Ontario Geological Survey
Miscellaneous Paper 115

Exploration Technology Development Program of the Board of Industrial Leadership and Development

Summary of Research 1981-1983

edited by
E.G. Pye and R.B. Barlow

Program funded by the Board of Industrial Leadership and Development

1983

Ontario

Ministry of
Natural
Resources

Hon. Alan W. Pope
Minister

W.T. Foster
Deputy Minister

©OMNR 1983
Printed in Canada

ISSN 0704-2752
ISBN 0-7743-8505-7

Publications of the Ontario Ministry of Natural Resources are available from the following sources. Orders for publications should be accompanied by cheque or money order payable to the *Treasurer of Ontario.*

Reports, maps, and price lists (personal shopping or mail order):
Public Service Centre, Ministry of Natural Resources
Room 1640, Whitney Block, Queen's Park
Toronto, Ontario M7A 1W3

Reports only (personal shopping):
Ontario Government Bookstore
Main Floor, 880 Bay Street
Toronto, Ontario

Reports and maps (mail order or telephone orders):
Publications Services Section, Ministry of Government Services
5th Floor, 880 Bay Street
Toronto, Ontario M7A 1N8
Telephone (local calls), 965-6015
Toll-free long distance, 1-800-268-7540
Toll-free from Area Code 807 0-ZENITH-67200

A project funded by the Board of Industrial Leadership and Development of the Government of Ontario.

Every possible effort is made to ensure the accuracy of the information contained in this report, but the Ministry of Natural Resources does not assume any liability for errors that may occur. Source references are included in the report and users may wish to verify critical information.

Parts of this publication may be quoted if credit is given. It is recommended that reference to this report be made in the following form for each individual paper:

Lazenby, P.G., and Becker, A.
1983: Grant 003 Redefinition of the INPUT® System; Part A—Instrumentation; p.1-9 *in* Exploration Technology Development Program of the Board of Industrial Leadership and Development, Summary of Research 1981-1983, edited by E.G. Pye and R.B. Barlow, Ontario Geological Survey, Miscellaneous Paper 115, 135p. Accompanied by 2 charts (coloured).

Scientific Editor: Guy Kendrick

1000-83-Tri-Graphic

INTRODUCTORY REMARKS
EXPLORATION TECHNOLOGY DEVELOPMENT PROGRAM

The favourable geology of Ontario and our previous success in discovering economic mineral deposits indicate that the resource potential of the province is high. At the same time, Ontario is one of the most extensively prospected areas in the world. Exploration has reached a stage of maturity such that most mineral deposits at or near the surface have been tested for their economic viability. It follows, therefore, that future success in mine discovery depends on our ability to detect and discriminate valuable mineral deposits at depths below the bedrock surface or below a concealing cover of glacial debris. This, in turn, necessitates continual updating of the technology base by developing and testing new methods and new instrumentation, specifically with Ontario in mind. The Exploration Technology Development Program was created in late 1981 to facilitate this need for more precise instrumentation required for deeper ground penetration.

With the implementation of the Ontario Geoscience Research Grants Program in the late 1970s, the Ontario Geological Survey developed a program of university research that serves to define the parameters of geological environments favourable to the occurrence of mineral deposits and devises methodologies to predict areas of valuable mineral resources. In the Cabinet submission that resulted in the establishment of the Ontario Geological Research Grants Program, however, it was recognized that this would be only the first step in addressing the exploration problem, and that the second step would be to devise a supplementary means to support the development of new field technology. To quote from the Cabinet submission of September 8, 1977:

> *As this [Ontario Geoscience] research program develops...we must then examine mechanisms at ensuring that Ontario-based research and development companies can take the ideas and concepts from this program and from other sources and put them into manufactured instrument packages for use by the private sector.*

The new Ontario Exploration Technology Development Program is viewed as helping to fill this need.

The Exploration Technology Development Fund is a program of mission oriented applied research in mineral exploration technology designed to encourage the advancement of exploration geophysics and geochemistry leading to the development of innovative technology specifically in those areas which support the mineral exploration industry in Ontario. This program promotes joint ventures in applied research and development with Ontario companies by providing funding for up to 3 years, with the Ontario Government financing 60% of all activities to a maximum contribution for an individual project of $150 000 per year.

The Canadian exploration technology industry, which is largely located in Ontario, has been in existence for approximately 30 years. It can easily be defined as a service industry which is currently active on a global scale, supplying a variety of contractable airborne and ground surveying techniques, as well as manufacturing survey systems for ground, airborne, and borehole logging applications. These companies on the whole are small scale, averaging about $1.0 million in gross sales per annum. Currently, 70% to 80% of gross sales revenue is derived from outside Canada.

The survival rate of companies included in this industry has been remarkable considering the exposure to severe fluctuations in exploration activity cycles which have taken place over this period. Research and development efforts within these companies, often amounting to 10% of gross sales, have been of paramount importance in realizing, firstly, the high survival rate and secondly, a respectable global market position. It is expected that funding provided by the Exploration Technology Development Program will significantly aid the industry in its continuing development of effective state-of-the-art technology.

The Exploration Technology Development Program receives financial support from the Board of Industrial Leadership and Development (BILD) and is administered by the Ontario Geological Survey of the Ministry of Natural Resources. BILD is the Cabinet Committee responsible for directing the province's economic development policies.

All technical matters of administration concerning the Exploration Technology Development Program are carried out by a Review Committee composed of 3 representatives from government agencies in Canada, 3 representatives of the university community, and 6 industry representatives. It is the responsibility of the Review Committee to review, rank, and recommend proposals for funding under the Program.

In order to receive funding support from the Program, companies are asked to submit project proposals to the Ontario Geological Survey by January 15. All submitted proposals are judged and ranked according to their relevance to exploration problems in Ontario and scientific merit by the Review Committee. All proposals must have an important economic impact in reducing the risks of mineral exploration, or contribute significantly to mineral resource management in Ontario.

The members of the 1982-1983 Committee included:

Dr. R.J. Uffen, Chairman	Queen's University
Dr. A.P. Annan	A-Cubed Incorporated
Dr. R.B. Band	Falconbridge Copper Limited
R.B. Barlow	Ontario Geological Survey
Dr. W.B. Coker	Kidd Creek Mines
L.S. Collett	Geological Survey of Canada
Dr. W.O. Karvinen	Karvinen and Associates
Dr. J.P. Lalonde	Government of Quebec
R.S. Middleton	Newmont Exploration of Canada
Dr. N.R. Paterson	Paterson, Grant, and Watson Limited
Dr. D.H. Watkinson	Carleton University
Dr. G.W. West	University of Toronto

During the 1982-83 year, 41 proposals were received from Ontario companies. Of these, 17 received funding towards the development of: airborne systems, borehole logging systems, ground portable systems, concepts and techniques in exploration geochemistry, laboratory support equipment not presently available in Ontario, data acquisition and signal processing hardware and software, and mineral deposit and overburden characterization studies. Grant allocations in support of these 17 proposals totalled $1 076 166.

The undersigned would like to thank the Chairman of the Program Review Committee, Dr. R.J. (Bob) Uffen and the rest of the members who gave freely of their time and expertise in reviewing and ranking proposals. Without their efforts, this program would not be possible. The work of the individual researchers and participating companies is also acknowledged, for without their time and perseverance, the objectives of the Program would not be realised. Thanks are due R.B. Watson who served as Grants Administrator and Secretary.

E.G. Pye
Director
Ontario Geological Survey

REFERENCES

Barlow, R.B.
1982: Directions for Research and Development in the 1980s; p.4-7 *in* Geoscience Research Grant Program, Exploration Technology in the 1980s, edited by E.G. Pye, Ontario Geological Survey, Miscellaneous Paper 105, 15p.

Pye, E.G.
1978: Mineral Exploration Trends and Problems; p.106-110 *in* A Submission to the Federal Government/Mining Association of Canada on the Proceedings of Two Exploration Sub-Group Workshops Held in February 1978, Preliminary Report, edited by R.V. Shank and U.E. Ruth.

1980: Introductory Remarks; p.v-vi *in* Geoscience Research Grant Program, Summary of Research, 1979-1980, edited by E.G. Pye, Ontario Geological Survey, Misscellaneous Paper 93, 262p.

CONTENTS

Introductory Remarks iii

Grant 003 Redefinition of the INPUT$^{(R)}$ System: Part A—Instrumentation, *P.G. Lazenby and A. Becker* 1

Grant 004 Electrical Parameters of Volcanogenic Mineral Deposits in Ontario, *Philip G. Hallof and James D. Klein* 11

Grant 005 Tin-Tungsten Analysis of Geological Samples Under Field Conditions, *J.D. Kinrade and J.C. Robbins* 27

Grant 009 High Sensitivity Portable/Base Station Magnetometer Based on Overhauser Effect, *I. Hrvoic and J. Myzyk* 39

Grant 010 Advanced Hardware and Software Development for Ground EM Prospecting, *J.C. Macnae and Y. Lamontagne* 45

Grant 011 Development of Computer Software for Geophysical Interpretation, *N.R. Paterson, F.S. Grant, and D.J. Misener* 53

Grant 012 A) Determination of Short-Lived Isotopes by Neutron Activation Analysis and B) Investigation of Commercial Viability of Prompt Gamma Analysis, *E.L. Hoffman et al* 63

Grant 014 Development of a Digital Pulse EM Receiver, *J. Duncan Crone* 71

Grant 018 Development of a Four Frequency Helicopter Electromagnetic System, *E.B. Morrison* 77

Grant 019 Development of a Portable Helium Detector, *G.M. Denham and R. Raz* 83

Grant 020 Application of Vibra-Corer Drills for Rapid Overburden Sampling, *C.W. Archibald* et al 85

Grant 023 Aeromagnetic Gradient Characterization of Altered Volcanic Rocks, *W.R. Lechow* 91

Grant 025 The Development of an Omni-Directional Multi-Frequency Airborne EM System, *S.J. Kilty* 99

Grant 028 TOTEM-2G Continuous Recording Ground VLF EM, *Alex Herz, A.B. Routledge, and K.D. Naujok* 107

Grant 030 A User-Friendly Electromagnetic Prospecting System, *Mitsuru Yamashita* 115

Grant 031 The Geoport Project, *D.J. Dodds* 125

Grant 039 Single Receiver, Frequency Scanning, Fixed Source Electromagnetic System, *Andrew Rogozinski* 131

CHARTS

(Back Pocket)

Chart A; Figure 4; Grant 023; (coloured)—
Colour contour map of total field (data supplied by Questor Surveys Limited).

Chart B; Figure 5; Grant 023; (coloured)—
Colour vertical gradient map (data supplied by Questor Surveys Limited).

Conversion Factors for Measurements in Ontario Geological Survey Publications

If the reader wishes to convert imperial units to SI (metric) units or SI units to imperial units the following multipliers should be used:

CONVERSION FROM SI TO IMPERIAL			**CONVERSION FROM IMPERIAL TO SI**		
SI Unit	*Multiplied by*	*Gives*	*Imperial Unit*	*Multiplied by*	*Gives*
			LENGTH		
1 mm	0.039 37	inches	1 inch	**25.4**	mm
1 cm	0.393 70	inches	1 inch	**2.54**	cm
1 m	3.280 84	feet	1 foot	**0.304 8**	m
1 m	0.049 709 7	chains	1 chain	20.116 8	m
1 km	0.621 371	miles (statute)	1 mile (statute)	**1.609 344**	km
			AREA		
1 cm^2	0.155 0	square inches	1 square inch	**6.451 6**	cm^2
1 m^2	10.763 9	square feet	1 square foot	**0.092 903 04**	m^2
1 km^2	0.386 10	square miles	1 square mile	2.589 988	km^2
1 ha	2.471 054	acres	1 acre	0.404 685 6	ha
			VOLUME		
1 cm^3	0.061 02	cubic inches	1 cubic inch	**16.387 064**	cm^3
1 m^3	35.314 7	cubic feet	1 cubic foot	0.028 316 85	m^3
1 m^3	1.308 0	cubic yards	1 cubic yard	0.764 555	m^3
			CAPACITY		
1 L	1.759 755	pints	1 pint	0.568 261	L
1 L	0.879 877	quarts	1 quart	1.136 522	L
1 L	0.219 969	gallons	1 gallon	**4.546 090**	L
			MASS		
1 g	0.035 273 96	ounces (avdp)	1 ounce (avdp)	28.349 523	g
1 g	0.032 150 75	ounces (troy)	1 ounce (troy)	**31.103 476 8**	g
1 kg	2.204 62	pounds (avdp)	1 pound (avdp)	**0.453 592 37**	kg
1 kg	0.001 102 3	tons (short)	1 ton (short)	**907.184 74**	kg
1 t	1.102 311	tons (short)	1 ton (short)	**0.907 184 74**	t
1 kg	0.000 984 21	tons (long)	1 ton (long)	**1016.046 908 8**	kg
1 t	0.984 206 5	tons (long)	1 ton (long)	**1.016 046 908 8**	t
			CONCENTRATION		
1 g/t	0.029 166 6	ounce (troy)/ ton (short)	1 ounce (troy)/ ton (short)	34.285 714 2	g/t
1 g/t	0.583 333 33	pennyweights/ ton (short)	1 pennyweight/ ton (short)	1.714 285 7	g/t

OTHER USEFUL CONVERSION FACTORS

1 ounce (troy)/ton (short)	20.0	pennyweights/ton (short)
1 pennyweight/ton (short)	0.05	ounce (troy)/ton (short)

NOTE—Conversion factors which are in bold type are exact. The conversion factors have been taken from or have been derived from factors given in the Metric Practice Guide for the Canadian Mining and Metallurgical Industries published by The Mining Association of Canada in cooperation with the Coal Association of Canada.

Grant 003 Redefinition of the INPUT$^{(R)}$ System: Part A—Instrumentation

P.G. Lazenby and A. Becker

Questor Surveys Limited, Mississauga

ABSTRACT

Between 1960 and 1980, many improvements were made to the INPUT$^{(R)}$ airborne electromagnetic system. These mostly were related to new developments in electronic and aviation technology. The objective of this research project is a major advance in system capabilities in terms of depth penetration, resolution, and discrimination. Redesign of the transmitter and towed sensor and replacement of the analog receiver with digital equipment have been the primary goals in the work undertaken to date.

A DC-3 aircraft was dedicated to serve as a flying laboratory for the duration of the project. Extensive modifications were made to mount the redesigned transmitter and to permit in-flight retrieval of the towed sensor. Standard survey equipment was installed alongside the experimental instruments for comparison purposes, and test flights using a high speed digital data acquisition system were made for spectrum analysis purposes. This was then replaced by a microprocessor-controlled digital detector capable of automatically carrying out the required functions such as compensation, spike rejection, and digital filtering. Lastly, the towed sensor incorporating orthogonal coils and new ideas for reducing motion noise was designed, constructed, and test flown.

INTRODUCTION

The filing of a patent application in mid 1958 by A.R. Barringer for the INduced PUlse Transient (INPUT$^{(R)}$) airborne electromagnetic apparatus signaled a new approach to mineral exploration. High detection efficiency was to be attained by:

1. developing a high power pulsed primary magnetic field
2. measuring the induced secondary field in the absence of the primary excitation
3. using the characteristics of the secondary field transient for anomaly discrimination

Initial patents for the invention were granted in the United Kingdom, the United States, and Canada in 1959, 1962, and 1963 respectively. First results obtained with the newly developed Mark II INPUT system were first published by Barringer 20 years ago (Barringer 1962) and clearly showed that the new apparatus fulfilled the high expectations that were held for it. Further development and improvement of the prototype apparatus led to the Mark V production equipment described by Boniwell (1967).

In 1970, revisions to the system were once again introduced by Questor Surveys Limited. The object of that development program was to improve the system performance by updating the signal processing techniques used in the detector, and also to improve the performance of the aircraft itself by replacing the time-honoured Canso with a modern airplane. Work done under this program resulted in the Mark VI Barringer/Questor INPUT system. This apparatus was first mounted on a Short Brothers Skyvan aircraft and later on a Britten-Norman Trislander. Both aircraft required considerable structural modifications in order to carry a transmitter loop of a size equalling that of the large loop carried by the Canso. As shown by Lazenby (1973), the new Mark VI INPUT system exhibited a large improvement in signal-to-noise ratio and anomaly resolution when compared to the Mark V results. Becker (1979) makes a direct comparison between results obtained in 1965 with Mark V equipment and the results obtained with Mark VI equipment in 1975 over the identical conductor. This data most clearly illustrates the direct relation between technological development and survey data quality.

To date, over 1½ million survey line miles have been flown with the INPUT system. Of this total, about 300 000 line miles or 20% of the worldwide mileage were flown in Ontario. The system was directly involved in the discovery of 15 economical ore deposits with an aggregate worth in excess of $6 billion; about ⅓ of these deposits are located in the Province of Ontario (such as the South Bay, Mattabi, Lyon Lake, and Detour River deposits).

In spite of the proven capability of the Mark VI INPUT system, as demonstrated by the confirmed detection of good conductors in a resistive environment at depths in excess of 250 m and by its capacity for discrimination between surficial and bedrock conductors, it appears that the full potential of this airborne electromagnetic system is not being realized. While adhering to the principles behind the INPUT apparatus first formulated nearly 20 years ago, significant improvements to the system can now be made by taking advantage of newly developed digital technology. Such a modification should result in an increased anomaly resolution for deep as well as shallow conductors and in increased capacity for defining bedrock mineralization in areas of highly conductive overburden.

PROJECT OBJECTIVES

The objective of the research project described below is to advance the standards of performance set by the Mark VI version of the INPUT airborne electromagnetic exploration system. Specifically, the work encompassed by this project is intended to result in an improved airborne electromagnetic system which will exceed the depth of penetration currently attainable. In addition to an increase in depth penetration, the redefined system should allow for use in electrically conductive terrains by providing a higher degree of discrimination against surficial conductors.

Before the stated geophysical objectives can be attained, they must be translated into precise technological modifications that will yield the required improvements. In particular, it is necessary to correctly identify the changes that should be made to the 3 subsystems that constitute the INPUT apparatus. Thus consider:

1. the transmitter subsystem, which contains the power source, the transmitter loop, and the switching and pulse-forming electronics
2. the receiver subsystem, which contains the receiver coil or coils and associated preamplifier electronics, the bird which houses the equipment, and the tow cable that connects this subsystem to the aircraft
3. the detector subsystem, which encompasses all the electronic circuitry (analog and/or digital) necessary for the detection and recording of the secondary magnetic field transients

The geophysical objectives of this research project should be attained by making the appropriate improvements to all 3 subsystems so that the signal-to-noise ratio for the anomalies detected by the redefined system should be increased.

In particular, it is expected that significant gains in system performance can be made by redesigning the transmitter subsystem to allow for a high power, long duration primary pulse. Further improvements can be made by redesigning the receiver subsystem so that motion-induced noise also should be substantially decreased. Finally, the replacement of the present analog receiver subsystem with modern digital equipment should allow for very sophisticated signal processing to optimize the received signal-to-noise ratio under any given set of circumstances.

FACILITIES

The first phase of this research project (October 1981-March 1982) centred around the establishment of proper facilities indispensable for acquiring the fundamental data on which the new equipment designs would be based. To this effect, Questor Surveys Limited dedicated a DC-3 aircraft to serve exclusively as a flying laboratory for the duration of the project. The airplane, CF-YED shown in Figure 1, was equipped with a high power transmitter subsystem, including a large area loop of novel design. Here, 6 turns are spaced in a flat ribbon configuration as opposed to the conventional 4-turn loop of cylindrical cross section. The transmitter is powered by an on-board auxiliary power unit (APU) made up of 3 28V-100A generators driven by an Onan engine. The new unit has a 7.5 kw capacity; its performance can be compared with that of the standard Mark VI system as shown in Table 1. The indicated 80% increase in transmitter moment allows the acquisition of experimental data of superior quality.

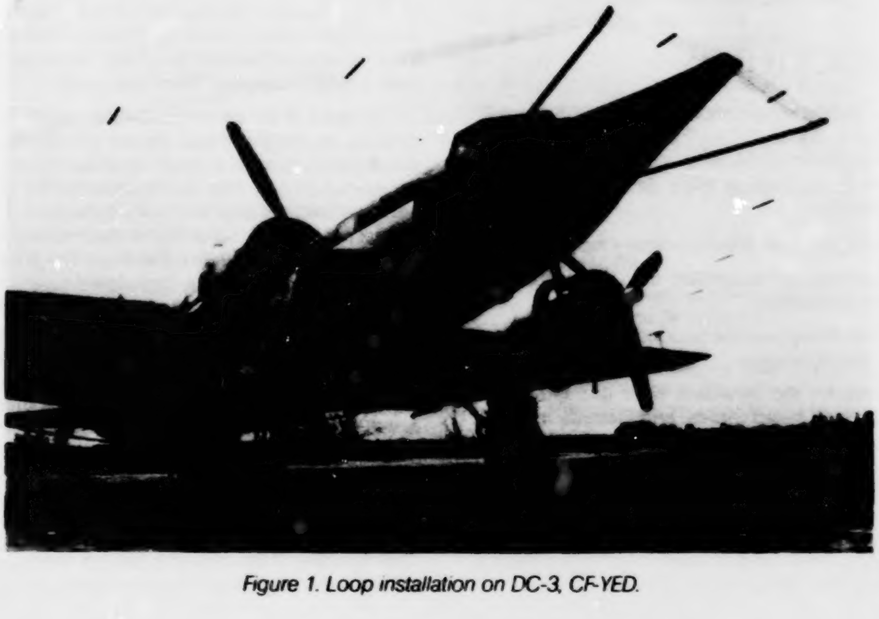

Figure 1. Loop installation on DC-3, CF-YED.

TABLE 1: TRANSMITTER SUBSYSTEM CHARACTERISTICS.

	STANDARD MARK VI	NEW
EXPERIMENTAL		
Loop turns		6
Loop area – M²	186	232
Peak current – A	285	270
Dipole moment – MKS	2.1 x 10^5	3.8 x 10^5
Power consumption – kW	2.8	4.4
Pulse width – mS	1/fixed	2/variable

To facilitate the redesign of the receiver subsystem, the aircraft has been modified to allow the installation of a large (152 cm by 51 cm) hatch. This hatch is equipped with double safety doors, only 1 set of which can be opened at a time. It allows the retrieval of the bird in flight and the adjustment of its configuration without the necessity of a landing. Figure 2 shows the hatch; the bird reposes on the closed inner doors. The winch assembly is shown in the foreground. In addition to the hatch, the aircraft is equipped with a periscope through which the bird motion can be visually monitored.

To monitor progress and to evaluate the various modifications as they are made, we have also installed a conventional Mark VI analog detector. This equipment operates at all times in parallel with any new detector and provides an instantaneous comparison between the 2 systems.

The aircraft is equipped to carry an experimental, very high speed digital data acquisition system intended to provide design data for the new digital detector. This system acquires and loads data on tape at rates up to 20 000 samples per second. It consists of an 8th-order Butterworth 10 kHz low-pass anti-aliasing filter and gain control followed by a 16-bit A-D converter. The data is first stored in a pair of 8K FIFO buffers which operate in ping-pong fashion. The data is taken directly from the buffers via an IEEE 488 bus by a Dylon 1015 formatter which transfers it to the tape drive. The whole assembly, including the 9 track, 114 cm/second, Kennedy tape deck, is controlled by a user-friendly HP 85 calculator.

Finally, and most recently, the aircraft is equipped with an RMS Limited GR33 recorder. This piece of equipment allows the recording of all the data acquired by the flying laboratory. Data inputs, whether analog or digital, are automatically scaled and can be displayed across the full 330 mm paper width.

In addition to the equipment described above, the aircraft carries the usual complement of ancillary survey equipment. This includes a Sperry radio altimeter and a 35 mm frame camera for flight path recovery. Provision is made for the installation of a proton magnetometer, and, if necessary, auxiliary Doppler or Loran C navigational aids.

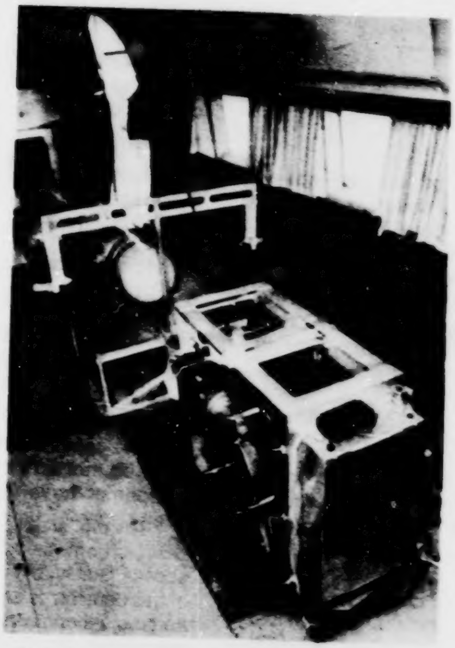

Figure 2. Bird launching and retrieval facility.

NEW INSTRUMENTATION

EXPERIMENTAL HIGH SPEED DATA ACQUISITION SYSTEM

In order to obtain design data for the new digital receiver, a number of test flights were made with the experimental high speed data acquisition system. The full power of this type of apparatus can be appreciated by examining the data samples shown in Figure 3. Here, the system was operating while the primary pulse was on. Data was acquired at about 20 000 samples/second or one sample every 50 microseconds. Note the clear resolution of an atmospheric event which was superimposed on the primary pulse shown in the lower trace.

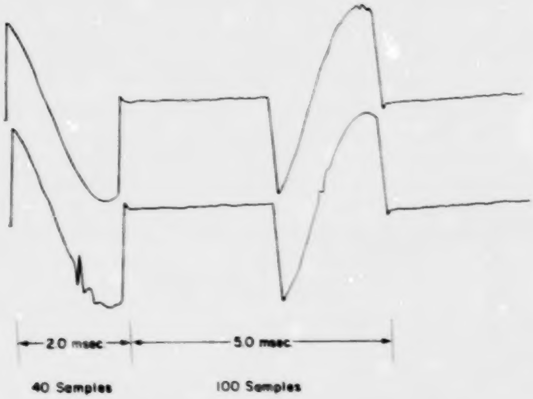

Figure 3. Digital data recording.

When flown with the transmitter off, the high speed data acquisition system enabled us to obtain data on the various sources of system noise. Figure 4 once again illustrates the high resolution capability of the data acquisition system. Here, the atmospheric noise spectrum in the upper end of the audio frequency range is shown. Note the characteristic 8 kHz broad thunderstorm energy peak. Superposed on the natural noise we find a sharply defined peak at about 12 kHz probably associated with a navigational aid.

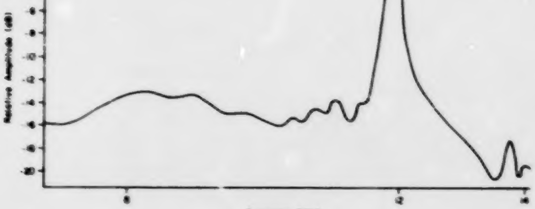

Figure 4. High frequency noise spectrum.

The flexibility of this new diagnostic tool can be further illustrated by considering the other extremity of the noise spectrum. The results at the sub-audio end of the frequency range are shown in Figure 5. Here, the noise can be attributed to the turbulent motion of the bird and receiver coil in the earth's magnetic field. As before, we note the clear resolution of the peaks at 0.58 and 2.58 Hz which corresponds to the 2 dominant modes of bird and receiver coil motion.

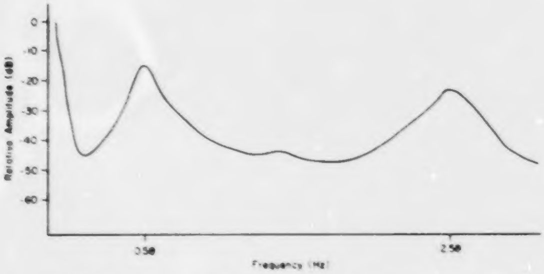

Figure 5. Low frequency noise spectrum.

DIGITAL DETECTOR

The digital detector is the heart of the redefined INPUT system. It fulfils all the functions which relate to the synchronous detection of the secondary field and its recording on digital magnetic tape. In particular, it is capable of the following operations:

1. transmitter triggering
2. coherent sampling and A-D conversion of receiver voltages
3. linear digital filtering
4. automatic compensation of system transient
5. automatic rejection of atmospherics
6. digital recording of acquired data
7. in-flight, real-time compilation of analog monitor records which confirm its own proper functioning

To track the received signals, this subsystem samples at a rate compatible with an 8 kHz signal bandwidth and has sufficient dynamic range to cover the anticipated 120 dB span of the received voltage.

The digital detector consists of a number of microprocessors controlled by an 8086 unit and linked by a direct access facility to a common memory. A synoptic diagram of the detector is shown in Figure 6. All real time filtering, compensation, and spike rejection is done by the array processor. The data is then channelled to the 8085 controller units. One of these units outputs the survey data to the tape drive while the other controls the analog monitor data. At present, the system accesses a number of

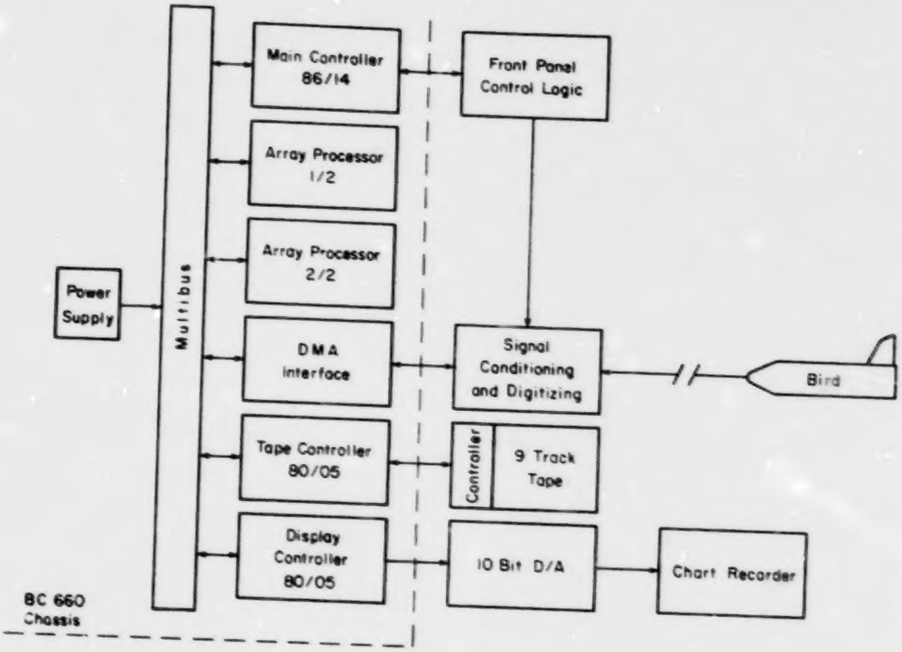
Main Controller 86/14
Front Panel Control Logic
Array Processor 1/2
Array Processor 2/2
Power Supply
Multibus
DMA Interface
Signal Conditioning and Digitizing
Bird
Tape Controller 80/05
Controller
9 Track Tape
Display Controller 80/05
10 Bit D/A
Chart Recorder
BC 660 Chassis

Figure 6. Synoptic diagram - Digital detector.

peripherals which, in addition to the digital tape drive, include dual floppy discs, a large CRT monitor, and an RMS chart recorder. At present, the digital detector has 1 signal channel. Provision was made, however, to easily expand this subsystem to 2 channels so that signals from a dual orthogonal coil system could be readily recorded.

The functioning of the digital detector can best be appreciated by illustrating its operation in direct comparison with the conventional analog detector. This was first done in the context of a laboratory scale model experiment using a low power pulse transmitter. Both detectors were connected in parallel to a common receiver coil. Provision was also made for injecting "atmospheric" noise and/or "motion" noise into the system. For the purpose of this comparison, the output of the digital detector was processed in an appropriate manner using stacking and running average filtering to produce 6 channels of analog output that closely correspond to the output of the analog detector.

The results of these tests are shown in Figures 7 and 8. Both of these illustrations show "anomalies" which attest to the close parallel functioning of the 2 units. Let us first

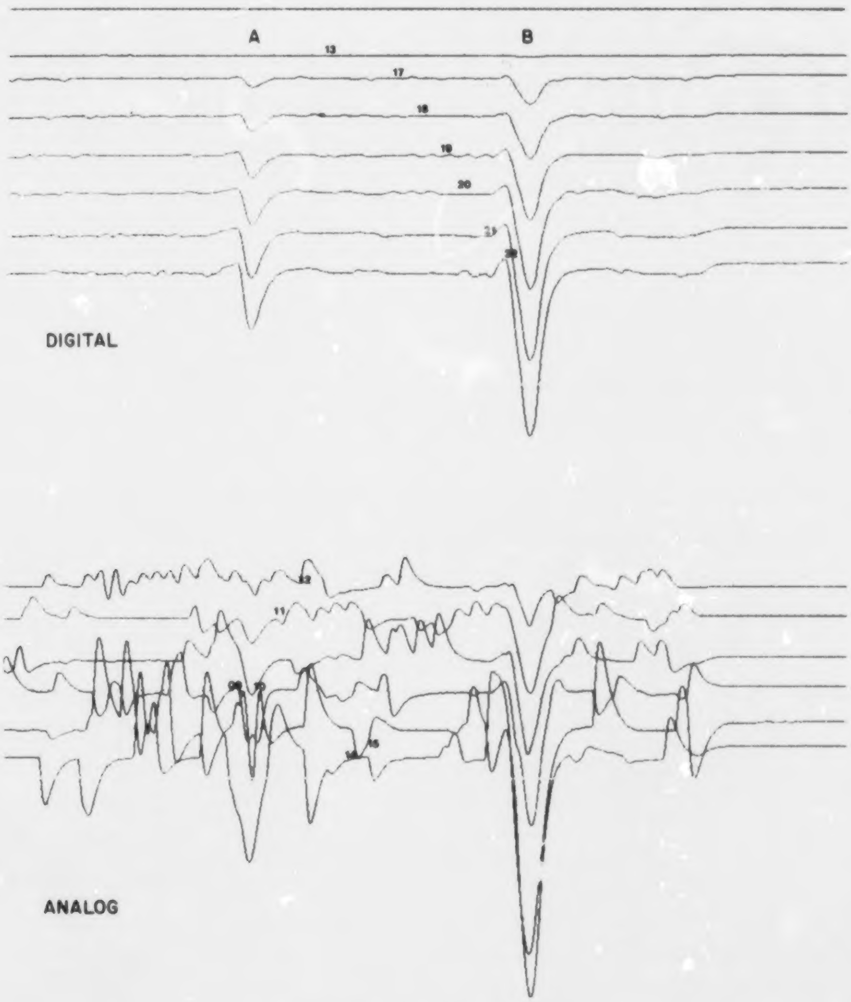

Figure 7. Automatic "spike" removal.

consider the atmospheric spike rejection capabilities of the digital system. As shown in Figure 7, both systems clearly indicate the large "B" anomaly. The small "A" anomaly however, which is clearly shown by the digital system, is totally obscured by the atmospherics on the analog output of the conventional detector. It should be noted that the atmospheric noise removal on the digital record is done without any loss in anomaly resolution or the introduction of any nonlinear effects into the system.

Equally important is the automatic compensation feature of the digital detector. The proper functioning of this aspect of the new apparatus is illustrated in Figure 8. The lower part of the illustration shows the effect of an uncompensated system transient caused by a variation in the primary signal. Such a variation is of course related to a change in the receiver-transmitter separation. With the exception of a small reflection of the event, in channel 1, the digital system automatically and fully compensates for any system transient. As shown further to the right, this again is done in a linear manner without any distortion of *bona fide* anomalies.

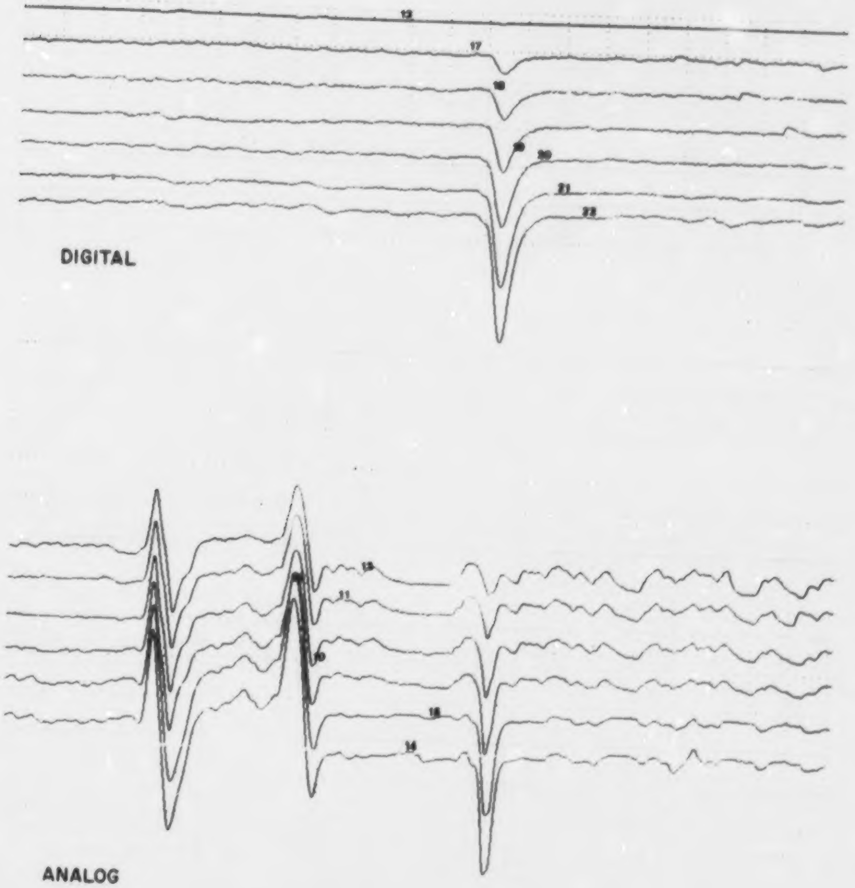

Figure 8. Automatic compensation.

NEW BIRD AND TWO-AXIS RECEIVER

To increase the INPUT system's capacity for defining the geometrical parameters of detected conductors, Questor Surveys Limited has designed an orthogonal coil receiver which senses the vertical and radial (horizontal) components of the secondary field. The 2-element receiver consists of a horizontal axis ferrite-cored solenoid lodged inside a vertical axis air-cored sensor. This combination provides for a most compact device. The new 2-component receiver is housed in a bird optimally designed for it. Figure 9 shows the new bird receiver coil assembly. In order to clearly show the vertical axis receiver, the horizontal coil device is omitted from the assembly. Because bird motion studies indicate that longitudinal motion is a source of system noise, the new bird, shown in Figure 9, differs from the conventional equipment. In particular, much care is taken to concentrate the mass at its centre of gravity and to position the stabilizers well aft of this point.

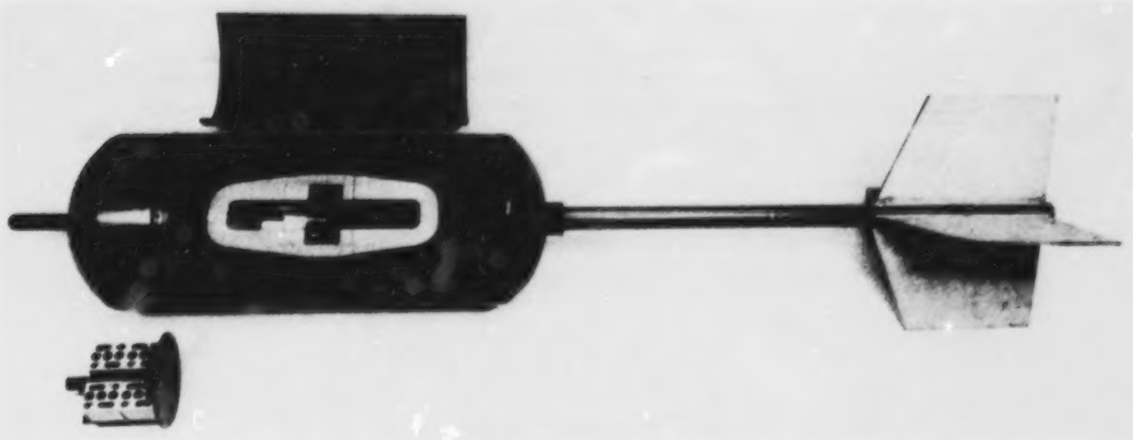

Figure 9. New bird and receiver.

Figure 10 shows a downdip record obtained with a prototype 2-coil receiver over the Cavendish test range. The data was recorded using 2 conventional analog detectors whose output is displayed on a standard Honeywell galvanometric recorder. Shortage of available recorder traces only allowed the display of 3 channels of transient data from the vertical axis receiver. Nevertheless, the advantages of a 2-coil receiver are clearly demonstrated by this illustration. Note in particular the subtle geometric differences between the 2 conductors that can be inferred from the vertical-axis coil data. These are much more difficult to perceive in the conventional horizontal axis record. It is also interesting to note that fairly severe spheric activity can be seen on the horizontal-axis receiver record. Due to the horizontal polarization of the interference, it is not sensed by the vertical axis receiver coil.

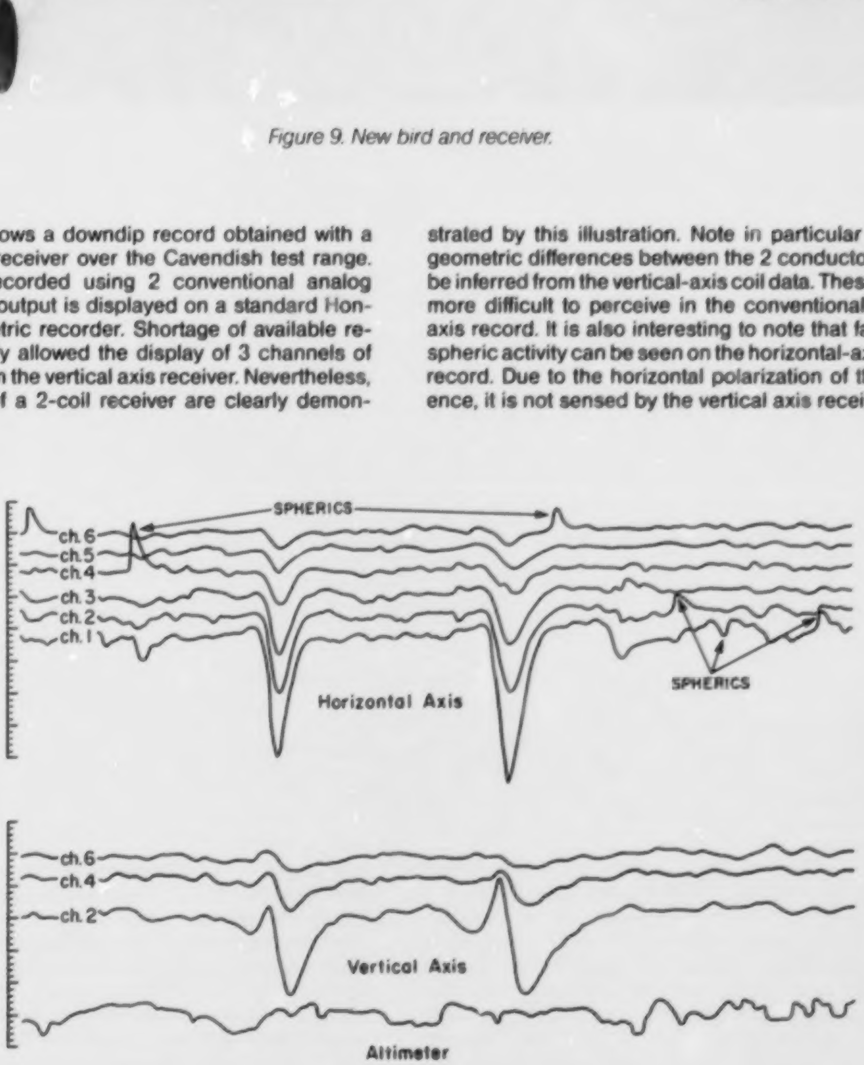

Figure 10. Dual receiver flight data.

DISCUSSION AND CONCLUSION

We are well advanced toward our goals of redefining the INPUT system in a way that will significantly improve its operating characteristics. In particular, at the completion of this research and development project, we expect to have an airborne electromagnetic exploration system of much-improved quality. This will be demonstrated by its superior penetration to deep targets, its large capacity for discriminating between different types of conductors, and above all, its ability to detect bedrock mineralization in areas of thick conductive surficial overburden.

To attain the desired geophysical objectives, we have assembled a new flying laboratory for airborne electromagnetic experiments. To date, this facility has provided us with much information on airborne electromagnetic system noise and its sources.

The main step toward our goal of an optimal airborne electromagnetic system was taken with the installation and testing of the digital detector. This device allows improved resolution of the secondary magnetic field. It also provides for the automatic rejection of 2 of the most common sources of airborne electromagnetic noise, system transients and atmospherics.

Comprehensive flight testing is planned for 1983 and 1984. This will allow us to perfect the software for the digital detector, optimize the receiver bird, and, above all, gain experience with the new geophysical apparatus.

REFERENCES

Barringer, A.R.
1962: New Approach to Exploration-The INPUT Airborne Electrical Pulse Prospecting System; Mining Congress Journal, October.

Becker, A.
1979: Airborne Electromagnetic Methods in Geophysics and Geochemistry in the Search for Metallic Ores; Geological Survey of Canada, Economic Geology Report 31, P.J. Hood (editor), p.33-43.

Boniwell, J.B.
1967: Some Recent Results with the INPUT Airborne EM System; Canadian Institute of Mining and Metallurgy Bulletin, Volume 60, Number 659, p.325-332.

Lazenby, P.G.
1973: New Developments in the INPUT Airborne EM System; Canadian Institute of Mining and Metallurgy Bulletin, Volume 66, Number 732, p.96-104.

Grant 004 Electrical Parameters of Volcanogenic Mineral Deposits in Ontario

Philip G. Hallof and James D. Klein
Phoenix Geophysics Limited, Willowdale

ABSTRACT

The object of this research project is to characterize the electrical properties of various rock types associated with metallic mineral deposits in Ontario. Included are the ores themselves, Cu-Pb-Zn sulphides, Ni sulphides, and Au-Ag bearing sulphides; and non-economic materials which have a similar geophysical response, for example, graphite, magnitite, clays, and pyrite.

The primary use for this information will be to aid in the evaluation of the economic potential of spectral IP Phase Anomalies which are due to deep-seated sources. Such anomalies can now be accurately measured with new equipment (the Phoenix IPV-3 Receiver), but are expensive to test with drilling. Specifically, accurate knowledge of the spectral characteristics of these various rock types can aid in (1) separation of EM coupling from multifrequencey IP data; (2) distinguishing various types of economic mineralization from non-economic sources, for example, massive sulphides from graphite, and nickeliferous pyrrhotite from magnetite; and (3) estimating the volume percent of conductive mineralization.

The proposed research will consist primarily of measurement of electrical response of the above-mentioned types of mineralization in situ. Measurements will be conducted in, and adjacent to operating mines with a low power battery operated transmitter and Phoenix IPV-3 receiver. Additionally, laboratory measurements of electrical response of hand speciments and detailed geologic descriptions will be used to provide the needed tie between theoretical models and the in situ measurements.

INTRODUCTION

The use of the Cole-Cole dispersion equation to describe the IP phenomena was first proposed by William H. Pelton in 1977, in his Ph.D. thesis. Since these proposals were published in 1978 (Pelton *et al.* 1978), there has been a great deal of discussion among geophysicists regarding the validity of the Cole-Cole approximation.

In our work, we have come to use the Cole-Cole equation response as being almost equivalent to the actual measured spectral response. For many natural and artifical rocks, the Cole-Cole equation has been found to be not only adequate, but indeed, an excellent representation of the measured IP spectral response.

The 4 parameters (Ro, m, τ, and c) will adequately describe any IP response that has been measured, even over as many as 6 or 7 decades of frequency. Further, it is possible to relate each of the 4 parameters to a physical property of the rock and contained metallic mineralization.

This usefulness of the Cole-Cole dispersion equation has been confirmed by the 1000s of spectral IP measurements recently made during a test program in 7 mines in Ontario. Measurements were made using 1 m and 2 m electrode intervals (dipole-dipole configuration and gradient array) in underground stopes and drifts, as well as open-pit mines. With almost no exceptions, these spectral responses can be exactly described by a single set of Cole-Cole parameters.

In many cases, the chargeability (m) approaches the theoretical maximum of 1.0. The frequency exponent (c) is often nearly equal to the theoretical value of 0.5, for spheres with a single size.

As would be expected, some of the measurements within massive sulphide ore zones result in very low resistivity values. However, the IP effects can still be accurately measured and the Cole-Cole approximation is representative. This is true, regardless of the location of the volcanogenic deposit being studied.

If the texture of the metallic ore was of disseminated or veinlet type, the Cole-Cole parameters will reflect this change. Nevertheless, the Cole-Cole dispersion is still an excellent approximation.

Even in the case of the nickel-copper ores at Sudbury (both disseminated and massive), the highly conductive sulphide zones (which give rise to $m > 0.9$) have IP spectra which can be described by a single Cole-Cole dispersion.

Occasionally, 2 types of metallic mineralization, with widely separated grain size, are present. In this situation, it is sometimes possible to see 2 distinct Cole-Cole dispersions, rather than a single dispersion with a small (c) value (i.e. $c < 0.25$). The "flat" spectral response indicates a broad distribution of grain sizes or a multiple grain size population.

LARGE AND UNIFORM ORE ZONES

We have found that some large zones of metallic mineralization are extremely uniform in their texture and therefore in their electrical parameters. The massive silver-zinc mineralization exposed in the 550-1040 Sill Drive at the Mattabi Mine at Ignace, Ontario is very uniform.

A dipole-dipole survey ($X = 1.0$ m; $n = 1,2,3,4,5,6$) was completed along a line 20 m long. The apparent resistivities ranged from 0.05 ohm-m to about 1.0 ohm-m. This was a larger variation than was observed in the other electrical parameters.

Only the 12 spectral plots measured for $n = 1$ are enclosed here. However, all of the $n = 2$ and many of the $n = 3,4$ spectral measurements were accurate enough to permit inversion. Those enclosed are entirely typical. All of the spectral curves show the steep flanks ($c \approx 0.5$) that indicate a single, unique size for the polarizable metallic particles. The time-constant (τ) values are grouped between 0.1 and 10 seconds. This is typical for massive volcanogenic sulphides and indicates a fairly small grain size.

The uniform character of the electrical parameters measured for this particular ore zone of massive sulphide can be seen in the histograms for the 24 $n = 1$ and $n = 2$ spectral plots.

MOST ORE DEPOSITS CONTAIN SEVERAL TEXTURES

The classic volcanogenic deposit described by geologists studying ore genesis can be expected to have variations in metallic sulphide minerals as well as in texture. One such deposit is the "F-Group" orebody at the Mattabi Mine in the Sturgeon Lake Mining Camp. A gradient-array survey was completed in an area 6 m by 48 m. The measurements crossed the several types and textures of ore that were described by the mine geologists.

The variations measured in the electrical parameters across the "F-Group" orebody can be studied from the contoured plan map. The lowest resistivities are within the massive ore; the highest apparent resistivities are within the non-porous, silicified zone. The entire region is anomalous, but the IP effects vary considerably across the zone of mineralization.

The time-constant (τ) also varies considerably across the various types of ore mineralization. The spectral plots show that the time-constant is directly related to the grain size and texture of the metallic minerals present.

The veinlet chalcopyrite (stringer copper) ore is present in the footwall of the mineralization. The resistivities are moderately low and the IP effects are moderately high. The time-constants for this type of mineralization are always larger than for the massive ore; the value of 11.0 seconds shown here are at the low end of the time-constant range usually found for this type of mineralization. The (c) values measured for this type of mineralization are usually small (0.20 to 0.30). This indicated a considerable distribution in the grain size population.

The disseminated chalcopyrite zone often is present above the stringer copper zone. The resistivities are higher and the IP effects lower. The smaller grain size is reflected in the smaller time-constant (τ) values. Often, the (c) value is closer to the theoretically maximum value of 0.50 for spheres. This indicates that the disseminated chalcopyrite more closely approximates a single grain size population.

The massive ores have a larger IP effect and a smaller time constant than the veinlet chalcopyrite ores. The apparent resistivities are lower in magnitude, but high-grade zinc ores often do not have a high conductivity. The (c) value for massive ores can vary from a maximum of 0.50 (see previous section) indicating a single grain size population to values as low as 0.15 to 0.25, indicating a broad distribution of grain sizes.

At the "F-Group" orebody, there is a hanging wall ore zone of massive, extremely coarse grained chalcopyrite mineralization. The electrical parameters for this mineralization are much the same as for the massive zinc ore. However, the time-constant (τ) values are much larger. This must result from the larger grain size for the polarizable mineral particles.

TEXTURES AND PARAMETERS CORRELATE BETWEEN VOLCANOGENIC DEPOSITS

The variations in electrical parameters for the various types of mineralization at the "F-Group" orebody appear to correlate with the texture of the metallic particles. In particular, the time-constant values (τ) seem to correlate directly with the grain size of the metallic particles (Hallof, Cartwright, and Pelton 1979). The exponent of the frequency term (c) determines the slope of the phase versus frequency curve at high and low frequencies. For a single, sphere-like, population of grain sizes, $c \approx 0.5$; for a continuous distribution of grain sizes, the value will be much smaller ($c \approx 0.15$).

The recent program of test surveys has shown that if the texture is the same, the electrical parameter values are very similar for all volcanogenic sulphide deposits.

For massive zinc-silver ore, the conductivity is high, with moderately high IP effects. Even for completely massive ore, the (c) value is often nearly equal to 0.5; the time-constant (τ) values are usually moderate in magnitude ($0.05 < \tau < 5.0$ seconds). The time-constant values (τ) for massive sulphide are rarely as high as 10 seconds. This fact suggests that the grain size for the polarizable particles in a massive sulphide deposit is relatively small.

The disseminated sulphide portions of such deposits have very different parameters. The sulphide contents begin with very low concentrations. There is a continuous, gradational variation through heavily disseminated mineralization to those deposits that contain veinlets of chalcopyrite as well as disseminated chalcopyrite. At the other end of this spectrum, are the veinlet chalcopyrite or "stringer copper" portions of volcanogenic deposits.

The apparent resistivities for these types of ores can vary from high for weakly disseminated mineralization to low for heavily veined chalcopyrite. The IP effects (m) for all of these types of ore can be surprisingly high, even for the more disseminated zones. The time-constant values (τ) vary from very small ($\tau \leq 0.01$/second) for fine-grained, disseminated ore to very large ($\tau \geq 100$ seconds) for the high-grade, heavily veined chalcopyrite ore.

In many cases for both massive and disseminated ore, the value for (c) on the Cole-Cole spectral inversion is in the range 0.35 to 0.50. For this result, the grain size population must be closely grouped about a single, preferred size. If a normal distribution of grain size is present, the value for (c) will be close to 0.250.

For (c) values in the range 0.10 to 0.25, the spectral curves are very "flat". In this situation, the IP dispersion is spread over a wide frequency range. Even for large (m) values, the maximum phase shifts measured, at any given frequency, are not large in magnitude. Theoretical work has shown (Hallof, Cartwright, and Pelton 1979) that the low (c) values arise from a continuous distribution of grain size, or from a dual population, with 2 (or more) distinct grain size populations.

If the 2 Cole-Cole dispersions are separated enough in time, it is possible to identify the character of the curve. If the resulting complex curve is quite flat, without much character, it is still often possible to obtain a "good fit" to the results by using 2 sets of Cole-Cole dispersion parameters. However, it must be kept in mind that these inversions are usually not unique. The statistical data (large standard deviations and high correlation factors) usually indicate this fact. It is often more satisfactory to "fix" certain of the parameters so that fewer variables are determined by the inversion.

The parameters from all of the spectral plots measured during the test surveys (all those accurate enough to make computer inversion possible) have been used to form a data base that can be displayed in many ways. The data can be displayed to study a particular type of ore, to study variations between ore types, or to study the same ore type from different locations.

SULPHIDE PARAMETERS VERSUS GRAPHITE PARAMETERS

In a previous paper, Hallof, Cartwright, and Pelton (1979) discussed the spectral parameters of graphite and proposed an explanation for the fact that graphite always has a large grain size and therefore a large time-constant (τ). According to Hallof, Cartwright, and Pelton (1979), the definition of graphite is very simple: 'Graphite is the amorphous form of the element, carbon, that conducts electricity.' Not only does graphite conduct electricity, it conducts it very well. Only some of the metals and metallic sulphide minerals have a higher conductivity. Petrographic tests on polished sections and thin sections have been developed to identify the graphite form of carbon.

The world of geology has abundant, black, carbonaceous rocks that do not contain graphite! These rocks, usually shales, argillites, water lain tuffs, and so on, do not have a high conductivity; their resistivities are usual for fine-grained, relatively porous rocks. Many of these rocks do exhibit moderate IP effects due to a few percent contained pyrite. The fine-grained pyrite is formed within the same reducing environment that created the carbonaceous sediments.

It has been the author's experience (throughout Canada, the United States, and Australia) that the metamorphic processes that finally convert amorphous "carbon" to conductive "graphite", invariably result in a large grain size for the polarizable particles. Thus, the spectral response for this type of source always has a large time-constant (τ).

The recent test surveys at the Kidd Creek Mine near Timmins, Ontario resulted in data that permits this matter to be studied further. A survey line, 15 m long, was surveyed in a cross-cut that passes through sulphide mineralization and graphitic material. Low apparent resistivities and high IP effects were measured along the entire line. Both types of sources can cause strong IP and resistivity anomalies.

The spectral plots show low resistivity values and high IP effects for all of the dipole-dipole pairs along the line. The massive sulphide parameters are much the same as have been seen elsewhere. Indeed, except for the time-constant (τ), the spectral parameters are much the same as those from the graphitic material. The (τ) values from the massive sulphide mineralization are moderately low.

Within the graphite zone, the apparent resistivities range from moderately low to very low; the IP effects are large in magnitude. The time-constant (τ) values are appreciably larger in magnitude than the authors have measured in volcanogenic, massive sulphide deposits. The values range from 50 seconds to 5000 seconds. These values are exactly the same as the authors have recorded over graphite deposits from the Bathurst mining area in New Brunswick to the Anvil mining area in the Yukon Territory.

Due to the complexity of the geology along the line surveyed, many of the spectral plots are influenced by more than 1 type of mineralization. Most of these plots show the "flat" shape ($c \simeq 0.125$) of multi-spectra. However, in a few positions the 2 Cole-Cole dispersions can be identified.

The plot of the parameters for massive sulphide mineralization and graphitic material at the Kidd Creek Mine show that the 2 highly conductive sources can perhaps be identified by the very different time-constant (τ) values. However, a review of the spectral plots previously presented for veinlet copper mineralization, will show that the texture for that type of ore frequently gives grain sizes (and therefore time-constants) that are as large as those for graphitic material. Therefore, a strong IP anomaly that exhibits a small time-contant can be expected to be disseminated, or massive, sulphide mineralization. An IP anomaly with a large time-constant will probably have a graphitic source; however, it must be kept in mind that a possible alternative would be veinlet chalcopyrite.

CONCLUSIONS

It is worth repeating here that the 70, or so, spectral IP plots presented here are typical of the several 1000s that have been measured within sulphide ore zones in Ontario. With almost no exceptions, the Cole-Cole dispersion equation can be used to accurately describe the measured data. The 4 parameters: Ro, m, c, and τ are therefore all that is necessary to catalogue the responses obtained.

The test surveys in 7 mines in Ontario have resulted in considerable insight into the causes and controls for the induced polarization phenomena. From this work, it seems clear that the texture (the grain size of the polarizable particles and the distribution of the grain sizes of the metallic particles present) of the metallic mineralization is much more important than the type of metallic minerals present.

Additional, perhaps more definitive, data will become available as a result of the next stage of study planned. Large hand specimens of mineralization were taken from within each 1 m, or 2 m electrode interval used during the spectral IP test surveys. These several hundred samples are now being prepared for petrographic examination as well as spectral IP measurements in the laboratory.

The results of the petrographic descriptions and the parameters obtained by computer inversion of the spectral IP measurements will then be compared and correlated. Finally, an attempt will be made to correlate all of this information with the data measured using X = 1.0 m and X = 2.0 m.

ACKNOWLEDGMENTS

The geophysical research described above was funded, in part, by the Ontario Geological Survey, Ontario Ministry of Natural Resources, through the Exploration Technology Development Program.

The measurements in operating mines, both open-pit and underground, would not have been possible without the support and cooperation of the management and mining staff of the mining companies involved. The individuals are too numerous to mention, but we would like to take this opportunity to thank all those who participated at: Noranda Mines (all Ontario mining operations), Kidd Creek Mines Limited, and Falconbridge Nickel Mines Limited (Sudbury Mining Division).

SELECTED REFERENCES

Dey, A., and Morrison, H.F.
1973: Electromagnetic Coupling in Frequency and Time-Domain Induced Polarization Surveys over a Multilayered Earth, Geophysics, Volume 38, Number 2, p.380-405.

Foster, R.N.
1933: Mutual Impedance of Grounded Wires Lying on or Above the Surface of the Earth; Bell Systems Technical Journal, Volume 12.

Grant, F.S., and West, G.F.
1965: Interpretation Theory in Applied Geophysics; McGraw Hill, New York, 583p.

Hallof, P.G.
1965: The Proper Choice of Frequencies for Induced Polarization Measurements; Presented at the S.E.G. Annual Meeting, Dallas, Texas.

1974: The IP Phase Measurement and Inductive Coupling; Geophysics, Volume 39, p.650-665.

Hallof, P.G., Cartwright, P.A., and Pelton, W.H.
1979: The Use of the Phoenix IPV-2 Phase IP Receiver for Discrimination Between Sulphides and Graphite; Presented at the S.E.G. Annual Meeting, New Orleans, Louisiana.

Hallof, P.G., and Pelton,, W.H.
1980: The Removal of Inductive Coupling Effects from Spectral IP Data; Presented at the S.E.G. Annual Meeting, Houston, Texas.

Hohmann, G.W.
1973: Electromagnetic Coupling Between Grounded Wires at the Surface of a Two-Layer Earth; Geophysics, Volume 38, p.854.

1975: Three-dimensional Induced Polarization and Electromagnetic Coupling; Geophysics, Volume 40, p.309-324.

1977: Numerical IP Modelling: Induced Polarization for Exploration Geologists and Geophysicists, The University of Arizona, March 14-16, 1977.

Millett, F.B.
1967: Electromagnetic Coupling of Co-linear Dipoles on a Uniform Half-Space; *in* Mining Geophysics, Volume 2, Tulsa, S.E.G.

Ness, N.F.
1957: EM Coupling of Finite Co-Linear Dipoles Over a Uniform Half-space; MIT Computer Centre Report.

1960: EM Coupling of Finite Co-Linear Dipoles Over a Two-Layer Half-Space; Private Report by McPhar Geophysics Limited.

Pelton, W.H., Ward, S.H., Hallof, P.G., Sill, W.R., and Nelson, P.H.
1978: Mineral Discrimination and Removal of Inductive Coupling with Multifrequency IP; Geophysics, Volume 43, p.598-609.

Riordan, J., and Sunde, E.D.
1933: Mutual Impedance of Grounded Wires Lying On or Above the Surface of the Earth; Bell Systems Technical Journal, Volume 12.

Wynn, J.C., and Zonge, K.L.
1975: EM Coupling, Its Intrinsic Value, Its Removal and the Cultural Coupling Problem; Geophysics, Volume 40, p.831-850.

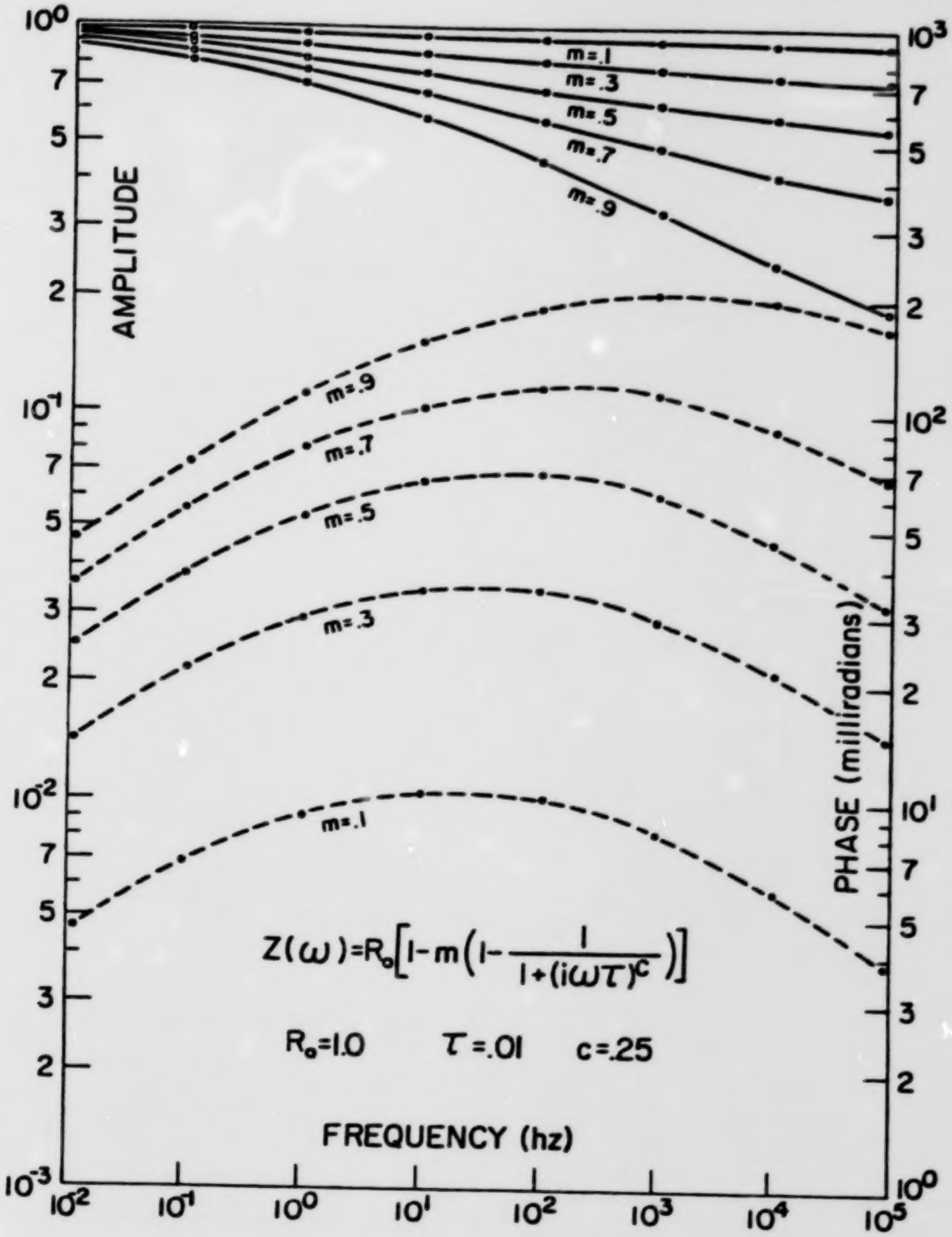

Figure 1. Calculated example for impedence of Cole-Cole dispersion.

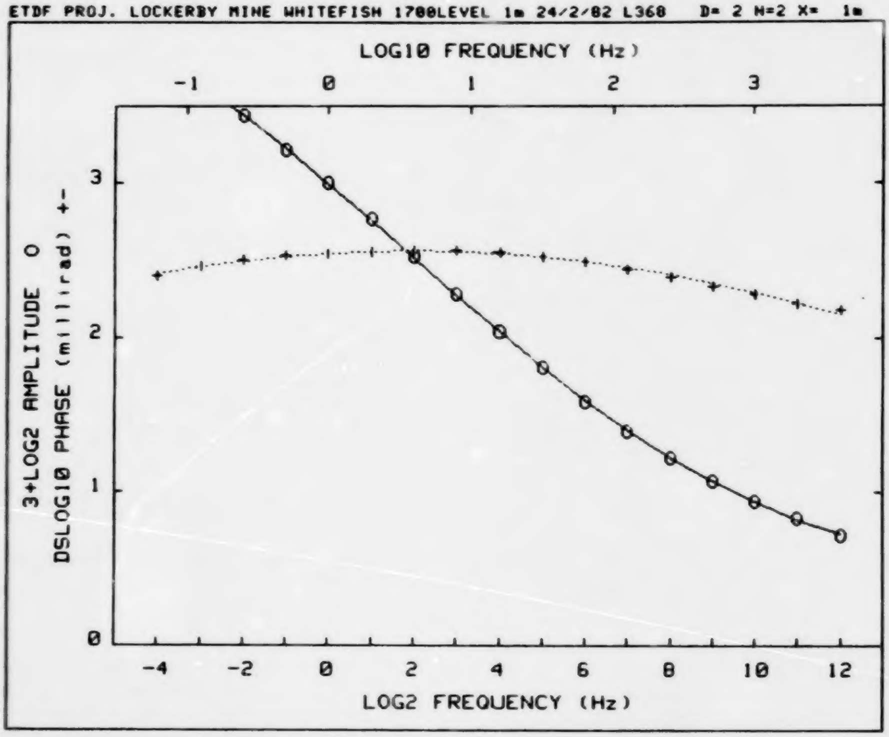

DISSEMINATED NICKEL-COPPER ORE

ETDF PROJ. LOCKERBY MINE WHITEFISH 1700LEVEL 1m 24/2/82 L368   D= 2 N=2 X= 1m

```
CRL:     Number of dispersions= 1

Iter Lambda     Rchsq     R0      M1       T1      C1
  0  1.E-02   .00015  3.298   .952  2.8E+00  .361
  1  1.E-02   .00015  3.298   .952  2.8E+00  .361

Pct Std Deviations        2.9      .2    13.7      .9

Correlation Matrix    1.000
                       .964  1.000
                       .981   .968   1.000
                      -.784  -.878   -.871  1.000

Apparent Resistivity Measured at 1 Hz is 4.660

Apparent Resistivity Calculated from Inductive Coupling is 0.000
```

Figure 2. Diagram illustrating disseminated nickel-copper ore.

```
ETDF PROJ. MATTABI MINE IGNACE550-1040 SILL.DR. 1m 3/82 L373   D= 1 N=1 X=  2m
```

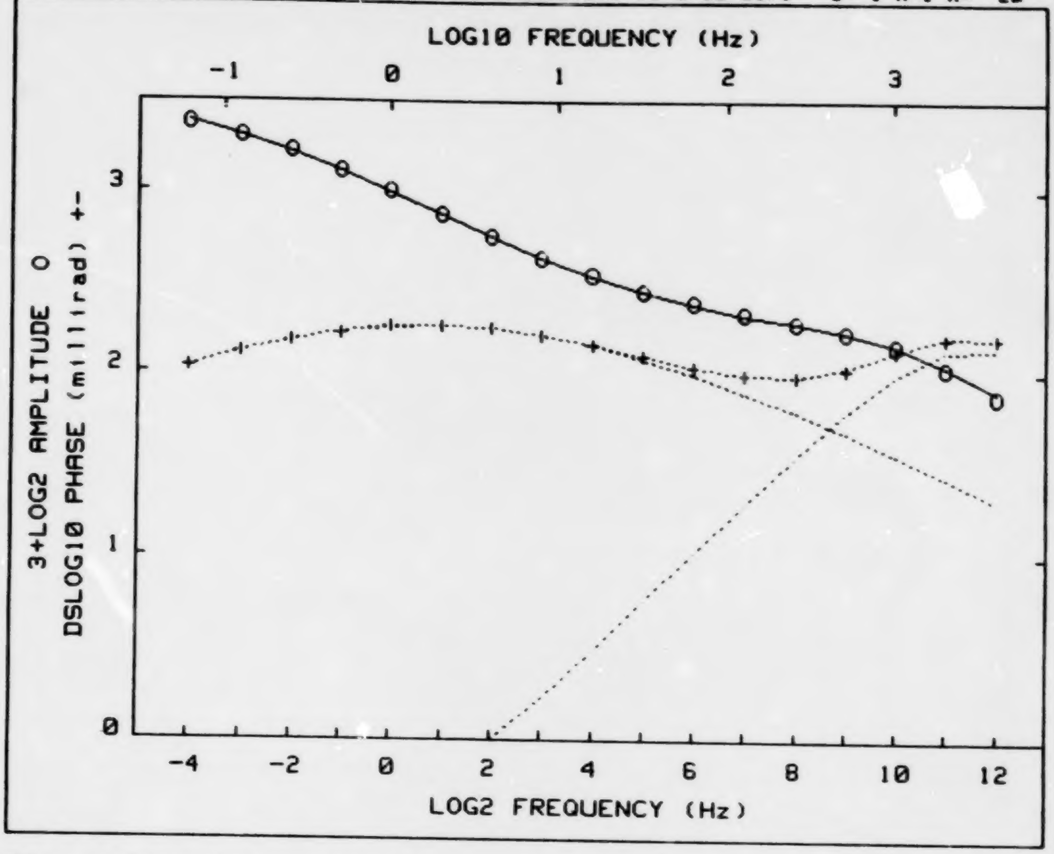

```
CRL:     Number of dispersions= 2

Iter Lambda      Rchsq      R0       M1        T1       C1       M2       T2      C2
  0  1.E-02     .00070   1.477     .612   2.1E-01   .500     .266   8.0E-05 1.000
  1  1.E-02     .00008   1.525     .632   2.6E-01   .453     .276   6.9E-05  .913
  2  1.E-03     .00005   1.544     .637   2.8E-01   .446     .285   6.4E-05  .891
  3  1.E-04     .00005   1.545     .637   2.9E-01   .446     .285   6.4E-05  .892

Pct Std Deviations          .6       .6       3.3      1.2      3.4       3.6     2.5

Correlation Matrix      1.000
                         .882   1.000
                         .858    .630    1.000
                        -.787   -.928    -.622   1.000
                        -.439   -.695    -.160    .655   1.00P
                         .032    .085    -.037   -.056   -.625    1.000
                         .394    .661     .108   -.603   -.938     .579   1.000

Apparent Resistivity Measured at 1 Hz is  .100

Apparent Resistivity Calculated from Inductive Coupling is  .115
```

Figure 3. Diagram illustrating sulphide ore.

MASSIVE ZINC ORE

NORANDA MATTABI MINE ONTARIO AREA-A 1m 15/12/81 L362 D= 6 N=4 X= 1m

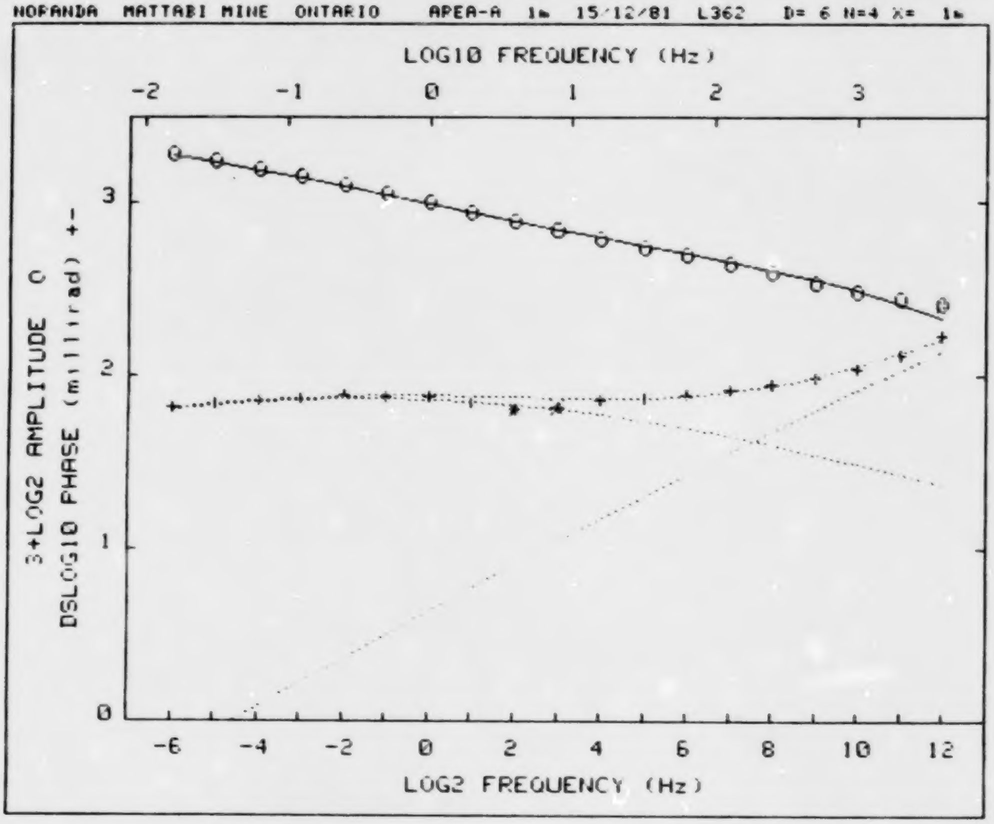

```
CRL:     Number of dispersions= 2
C1=.25     fixed

Iter Lambda    Rchsq     R0     M1      T1      M2      T2      C2
  0  1.E-02   .00024  1.558   .523  3.4E+00  .449  2.7E-06  .407
  1  1.E-02   .00020  1.561   .529  3.0E+00  .444  2.6E-06  .408
  2  1.E-03   .00018  1.544   .531  2.3E+00  .470  2.1E-06  .418
  3  1.E-03   .00017  1.541   .532  2.1E+00  .498  1.7E-06  .420
  4  1.E-03   .00017  1.540   .532  2.1E+00  .522  1.5E-06  .417
  5  1.E-03   .00017  1.540   .532  2.1E+00  .544  1.3E-06  .413

Pct Std Deviations         1.1    2.0     38.3  121.1  1496.2   23.6

Correlation Matrix       1.000
                         -.512  1.000
                          .892  -.814   1.000
                          .531  -.865    .725  1.000
                         -.539   .866   -.729  -.999   1.000
                         -.630   .930   -.829  -.971    .975  1.000

Apparent Resistivity Measured at 1 Hz is 10.04

Apparent Resistivity Calculated from Inductive Coupling is  .127
```

Figure 4. Diagram illustrating massive zinc ore.

MASSIVE ZINC ORE

NORANDA MATTABI MINE ONTARIO AREA-A 1m 15/12/81 L362 D= 6 N=3 X= 1m

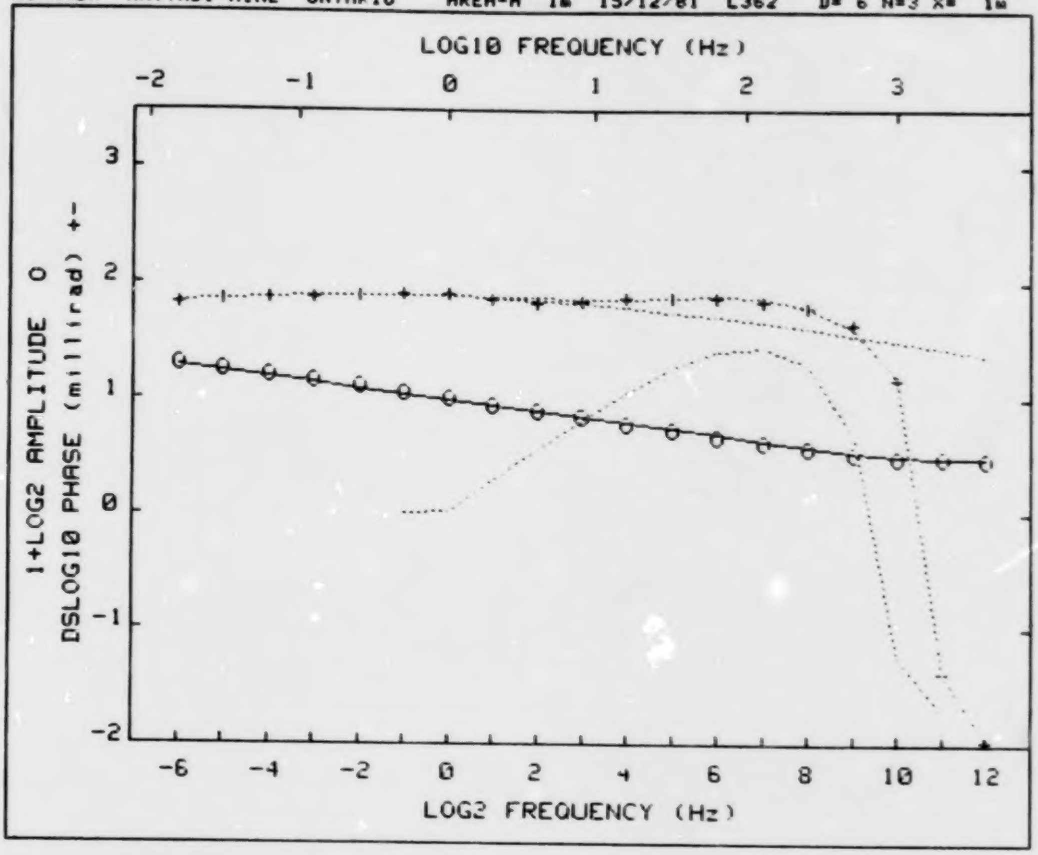

```
CRL:     Number of dispersions= 3   Negative.
C1=.25  M3=1  C3=1     fixed

Iter Lambda    Rchsq    R0     M1      T1     M2      T2     C2      T3
  0  1.E-02  .00031  1.579   .554  2.7E+00  .037  1.5E-03  .853  2.1E-06
  1  1.E-02  .00031  1.579   .554  2.7E+00  .037  1.5E-03  .854  2.1E-06

Pct Std Deviations     1.4    1.0     35.7   18.0    13.0    9.1     2.8

Correlation Matrix    1.000
                       .040  1.000
                       .905  -.337   1.000
                       .650  -.692    .864  1.000
                       .357  -.543    .496   .696   1.000
                      -.533   .582   -.706  -.847   -.655  1.000
                      -.664  -.031   -.639  -.369   -.364   .110   1.000

Apparent Resistivity Measured at 1 Hz is 10.04

Apparent Resistivity Calculated from Inductive Coupling is  .040
```

Figure 5. Another diagram illustrating massive zinc ore.

DISSEMINATED COPPER-ZINC ORE

ETDF PROJ. LYON LAKE MINE 320LVL CREEK ZONE 2m 3/16/82 L372   D= 9 N=3 X= 2m

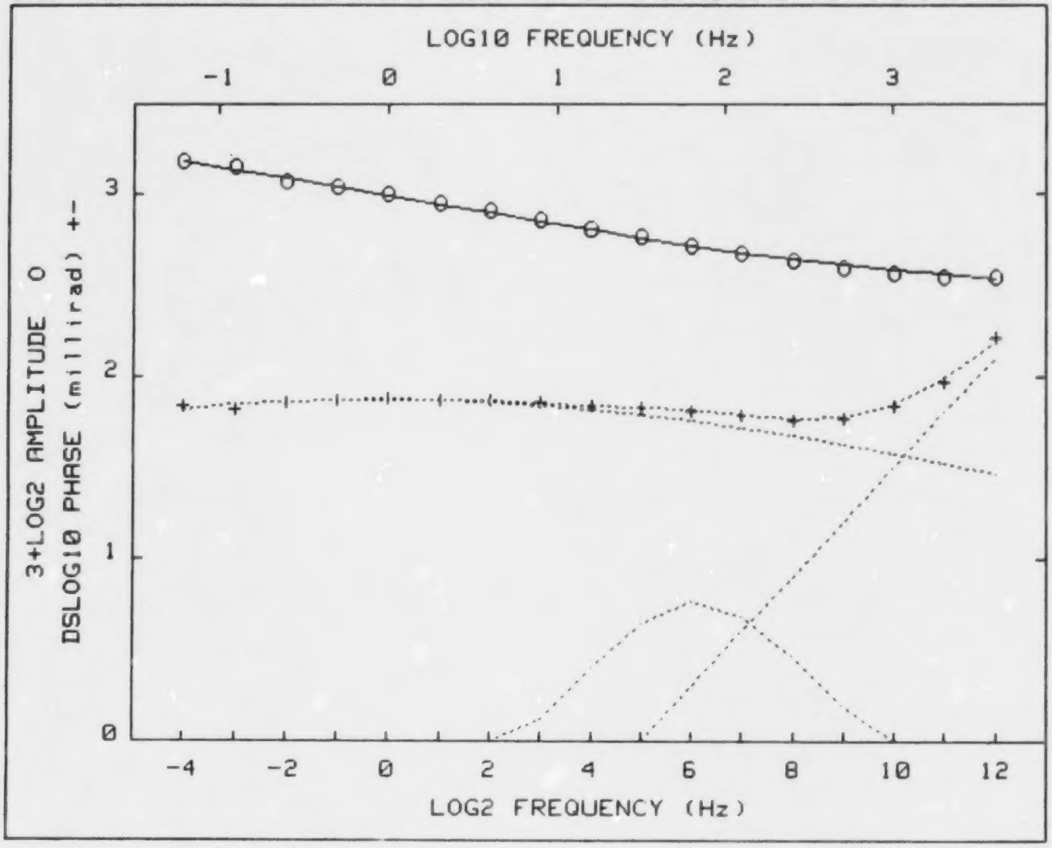

```
CRL:     Number of dispersions= 3
C1=.25   C2=1   C3=1     fixed

Iter Lambda     Rchsq     R0      M1      T1       M2      T2       M3     T3
  0  1.E-02    .00014   1.464    .535  7.6E-01   .011  2.3E-03   .971  5.1E-06
  1  1.E-02    .00014   1.464    .534  7.6E-01   .012  2.3E-03   .983  5.1E-06

Pct Std Deviations         .9      .7    19.4     47.5    37.6     71.0    72.9

Correlation Matrix      1.000
                         .285   1.000
                         .890   -.104   1.000
                         .551   -.527    .778   1.000
                        -.090   -.202   -.057    .055   1.000
                        -.217    .170   -.241   -.161   -.084   1.000
                         .237   -.183    .268    .184    .093   -.999   1.000

Apparent Resistivity Measured at 1 Hz is 5.810

Apparent Resistivity Calculated from Inductive Coupling is 2.962
```

Figure 6. Diagram illustrating disserninated copper-zinc ore.

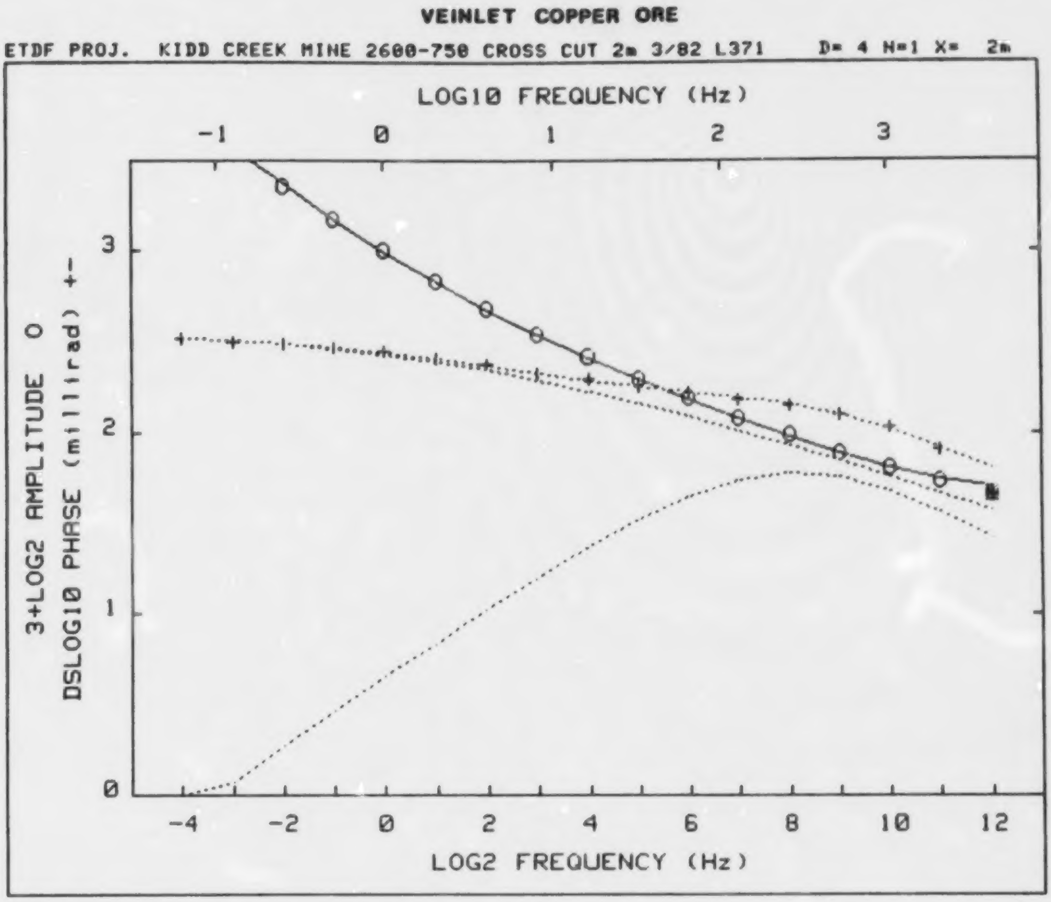

```
CRL:     Number of dispersions= 2

Iter Lambda     Rchsq    R0      M1       T1      C1      M2      T2      C2
  0  1.E-02    .00009  8.208   .944   3.2E+02  .334    .193  6.6E-04  .649
  1  1.E-02    .00008  8.235   .944   3.3E+02  .334    .193  6.6E-04  .649
  2  1.E-02    .00008  8.259   .944   3.3E+02  .334    .192  6.6E-04  .650

Pct Std Deviations     24.6     1.8    184.0     6.3    29.2    18.8    11.1

Correlation Matrix    1.000
                       .990   1.000
                       .996    .996    1.000
                      -.935   -.973    -.960   1.000
                      -.787   -.865    -.822    .934   1.000
                      -.534   -.635    -.572    .727    .883    1.000
                       .652    .740     .685   -.809   -.946    -.873   1.000

Apparent Resistivity Measured at 1 Hz is 9.670

Apparent Resistivity Calculated from Inductive Coupling is  .005
```

Figure 7. Diagram illustrating veinlet copper ore.

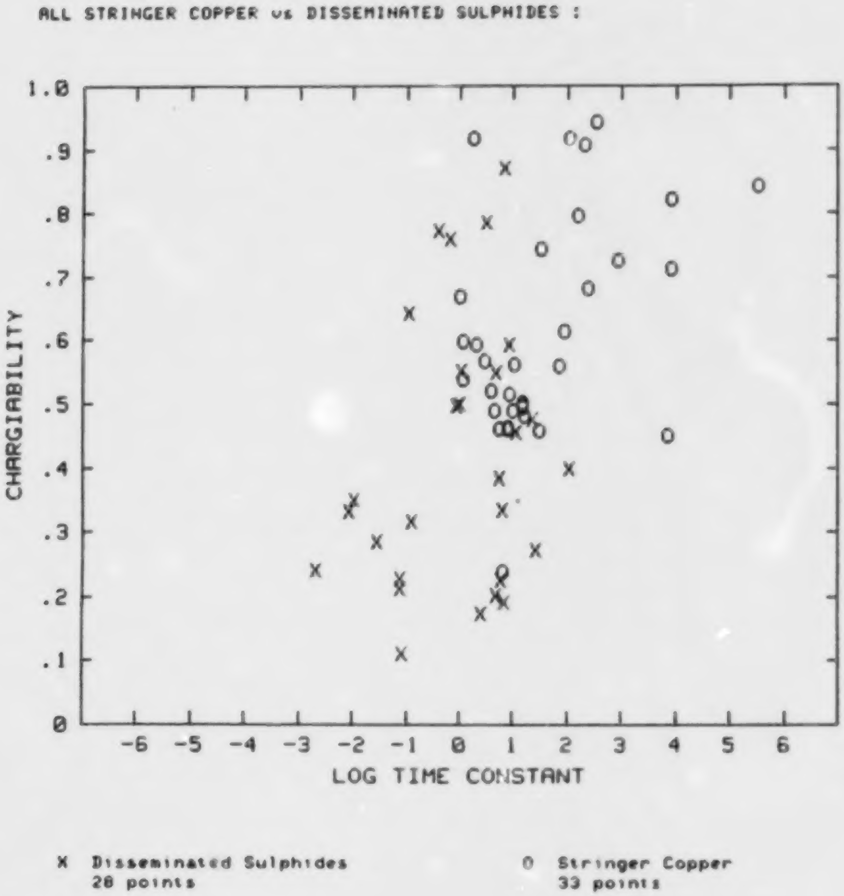

Figure 8. Diagram showing all stringer copper versus disseminated sulphides.

MASSIVE SULPHIDE ORE

```
ETDF PROJ. KIDD CREEK MINE 2600-03FRINGE DRIFT 1m 3/82 L370      D= 1 N=1 X=  1m
```

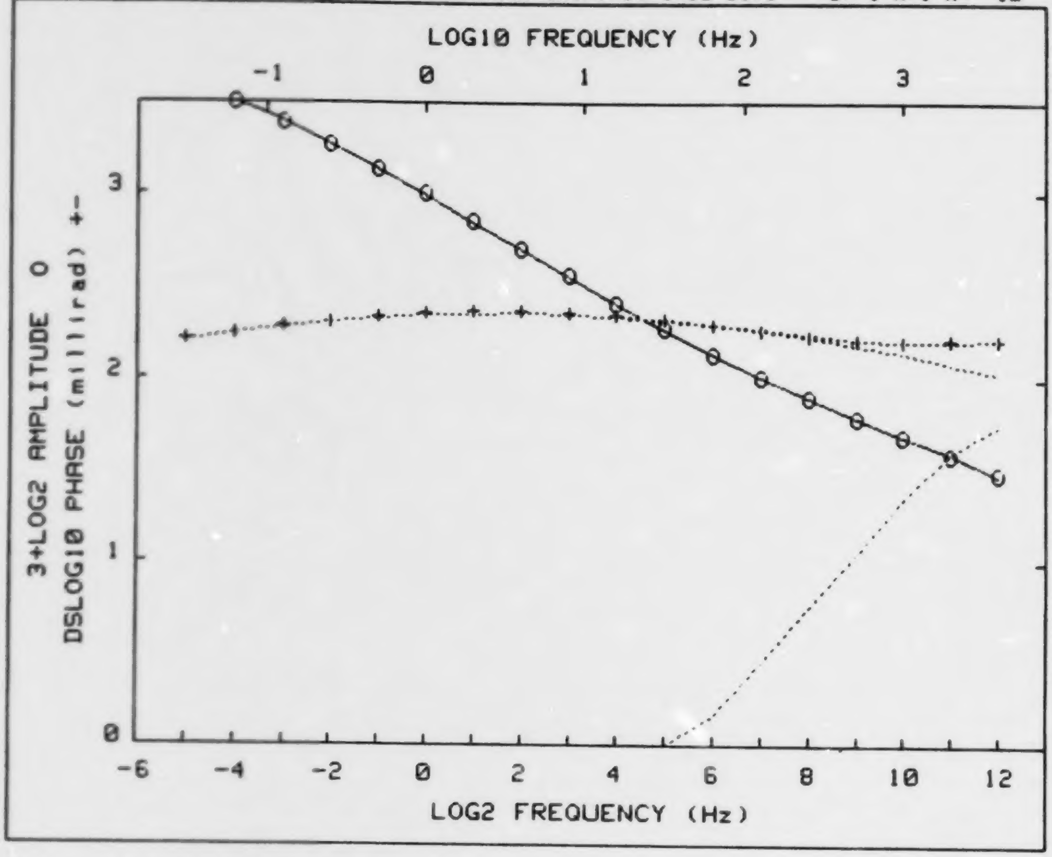

```
CRL:      Number of dispersions= 2
C2=1      fixed

Iter Lambda     Rchsq     R0      M1      T1      C1      M2       T2
  0  1.E-02    .00000   2.451   .887  2.0E+00  .286    .109   3.3E-05
  1  1.E+06    .00000   2.451   .887  2.0E+00  .286    .109   3.3E-05

Pct Std Deviations        1.9      .5    13.7     1.7     8.2     16.4

Correlation Matrix      1.000
                         .933   1.000
                         .990    .914   1.000
                       -.906   -.979   -.909   1.000
                       -.346   -.372   -.347    .402   1.000
                       -.317   -.497   -.281    .447   -.397    1.000

Apparent Resistivity Measured at 1 Hz is 5.280

Apparent Resistivity Calculated from Inductive Coupling is  .210
```

Figure 9. Diagram showing massive sulphide ore.

GRAPHITE ZONE

ETDF PROJ. KIDD CREEK MINE 2600-03FRINGE DRIFT 1m 3/82 L370   D=10 N=1 X= 1m

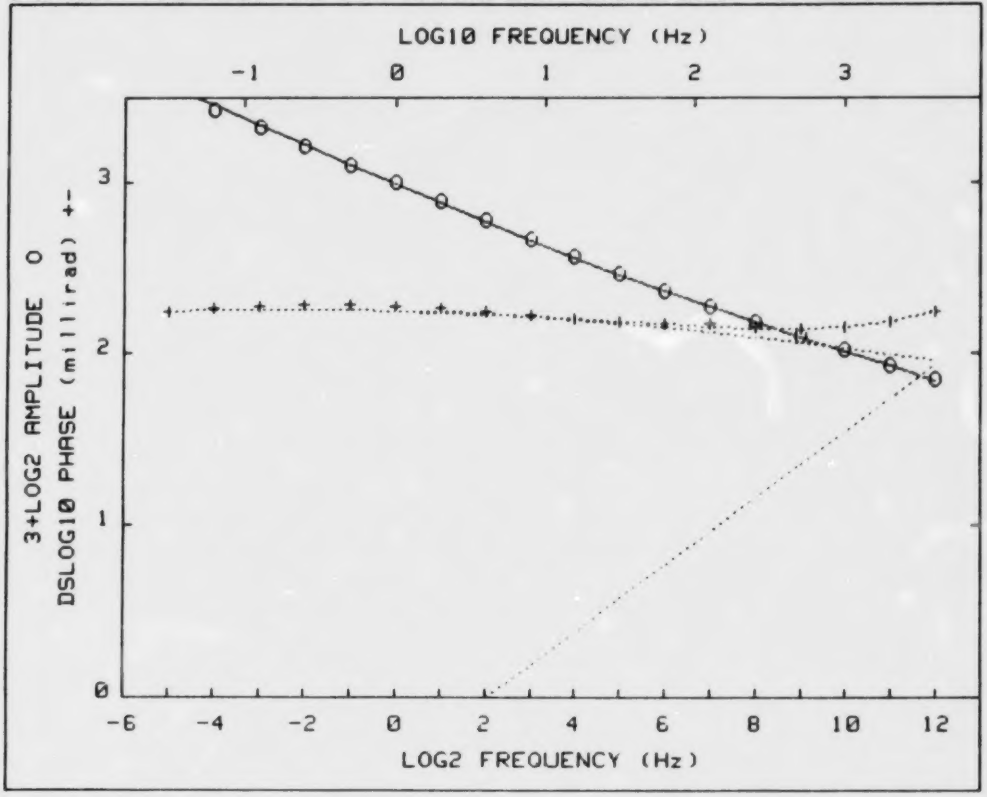

```
CRL:     Number of dispersions= 2
M2=1     fixed

Iter Lambda     Rchsq     R0      M1      T1      C1      T2      C2
  0  1.E-02   .00038   3.842   .911  1.4E+02  .214  1.1E-06  .663
  1  1.E-02   .00026   3.798   .906  1.5E+02  .215  1.1E-06  .600
  2  1.E-03   .00025   3.951   .910  2.1E+02  .212  1.1E-06  .607
  3  1.E-03   .00025   4.089   .915  2.8E+02  .208  1.2E-06  .623
  4  1.E-03   .00025   4.215   .919  3.6E+02  .205  1.2E-06  .639
  5  1.E-03   .00025   4.334   .922  4.6E+02  .203  1.2E-06  .654

Pct Std Deviations       22.5     2.9    474.7    10.3     42.4    22.8

Correlation Matrix      1.000
                         .984   1.000
                         .999    .987    1.000
                        -.965   -.994    -.973   1.000
                         .330    .438     .333   -.445    1.000
                         .652    .762     .659   -.777     .875   1.000

Apparent Resistivity Measured at 1 Hz is 34.25

Apparent Resistivity Calculated from Inductive Coupling is  .125
```

Figure 10. Diagram showing graphite zone.

GRAPHITE ZONE WITH FINE-GRAINED SULPHIDES

```
ETDF PROJ. KIDD CREEK MINE 2600-03FRINGE DRIFT 1m 3/82 L370    D= 3 N=2 X=  1m
```

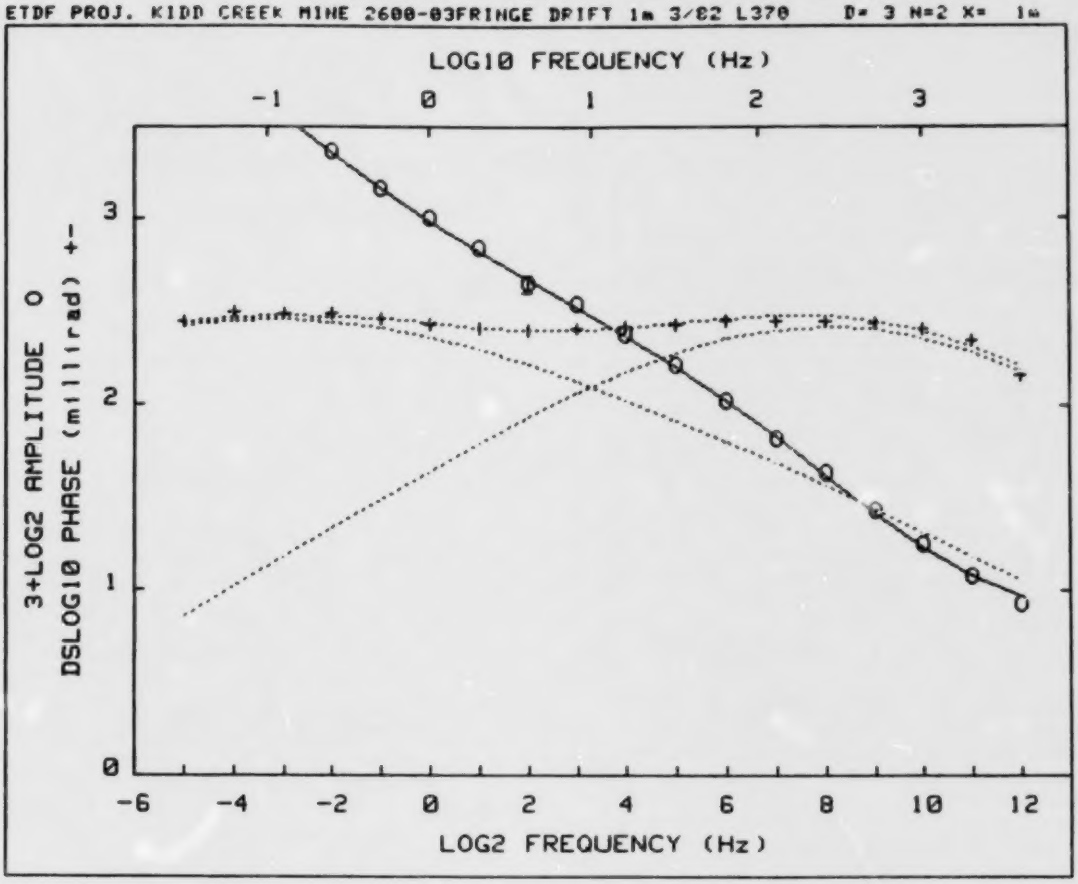

```
CRL:     Number of dispersions= 2

Iter Lambda     Rchsq     R0      M1       T1      C1      M2       T2      C2
  0  1.E-02    .00042  3.637    .814  1.1E+01   .442    .705  1.9E-03   .536
  1  1.E-02    .00041  3.685    .819  1.2E+01   .437    .702  1.8E-03   .538

Pct Std Deviations     13.5     5.3     73.8    10.4     5.2     35.3     5.3

Correlation Matrix    1.000
                       .957   1.000
                       .995    .942    1.000
                      -.938   -.986    -.933   1.000
                      -.754   -.907    -.725    .893   1.000
                      -.726   -.890    -.694    .875    .973    1.000
                       .530    .717     .492   -.674   -.912    -.885   1.000

Apparent Resistivity Measured at 1 Hz is  .180

Apparent Resistivity Calculated from Inductive Coupling is  .000
```

Figure 11. Diagram showing graphite zone with fine-grained sulphides.

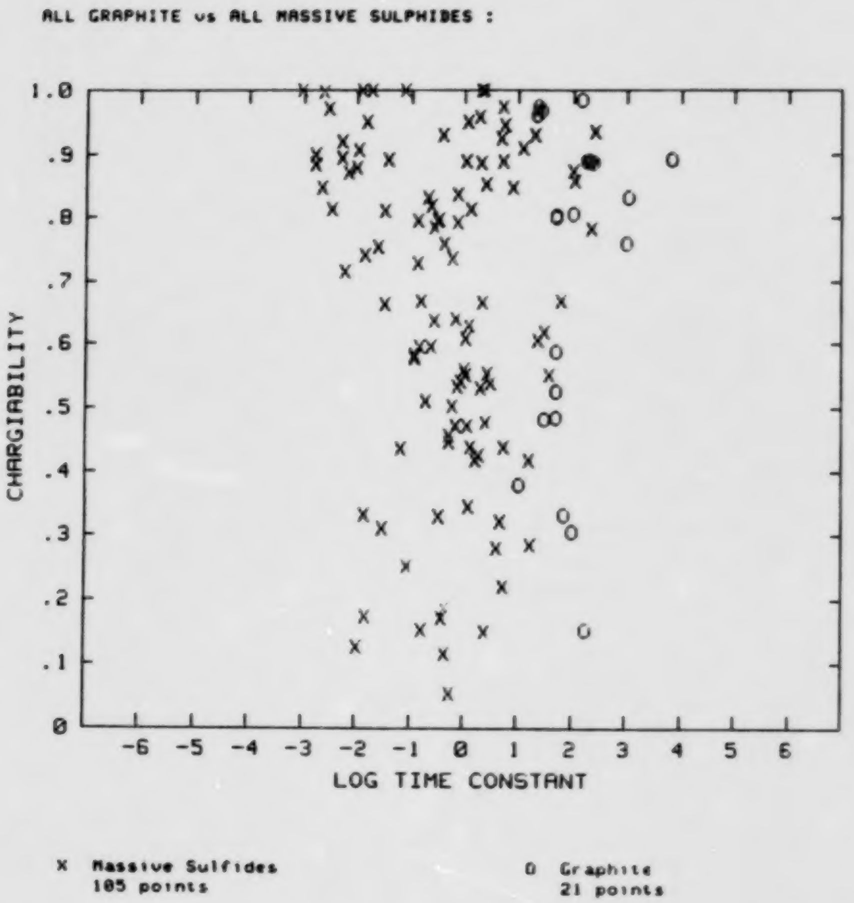

Figure 12. Diagram showing all graphite versus all massive sulphides.

Grant 005 Tin-Tungsten Analysis of Geological Samples Under Field Conditions

J.D. Kinrade and J.C. Robbins
Scintrex Limited, Concord

ABSTRACT

The determination of tin and tungsten in geological samples under field conditions has been divided into 2 areas of research: "in-field" chemistry and "in-field" instrumentation. The analytical technique chosen was molecular fluorescence. Tin was determined as the fluorescent oxine complex and tungsten as the morin complex. Research in the Scintrex Limited laboratory led to the development of a new class of low temperature fluxes designated "FX-2" for tin sample decomposition and "TR-1" for tungsten sample decomposition.

Repeated analyses of 14 samples of widely varying mineral type and tungsten content have indicated promise using the fusion-fluorescence technique. At present, however, tin recoveries from soil and rock samples show poor precision. This is believed to be due to the incorporation of a fraction of the tin in minerals such as biotite, hornblende, muscovite, and garnet which are not readily decomposed.

When considering other possible uses for fluxes TR-1 and FX-2, it was found that a number of other metals and metal oxides could be made soluble by these fluxes. Preliminary work using gold-bearing samples, flux FX-2, and atomic absorption spectrometry showed very good recoveries from samples containing microgram and nanogram quantities of gold.

INTRODUCTION

This project is concerned with the development of in-field methods and equipment for the determination of tin and tungsten in geological materials.

The term "in-field" refers not only to the use of equipment in a bush camp or drill site, but also to locations where the technical services of a modern, well-equipped laboratory may be absent.

Tin and tungsten have been chosen as part of the geochemically important suite of the lithophilic elements, tin, tungsten, molybdenum, (and fluorine). There is considerable interest in these elements both in mineable amounts and as pathfinders to ore deposits.

As so-called "strategic" metals, one could anticipate significant future exploration efforts in North America for both tungsten and tin, especially the latter. A recent compilation of mineral resources (Derry 1980) lists North American reserves of tungsten as 14.8% of world reserves compared to a total of 48.6% for China and the U.S.S.R. combined. There are apparently no significant reserves of tin in North America. Some 55% of world reserves of tin occur in the Far East (Malaysia, Thailand, and so on). Russia and China together account for a further 22.5%.

In Ontario, tungsten and tin have not been mined as primary products. Tungsten was, however, recovered as a by-product of gold mining at the Hollinger Mine in the Timmins area during World War II and tin has been recovered as a by-product of base-metal mining at the Kidd Creek massive sulphide deposit. Some apparently uneconomic tin (cassiterite) showings in veins or greisen were found in northwestern Ontario during the 1920s and 1930s (Mulligan 1974). Tungsten occurrences in Ontario have been found in association with gold mineralization, although at least 1 showing of coarse scheelite in non-auriferous quartz has been recorded (Little 1958). In the Sudbury region, several small deposits of scheelite in quartz-carbonate veins associated with Nipissing Diabase are known (Card 1976).

The Fostung Prospect in Foster Township, southeast of Espanola, consists of a number of mineralized skarns in the Espanola Formation near intensely altered gabbroic intrusions. Scheelite is the principal economic mineral ranging from trace amounts to 0.38% W, although powellite and various sulphide rocks are also present (Union Carbide Exploration Company 1978; Wright 1979).

Determinations of tin and tungsten at trace levels in soils, stream sediments, and other similar deposits are used as guides to prospecting for economic concentrations. Lithogeochemical studies applied to exploration have shown that tin is one of the very few trace elements that, on a regional scale, is enriched in intrusive rocks in many parts of the world. Tin-bearing granites typically may contain 20 to 30 ppm Sn compared to "barren" granites which carry less than 5 ppm Sn (Govett and Nicol 1979; Juniper and Kleeman 1979). Conversely, although mean tungsten values may not be high, the form of the frequency distribution may be significant. Distribution of tungsten in "barren" plutons is only slightly skewed, but the distribution in so-called "mineralized" plutons has a more marked, positive skew (Garrett 1971).

As a possible pathfinder to other metals, it has been noted that tungsten is widely associated with both gold-quartz mineralization (Boyle 1979, p.155-156) and disseminated (Carlin-type) gold mineralization (Radtke *et al.* 1972). The enrichment of tungsten at the Dickenson Mine, northwest Ontario, is 100-times background. Kerrich (1980) stated "The higher ambient temperatures of hydrothermal gold systems compared to submarine geothermal convection may promote aqueous transport of relatively insoluble metals. The extent of enrichment of W, Cr, Ni, and Pd for lode gold deposits is much greater than is typical for massive base-metal sulpides".

Both scheelite and cassiterite have high specific gravities, and are chemically resistant minerals. Scheelite is considerably more friable than cassiterite and infrequently forms economic placer deposits, but both minerals can be expected to form significant dispersion trains in stream sediments, and under favourable conditions in other mechanically dispersed mineral trains, for instance in basal till.

Table 1 (Rosler and Lange 1972) presents the elemental abundances of tin and tungsten. Examination of these data reveals that an analytical method is required which has a detection limit of at least 1 microgram/gram for tin or tungsten in a sample. This requirement must be viewed in light of the sensitivity available from methods in common usage by service laboratories (E. Brooker, President, X-ray Assay Laboratories, personal communication, 1982). Three techniques are routinely available for the determination of tin; these are x-ray fluorescence (XRF), spark or arc emission spectroscopy, and plasma emission spectroscopy. X-ray fluorescence has the advantage of using a solid sample for analysis, but suffers from poor sensitivity (the detection limit is approximately 100 μg/g). Arc or spark emission spectroscopy again uses a solid sample and has a more reasonable detection limit of 3 μg/g. This technique, however, only uses 10 mg of sample per analysis. As a result, sample inhomogeneity is a problem. Plasma emission spectroscopy has a detection limit of approximately 20 μg/g for tin. Prior to the plasma emission analysis, a metaborate fusion is performed on the sample. Two techniques are commonly used for tungsten analysis, x-ray fluorescence and neutron activation. Again, XRF suffers from poor sensitivity (approximate detection limit 100 μg/g). Neutron activation has good sensitivity (approximate detection limit 1 μg/g), but the instrumentation is not readily available.

IN-FIELD CHEMISTRY

The analytical techniques just cited, except for plasma emission spectroscopy, are frequently used with solid samples. Better sensitivity requires some form of sample decomposition.

There are 2 main choices for sample decomposition, acid attack or fusion. In general, a vigorous acid attack lends itself more to laboratory rather than field usage since large volumes of acid are commonly used, and often specialized containers are required. These procedures then become both tedious and time-consuming. Various examples from the literature are presented in Table 2.

TABLE 1: ELEMENTAL ABUNDANCES OF TIN AND TUNGSTEN.

Material	**Tin**	**Tungsten**
Ultramafic rocks	0.5 μg/g	0.1 μg/g
Mafic rocks	1.5	0.7
Granitic (high Ca) rocks	1.5	1.0
Granitic (low Ca) rocks	3.0	1.5
Syenitic rocks	–	1.3
Lithosphere	2.5	1.3
Shales	10.0	2.0
Sandstones	–	1.6
Carbonates	–	1.6
Seawater	0.0003	0.0001

TABLE 2: ACID DECOMPOSITION OF SOLID SAMPLES.

Tin

a) HC1, 250°C, 24 hours (Wichers 1944).

b) H1, sealed under nitrogen, 110°C, 20 minutes (Phillips 1960).

c) HC1-HF-H_2O_2, sealed teflon container, 24 hours, anion exchange, solvent extraction, colorimetric determination, sensitivity 0.1 μg/g (Smith 1971).

Tungsten

a) HC1-HNO_3, 5 hours (Scott 1928).

b) HNO_3-HF, teflon container (Quin 1973).

c) HF-HNO_3-$KC10_4$, platinum dish (Bottei 1968).

d) HF-$HClO_4$, 24 hours, 2 extractions, isotope dilution analysis, sensitivity 2 μg/g (Lillie 1973).

The alternative to acid attack is fusion of the sample with an inorganic salt, a flux which melts at a reasonable temperature, and yet is capable of a vigorous chemical attack on the sample. Existing fusion procedures, however, suffer from a number of shortcomings which include the use of toxic and/or corrosive chemicals, the common requirement for expensive containers (for example, platinum, zirconium, silver) and, frequently, the requirement for high temperatures. Table 3 lists some of the fusion procedures which have been used.

All of these earlier developed methods, both fusion and acid decomposition followed by analytical measurement, tended to be very time-consuming and involved multiple chemical steps before the final determination could be performed. Much of the earlier work also was carried out on samples having reasonably simple matrices (for example, ores, concentrates, alloys (Sprenz and Prager 1981; Capacho-Delgado and Manning 1965; Sattur 1966), whereas a practising laboratory encounters much more varied and complex samples. The earlier works also make no mention as to the form of the metal in geological samples. For example, did the tin occur in discrete minerals and, if so, in which minerals (cassiterite, stannite, malayaite and so on) or was the tin lattice-bound?

The Scintrex Limited laboratory often encountered poor recoveries and various matrix problems when employing the published methods, for example, the popular ammonium iodide sublimation method for tin (Bowman 1968; Yim 1979; Bond *et al.* 1970). This particular method was found to be usable, though precision tended to be poor. The sublimation readily decomposed cassiterite, but proved quite ineffective for samples having lattice-bound tin. To further complicate the use of this method, near the latter part of 1980, problems arose with the supply and quality of ammonium iodide. The price of the salt increased about tenfold and the available material was found to be contaminated with some constituent (insoluble organic (?) material) which would, after sublimation, strongly adsorb tin in the subsequent aqueous solution. All attempts to purify or synthesize a better grade of ammonium iodide failed. These problems catalyzed the search for a more dependable method.

Since the goal of this investigation was "in-field" methodology, research was directed towards developing low temperature and reasonably neutral fluxes, which would readily decompose samples of varying geological composition, and would be safe to handle and transport. To date, the end result of this study has been the generation of a number of hitherto unreported 2-, 3-, and 4-component powder fluxes and an extraction-fluorescence analytical method.

The procedure developed for the determination of tin is as follows:

> A 0.5 g sample, or more if desired, is mixed with 5 g of flux FX-2, placed in a glass test tube and heated for 5 minutes, either individually over a propane flame, or in a batch with an electric heater. The tube is then allowed to cool, 25 ml of an acetate buffer (0.3% v/v acetic acid) are added and the pH is adjusted to 1.7. Five ml of a butylacetate-oxine solution (1% w/v oxine in butylacetate) are added, and the tube is shaken for 2 minutes. The butylacetate phase is backwashed for 30 seconds with a pH 1.5 acetate buffer solution (0.3% v/v acetic acid) to remove any co-extracted complexes of elements which interfere with the determination. Finally, the fluorescence of the butylacetate layer is measured (excitation 372 nm, emission 525 nm).

The procedure for the determination of tungsten is as follows:

> A 0.5 g sample is mixed with 5 g of flux TR-1, placed in a glass test tube and heated for 5 minutes. The tube is allowed to cool, 25 ml of buffer solution (0.3% v/v acetic acid, 0.3% v/v phosphoric acid, 0.02% w/v sodium fluoride) are added, and the pH is adjusted to 4.4. One ml of morin solution (0.18 g in 100 ml acetone) and 5 ml of heptane are added and the tube is shaken for 1 minute. The fluorescence of the aqueous phase is measured (excitation 417 nm, emission 500 nm).

TABLE 3: FLUX DECOMPOSITION OF SOLID SAMPLES.

Tin

a) NaF-H_3BO_3, platinum crucible, polarographic determination, sensitivity 10 μg/g (Bond 1970).
b) KCN, clay crucible (Scott 1928).
c) Na_2O_2, nickel crucible (Scott 1928).
d) Na_2O_2-NaOH, nickel crucible (Holtje 1937).

Tungsten

a) KOH, silver crucible, 450°C (Sajo 1955).
b) Na_2O_2, silver crucible (Hempel 1893).
c) $Ba(NO_3)_2$, tetraborate, 1200°C (Harris 1979).
d) Na_2CO_3, platinum crucible, 880°C (Sprenz 1981).
e) NaOH-Na_2O_2, platinum crucible (Vajda 1971).

DETAILED DEVELOPMENT OF THE CHEMICAL PROCEDURE

FUSION

TIN

Tin, in the absence of complexing agents, is only stable in aqueous solutions at a pH <2 or >9 (Smith 1971). Therefore, a very acid or very basic flux is required to render tin compounds water soluble.

Initially, basic fluxes were applied to tin-bearing samples. Two problems arose. First, glassware could not be used to carry out the fusion as it was attacked by the flux. Iron crucibles were found to be satisfactory, with minimal attack on the crucible. The second more serious problem was associated with the acidification of the strongly basic solution resulting from the fusion. As will be described later, this acidification was necessary since an extraction at pH 2 was carried out just prior to the fluorescence measurement. On acidifying the basic solution, it passed through the SnO_2 stability field (Pourbaix 1968) with the concomitant precipitation of the tin. As a result of these problems, an acid flux was sought. The acid fluxes reported in the literature (for example, bisulfate, pyrosulfate, borax (Scott 1928; Skoog and West 1969; Willard *et al.* 1956)) failed to dissolve tin ore. Therefore, research was conducted on a new generation of acid fluxes, the end result being a flux designated FX-2.

TUNGSTEN

Tungsten in the absence of complexing agents, is only soluble in aqueous solutions having a pH greater than approximately 4 (Pourbaix 1968). Therefore, any flux should be neutral to slightly basic, not so basic that it would attack the glass container. Tungsten commonly occurs in skarn deposits, in which carbonate may be abundant. The carbonate can disrupt the properties of any given flux since carbonate is a high melting point, strong basic flux (Scott 1928; Skoog and West 1969; Willard *et al.* 1956). Research work resulted in the development of a new neutral flux (TR-1) with a high buffering capacity for any carbonate present in the sample.

EXTRACTION - FLUORESCENCE

The tin and tungsten were brought into solution for the subsequent determination. The molecular fluorescence technique was chosen; it offers good sensitivity and reasonable (although by no means complete) freedom from interference. The equipment and technique also can be readily used in the field. The equipment can be built to be portable, rugged, and practical. Fluorimetric methods for tin (Pal and Ryan 1969) and tungsten are described in the literature (Kirkbright *et al.* 1966). Pal and Ryan (1969) reported the use of 8-hydroxyquinoline-5-sulphonic acid to form a fluorescent complex with tin. This method was evaluated as part of a joint development program with A.B.P. Lever at York University who found considerable difficulty with high background fluorescent levels in the reagent even after repeated steps of re-purification. The use of carminic acid by Kirkbright *et al.* (1966) for tungsten was found to be only marginally sensitive for the geological applications considered.

A more satisfactory method was developed using the extraction of tin as the fluorescent oxinate and the formation of the fluorescent tungsten-morin complex.

TIN

Oxine is well known to be a fluorescent reagent and the tendency to form fluorescent compounds is greater for the parent oxine molecule than for its derivatives such as 8-hydroxyquinoline-5-sulphonic acid (Zolotov 1970). Earlier methods had been developed for the extraction of tin with oxine (Eberle and Lerner 1962; Amano 1960; Stary 1963); however, these procedures were not found to have been optimized. Given the present experimental conditions (geological sample, flux matrix, etc.), the optimal conditions for the extraction and fluorescence analysis were determined. Figure 1 shows the excitation and emission spectra for oxine, tin oxinate, and tungsten oxinate.

The optimum pH range for extraction of tin was found to be 1.4 to 1.8. A linear fluorescence response is obtained for tin concentrations up to 400 ng/ml with a corresponding detection limit of 1 ng/ml tin in solution.

At present, no other cations have been found to interfere with the determination of tin.

Table 4 summarizes the results for the analysis of some tin-bearing samples. The scatter in the results was probably due to the capacity of such minerals as biotite, hornblende, muscovite, and garnet to incorporate extraneous ions such as tin in their structures. The tin could replace any or all of the following: Mg, Fe(II), Fe(III), Ti, Al, Mn, and Li (Flinter 1971; Hesp 1971; Mulligan and Jambor 1968; McIver and Mihalik 1975). In turn, these minerals are not readily decomposed.

Research in the laboratory has indicated that the so-called total decomposition methods recommended in the literature using acid digestion of tin-bearing samples are also not effective. In the past, workers have used hydrofluoric acid-sulphuric acid (Agterdenbos and Vlogtman 1972; Huffman and Bartel 1964), perchloric-nitric-hydrofluoric (Terashima 1982) and hydrochloric-hydrofluoric acids (Smith 1971). Open teflon beakers and closed polyethylene bottles that contained various acid and acid-salt combinations (sulphuric-hydrofluoric, sulphuric-hydrofluoric-hydrochloric, sulphuric-hydrofluoric-nitric, sulphuric-hydrofluoric-potassium persulphate and sulphuric-hydrofluoric-nitric-sodium bromide) were employed by the authors in the Scintrex Limited laboratory. The recovery of tin from both samples and reagent grade tin oxide was very poor.

TUNGSTEN

Initial work with tungsten also made use of the fluorescent reagent oxine. The excitation and emission spectra for

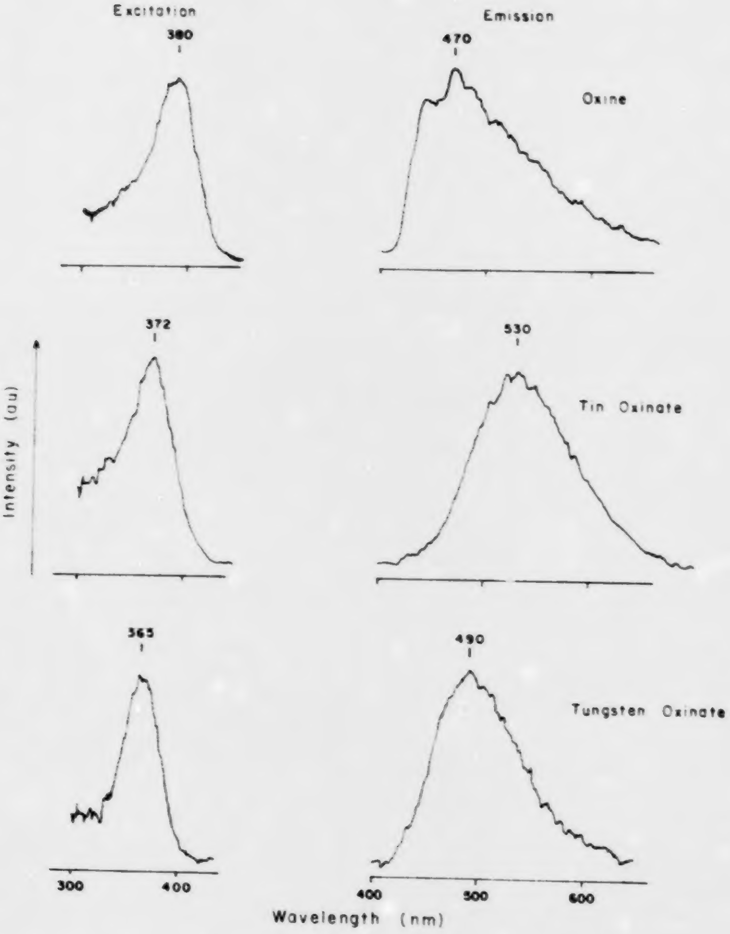

Figure 1. Excitation and emission spectra for oxine, tin oxinate, and tungsten oxinate.

TABLE 4: TIN IN GEOLOGICAL SAMPLES.

Sample	XRF	Fusion-Fluorescence	% Recovery
GC-1 (skarn)	20 μg/g	11, 11 μg/g	55
HM-2 (skarn)	20	7, 6, 5, 11	36
LM-5 (quartzite)	40	59, 57, 41, 41	124
2942 (soil)	74	108	146
JB-3 (skarn)	80	89, 94	114
BC-4 (skarn)	80	85, 91	110
BC-5 (skarn)	80	85, 76, 113, 76, 74	106
JB-1 (skarn)	100	92, 97	95
1658 (silt)	112	52	46
5158 (soil)	129	208	161
BC-7 (skarn)	140	104, 97, 97	72
JB-2 (skarn)	160	114, 122	74
5149 (soil)	229	243, 160, 154, 145, 153	75
4318 (soil)	447	104	23
24448 (greisen)	600	321, 178, 168	37
BC-6 (skarn)	600	291, 262, 305, 344, 318	51
24465 (greisen)	700	183	26
4326 (soil)	767	138	18
24463 (greisen)	1900	381, 489, 660	27
24460 (greisen)	2600	916, 442, 532	24
24449 (greisen)	3600	767	21

TABLE 5: TUNGSTEN IN GEOLOGICAL SAMPLES.

Sample	XRF	Fusion-Fluorescence	% Recovery
Fluorescent Reagent: Oxine			
BC-5 (skarn)	430 μg/g	540, 456 μg/g	116
BC-4 (skarn)	630	524, 552	85
PSK-1 (pyrrhotite)	950	1137	120
JB-1 (skarn)	1030	1030	100
JB-3 (skarn)	1400	1090	76
TB-1 (skarn)	2400	2556	107
JB-2 (skarn)	4400	4600	105
Fluorescent Reagent: Morin			
BC-1 (skarn)	8	7	88
BC-2 (skarn)	13	13	100
V11-1 (quartzite)	13	10	77
PM1-5 (mudstone)	14	8	57
PM1-2 (skarn)	20	11	55
HM-1 (skarn)	99	78	79
PSK-1 (pyrrhotite)	950	313	33
JB-1 (skarn)	1030	719	70
JB-3 (skarn)	1400	984	70

oxine and tungsten oxinate are shown in Figure 1. The sensitivity of this system (approximately 250 ng/ml tungsten in solution), however, left much to be desired. As a result, energies were directed towards finding a reagent producing a more fluorescent tungsten complex. A.B.P. Lever at York University conducted preliminary research on the reagent morin (3, 5, 7, 2', 4' pentahydroxyflavone) and since this reagent showed some promise, further study was carried out.

Experimentally, it was found that the optimum technique for measuring the fluorescence was to add 1 ml of a morin-acetone solution (0.18 g morin in 100 ml acetone) to 25 ml of sample solution buffered with acetic-phosphoric acid (0.3% v/v acetic acid and 0.3% v/v phosphoric acid) and adjusted to pH 4.4. The excitation and emission spectra for the tungsten-morin complex are shown in Figure 2.

A linear response was obtained for tungsten concentrations up to approximately 250 ng/ml with a corresponding detection limit of 1 ng/ml tungsten in solution.

Several ions were found to interfere with the tungsten-morin fluorescence; however, with the exception of molybdenum, the effect of these ions could be eliminated. Tin (IV) and zirconium (IV) were masked by the phosphate in the

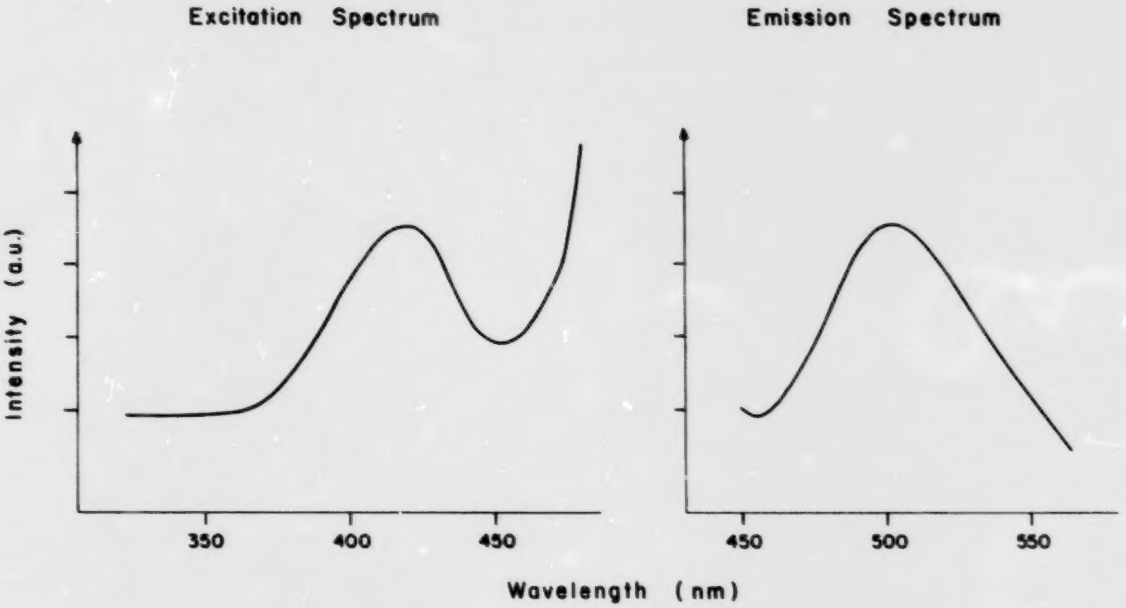

Figure 2. Excitation and emission spectra for the tungstenmorin complex.

buffer. Iron (III) and copper (II) were found to produce strongly absorbing morin complexes, but these could be separated from the tungsten by extracting with 5 ml of heptane. Aluminium (III) produces an absorbing morin complex, however, flux TR-1 had little effect on aluminium compounds and therefore the effect of any aluminium in a sample was found to be negligible. Fluoride was found to be effective in suppressing low levels of aluminium ion, and, therefore to allow for any traces of aluminium (III) in the sample solution, the buffer was modified to contain 0.3% acetic acid, 0.3% phosphoric acid, and 0.02% sodium fluoride.

Molybdenum (VI) was found to form a strongly absorbing morin complex. The absorbance of this complex is linear up to 4000 ng/ml with a corresponding detection limit of 10 ng/ml molybdenum in solution. All attempts to mask or separate molybdenum from tungsten failed.

Figure 3 shows the effect of varying amounts of molybdenum on 100, 150, 200, and 250 ng/ml quantities of tungsten. Given that tungsten fluoresces and molybdenum absorbs, there exists the possibility that molybdenum could also be determined in geological samples. Tungsten appears to be the only interferent on molybdenum. Figure 4 shows the effect of varying concentrations of tungsten on molybdenum absorbance.

At present, it may not be chemically possible to separate molybdenum from tungsten, however, it may be possible mathematically. Figures 3 and 4 represent 2 equations for 2 families of spectral lines; absorbance and fluorescence are read from the instrument and the unknown concentrations of tungsten and molybdenum (2 equations with 2 unknowns) can be calculated.

Table 5 summarizes the results for the analysis of some tungsten-bearing samples using flux TR-1 for sample decomposition and either oxine or morin as the fluorescent reagent. These results indicate that the fusion-fluorescence method for tungsten has promise. Further sample analyses will be required to verify this.

METAL UPTAKE BY FLUX TR-1 AND FX-2

To date, most of the work on the fluxes has been with respect to tin and tungsten. Table 6 lists some preliminary measurements on the uptake of various tungsten compounds and other metal oxides. The acid flux FX-2 was also found to readily dissolve platinum and gold and the minerals ilmenite ($FeTiO_3$) and chromite ($(Mg,Fe)\ Cr_2O_4$). This preliminary work thus indicates that the fluxes may also be used for the decomposition of samples which are to be analyzed for metals other than just tin and tungsten. Some work was conducted on gold-bearing samples using flux FX-2 and the Scintrex atomic absorption spectrophotometer AAZ-2. Table 7 lists some of the experimental results obtained from the fusion-atomic absorption results. Comparing these values with those obtained by other laboratories and/or methods, a reasonably good agreement is found. Note also that only 1 g of sample was used for the fusions, while all other work was conducted with 10 to 25 g of sample.

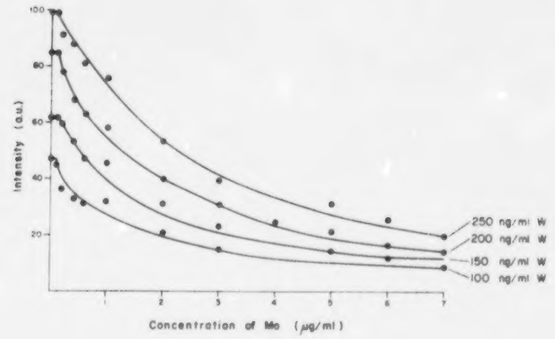

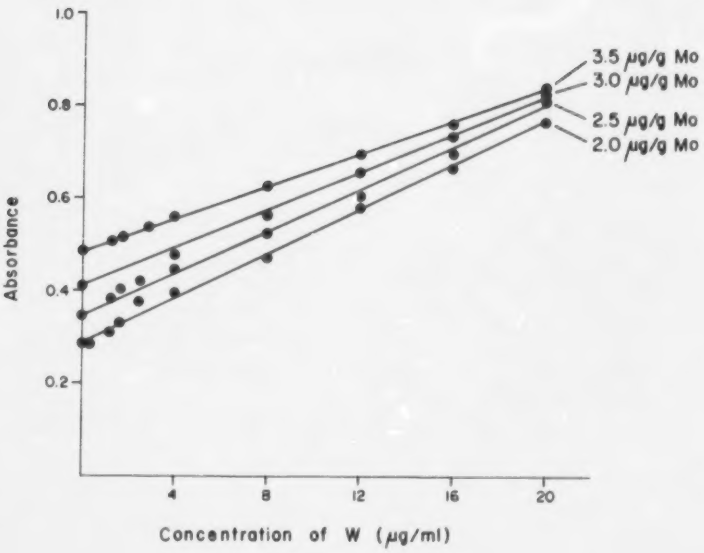

Figure 4. Effect of varying amounts of tungsten on the absorbance of given amounts of molybdenum.

TABLE 6: SOLUBILITY OF METAL COMPOUNDS IN FLUXES.

Metal Compound	Weight Taken Up By 3 g Flux
Flux FX-2	
ZrO_2	200–300 mg
TiO_2	200–300
CuO	500
Nb_2O_5	200
Ta_2O_5	50–100
Flux TR-1	
W	> 7500
WO_3	> 7500
$CaWO_4$	> 1600
MoO_3	> 13 500
Al_2O_3	not detectable

TABLE 7: GOLD ANALYSES METHODS COMPARISON.

Sample	X-Ray Assay F.A. Plasma	T.S.L. F.A. A.A.	Hot Bromine Solvent Extraction AAZ-2	Bondar and Clegg F.A. A.A.	Fusion–AAZ-2
	ppm	ppm	ppm		ppm
B122989–Tailings			1.2		0.98
B123033–Tailings			14.7		11.5
23163–Gossan		6.8	10.0		6.3
23119–Gossan		3.4	4.9		4.0
23154–Gossan		6.9	12.6		11.4, 12.6
3305–Rock pulp (ID.?)	5.0	4.4	3.9		5.3
3301–Rock pulp (ID.?)	2.7	1.7	3.1		1.6
3309–Rock pulp (ID.?)	2.9	1.7	1.6		2.8
	ppb	ppb	ppb	ppb	ppb
3389–Rock pulp (ID.?)	140	170	158		201
3385–Rock pulp (ID.?)	380	350	355		428
RL-1–Massive Sulfide		280–320			342
UM-1–Ultramafic				65/50	79
UM-3–Ultramafic				205	158
					ppm
3305	(5.0)	(4.4)	(3.9)		5.6
Test of					5.3
homogeneity:					6.0
6 fusions using					5.7
1 gram of					5.1
sample each					5.9
time					

Abbreviations

F.A.:	Fire Assay
A.A.:	Atomic Absorption Spectrometry
T.S.L.:	Technical Service Laboratories

IN-FIELD INSTRUMENTATION

The fluorometer constructed for making high sensitivity tin and tungsten measurements consisted of a modulated mercury discharge lamp in combination with a sample cuvette and photomultiplier combination.

The mercury lamp used was a phosphor-coated type in which the primary 237 nm radiation is converted by the phosphor to an emission band at 365 nm. The modulation frequency was approximately 5 kHz.

The light was focussed on the cuvette, the fluorescence being observed at right angles by a 6199 end-on photomultiplier to be isolated by a liquid filter (potassium dichromate) to reduce scattered ultraviolet.

The signal from the photomultiplier tube was amplified and "synchronously detected" using a Princeton Applied Research lock-in amplifier model HR-8. Since the radiative lifetime of the organic complexes measured was extemely short, no attempt to measure out-of-phase components was made.

SUMMARY

The present research program has been concerned with the development of in-field methods and equipment for the determination of tin and tungsten in geological materials.

The analytical technique chosen for the measurement of these metals was molecular fluorescence. Tin was determined as the fluorescent oxine complex and tungsten as a morin complex. In order to render the tin and tungsten water soluble and thus available for analysis, fusion was chosen as the most appropriate in-field means of decomposing geological material. Existing fusion procedures were found to suffer from a number of shortcomings and therefore research was directed towards developing a new class of low melting point fluxes. As a result of the difference in chemistry of tin and tungsten, it was found necessary to develop 2 different fluxes, 1 for tin (FX-2), and 1 for tungsten (TR-1).

The procedures involve mixing a 0.5 g sample with 5 g of flux in a glass test tube and fusing for 5 minutes, either individually over a propane flame, or in a batch with an electric heater. The tube is allowed to cool, a buffer solution is added, and the solution pH is adjusted to the appropriate value. For tin, 5 ml of an oxine solution are added, the tin is extracted, and the fluorescence measured. In the case of tungsten, 1 ml of a morin solution is added to the sample solution, interfering ions are extracted from the tungsten, and the fluorescence of the tungsten morin complex is measured.

The analytical working range for tin in solution is 25 to 400 ng/ml and for tungsten is 25 to 200 ng/ml. No other metal ions have been found to interfere with tin, and molybdenum was found to be the only metal which interfered with tungsten. Molybdenum, however, may be determined by absorption with tungsten simultaneously measured by fluorescence.

Repeated analyses of 14 samples of widely varying mineral type and tungsten content have indicated promise using the fusion-fluorescence method. At present, tin recoveries from soil and rock samples show poor precision. This is believed due to the incorporation of a fraction of the tin in minerals such as biotite, hornblende, muscovite, and garnet which are not readily decomposed.

As a route to other possible uses for fluxes TR-1 and FX-2, it was found that a number of other metals and metal oxides could be made soluble by these fluxes.

Preliminary work using gold-bearing samples, flux FX-2, and atomic absorption spectrometry showed very good recoveries from samples containing microgram and nanogram quantities of gold.

REFERENCES

Agterdenbos, J., and Vlogtman, J.
1972: Talanta, Volume 19, p.1295.

Amano, H.
1960: Science Reports for the Research Institute Tohoku University, Volume A12, p.24.

Bond, A.M., O'Donnell, T.A., and Waugh, A.B.
1970: Analytical Chemistry, Volume 42, p.1168.

Bottei, R.S., and Br. Ambrose Trusk
1968: Analytica Chimica Acta, Volume 41, p.374.

Boyle, R.W.
1979: The Geochemistry of Gold and its Deposits; Geological Survey Canada, Bulletin 280.

Bowman, J.A.
1968: Analytica Chimica Acta, Volume 42, p.285.

Capacho-Delgado, L., and Manning, D.C.
1965: Perkin Elmer Atomic Absorption Newsletter; Volume 4, p.317.

Card, K.D.
1976: Geology of Espanola, Whitefish Falls Area, District of Sudbury; Geoscience Report Number 131.

Derry, D.R.
1980: A Concise World Atlas of Geology and Mineral Deposits; Mining Journal Books, London.

Eberle, A.R., and Lerner, M.W.
1962: Analytical Chemistry, Volume 34, p.627.

Flinter, B.H.
1971; Geochemical Exploration; Canadian Institute of Mining and Metallurgy, Special Volume Number II (Boyle, R.W., Editor), p. 323.

Garrett, R.G.
1971: Molybdenum, Tungsten, and Uranium in Acid Plutonic Rocks as a Guide to Regional Exploration, Southeast Yukon; Canadian Mining Journal, Volume 92, Number 4, p.37.

Harris, A.M., and Hingle, D.N.
1979: X-ray Spectrometry, Volume 8, p.129.

Hempel, W.Z.
1893: Z. Anorg. Allgem. Chem., Volume 3, p.193.

Hesp, W.R.
1971: Geochemical Exploration; Canadian Institute of Mining and Metallurgy, Special Volume 11 (Boyle, R.W., Editor) p. 341.

Holtje, R., and Schlegel, H.
1937: Z. Anorg. Allgem. Chem., Volume 231, p.97.

Huffman, C., and Bartel, A.J.
1964: Ion-Exchange Separation of Tin from Silicate Rocks; United States Geological Survey, Professional Paper 501-D, p.131.

Juniper, D.N., and Kleeman, J.D.
1979: Journal of Geochemical Exploration, Volume 11, p.321

Kerrich, R.
1980: Archean Gold-Bearing Chemical Sedimentary Rocks and Veins: A Synthesis of Stable Isotope and Geochemical Relations; p.144-167 *in* Genesis of Archean, Volcanic-Hosted Gold Deposits, Symposium Held at the University of Waterloo, March 7, 1980, Ontario Geological Survey, Miscellaneous Paper 97, 175p.

Kirkbright, G.F., West, T.J., and Woodward, C.
1966: Talanta, Volume 13, p.1637.

Lillie, E.G., and Greenland, L.P.
1973: Journal of Research, United States Geological Survey, Volume 1, p.555.

Little, H.W.
1958: Tungsten Deposits of Canada; Geological Survey of Canada, Economic Geology Report Number 17.

McIver, J.R., and Mihalik, P.
1975: Canadian Mineralogist, Volume 13, p.217.

Mulligan, R.
1974: Geology of Canadian Tin Occurrences; Geological Survey of Canada, Economic Geology, Report Number 28.

Mulligan, R., and Jambor, J.L.
1968: Tin-Bearing Silicates from Skarn in the Cassiar District, Northern British Columbia; Canadian Mineralogist, Volume 9, Part 3, p.358.

Pal, B.K., and Ryan, D.E.
1969: Analytica Chimica Acta, Volume 48, p.227.

Phillips, S.L.
1960: Analytical Chemistry, Volume 32, p.1062.

Pourbaix, M.
1968: Atlas of Electrochemical Equilibria; Pergamon Press, Oxford.

Quin, B.F., and Brooks, R.R.
1973: Analytica Chimica Acta, Volume 65, p.206.

Radtke, A.S., Heropoulos, C., Fabbi, B.P., Scheiner, B.J., and Essington, M.
1972: Economic Geology, Volume 67, p.975.

Rosler, H.J., and Lange, H.
1972: Geochemical Tables; Elsevier Publishing Company, Amsterdam.

Sajo, I.
1955: Acta Chimica Academy of Science, Hungary, Volume 6, p.233.

Sattur, J.W.
1966: Perkin Elmer Atomic Absorption Newsletter; Volume 5, p.37.

Scott, W.W.
1928: Chemical Methods for the Analysis of Metallurgical Products; D. Van Nostrand Company, New York.

Skoog, D.A., and West, D.M.
1969: Fundamentals of Analytical Chemistry; Holt, Rinehart, and Winston, New York.

Smith, J.D.
1971: Analytica Chimica Acta, Volume 57, p.371.

Sprenz, E.C., and Prager, M.J.
1981: Analyst, Volume 106, p.1210.

Stary, J.
1963: Analytica Chimica Acta, Volume 28, p.132.

Terashima, S.
1982: Geostandards Newsletter, Volume 6, p.77.

Union Carbide Exploration Corporation
1978: Unpublished Geological Report, Assessment File 22863; Assessment File Research Office, Ontario Geological Survey, Toronto.

Vajda, F.
1971: Kut. Intex., Kozlem, Volume 15, p.55.

Wichers, E., Schlecht, W.G., and Gorde, C.L.
1944: Journal of Research, National Bureau of Standards, Volume 33, p.451.

Willard, H.H., Furman, N.H., and Bricker, C.E.
1956: Elements of Quantitative Analysis; D. Van Nostrand Company, New Jersey.

Wright, J.L.
1979: Magnetometer and V.L.F. Surveys, Fostung Township, Project 3115; St. Joseph Explorations Limited, Assessment File 23168, Toronto.

Yim, W.W.S.
1979: Bulletin of the Geological Society of Malaysia, Volume 11, p.375.

Zolotov, Yu. A.
1970: Extraction of Chelate Compounds; Ann Arbor-Humphrey Science Publishers, Ann Arbor.

Grant 009 High Sensitivity Portable/Base Station Magnetometer Based on Overhauser Effect

I. Hrvoic and J. Myzyk

Gem Systems, Incorporated, Toronto

ABSTRACT

The Overhauser Effect allows for increased proton polarization via nonlinear RF pumping. This is obtained at substantial savings of power and time in comparison to classical proton precession magnetometers. The microprocessor controlled portable/base station magnetometer Model GSM-10, based on Overhauser Effect, will have 0.1 nT (gamma) sensitivity, twice per second resolution with 0.5 litre sensor volume and few Ws per reading, nonvolatile memory for data storage, digital output to drive a printer or a computer compatible interface, and will be compatible with Lamontagne Geophysics Field Computer Model GFC-1 and Hewlett-Packard HP-85. The miniature magnetometer will weigh only 4.5 kg complete with sensor, staff, and console with batteries. The special sensor has been constructed and successfully tested. A strong Overhauser Effect-based signal is generated using a local RF generator and a software generated sequence of pulses. Steady RF polarization allows for the increased rate of generating the proton precession signal. A high stability temperature compensated frequency source increments the counter whose status is latched in synchro with the precession frequency zero crossings. The timing information is stored and used for calculation of an average period of the precession frequency, followed by a reciprocation and conversion into units of the applied magnetic field.

The very compact design of the magnetometer allows for storage of up to nearly 9000 readings in a portable mode, or about 24 000 readings in a base station mode. Full data labelling with an octant of directions, precise timing of readings, scanning of accumulated data, nonvolatile memory, and many other features make the GSM-10 one of the most advanced and sophisticated portable magnetometers presently available. The development and the future product has been licensed by Canadian Patents and Development Limited (Hrvoic and Humski 1976).

INTRODUCTION

Overhauser Effect or Dynamic Polarization (Abragam 1961; Schumacher 1970) is a term used for polarization of a proton-rich sample, via an RF saturation of electron spin resonance lines of free electrons, introduced into the liquid by a small amount of so called "free radical". The polarization is much superior to and much less power consuming than classical DC polarization used in proton precession magnetometers. The measurement rate is potentially higher, since the polarization and frequency determination can be concurrent. Other characteristics of the proton precession method of field measurement are unchanged, the most important is an absolute accuracy of 0.5 nT (gamma) and repeatability better than 0.1 nT (gamma) depending on the sensor size and electronic circuitry.

Overhauser Effect applied to a proton magnetic resonance can lead to a variety of precise field measurements. The attractive features in a portable/base station magnetometer are small size, weight, low power consumption, high absolute accuracy, and ease and speed of operation. Combined with a CMOS low power microprocessor, sufficient memory for a full day's operation, and computer compatibility, the magnetometer becomes a powerful tool in mineral and oil exploration, monitoring of temporal activities, archaeological research, earthquake prediction, and weapons detection.

METHOD OF MEASUREMENT

GEM Systems Incorporated portable/base station magnetometer Model GSM-10 uses a nitroxide free radical 2, 2, 4, 4, tetramethyl oxazolidine-3-oxyl (licensed by Canadian Patents and Development Limited) in a solvent such as methanol, dimethoxyethane. A specially prepared sensor serves as an RF resonator at 62.6 MHz, saturating one of the free radical's electron spin spectral lines. The increase in proton polarization is of the order of several thousand.

The pulsed method is used to deflect the increased proton magnetization into a plane of precession around the magnetic field to be measured. The pulse is a 90° or $\pi/2$ pulse of submillisecond duration. A pair of coils serves as both deflection and pick-up coils for the proton precession signal (Figure 1).

The precession signal is amplified and band-pass filtered. A high frequency counter, counting a high stability reference frequency, is latched synchronously to the zero crossings of the precession frequency. Time intervals thus obtained are stored into the memory, averaged, and converted into a frequency, and further converted into units of the measured magnetic field; precession frequency is strictly proportional to the applied magnetic field. A RCA microprocessor CDP1805 controls a measuring sequence, signal monitoring and diagnostics, storage of the results of measurement in CMOS nonvolatile memory, transfer of data to and from peripherals, and communi-

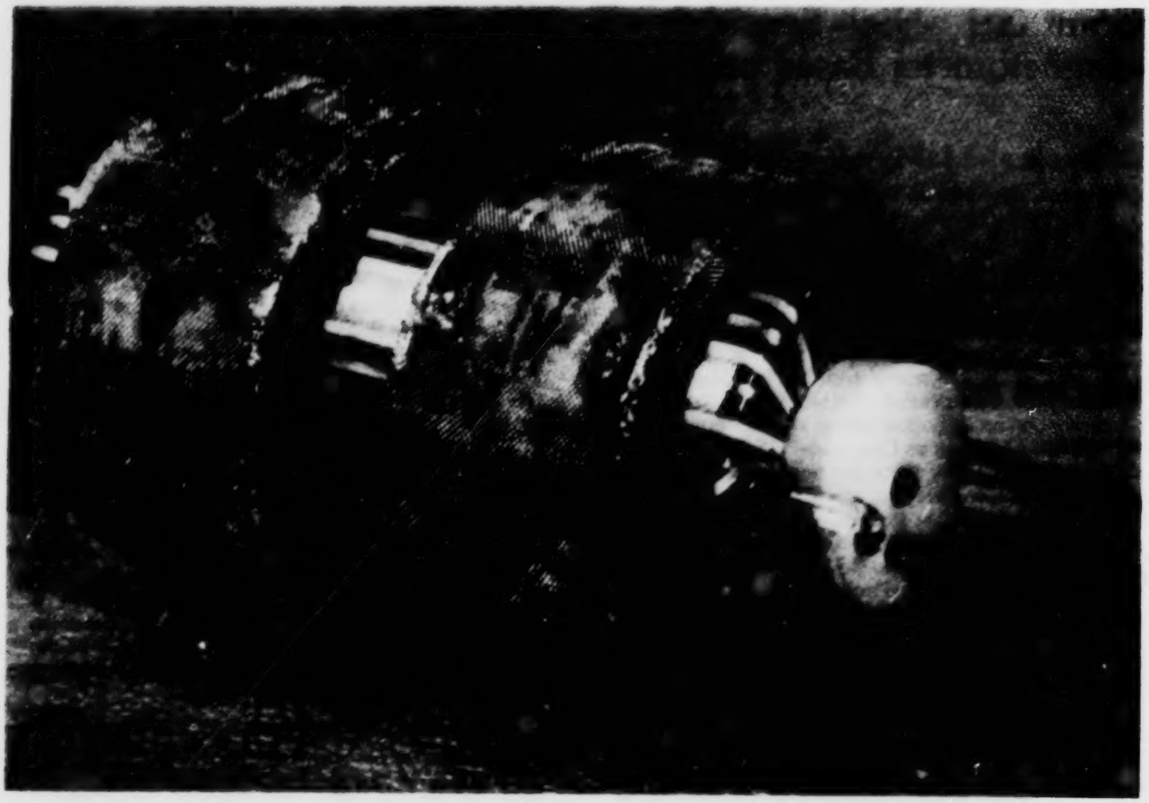

Figure 1. Photograph of a proton precession device.

cation with operator via keyboard. A custom made LCD display helps monitor operation of the instrument, the display will allow for storage of labels, scanning of memory, input from other units and automatic correction of diurnal variations, output to printers, cassette tape recorders or computers, and in particular to the Lamontagne Geophysics Field Computer GFC-1. Each magnetometer is easily converted into a base station with up to 2 readings per second, sufficient to support ground or airborne surveys.

INSTRUMENT ORGANIZATION

A major effort has been made in the past 12 months to develop the instrument's software, all written in Assembler Language to compact (reduce the size of) the programs and maximize the speed of processing. Some minor modifications to the hardware also were made. Packaging has been completed. Front panel dimensions are only 10 by 16 cm (Figure 2); much of the surface of the panel is taken up by a keyboard, large LCD display, and sensor and bus connectors.

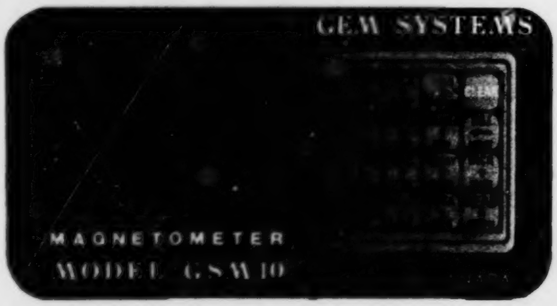

Figure 2. Photograph of a front panel device.

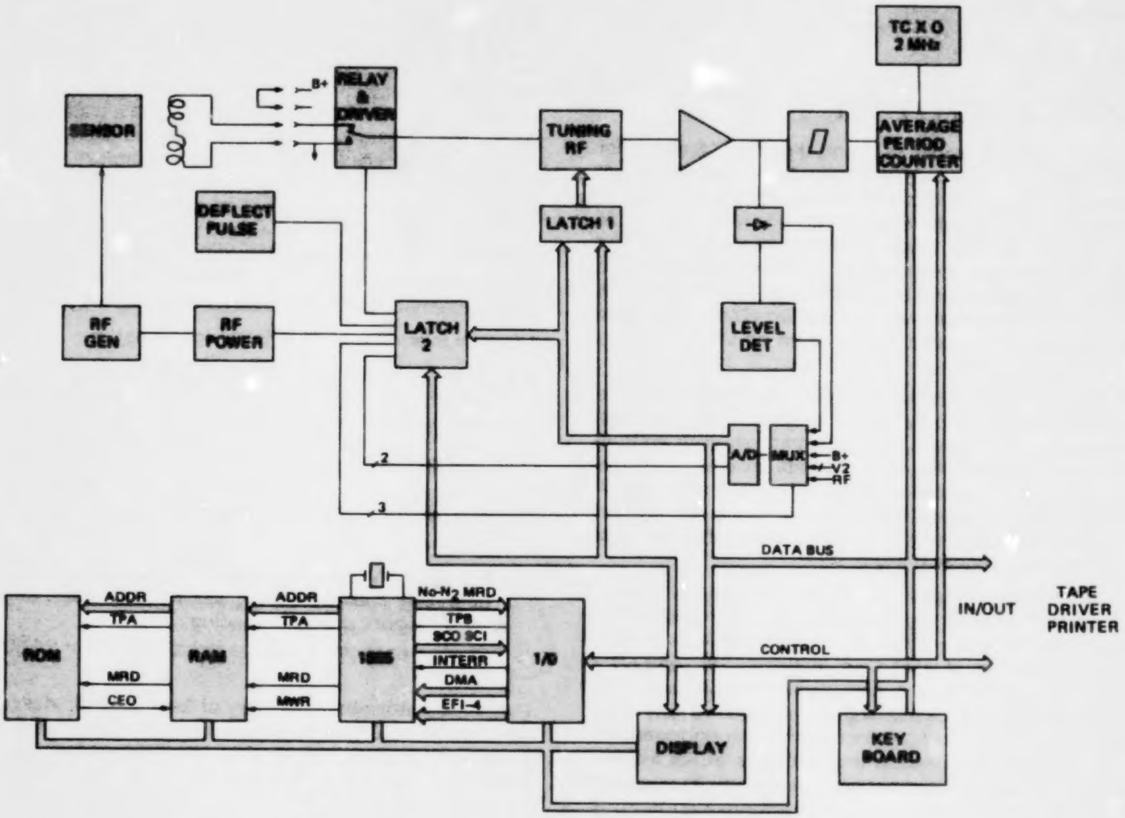
SENSOR
B+
RELAY & DRIVER
TUNING RF
TCXO 2 MHz
AVERAGE PERIOD COUNTER
DEFLECT PULSE
LATCH 1
RF GEN
RF POWER
LATCH 2
LEVEL DET
A/D
MUX
B+
V2
RF
2
3
DATA BUS
IN/OUT
TAPE DRIVER PRINTER
CONTROL
ROM
ADDR
TPA
MRD
CEO
RAM
ADDR
TPA
MRD
MWR
1805
No-N2 MRD
TPB
SCO SCI
INTERR
DMA
EF1-4
I/O
DISPLAY
KEY BOARD

Figure 3. Instrument block schematic diagram.

The depth of the console is 21 cm; ⅓ of which is reserved for a detachable battery pack. Rechargeable nickel-cadmium batteries are used in standard configuration; other types of batteries are optional. The instrument's block schematic diagram is shown in Figure 3.

The generation of the precession frequency, tuning of the analogue circuitry, and monitoring of vital parameters are all under the control of a RCA CDP1805 microprocessor. The operator uses a special 16 key keyboard (Figure 3) with 31 different commands plus numerical entries to control the magnetometer. Every operation is confirmed on a special display (Figure 2) guiding the operator through sometimes complex operations of setting field labels, timing, synchronization with other GSM-10 units, or scanning of stored data.

A number of parameters like battery voltage, polarizing current, signal strength, and decay time are monitored and displayed as a warning if they exceed the preset limits.

OPERATING MODES

The GSM-10 has 2 basic modes of operation:

BASE STATION

In the base station mode, the magnetometer is presumed to operate at one place recording the time variations (diurnals) of the magnetic field.

An 8 digit label and the date are entered before the operation of the instrument starts. The time of day is set precisely, along with the increment of time between the readings. Only the time of reading and magnetic field are recorded in this mode allowing for about 8000 readings with normal memory capacity (16K) and 24 000 with the maximum memory capacity (48K). The final time of recording is entered into memory. The base station operates until the final time is reached, or the available memory is filled with data.

MOBILE FIELD UNIT

When used as a mobile field unit, the GSM-10 allows for time synchronization with the base station and (if desired) readings can be taken exactly in step with the base station readings. The operator does not have to note the precise time of the reading; instead the instrument will wait and take the reading at the proper time, that is, each 3 seconds if both the mobile and base station units are set to this interval. This feature allows precise diurnal correction even during strong magnetic storms since no interpolation is necessary.

The operator can initially enter the full label (line and station numbers and the octant of directions), and label interval (station interval), to be automatically updated from reading to reading. After this, the data collection consists of moving to a new station and pressing a READ button. If the operator is not satisfied he can reject the reading and repeat the measurement. A change of label or label increment is allowed at any time.

To change the label, the operator must enter a code, characteristic for a specific instrument, to "unlock" the label. This will prevent misuse or accidental loss of data. Data, in the form of label, time, magnetic field, and error code are stored into a nonvolatile memory and fully protected against overwriting or erasure. At any time during the survey, the operator can scan through collected data using SCAN function and setting a SCAN INCREMENT to a negative number to go backwards through the data or a positive number to go forwards. Any step, from ±1 to ±99 is allowed. When scanning, the operator can select the labels, times, or magnetic fields to be displayed, the other 2 parameters being readily displayable at a press of the proper button. To return to the "on line" readings, the CLEAR button is pressed, and the survey can continue immediately.

At any time, a particular label, time of reading, or magnetic field can be located by using a FIND function. The GSM-10 has a 37 pin bus (Figure 2) to communicate with various peripherals; a special cable makes it compatible with the Centronics type printer. Any stored data can be printed. In base station mode, the printout will show times of reading, magnetic field, first difference, a base correction, and the error code. Approximately 50% of the printer scale is used for 2 analogue traces of ±4 nT and ±80 nT full scale. In field mode, the format is different. It will show full label, time of reading, uncorrected magnetic field, base correction (if available), corrected field (if reduction has been done previously), first difference, and error code. Again, about 50% of the paper is used for a 2 scale analogue record of corrected (if corrected) or raw data.

Neither reduction of data nor printouts will destroy the original data in memory. Only deliberate memory erasure will destroy the collected data. To safeguard this, there is a special code preventing tampering with the data at any time. The magnetometer has a concealed ON/OFF switch. When switched off, the synchronisation or real time will be lost. Disconnecting the sensor will only reset the microprocessor and somewhat reduce the power consumption.

SPECIFICATIONS

Resolution: 0.1 nT (gamma)

Accuracy: 0.5 nT (gamma) over operating range

Range: 20 000 to 100 000 nT (gammas), 23 overlapping steps, automatic tuning, manual initial set-up

Gradient tolerance: up to 5000 nT (gammas)/m

Operating modes: (all are keyboard selectable)

> Mobile field unit: Memorizes a full label, time of reading, and magnetic field, automatic label increment, automatic cycling time of the reading to coincide with the base station timing, field data scanning, error code for poor quality of reading
>
> Storage capacity: 3000 readings, 6000, or 9000 optional
>
> Base station: Stores time and magnetic field. Present operating interval from 0.5 seconds to 1 hour, error code for poor quality of reading
>
> Storage capacity: 8000 readings, 16 000, or 24 000 optional

Playback: Automatic correction of field data for diurnal variation. Printouts or storage on cassette tape of: label, time, error code, original data, first difference, base correction, and corrected data. Reduced data storage capacity (without alteration of raw data) readings optional. Printout of label based profiles. In-field data gridding and contouring via Lamontagne Geophysics Field Computer GFC-1. Model fitting programs.

Input/Output: 37 pin parallel output provides for base station - field unit - printer/cassette tape/FC-1 mating. Precession frequency available for telemetering

Power requirements: 12 V 120 mA, 15 mA standby

Power source: Internal 12 V 2.2 Ah Rechargeable Ni-Cd batteries, others optional

Battery charger: 110/220 V 50/60 Hz output 200-350 mA (constant current, selectable) 14-20 V

Operating temperature: -40°C to +60°C

Dimensions: Console - 10 by 16 by 21 cm

Sensor staff: 4 sections 45 cm (18") each

Weight: 4.5 kg total (console with batteries, sensor, staff)

The 37 pin data connector will, in future, serve also to transfer the collected data to magnetic tape and directly to some computer such as the Lamontagne Geophysics field computer GFC-1 or the Hewlett Packard HP-85. The software development has been done in cooperation with Lamontagne Geophysics Limited of Toronto.

CONCLUSION

Over the past 12 months, we have made progress in the development of the Overhauser Effect portable/base station magnetometer: the software has been written and tested, and the packaging has been completed. The task of organizing a complex software and limiting its size to 16K was a major one and considerably larger than anticipated. This is the main reason that the instrument falls somewhat short of being fully completed. GEM Systems Incorporated, however, will complete the testing and soon market the instrument using its own resources. The major advantages of the GSM-10 are the high precession and sensitivity, high speed of data collection, low power consumption, reasonable size and weight, and the large storage capacity.

REFERENCES

Abragam, A.
1961: Principles of Nuclear Magnetism, Oxford University Press.

Schumacher
1970: Introduction to Magnetic Resonance; W.A. Benjamin, New York.

Hrvoic, I., and Humski, K.
1976: Canadian Patent 1001232, U.S. Patent 3,966,409, Granted to Canadian Patents and Development Limited.

Grant 010 Advanced Hardware and Software Development for Ground EM Prospecting

J.C. Macnae[1,2] and Y. Lamontagne[1]
[1]Lamontagne Geophysics Limited, Toronto
[2]Geophysics Laboratory, Department of Physics, University of Toronto

ABSTRACT

Support from the Exploration Technology Development Fund is enabling Lamontagne Geophysics Limited to conduct research and development to improve EM prospecting in 4 different categories:

1. The development, to field testing stage, of a backpackable automatic borehole logging system with a 10M BAUD fibre optic data link.
2. Preliminary development of a high power, efficient, EM transmitter.
3. Optimization of the signal/noise (S/N) parameter by advanced signal processing techniques. S/N improvements of between 3.5:1 and 6:1 have been routinely achieved without any increase in transmitter power.
4. Development of the processing and interpretational capability of ground and borehole EM, including programming, scale model studies, and theoretical research.

INTRODUCTION

The aim of this research project was to improve the detection and interpretational capability of wideband time-domain EM systems in general, and the UTEM system in particular.

To improve detection, several avenues were chosen. Those chosen for hardware development are: a borehole subsystem to extend the search to greater depths than could be reached by surface surveys alone; and a high power transmitter to increase the signal level, and hence the signal/noise ratio. A research project was also undertaken with respect to signal/noise ratios.

To improve interpretational capability, it was felt that a program of scale modeling was required to fill obvious gaps in the literature for fixed transmitter geometry EM systems. Also, an investigation was needed into the best way to use such models (and other computational models) to interpret field data.

BOREHOLE UTEM SYSTEM

A borehole subsystem is a necessary part of a complete, deep penetration EM system. This arises from the need to use the equipment as a primary reconnaissance tool, and as a means of ensuring that when deep conductors are detected by surface measurements, the resulting drilling intersects the main conductor which has been detected. The small surface anomaly amplitude and broad shape, arising from a very deep conductor, means that interpretation often poorly locates the target, particularly if other conductors are present.

Existing hardware, namely the UTEM 3 receiver, transmitter, and playback computer, was to be used as a basis for the development. New development consisted of a borehole coil sensor, encoder-decoder, fibre optic transmission cable, winch, position and tension encoders, and an automatic programmable controller. The initial objectives and current status are:

OBJECTIVES

1. A 2 km depth capability with a cable weighing about 25 kg and with strength in excess of 100 kg.
2. Avoidance of ground loops and stray coupling. The probe will be electrically self-contained and shielded.
3. Development of a sealed, ferrite cored probe shielded and guarded with an effective area of 100 m^2, 3.0 cm in diameter to fit in Ex or larger size holes.
4. Conversion of coil output to pulse width modulated signal for transmission by fibre optic cable.
5. Conversion of signal back to analogue amplitudes for normal sampling by the receiver. This re-conversion would take place in the controller/interface unit at the surface.
6. Use of a light-weight winch with position encoder with electrical connection to the controller to position the probe under program control by use of a stepping motor.
7. Microprocessor based controller to select the desired depths according to the user program and control the receiver function.
8. Use of a slip clutch and pretensioner to detect blockages automatically. Similar hole bottom detection.
9. Threshold levels that can be set on any channel for automatic anomaly detection and detailing.

BOREHOLE UTEM FIRST TEST

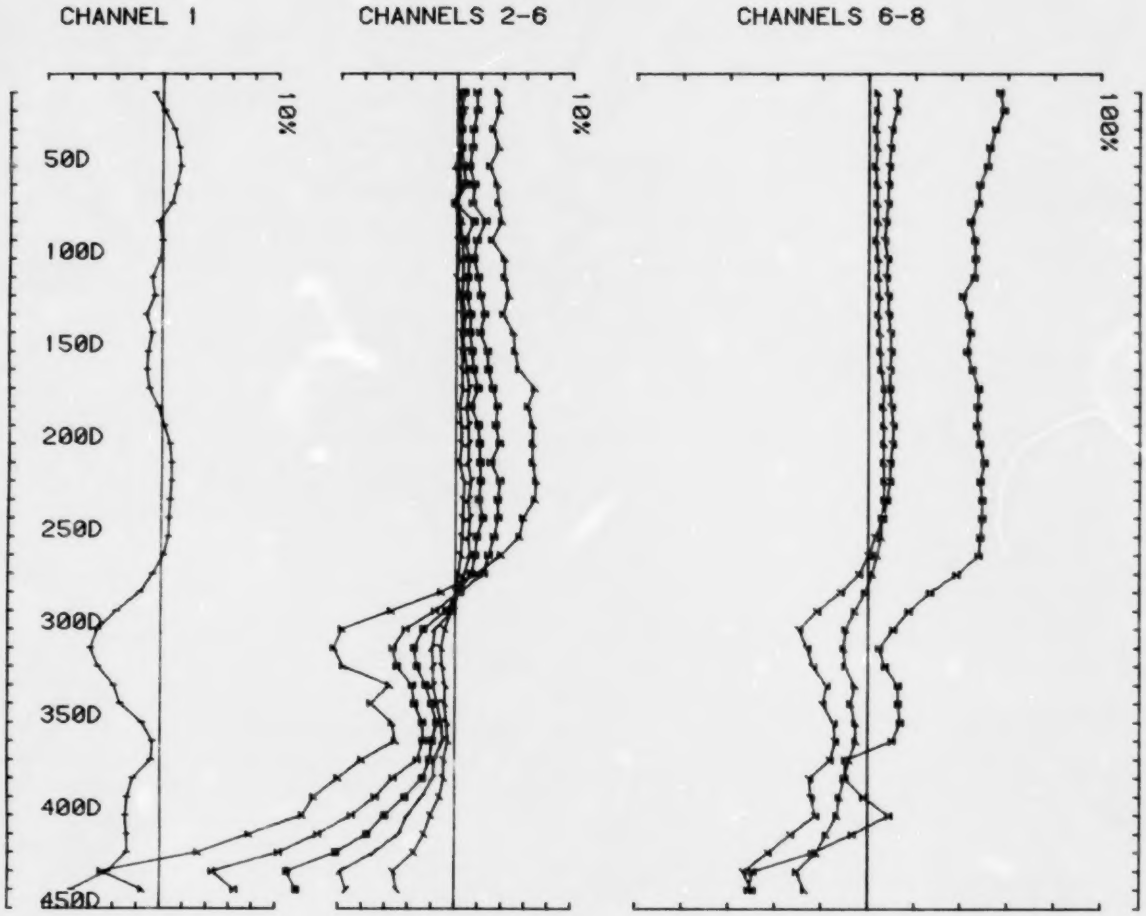

FIG 1 - PLOT OF THE FIRST DOWN-THE-HOLE MEASUREMENTS WITH THE NEW FIBER OPTIC BOREHOLE UTEM SYSTEM DURING EQUIPMENT TESTING AT GERTRUDE.

DDH 9266 DEPTH INTERVAL: 10 M MEASUREMENT TIME: 65 MIN
LOOP: 500 M E-W BY 450 M N-S ENTIRELY TO THE NORTH OF DDH 9266
CENTRE OF SOUTH LOOP SIDE 150 M NORTH OF COLLAR

UTEM SURVEY **conducted by** HU AW YL **Job** 9266
Project Area BH TEST GERTRUDE **Survey for** LGL **freq(hz)** 30.974

Figure 1. Plot of the first down-the-hole measurements made with the new fibre optic borehole UPEM system during equipment testing at Gertrude.

CURRENT STATUS (OF OBJECTIVES)

1. Achieved with custom fibre-optic cable design.
2. Achieved
3. Achieved. Effective area is 300 m^2.
4. After close to a year of severe technological problems, the encoder has been finalized. Chief problems arose in minimizing the component count so that a long thin circuit board was feasible, and in finding small enough components that would fit in the dimensions forced by criterion 3.
5. The decoder on surface has been constructed and fully tested.
6. Completed. Lighter DC servo motor used.
7. Currently being refined.
8. Mechanically completed, interfacing to microprocessor in progress. Electronic torque limiter used.
9. Being implemented in conjunction with 7 above.

At the time of writing, the borehole system is being field tested (Figure 1). The problems of introducing fibre-optic data link technology to borehole geophysics proved to be formidable. It was initially estimated that a few weeks would be sufficient to design a data encoder-decoder system. In fact, the design process had to be repeated from scratch 3 times because the first 2 attempts ran into difficult problems. Other than this, the remaining development was performed in about the time scheduled.

Since the project commenced, other research on fibre optics for borehole application has been reported. Gould (1981) reported on a fibre optic system developed by Optelecom Incorporated for the United States Department of Energy for radiometric application, where, with a 5 cm diameter downhole electronic casing, each fibre optic cable was capable of only 2 M bit/second, requiring 2 fibre optic cables going uphole for a total of 4 M bit/second data rate. The development by Lamontagne Geophysics Limited of error free 10 M bit/second in one cable, with downhole electronics contained in a casing diameter of 3.0 cm can thus be evaluated as a significant advance over known results.

SIGNAL/NOISE OPTIMIZATION

Several techniques have been found to be useful for rejecting noise in time-domain EM systems. One major difference between the type of signal processing used in EM sytems and that used in other areas, such as seismic surveying, is that the EM system processing is usually constrained to be primarily in real-time. This is not a fundamental requirement. It arises because the field crews required to perform a survey are typically small, and usually have limited access to major computers and mass data storage at the data acquisition point.

Virtually all controlled source EM systems transmit a repetitive signal and use some form of synchronous detection and averaging (stacking) to enhance the signal relative to the noise background. Because the sensors, amplifiers, and signal conditioning circuits in a time-domain EM system are broadband, it is sometimes assumed that any time-domain EM system must have signal to noise characteristics which are inferior to a frequency-domain unit. This is not so, however, because the averaging procedures employed reduce the effective bandwidth of the system to incoherent noise while still performing a broadband measurement of signal. Basically, synchronous averaging causes the instrument's spectral response to be collapsed to a multitude of narrow spectral lines centred on odd harmonics of the signal's base frequency. The system response to different types of noise may be calculated for various stacking and processing techniques such as those shown in Figure 2. Some tradeoffs, however, must be made in designing a practical signal acquisition system.

Synchronous detection is a powerful rejector of incoherent noise that has a stationary statistical character. However, not all noise has this characteristic. Steady powerline noise is a highly coherent signal. Powerline transients and local spheric activity often occur sporadically on the time scale of a single EM measurement, and when the total number of noise events is small, the resulting noise is not stationary in a statistical sense. Both tapered and randomized stacking (Figure 2) were studied and found to be able to improve noise rejection for this type of noise.

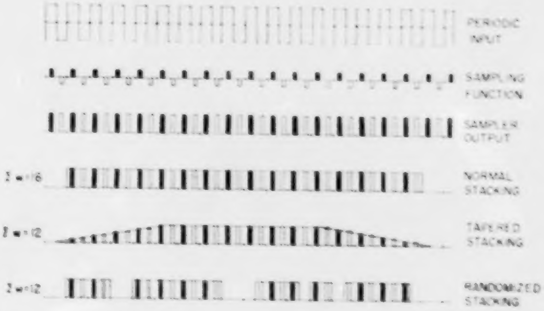

Figure 2 Different averaging methods. The sampling function produces an output of one sign for synchronous input. Normal stacking accepts data continuously. Tapered stacking accepts data with a weighting dependent on time; that shown here is linearly tapered. To ensure that no zero bias is introduced, randomized stacking contains equal numbers of half cycles that were of opposite sign before sampling.

When a coil sensor is used to measure the magnetic field, much of the noise energy from spheric sources lies in the high frequency part of a typical system's bandwidth. When wideband noise is "coloured", a standard technique to improve signal to noise ratios consists of adding a filter to the receiving circuitry to "whiten" the noise, with a corresponding inverse filter being applied to the transmitted waveform.

Analogue bandpass filtering techniques are commonly used in all EM systems. For example, if system design characteristics require a linear bandwidth for signals only up to a certain limit, a high cut filter eliminates noise above this frequency. It is also possible to redistribute the power in the transmitted spectrum and compensate in the receiver by filtering the signal and noise. Such techniques, known as pre-emphasis, prewhitening, and deconvolution are well known in many fields such as audio engineering. The main obstacle to their use in EM is the necessary preservation of phase characteristics in filters.

For real-time operation of complex filters, the major constraint is that of realizability. There are a very limited class of prewhitening filters whose inverses can be exactly realized. Prewhitening has wideband effects and as a result is best understood by looking at the response of the spectral sensitivity envelope of each time channel. Figure 3 shows the sensitivity envelope of a system with prewhitening, using a filter with 10:1 high:low frequency gain and time constant .003/f_0. The effect of the filter in reducing noise in the high frequency part of the spectrum is evident. By comparison with Figure 4, this particular example of prewhitening has little advantage at low frequencies, but the high frequency sensitivity to noise is reduced 20 dB.

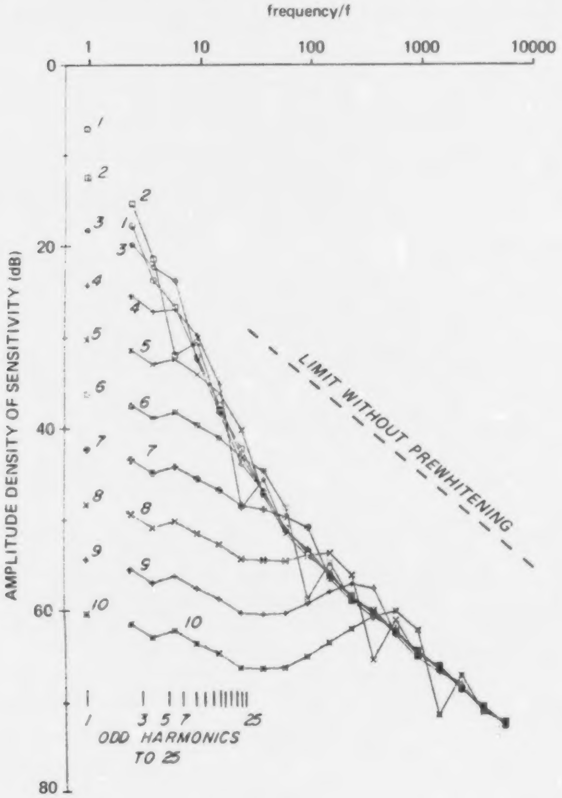

Figure 3. Spectral envelope showing the effects of prewhitening. The particular filter has a low:high gain ratio of 10:1 and a time constant 0.003/f_0.

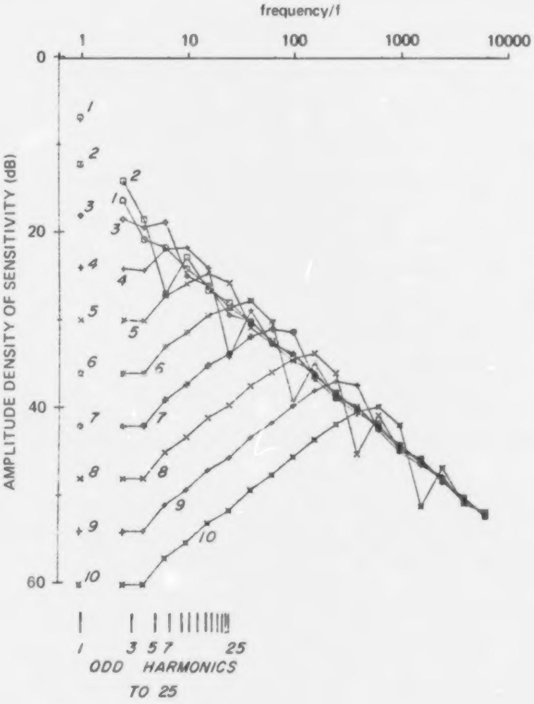

Figure 4. Amplitude density (root sum power per fifth decade) vs frequency of the noise sensitivity spectrum.

Optimization of prewhitening is a complex process, as the actual noise spectrum is not time invariant. It is necessary also to take account of achievable voltage or current limits in calculating the redistribution of power within the transmitter waveform. With the UTEM system, a signal/noise ratio improvement of 3:1 on long delay time channels and 6:1 on short delay time channels has been established to be routinely achievable without any increase in peak transmitter power or stacking time. Since stacking generally improves the signal/noise ratio with a SR/T factor, use of prewhitening corresponds to the increase in precision that would be obtained by stacking from 9 to 36 times longer! An improvement of this order required implementation of filters with multiple rather than single time constants to closely match the transmitted spectrum to the noise

This study has been written up for publication and was submitted to GEOPHYSICS in 1982, as "Noise Processing Techniques for Time Domain EM Systems" by J. Macnae, Y. Lamontagne, and G.F. West.

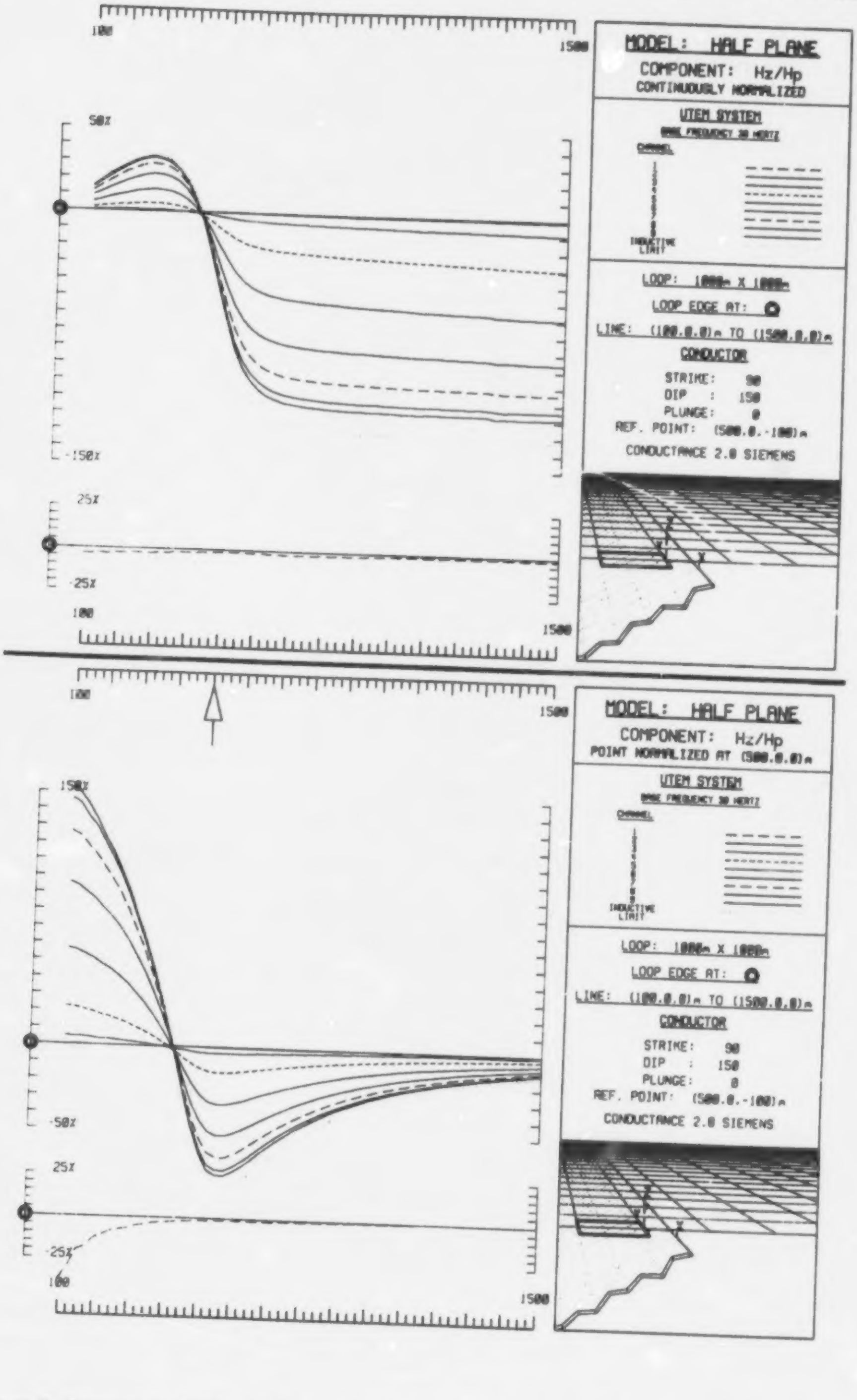

Figure 5. Example of UTEM scale model data over a dipping half plane. The dotted curve is the theoretical inductive limit.

DATA PROCESSING AND INTERPRETATION

SCALE MODEL STUDIES

About half of the scale models necessary for the planned comprehensive set of type curves were completed by summer students during 1982. The results have been compiled and are commercially available in a 5-volume set and have been used to upgrade interpretational techniques. Interpretational programs available on the GFC-1 computer now include the horizontal thin layer, homogeneous half space, approximate layered earth, and inversion to a "quasi-plate" model. Further development of more general routines was not attempted due to the size/speed limitations of current microcomputers. Figure 5 shows an example of scale modelling data in final presentation form.

Further developments planned in 1983/84 are the continuation of the scale modelling project to cover problems with overburden cover, of relevance to exploration in northern Ontario, and systematic modelling of borehole geometries necessary for proper interpretation. Work by J.S. Holladay (Graduate student, University of Toronto, personal communication, 1982) showed that it should be possible to transform this UTEM scale model data into the equivalent responses for other large loop systems such as Crone PEM or Geonics EM37, and this will be further studied.

INTERPRETATIONAL STUDIES

The interpretational value of horizontal as well as vertical components was studied to aid in survey design. It is easy to show that the secondary EM magnetic field on the surface from a fixed transmitter source is a potential field. As such, Laplace's equation indicates that both horizontal components can be predicted from a knowledge of the vertical component alone. This, as is common to most potential field operations such as upward continuation,

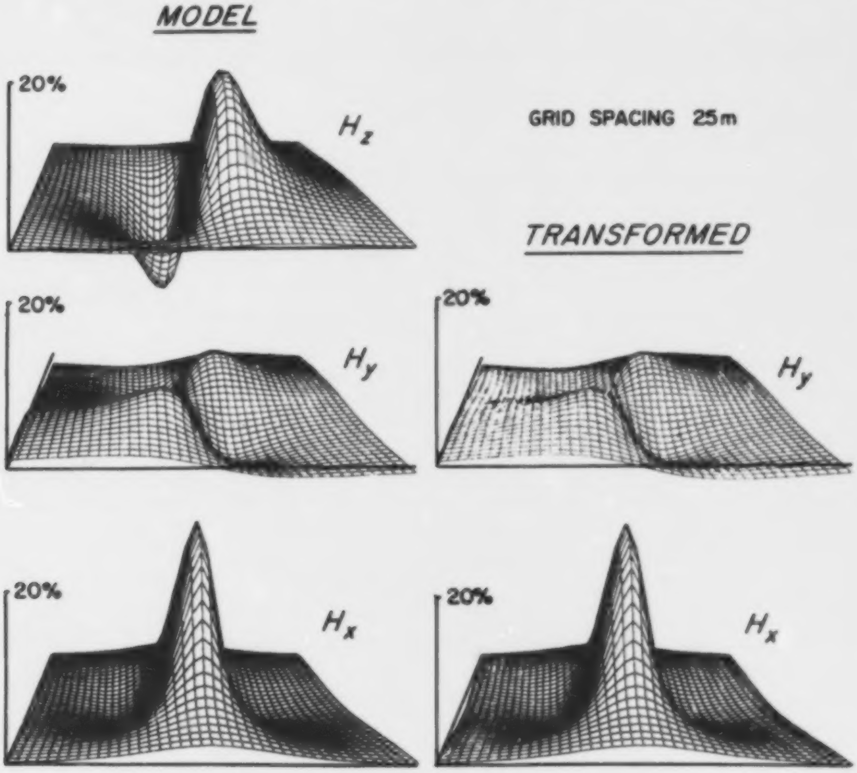

Figure 6. Directly computed vertical H^s_z and horizontal H^s_x, H^s_y UTEM channel 5 response over a conductive plate, together with H^s_x, H^s_y components computed from the spatial variation of H^s_z by a 2-dimensional, quadrature phase, amplitude invariant filter. The transmitter loop is the same size as the plotted grid and located immediately to the right of each plot.

was found to be best performed in the wavenumber (Fourier) domain.

After development of the required filters, testing was done on both model and field data to investigate the stability of the vertical component to horizontal component transform.

Program PLATE (Dyck *et al.* 1980) is a standard computer package for modelling for the EM response of thin, rectangular conductors located in a resistive environment. The program was used to compute the response in channel 5 (mean delay time 0.8 ms) of the UTEM time-domain EM system to a vertically dipping, thin plan conductor of strike length 500 m, depth extent 250 m, depth to top 50 m, and conductance 10S. All 3 components H_x^s, H_y^s, H_z^s were calculated directly by the program. The vertical component data were then Fourier transformed to the wavenumber domain using a standard library FFT routine, the transformation filter applied, and the data inverse Fourier transformed to yield predicted horizontal H_x^s, H_y^s components. Figure 6 shows the results over a 1000 m by 1000 m grid, with 25 m line/station spacing. The normalization used for expressing secondary fields as a percentage is the value of the primary field on the surface at a point located directly above the centre of the conductor. The difference at any point between transformed and directly modeled horizontal components is less than 3% of the peak H_x^s amplitude. A close examination of this transformed data shows that some ripple is visible near the grid edges which is seen clearest on the H_x^s plot. This ripple (or ringing) is an artefact of discrete Fourier Transforms when discontinuities exist at the edge of the data grid. Thus, theoretical model data can be stably transformed.

Figures 7 and 8 show examples of field data selected to show 2 different problems that may occur in practice due to undersampled data. Both examples show profiles taken in the horizontal X direction. Figure 7 shows some UTEM data from the Cavendish test site, plotted as a secondary field normalized to the constant primary field at the station closest to the conductor. The original plots of the UTEM multichannel response, which are plotted with a different convention, namely continuous normalization to local primary field, on 6 lines of the grid, may be found in Macnae (1980). Figures 7 and 8 show the channel 5 response (mean delay time 0.8 ms). It is clear that the H_z^s anomaly is undersampled near the H_z^s crossover. The difference between transformed and measured H_x^s amounts to about 20% of the peak-to-peak H_z^s response; what has clearly occurred here is that the station spacing is too large to estimate the high wavenumber components. The depth to the top of the conductive material is known to be only a few metres for this conductor.

Figure 8 shows an example from a much deeper conductor where the anomaly is much longer than the survey line. The main problem in this case is that the low wavenumber components of the anomaly in the X direction can not be determined from the data. As a result, the transformed H_x^s data are significantly different from the measured H_x^s data. In cases such as these, the discrete Fourier transform applied directly to the data assumed a spatial repetition of the survey data that is unrealistic. Discrete Fourier transforms have this property as is discussed in many texts (Kanasewich 1975). Common practice in 2-dimension Fourier processing of airborne magnetic data, for example, is to predictively taper the data outside the survey area to improve base-level estimation. Depending on how tapering is done, however, there are significant effects in the estimation of the amplitude of long wavelength (low wavenumber) components. Figure 7 shows the change in predicted H_x^s response when the actual data was empirically "tapered" by simply folding the response about the leftmost point on the plot. The calculated H_x^s response differs from the measured response essentially by only a monotonically decreasing amount of about 10% per km; this is equivalent to a poor estimate of only 1 very long wavelength, which if added, would significantly reduce the difference between the actual and predicted data.

These 2 examples show that horizontal H_x^s data may often be poorly estimated from vertical H_z^s data in the usual cases with undersampled real data. The essential object of any survey, however, is not the measurement of the data itself, but rather the interpretation of this data in terms of a reasonable geological model. If enough data points are read to adequately sample an anomaly for detailed interpretation, then the horizontal component data are essentially redundant.

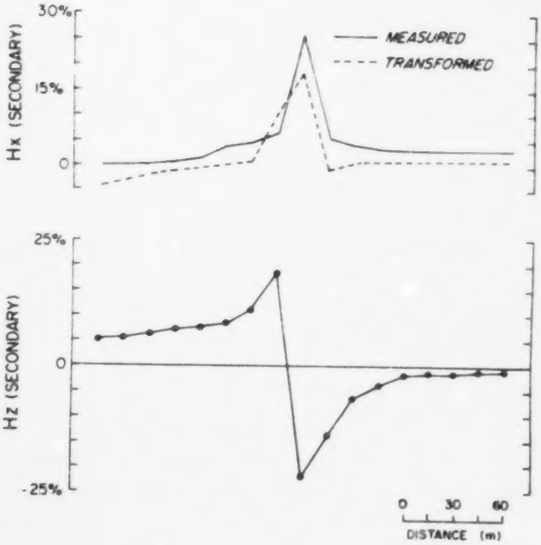

Figure 7. Example of transformation of H_z^s data to the horizontal H_x^s component showing the effect of insufficient sampling density. The transformation was performed in 2 dimensions on 6 lines of data, of which only 1 is shown here.

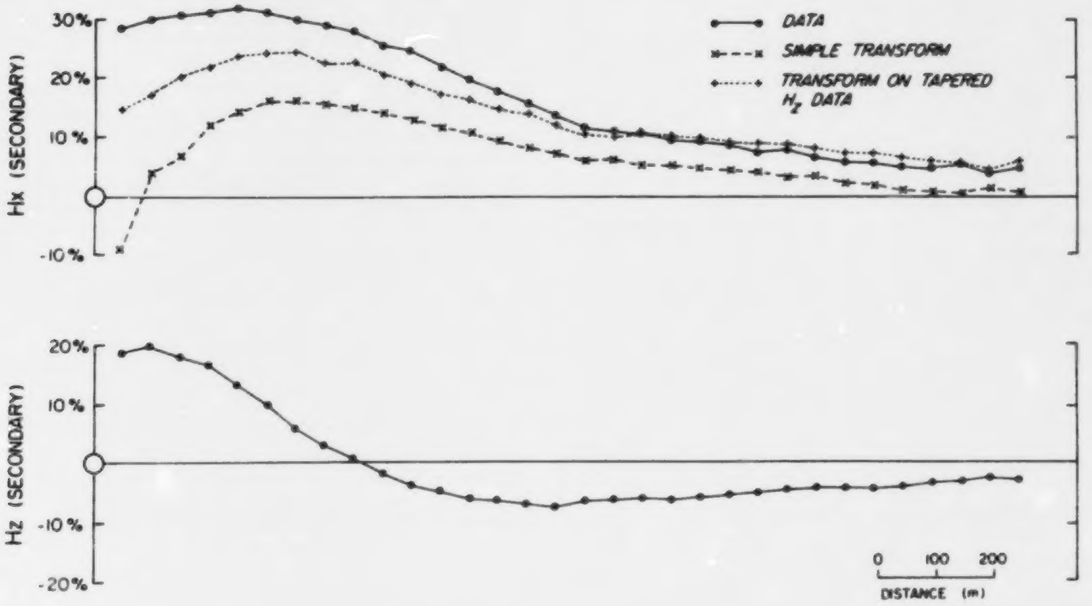

Figure 8. Example of transformation of vertical H_z^s data to horizontal H_x^s component. The survey line of length 1.5 km is too short to fully map out the anomaly. The simple discrete transform applied implicitly assumes a spatial repetition of the H_z^s data which is unrealistic. The transform using an empirical extrapolation to taper the H_z^s data differs from the measured H_x^s data by 1 wavenumber component corresponding locally to a slope of 10% per km.

CONCLUSION

Work continues both on the hardware and software developments discussed. The advances in equipment and interpretational tools already developed, should indeed greatly improve the success of the search for deeply buried conductors in Ontario.

REFERENCES

Dyck, A.V., Bloore, M.A., and Vallee, M.A.
1982: User Manual for Programs: Plate and Sphere; Research in Applied Geophysics Number 14, Geophysics Laboratory, Department of Physics, University of Toronto, January 1980.

Gould, G.
1981: Fibre Optic Data Transmission System for Borehole Logging; United States Department of Energy, Final Report of Contract DE-AC13-78GJ01664.

Kanasewich, E.R.
1975: Time Sequence Analysis in Geophysics; University of Alberta Press, Edmonton.

Macnae, J.C.
1980: The Cavendish Test Site: A UTEM Survey Plus a Compilation of Other Ground Geophysical Data; Research in Applied Geophysics Number 12, Geophysics Laboratory, University of Toronto.

Grant 011 Development of Computer Software for Geophysical Interpretation

N.R. Paterson, F.S. Grant, and D.J. Misener
Paterson, Grant, and Watson Limited

ABSTRACT

Software has been developed to assist in the interpretation of airborne EM, magnetometer (including gradiometer), and gravity data. Emphasis has been placed on techniques of direct application to current exploration problems in Ontario. Three programs (AEMINV, MAGMOD 1.4, and SDSUSC) have been applied to exploration data, and are now in routine use by the mining industry, either through Paterson, Grant, and Watson Limited, or via the public service library of Dataplotting Services Limited. Two gravity interpretation programs have also been developed in conjunction with the Ontario Geological Survey. Work is continuing to further develop the techniques of variable depth (height) magnetic susceptibility mapping, 2-layer EM inversion, and magnetic gradiometer modelling.

OBJECTIVES

Although numerous programs exist for processing and interpreting geophysical data, many of them have been prepared for research purposes and have limited application to exploration.

With the advent of routine digital recording of multichannel, high resolution, wide-band data sets, and the growing availability of high speed computers (Paterson *et al.* 1982), the need for user-friendly processing and interpretation software is urgent.

The ETDF grant was awarded to assist in the development, testing, and application of a variety of software designed to meet the current priorities of exploration organizations in Ontario.

FIELDS OF STUDY

AIRBORNE EM

There have been rapid improvements in the field of multi-channel airborne EM (AEM), both fixed-wing and helicopter, in recent years. It is common (Paterson *et al.* 1982; Pitcher *et al.* 1980; Fraser 1979) for 6 channels of EM data, of several different frequencies and/or coil separations, to be recorded simultaneously at intervals of <1 second. Obviously, such data can, if properly assimilated, reveal a great deal about the conductivity distribution of the ground surveyed. Attempts at half-space and 2-layer modelling (Pitcher *et al.* 1980; Fraser 1979; Palacky 1981) have been successful in producing "apparent resistivity" maps which assist in recognizing local conductors and (in areas of residual soil) in lithologic mapping. Where a conductive overburden overlies the bedrock, for example most of the Canadian Shield, the existing methods have limited application. None are directly available to industry geophysicists.

A need was identified for a rapid, economical program to derive the parameters of a 2-layer earth (Figure 1) in which the conductivity and thickness of the overburden, as well as its depth below the sensor, would be allowed to vary in order to produce an optimum "fit" to the observed data. Edwards (Edwards *et al.* 1981) developed a program based on earlier work by Wiggins (1972), by which model

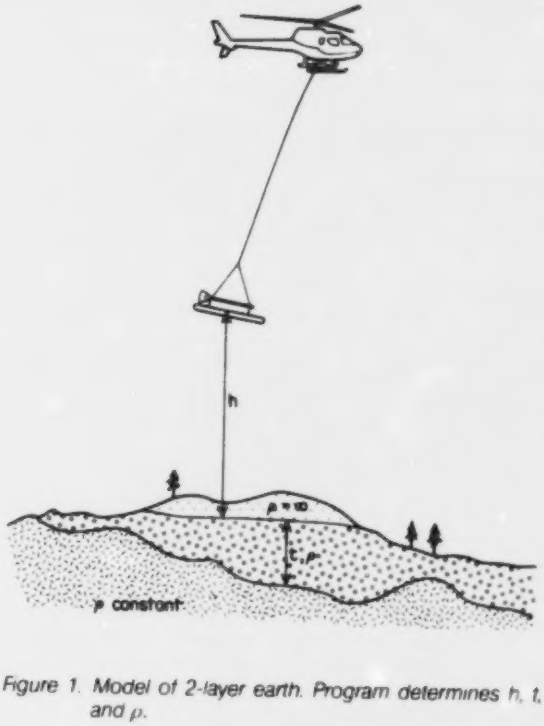

Figure 1. Model of 2-layer earth. Program determines h, t, and ρ.

parameters are decomposed in such a way that the effects of fractional changes are independent of one another and the parameters can therefore be identified and determined.

With the help of R.N. Edwards, this technique of eigenvector decomposition was applied successfully in April 1982 to a helicopter EM data set (Paterson *et al.* 1982). Subsequently, more than 4000 line km of helicopter EM data have been inverted using steadily improved versions of the program. Copies of the programs are currently in use by 2 survey contractors. The cost of running the program on the VAX/11/780 computer is roughly $1.00 per km, with data points at approximately 50 m intervals along the profile.

The calculated parameters are normally listed, together with the observed and fitted data values, their RMS error, and the critical eigen statistics, for each point on the profile. Selected data are then plotted as stacked profiles (Figure 2) and (usually) contours of conductance or resistivity of the upper layer (Figure 3). Overburden thickness can be derived uniquely only within its determinable range, which is normally about 0.2 to 0.7 times the flying height of the sensor. Outside this range, it can be approximated by multiplying the conductance values on the contour map by the average local overburden resistance, estimated from the stacked profiles.

Advantages of the 2-layer model, and, particularly, the method of inversion, include:

1. Bedrock conductors are usually "flagged" by sharp spikes in the RMS error profile (*see* Figure 2).

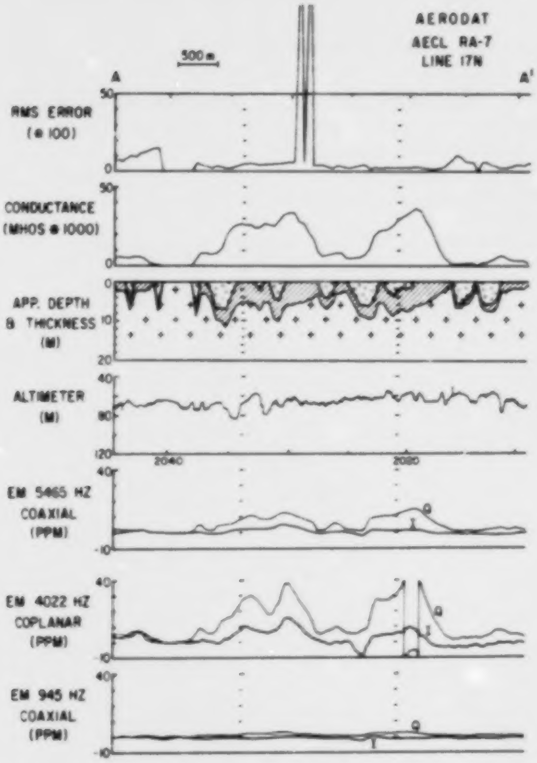

Figure 2. Stacked profiles; 3-frequency helicopter EM responses and 2-layer inversion. Conductance refers to crosshatched layer. Overlying layer is assumed to be non-conductive and is obtained by subtracting altimeter reading from calculated value of h (Figure 1). RMS error represents fit of model data to observed EM response. Spikes may be indicative of bedrock conductors.

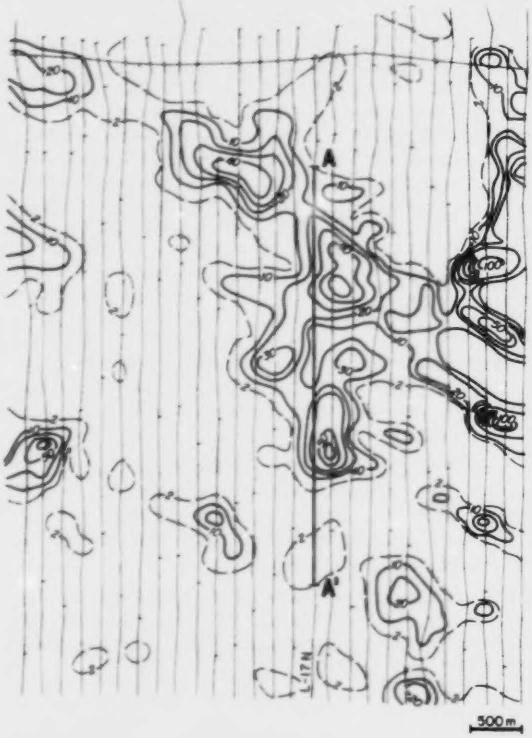

Figure 3. Apparent conductance contours, same area as Figure 2 (see Profile AA'). Fairly reliable overburden thickness can be derived by multiplying conductance by average local resistivity even when the inversion method cannot uniquely separate t from ρ. Contours represent the calculated conductance (conductivity x thickness), in milli-mhos, of the upper layer of a 2-layer earth model; the underlying half space is assumed to have a resistivity of 50 000 ohm-m.

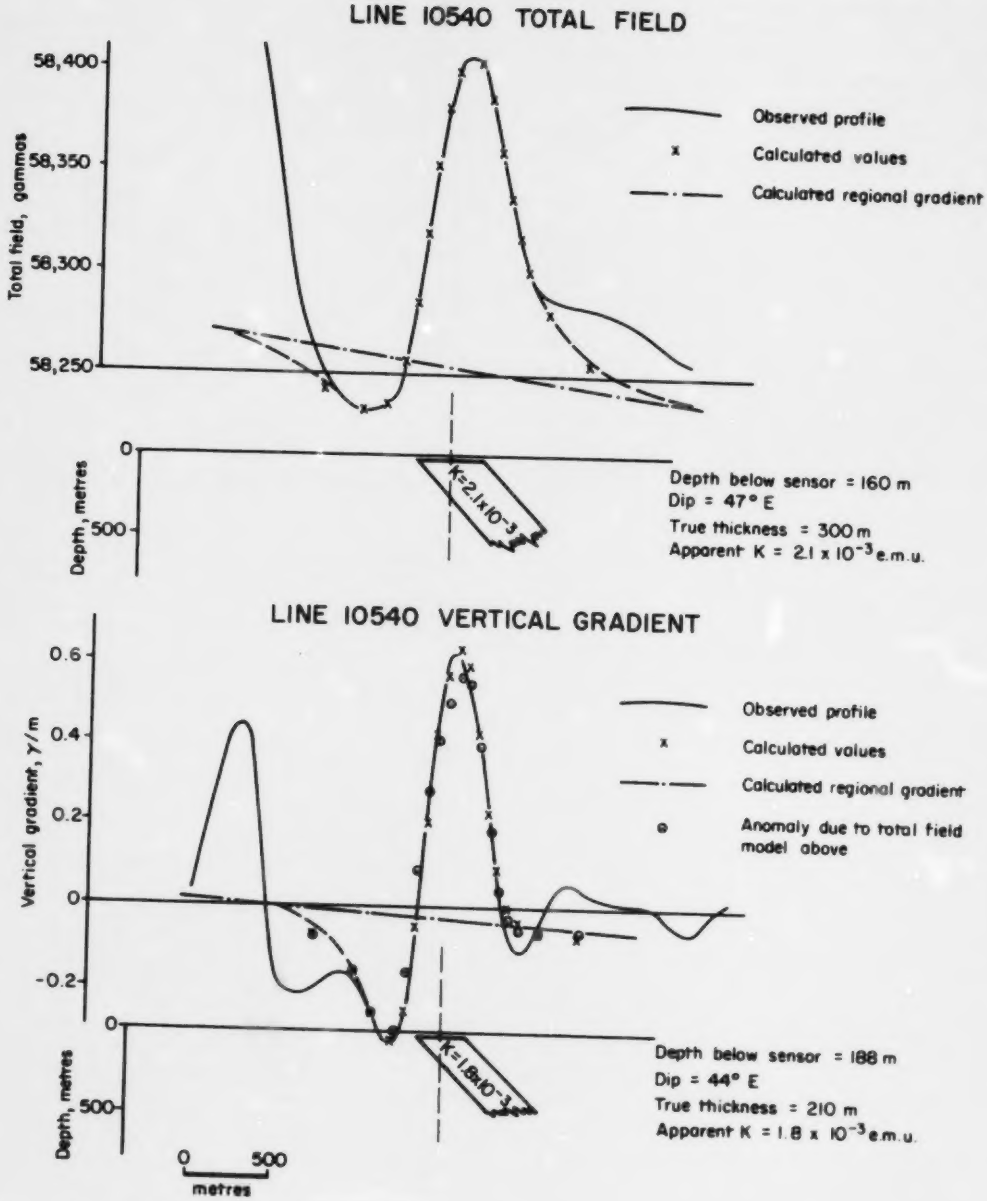

Figure 4. Magnetic anomaly inversion. Observed total field and vertical gradient anomalies are inverted to provide best-fitting 2-D, 2½-D, or 3-D magnetic source. Better accuracy is obtainable using gradient data.

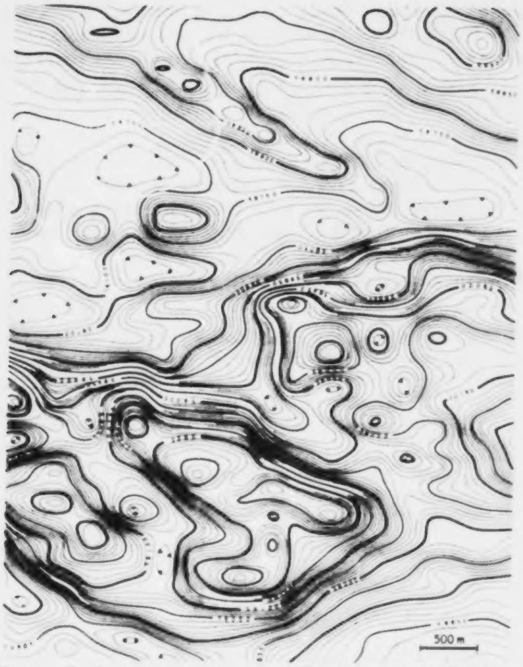

Figure 5. Aeromagnetic survey. Total magnetic field contours. Height 150 m. Line spacing 300 m. Contour interval 10 nT.

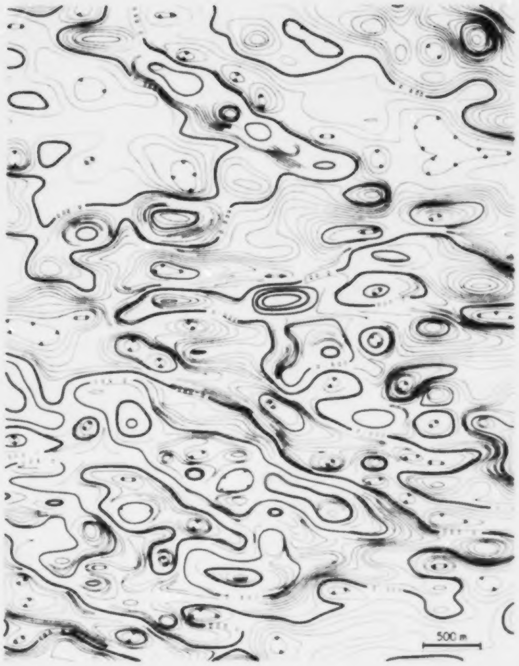

Figure 6. Aeromagnetic survey (see Figure 5). Vertical gradient contours. Contour interval 0.05 nTm.

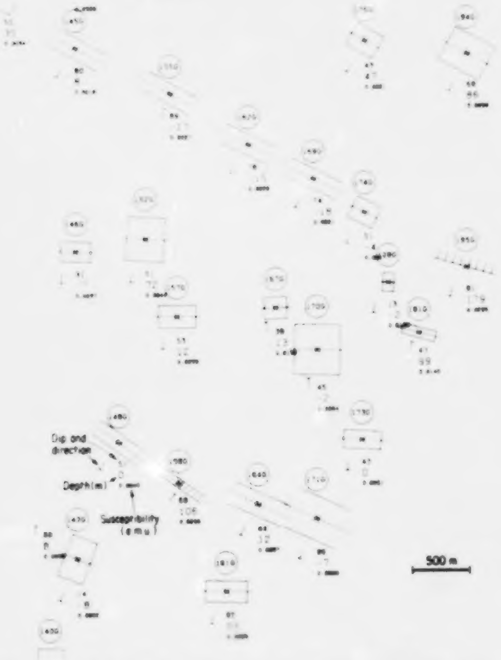
Dip and direction
Depth (m)
Susceptibility (emu)
500 m

Figure 7. Quantitative interpretation of Figure 6. Outlines of models interpreted from vertical gradient anomalies.

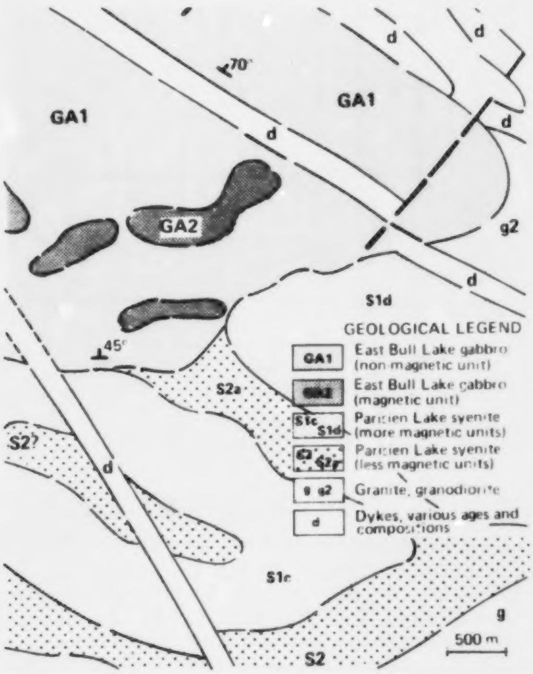
d
d
70°
GA1
GA1
d
d
GA2
g2
d
S1d
45°
S2a
S2?
d
S1c
g
S2
500 m
GEOLOGICAL LEGEND
GA1 East Bull Lake gabbro (non-magnetic unit)
GA2 East Bull Lake gabbro (magnetic unit)
S1c S1d Parisien Lake syenite (more magnetic units)
S2 S2r Parisien Lake syenite (less magnetic units)
g g2 Granite, granodiorite
d Dykes, various ages and compositions

Figure 8. Lithologic interpretation of Figures 5 and 6, incorporating data in Figure 7.

For the convenience of the reader, Figures 5, 6, 7, and 8 have been placed on 1 page. For further information on these figures, the reader is advised to contact the authors directly.

2. Within the range established by the operating system, changes in thickness and resistivity of the overburden are distinguishable from one another. Changes in depth to the top of the conductive layer are positively identified.
3. Since all the recorded EM data are used, there is no chance that a solution will be obtained that is incompatible with part of the data set.
4. The 2-layer model is more realistic than the half-space model in most of Canada. In areas of heavily weathered soils, a half-space version of the program can be adopted. In this case, the above 3 advantages are still valid.

Work is continuing in 1983 and 1984 on improvements to the above program. Also, an attempt will be made to develop a program that will accomodate multi-channel ground EM data.

VERTICAL MAGNETIC GRADIENT MODELLING

During the 1982 to 1983 fiscal year, a computer model-fitting program was developed to optimally fit the parameters of simple 2-D, 2½-D, and 3-D models to airborne or ground measurements of vertical magnetic gradient. This procedure, an extension of the company's MAGMOD computer program (Reeves 1981), is now in routine service, and has been available to industry users since 1982 through Dataplotting Services Limited's public library. Figure 4 illustrates the application to data in Northern Ontario.

The main advantages of modelling the gradient rather than (or in addition to) the total field include:

1. Gradient anomalies are sharper than total field anomalies and better resolved from the effects of adjacent bodies. There is therefore less distortion and a more accurate fit.
2. The base-level of the gradient anomaly is much easier to determine (1 less degree of freedom).

The gradient modelling technique has now been introduced as a subroutine to the company's semi-automatic version of MAGMOD (Reeves 1981) which allows large numbers of anomalies, recorded digitally during a survey, to be processed sequentially. This program has been used on several projects including the interpretation of the Geological Survey of Canada's airborne gradiometer survey of the AECL East Bull Lake (RA-7) research area, from which the following examples are drawn.

Figure 5 is an area of the total field anomaly map, and Figure 6 shows the same part of the vertical gradient anomaly map. Figure 7 shows the plan view of the models interpreted by analysis of this data. In total, over 200 anomalies were analyzed in this way, and very good agreement between model parameters for the total field and vertical gradient interpretations was demonstrated. Figure 8 is the final geological interpretation of the same part of the area, constructed with the aid of the modelling results.

The method is used also as the basis for preparing depth-to-basement maps as part of the process of mapping susceptibility on the basement surface. The following section describes the development of this new technique.

MAGNETIC INTERPRETATION (SUSCEPTIBILITY MAPPING)

Maps of apparent magnetic susceptibility have been a standard product of Peterson, Grant, and Watson Limited since 1973 (Grant 1973) and have been used in the preparation of pseudo-lithology maps of many km^2 of magnetically surveyed terrain. Versions of the program have been used, for example, by Bambrick *et al.* (1982) and Yunshen *et al.* (1982), to characterize the magnetic signatures of a variety of mineralized areas.

All of these techniques have, to date, involved operations such as downward continuation and reduction to the pole, all carried out, after Fourier transformation, in the wave number domain. All of them suffer from an assumption of uniform depth to the surface upon which the magnetic susceptibility is being calculated. In practice, as, for example, in the Hudson Bay or James Bay lowlands, the depth to the Precambrian basement can vary from a few m to several hundred m for a distance of a few km (Figure 9).

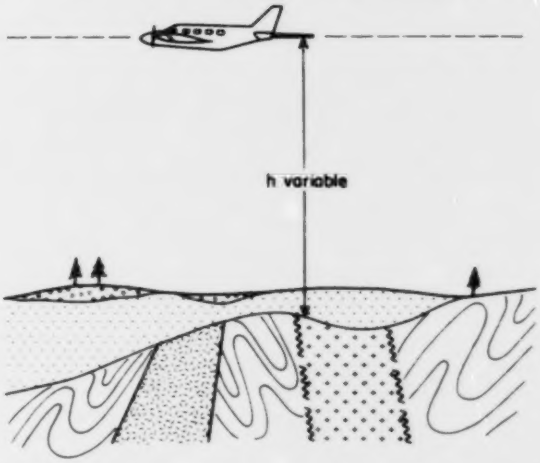

Figure 9. Aeromagnetic survey over basement of varying depth.

By assuming a constant depth, the calculated susceptibilities are not only incorrect, but the patterns are badly distorted, leading to poor definition of unit boundaries.

A spatial domain procedure (SDSUSC) has been developed that permits a depth to be assigned to each grid point of an X-Y gridded data set. The magnetic susceptibility is varied iteratively at each point until the calculated field on the surface of measurement is equal to the measured field (Figure 10).

Initial attempts to apply the method were unsuccessful. Resolution was poor and short wavelength noise was severe. After experimenting with several field data sets, it

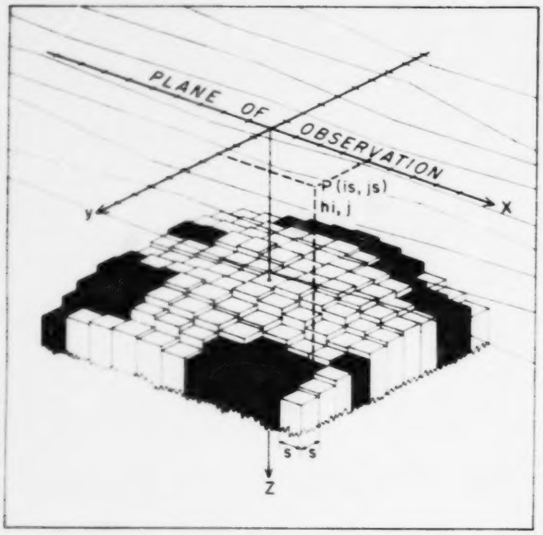

Figure 10. Method of calculating magnetic susceptibility of basement from a gridded set P (is, js) at variable height (h . j).

was decided to work with synthetic fields over simple bodies. Figure 11 illustrates the results of tests over a single prism, before and after program modifications.

The new program has been applied successfully to several sets of recent high resolution aeromagnetic data, including one over a major cratonic sedimentary basin. A portion of the total field data is illustrated in Figure 12. A regional depth to basement map (Figure 13) has been generated over the survey area using magnetic depths as calculated from the measured vertical magnetic gradient profiles (Reeves 1981). The depth within this part of the survey area varies from 126 m to over 800 m. The global minimum depth over the whole survey area was near the edge of the basin, a shallow 50 m. Initial susceptibility calculations were carried out using Fourier domain techniques assuming a uniform basement depth of 50 m below ground surface (Figure 14). This continuation depth was selected in order to approach the basement surface, and yet not unduly distort the shallower magnetic features. This initial susceptibility map has not shown the desired resolution of the deeper part of the basement, as evident in the region of the large anomaly in the centre of Figure 14. In order to obtain the required resolution at depth the susceptibility map would have to be calculated at a depth of at least 500 m below ground. If this was done throughout the area, shallow sources would be unduly amplified and badly distorted.

The solution to the problem lies in generating the susceptibility map on an uneven bedrock surface. Combining the total field map and the depth-to-basement map, a susceptibility map of the "true" basement surface may be generated (Figure 15) using the SDSUSC program.

The deeper regions of the area have been resolved to the same detail as the shallow regions, and magnetic signatures can be interpreted (Figure 16) with more confidence across the sloping basement surface.

The underlying algorithm upon which the SDSUSC program is based superimposes a grid (*see* Figure 10) having the same dimensions as the gridded data set upon the magnetic basement surface. Each cell of the grid represents the top of a square-ended, vertical-sided prism which is inductively magnetized in the earth's magnetic field. The magnetic susceptibilities of the prisms are calculated such that their aggregate magnetic field intensities or their vertical gradients match the geomagnetic anomaly values (with the geomagnetic component removed) at all grid points of the data set. Since the inversion of very large matrices is impractical, the calculations are performed by successive approximation using only the prisms contained within a "window" of a certain size surrounding the point at which the calculation is made. Special techniques are used for compensating the solutions for the finite window size, and for accelerating the convergence of the calculations in troublesome areas.

In making the calculations, the actual elevations of the prisms and the actual heights of the grid points (that is, the actual vertical distances between the grid points and the magnetic basement surface) are used, so that the magnetic basement surface need no longer be considered to be horizontal, and the survey data need no longer be assumed to have been acquired at a constant (barometric) elevation. This allows for the calculation of apparent susceptibilities on uneven surfaces and, by extension, for the continuation of magnetic fields between general surfaces.

GRAVITY INTERPRETATION

Two new programs for interpreting gravity survey data were developed in conjunction with the Ontario Geological Survey during 1982. The first is for calculating bottom elevations of basin-like structures in which the density varies laterally. It is an extension of the conventional basin-fitting algorithm (fixed upper surface, variable lower surface) which allows each vertical prism to have a different density contrast. The second program calculates an apparent bedrock density down to given depth from gridded Bouguer gravity data, using Fourier domain operations. This algorithm, like the first, assumes that density varies laterally but not vertically.

Both of these programs were used in the interpretation of a large-scale gravity survey in central Ontario (Gupta and Grant 1982). It was demonstrated that because the densities of rocks are determined by their major component mineralogy, apparent density is particularly effective for mapping lithologies. In addition, the 3-D picture that was obtained by using a combination of apparent densities and actual measurements determined from more than 2800 samples, introduced an important new dimension to the structural interpretation of major intrusive bodies within the area.

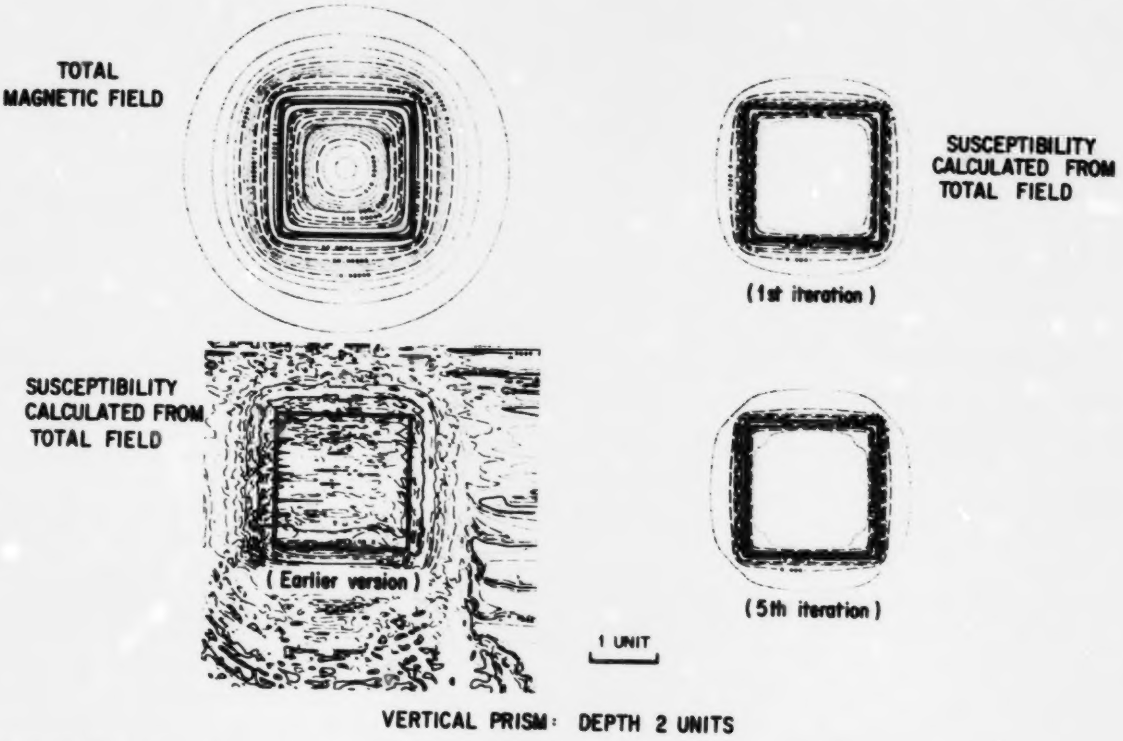
TOTAL MAGNETIC FIELD
SUSCEPTIBILITY CALCULATED FROM TOTAL FIELD
(1st iteration)
SUSCEPTIBILITY CALCULATED FROM TOTAL FIELD
(Earlier version)
(5th iteration)
1 UNIT
VERTICAL PRISM: DEPTH 2 UNITS

Figure 11. Calculation of magnetic susceptibility from synthetic total field data over a vertical prism. Development of the method.

A version of the method (DENS3-D) has been used to interpret the structure of the gabbro-anorthosite intrusion at East Bull Lake (AECL RA-7). Figure 17 shows the depth to the base of the sill, calculated on a 500 m by 500 m grid using the results of detailed surface density measurements.

FUTURE PLANS

In the current (and final) year of the program, emphasis will be placed on completing the work described in this paper. In addition, attempts will be made to develop user-friendly software for:

1. 2-layer inversion of ground EM data
2. rapid and systematic forward modelling of 1-, 2- and 3-D susceptibility distributions
3. colour presentations of multi-channel gamma-ray spectrometer data to reveal both relative and absolute element abundances

ACKNOWLEDGMENTS

The Company is grateful to the Ontario Ministry of Natural Resources for its financial assistance and for the cooperation of the staff of the Ontario Geological Survey in various aspects of the work.

The authors wish to thank Atomic Energy of Canada Limited for permission to publish examples from studies made at the East Bull Lake research area.

The following made valuable contributions to the work described in this paper: R.N. Edwards, P.W. Walker, I.N. MacLeod, S.W. Reford, C.V. Reeves, and J.D. Panar.

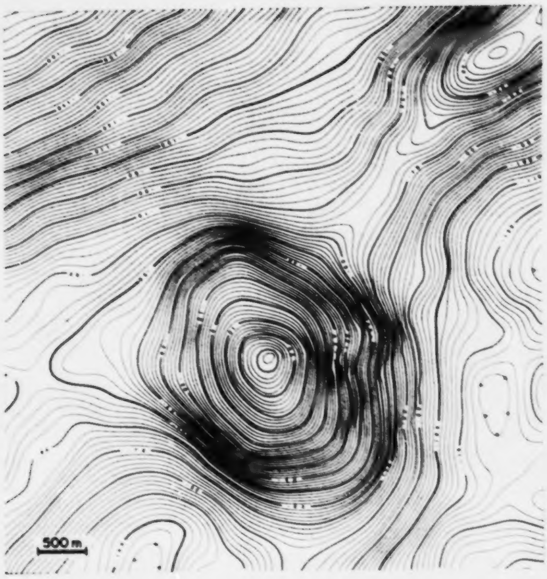

Figure 12. High resolution aeromagnetic survey over a major cratonic basin. A base level of 61 000 nT has been removed. Contour interval 2 nT.

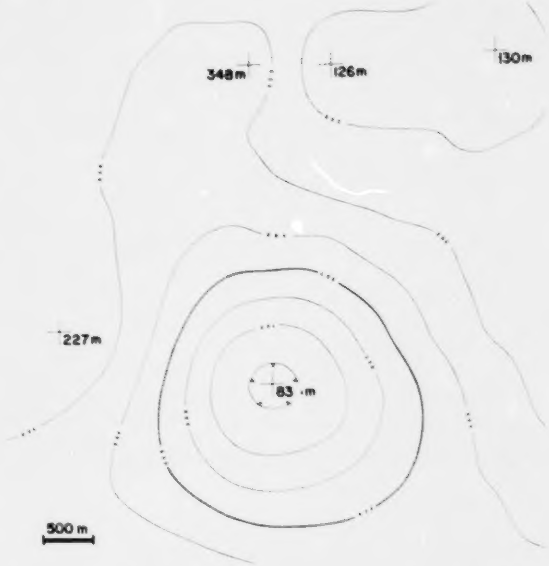

Figure 13. Basement depth contour map generated from calculated vertical magnetic gradient model depths. Contour interval 100 m. Depths measured below ground surface; flight elevation 150 m above ground surface.

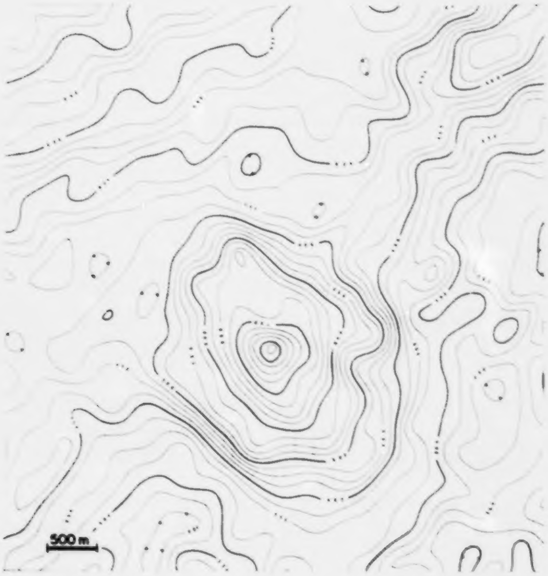

Figure 14. Apparent magnetic susceptibility map, assuming basement depth of 50 m below ground surface. Contour interval 200 x 10^{-6} emu.

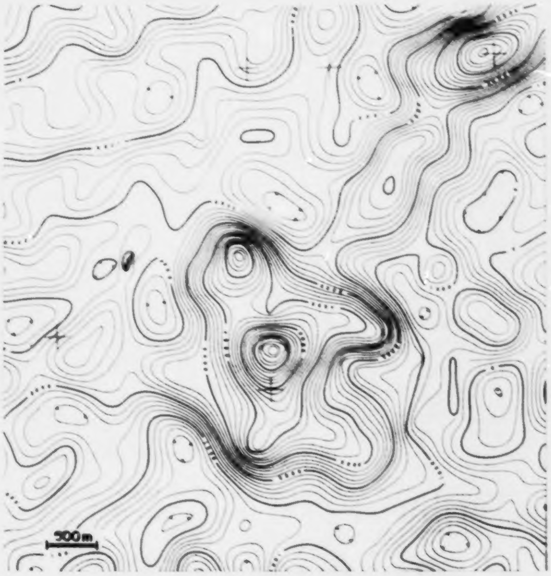

Figure 15. Variable depth susceptibility map calculated for the basement surface defined in Figure 13. Contour interval 200 x 10^{-6} emu.

For the convenience of the reader, Figures 12, 13, 14, 15 have been placed on 1 page and figure 16 on the facing page. For further information on these figures, the reader is advised to contact the authors directly.

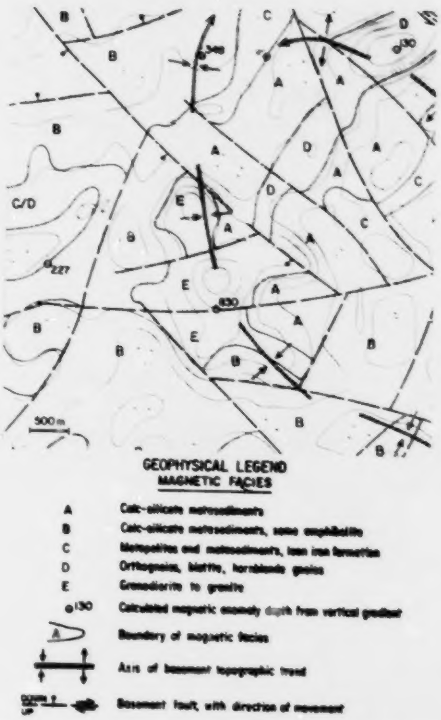

B
C
D
A
C/D
E
227
830
130
500m
GEOPHYSICAL LEGEND
MAGNETIC FACIES
A Calc-silicate metasediments
B Calc-silicate metasediments, some amphibolite
C Metapelites and metasediments, lean iron formation
D Orthogneiss, biotite, hornblende gneiss
E Granodiorite to granite
130 Calculated magnetic anomaly depth from vertical gradient
Boundary of magnetic facies
Axis of basement topographic trend
Basement fault, with direction of movement

Figure 16. Geological interpretation of variable depth susceptibility map.

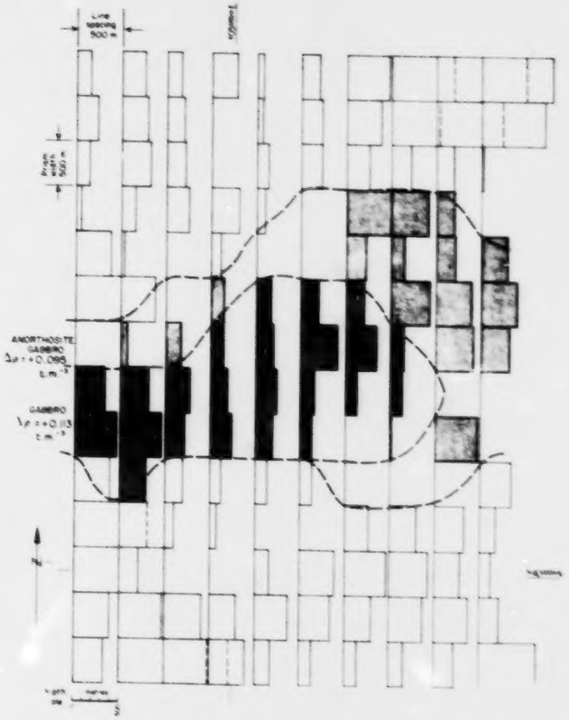

Line spacing 500 m
ANORTHOSITE GABBRO Δρ = +0.095 t.m⁻³
GABBRO Δρ = +0.113 t.m⁻³

Figure 17. 3-D inversion of gravity data based on detailed surface density measurements.

REFERENCES

Bambrick, James, Letros, L., Strangway, David W., and Geissman, J.
1982: Apparent Magnetic Susceptibility (SUSC) Mapping in Theory and Practice; 52nd Annual Meeting, Society of Exploration Geophysicists, October 17-21, 1982, Dallas. Technical Program Abstracts and Biographies, p.238-241.

Edwards, R.N., Bailey, R.C., and Garland, G.J.
1981: Conductivity Anomalies: Lower Crust or Asthenosphere?; Physics of the Earth and Planetary Interiors, Volume 25, p.263-282.

Fraser, Douglas C.
1979: The Multicoil II Airborne Electromagnetic System; Geophysics, Volume 44, p.1367-1394.

Grant, F.S.
1973: The Magnetic Susceptibility Mapping Method for Interpreting Aeromagnetic Surveys; 43rd Annual International Meeting, Society of Exploration Geophysicists, Mexico City, November 1973. Preprint available from author.

Gupta, V.K., and Grant, F.S.
1982: Mineral Exploration Aspects of Gravity and Aeromagnetic Maps of Ontario; 52nd Annual Meeting, Society of Exploration Geophysicists, October 17-21, 1982, Dallas. Technical Program Abstracts and Biographies, p.371-372.

Palacky, G.J.
1981: The Airborne Electromagnetic Method as a Tool for Geological Mapping; Geophysical Prospecting, Volume 29, p.60-88.

Paterson, Norman R., Edwards, R.N., and Reford, S.W.
1982: Continuous Two-layer Inversion of Multi-coil EM Data; 9th Annual Meeting of CGU, York University, May 10-12, 1982. Technical Program Abstracts, p.20. Preprint available from authors.

Pitcher, D.H., Barlow, R.B., and Lewis, M.
1980: Tridem Airborne Conductivity Mapping as a Lignite Exploration Method; Canadian Institute of Mining and Metallurgy Bulletin, Volume 73, p.53-63.

Reeves, C.V.
1981: Optimising the Interpretation of Magnetic and Gravity Data by Computer Inversion of Numerous Selected Anomalies; 51st Annual International Meeting, Society of Exploration Geophysicists, Los Angeles, October 11-15, 1981. Technical Program Abstracts and Biographies, p.35-36. Preprint available from author.

Wiggins, R.A.
1972: The General Linear Inverse Problem: Implication of Surface Waves and Free Oscillations for Earth Structure; Reviews of Geophysics and Space Physics, Volume 10, p.251-258.

Yunshen, S., Urquhart, W.E.S., Strangway, D.W., and Fengxing, Sun
1982: Geological Interpretation of Aeromagnetic Surveys in the Precambrian of Quebec and China; 52nd Annual Meeting, Society of Exploration Geophysicists, October 17-21, 1982, Dallas. Technical Program Abstracts and Biographies, p.241-244.

Grant 012 A) Determination of Short-Lived Isotopes by Neutron Activation Analysis and B) Investigation of Commercial Viability of Prompt Gamma Analysis

A) E.L. Hoffman[1], P.C. Ernst[2],
A. Pidruczny[1], W. Hutton[1]
B) M.D. Higgins[1,3], M.G. Truscott[1,3],
E.L. Hoffman[1], D.M. Shaw[3],
M. Bergeron[3], G.H. Buffet[3],
J.R.D. Copley[2], W.V. Prestwich[4],
A. Pidruczny[1], and W. Hutton[1]
[1]Nuclear Activation Services Limited, McMaster Nuclear Reactor, 1280 Main Street West, Hamilton
[2]McMaster Nuclear Reactor, McMaster University, Hamilton
[3]Geology Department, McMaster University, Hamilton
[4]Physics Department, McMaster University, Hamilton

ABSTRACT

The development of the short-lived neutron activation analysis (SLNAA) facility is described. This system is now providing commercial analysis for certain, selected, trace elements. The low-cost multielement capability should be completed in the coming year. Data for Se and In on some selected international standard are presented.

The prompt neutron activation analysis (PGAA) gamma facility is described with data for B and Gd presented on international standard materials. Some results on projects being conducted using the system are also discussed. Automation of this system is being undertaken this year, thus lowering the cost of analysis.

A) SHORT-LIVED ACTIVATION ANALYSIS

INTRODUCTION

Neutron activation analysis involves the bombardment of samples by neutrons produced in a nuclear reactor. The neutrons induce nuclear reactions among the elements in the sample, leading in many cases to the formation of radioactive isotopes. As these radioisotopes decay, they emit characteristic radiation. The measurement of the emitted radiation is achieved using high resolution, hyperpure germanium detectors linked to multichannel analyzer-computer systems. These systems can resolve the complex multielement gamma-ray spectra obtained from the activated sample.

The advantage of the technique is that the method can be very accurate; detection limits for many elements are much lower than those obtained by conventional techniques such as plasma emission, atomic absorption (both flame and flameless), or X-ray florescence. INAA (Instrumental Neutron Activation Analysis) is also a multielement technique where quantitative information can be obtained simultaneously on as many as 35 elements, all of this instrumentally with no chemical treatment required, eliminating the problems attendant on chemical treatment. All of this can be achieved in a reasonable time frame and at a competitive price relative to other analytical techniques.

Activation analysis involves the measurement of radiation emanating from an activated sample. One of the factors which governs the delay time after irradiation before counting the sample, is the radioisotopes' half-life. The half-life for different radioisotopes can vary from a fraction of a second to many years. Much of the work done prior to this Exploration Technology and Development Fund development program mainly involved the so-called long-lived isotopes which have half-lives of the order of hours, days, and years. These samples could be batch-irradiated, and are usually counted 4 to 8 days after irradiation.

The determination of short-lived radioisotopes on the other hand, or those with half-lives of seconds to minutes, involves a different type of procedure. The sample must be irradiated for a brief period, usually a few seconds. The sample which is contained in a "rabbit" (polyethylene capsule) is then transferred to a high resolution detector for immediate counting. The multielement gamma spectrum obtained is then analyzed.

The technology we have developed by designing, building, and operating our computer-automated delayed neutron counting facility was used extensively in the design of our new transfer system, essential for the short-lived radioisotope determinations. With this system samples are transferred from a sample loader station through a maze of polyethylene tubing to an appropriate sample irradiation facility. After a few seconds, the sample is usually transferred to the receiving station at the detector where the gamma radiation of the sample will be counted. For certain samples, it may be advantageous to wait a few minutes after irradiation to let certain highly active radioisotopes die away before counting. This can be done with our system by programming a delay-to-count time. All the above operations are done under microprocessor control with very little human interaction. The transfer system is linked to a Canberra Series 85 multichannel analyzer which is linked to a PDP 11/44 computer.

PROGRESS REPORT AND FUTURE PLANS

The microprocessor-controlled transfer system for the short-lived isotopes has been completed with the installation of a new sample receiving station and is currently operating satisfactorily. Replacement of the sample receiving station was necessary because of the diverse nature of the geological samples that were being tested. This required that the sample to detector distance be modified with virtually every sample being run. The new sample receiving (Figure 1) station changes the sample-to-detector distance an appropriate amount based on the activity of the sample. This last modification has allowed us to begin offering commercial analytical services for selected short-lived radioisotopes. The multielement capability of the system is not yet operational. The reasons for this are the length and complexity of the computer programs required to reduce the data. The existing PDP 11/34 computer with 256 kilobytes of memory (maximum), could not adequately handle the task and has been replaced with a PDP 11/44 computer, with 1256 kilobytes of memory and is expandable to 4000 kilobytes of memory. This, combined with the addition of floating-point hardware has enabled us to gain a factor of approximately 20 in speed thus reducing the computing time for each sample from 20 minutes to approximately 1 minute. The large number of samples

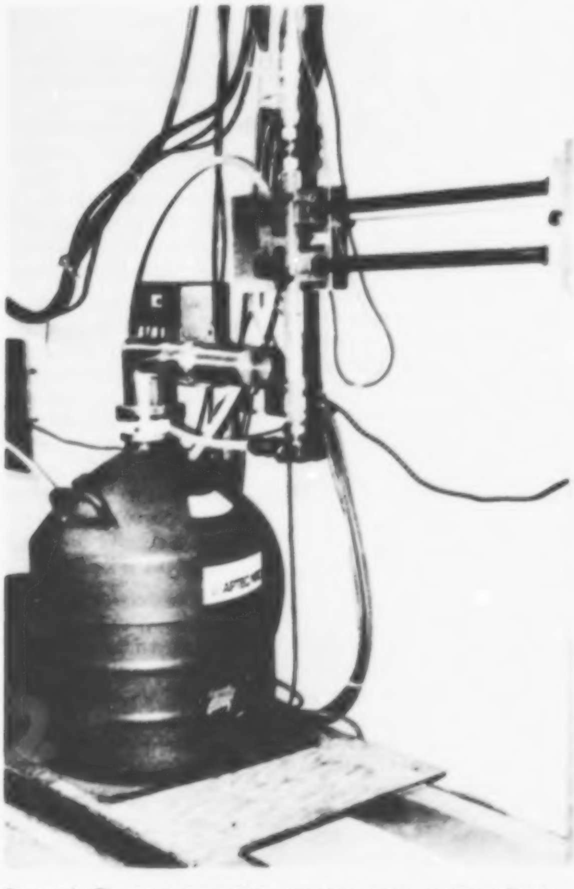

Figure 1. The programmable sample receiving station from the short-lived activation system.

anticipated for this system and the prompt gamma system have necessitated increasing the disc storage space from 20 megabytes to 180 megabytes. At the time of writing, this additional 160 megabyte disc drive has been delivered and is being installed. To further increase the power of the computing system, we are in the process of upgrading our operating system from RSX11M V3.2 to V4.0.

Programming to reduce the complex spectra will continue concurrently with the programming on the prompt gamma system. The basic mode of the programs is the same, with minor variations for each different mode of analysis. The programming task has been slower than anticipated due to the complexity of the job and the need for a higher speed processor which is now in place.

ANALYTICAL CAPABILITIES

We have ascertained that the neutron flux for both the thermal and epithermal irradiation sites varies by < 2% at 12 hours after startup until shutdown. Although standards are run along with the samples, this is done mainly as a check on the system rather than for calibration purposes.

It is somewhat difficult to give detection limits for various elements because of the diverse matrices of samples being sent for analysis by this technique. For example, the detection limit for Se by this technique is as low as 0.04 ppm on vegetation, whereas it may vary on rock samples from 1 to 5 ppm depending on the nature of the samples (Table 1). Improvements on these detection limits may be achieved by cyclic activation analysis. For certain trace elements, data at low levels is very sparse. An example of this is In. Table 2 shows the recommended value versus that obtained by NAS on In.

Elements other than Se and In which have been determined using their short-lived isotopes include Al, Ba, Br, Ca, Cl, Cu, Dy, Eu, Hf, I, Mg, Mn, Nb, K, Na, Sr, S, Ti, U, and V. The determination of Eu via its short-lived isotope has in fact allowed us to introduce a rare earth mineral exploration package at about ¼ the cost of our rare earth research package (see NAS 1983 price list). We would hope to include many of the above elements in a multielement package to be available in the coming year.

B) PROMPT GAMMA ANALYSIS

INTRODUCTION

Prompt gamma neutron activation analysis (PGNAA) is based on the detection of gamma-rays emitted by samples during neutron irradiation. To utilize this technique, a beam of neutrons from the core of the reactor is obtained using a beam port. The sample is encapsulated in a teflon container and is then placed in the beam of neutrons. Interaction of the neutrons with the sample yields prompt gamma-rays, which are measured with a hyperpure germanium detector connected to a conventional multichannel analyzer-computer system.

The prompt gamma technique has several advantages. Since the response for all elements is instantaneous, all elemental contributions occur independent of timing. No *a priori* information regarding sample content is needed since it is not necessary to adjust irradiation and counting period parameters. There are also no half-life limitations. The gamma-rays continue to be emitted as long as the sample is being irradiated. All elements interact

TABLE 1: RECOMMENDED VALUES FOR Se ON SAME SELECTED INTERNATIONAL STANDARDS BY NUCLEAR ACTIVATION SERVICES LIMITED.

STANDARD	RECOMMENDED (ppm)	FOUND (ppm)
USGS-GxR-1	19 **	21
NBS-1632A	2.6 *	2.7
NBS-1633A	10.3 *	10
USGS-GxR-4	6 **	6.6
NBS-1577	1.1 *	1.1
IAEA A13	–	0.21,0.33,0.28,0.33
IAEA MA-A2	0.5→11.3 ***	0.26,0.14
IAEA H-4	0.28 ***	0.94,1.02,1.05 0.28,0.30

*U.S. National Bureau of Standards recommended
** Abbey 1980 recommended
*** I.A.E.A. recommended or suggested numbers

TABLE 2: RECOMMENDED VALUES FOR In VERSUS THOSE OBTAINED BY NUCLEAR ACTIVATION SERVICES LIMITED.

STANDARD	RECOMMENDED (ppm)	FOUND (ppm)
MP-1	690*	690

* CANMET
There is only one certified reference material for "In" in the ppm range

more or less, so the method is suitable for multielement analysis in geological samples. The method is particularly advantageous in those cases where neutron capture produces no suitable radioisotope for normal activation analysis. Some of the elements which have good potential by this method are Cd, Ni, Si, C, H, Ti, Fe, Cr, B, N, Al, Cu, Gd, and Nd.

DESCRIPTION OF THE PROMPT GAMMA NEUTRON ACTIVATION ANALYSIS FACILITY

Original development of this facility was initiated in the Physics department at McMaster University and continued in the McMaster Isotopic and Nuclear Geochemistry Studies (MINGS) research group with the cooperation of personnel from the McMaster Nuclear Reactor. The feasibility of constructing a dedicated facility which could be used for commercial analytical purposes has been undertaken over the past 2 years. The development as a geochemical research facility has now been extended to commercial applications, through agreement between D.R. Smith, Director, McMaster Nuclear Reactor, D.M. Shaw of the MINGS research group, and Nuclear Activation Services Limited (NAS), now that the feasibility stage has been completed successfully.

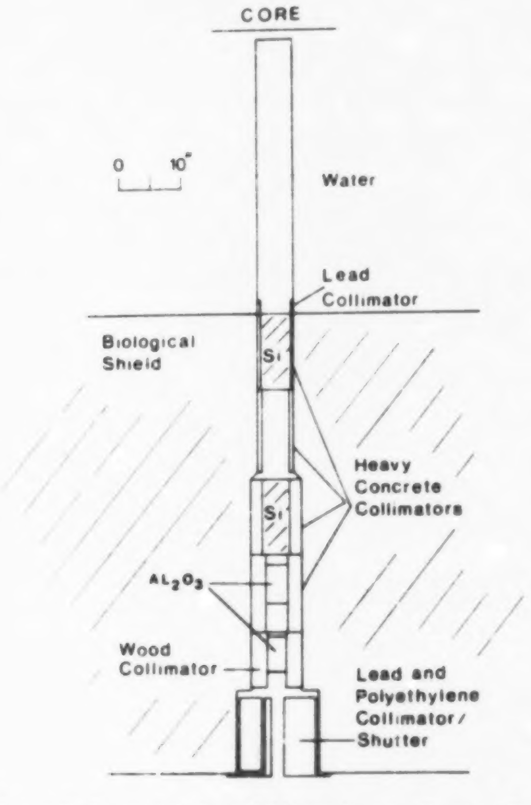

Figure 2 Beam-port 4 at McMaster Nuclear Reactor. The locations of the silicon (Si) and sapphire (Al_2O_3) crystals are indicated on the figure. The beam may be partially shut off by a rotatable shutter of lead and polyethylene.

During the last year, numerous modifications to the instrument have been completed. These have resulted in considerable improvement in performance. We do not envisage any major modifications in the immediate future, with the exception of changes to the sample handling system (see below). The beam ports at the McMaster Nuclear Reactor view the core directly, hence the beams have a large component of fast neutrons and gamma-rays. These must be removed for health reasons and to safeguard the detector. A combination of 60 cm of silicon crystals (12 cm diameter) and 30 cm of sapphire crystals (Figure 2) is used for this purpose. This arrangement gives approximately twice the neutron flux of earlier versions, where bismuth was used in place of one of the sapphire crystals. The neutron beam is shaped by lead, heavy concrete, wood, and polyethylene collimators. Final beam shape is controlled by a collimator-shutter of lead and polyethylene. The beam may be shut off by rotation of this assembly. However, beam cut-off is not complete as fast neutrons can still penetrate the shutter.

Once the beam enters the 'cave', it is constrained by a tunnel of $^{6}LiCO_3$ in wax (Figure 3). The beam is stopped by a block of $^{6}LiCO_3$ in wax, wrapped in aluminum foil. Tritium production does not appear to be excessive. The $^{6}LiCO_3$ block is set in a large block of barytes concrete (Figure 4). The thermal neutron flux at the sample position is 4×10^7 ns^{-1} cm^{-2} in a beam 5 cm by 7 cm. The fast neutron flux is too small to measure.

The gamma-ray detector is a 12% efficient intrinsic Ge detector specially manufactured to be free of boron-bearing components. It is situated 20 cm from the sample position. It must be well shielded from neutrons, which cause damage and extraneous gamma-rays. This is achieved by a 1 cm thick cap of $^{6}LiCO_3$ in wax, 4.5 to 20 cm of lead, 5 cm of wax, and 2 to 4 mm of boroflex (borated rubber). The thermal neutron flux through the detector is estimated to be approximately 1 $ns^{-1}cm^{-2}$. Data from the detector is analyzed using a Canberra Series 85 MCA and a combination of Canberra model 2020 amplifier and model 8621 ADC. The series 85 MCA is interfaced to the PDP 11/44 computer described under the previous section.

The encapsulation of the sample material at the present time involves the weighing of the powder into a 1 cm diameter teflon tube about 7 cm long with polyethylene plugs on each end. The sample is then manually placed on the end of a teflon rod and inserted into the neutron beam. All of these procedures are very time consuming and expensive with respect to labour and materials. As a result of this, the throughput of samples sent for commercial analysis by this technique has been slow and relatively expensive ($20 for the first element and $1 for any additional element determined at the same time).

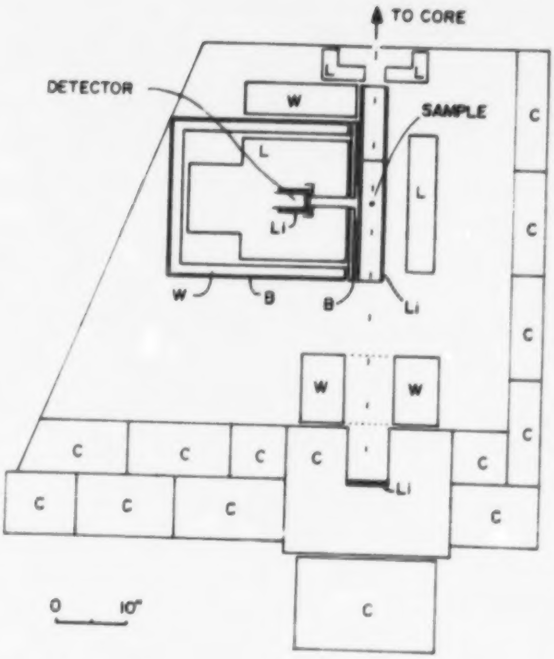

Figure 3 The filtered neutron beam enters the 'cave' at the tip of the diagram. The beam is constrained by lead (L) blocks and a tunnel of ^{6}Li Co_3 in wax (Li) when it passes in front of the detector. The beam is stopped by a barytes loaded concrete block (C) lined with ^{6}Li Co_3 in wax. The detector is shielded by boroflex (B), wax (W), lead (L) and ^{6}Li Co_3 in wax (Li).

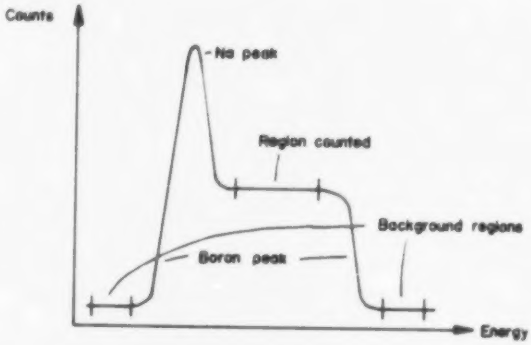

Figure 4 Gamma-ray spectrum of the Doppler widened boron peak at 478 KeV showing the interference from sodium.

Redesign of the sample container to a molded teflon vial with lid will lower these costs. Teflon is required because of neutron absorption and scattering by H in polyethylene.

A simplified version of the microprocessor-controlled transfer system developed for our short-lived activation project, is being designed. This would allow the rapid, unattended counting of samples as is the case with the type of system we are currently using for uranium analysis by delayed neutron counting. This simplification will lower the cost of the elemental analysis to a price range amenable to large scale geochemical projects (in the order $5 + $1 for each additional element range).

The automated counting of large numbers of samples by prompt gamma-analysis will generate vast amounts of spectral data which will have to be reduced. Modifications to the computer acquisition and storage system have been described under the previous section.

ANALYTICAL PERFORMANCE OF THE SYSTEM

During the past 2 years, we have been able to show the feasibility of determining a variety of elements by prompt gamma analysis to levels not attainable by other analytical techniques. Two of the more notable elements among these, have been boron and gadolinium. The ultimate sensitivity for B appears to be 0.1 ppm on a 3 g sample but that of Gd is also 0.1 ppm. The determination of the sensitivities for other elements is also underway at the present time. Although the throughtput of samples is very slow, commercial analyses for B and Gd are currently being provided.

Calibration of the system was achieved using synthetic boron and gadolinium standards. Data on these 2 elements on selected international rock reference materials are listed in Tables 3 and 4 respectively.

Extensive work on the determination and geochemistry of boron has been conducted by the MINGS group using this system. The following summary reflects their findings.

MINGS GROUP

The initial interest of the group was in the geochemistry of boron. A large amount of calibration data has been collected on this element. A filter-paper standard loaded with 50 μg of boron was analyzed 56 times from December 1982 to April 1983 in order to monitor variations in the flux of neutrons at the beam-port and to check the alignment of the sample holder. Standard deviation of all 56 measurements was 5%, roughly comparable with the error expected from counting statistics.

The primary calibration was the addition of standard boric acid solutions to a powdered peridotite that is almost free of boron, followed by drying to remove water. Twenty such standards between 2 and 1000 μg yielded a correlation coefficient of 0.999. To test the effects of rock matrix on count rate, rock standards were prepared with 50 and

TABLE 3: RECOMMENDED NUMBERS WHERE AVAILABLE FOR B VERSUS THOSE OBTAINED BY PROMPT GAMMA ANALYSIS ON SELECTED INTERNATIONAL STANDARDS.

STANDARD	RECOMMENDED (ppm)	FOUND (ppm)
CANMET SY-3	110	111,106
CANMET SY-2	85?	91,90
USGS GxR-2	44?	42
N1MG	8?	5.3
IAEA SOIL-5	63 *	86,82
NBS-1632A	53 **	52,53
NBS-1633A	39 **	38
CANMET MRG-1	13? ***	1.7,1.3
IAEA SL-1	39 *	38,36
USGS QLφ1	155	166
USGS MAG1	41	46
CANMET MA-1	*****	12,11
CANMET MA-2	*****	11,12
CANMET PR-1	*****	3.0,1.7
CANMET HV-1	*****	15,15
NBS-1571	33**** 32**	31,32
NBS-1577	3.2	3.0,2.9
IAEA V-9	*****	6.4
IAEA A-13	*****	1.8,1.4
IAEA H-4	*****	2.6,1.4
IAEA SD-N-1	*****	64,66

NOTES

All values are recommended numbers of Abbey (1980) except

* IAEA recommended numbers

** Gladney 1980

*** Previously recommended 5? Abbey (1977)

**** Certified NBS

***** No data available

TABLE 4: RECOMMENDED NUMBERS FOR Gd VERSUS THOSE OBTAINED BY PROMPT ANALYSIS ON SELECTED INTERNATIONAL STANDARDS.

STANDARD	RECOMMENDED (ppm)***	FOUND (ppm)
CANMET SY-3	55?	123,117
CANMET SY-2	*****	16,16
USGS GxR-2	*****	3.0
N1M G.	11?	11,9.6,12
IAEA SOIL-5	35? ** (typographical error?)	4.5,4.1
NBS-1632A	1.95*	2.0,1.8,2.0,2.0,1.9
NBS-1633A	16.3*	16,17
CANMET MRG-1	*****	3.6, 4.0
IAEA SL-1	12 **	7.6, 7.5
IAEA SD-N-1	*****	4.1,4.1
CANMET MA-1	*****	5.5,5.3
CANMET MA-2	*****	6.0,6.1
CANMET PR-1	*****	0.8,0.7
CANMET HV-1	*****	0.9,1.2
IAEA H4	*****	<0.1, <0.1
IAEA MAA-2	*****	<0.1,<0.1
IAEA V-9	*****	<0.1, <0.1
NBS -1577	<0.1*	<0.1,<0.1
NBS -1571	<0.1→0.1*	<0.1, <0.1

NOTES

All recommended numbers are those of Abbey (1980) except

* Gladney 1980

** IAEA information only values (non-certified)

*** No certified values are available

***** No information available

100 μg boron spikes in granite, shale, peridotite, and silica sand powder. There was no detectable effect of matrix on the count rates at these levels.

Tests were conducted to measure the effect of neutron self-shielding on the count rate. Very little effect was noted up to 1000 ppm. Samples with higher boron abundances than this are diluted with magnesia before analysis.

The calibration for boron indicates that the sensitivity is 0.7 counts $\mu gB^{-1}s^{-1}$, using the whole boron peak at 478 Kev. In order to avoid the Na peak at the lower end of the Doppler broadened boron peak, the MINGS group usually counts only on a flat region that covers half the peak (Figure 4). Experiments indicate that addition of up to 5% Na_2O has no detectable effect on the count-rate in this region.

Accuracy at low abundance levels is dominated by corrections for the boron blank. The system blank is 0.5 μg equivalent or 0.17 ppm in a typical 3 g sample. The regular sample package contributes a similar amount to the blank, but the samples can be irradiated in a low-blank package as required. The system blank is very stable, hence one can measure 0.1 ppm in a 12 hour irradiation of a 3 g sample.

International standard reference samples/and local standards were also analyzed, and an interlaboratory comparison was made with D.B. Curtis of Los Alamos National Laboratory, New Mexico (Table 5). Curtis uses U.S. National Bureau of Standards standard 1571, Orchard leaves, as his standard, as this is the only U.S. National Bureau of Standards reference standard certified for Boron at these abundance levels. We have used a chemical standard for our analyses. If we recalculate our data to give the certified value for NBS 1571, then there is good agreement between our data and that of Curtis.

Some current projects using the prompt gamma neutron activation analysis system includes the analysis of cherts from bedded siliceous sediments, nodules, and banded iron formations to test the feasibility of using boron as an indication of paleosalinity (Truscott and Shaw 1983). The abundances in spinel lherzolite xenoliths to determine the boron budget in the earth have been measured, which leads to the conclusion that condensation temperatures from the solar nebula appear to have been higher than previously estimated (Higgins and Shaw 1983). Alteration of basalts in marine and terrestrial environments has been monitored using boron abundances (Bergeron *et al.* 1983). A number of mineralogical projects are currently underway, and a project to discover if boron may be used as an indicator element in geochemical exploration for various metals is being planned.

CONCLUSIONS

The current year should see the completion of both the short-lived activation project and the complete automation of the prompt gamma facility. This will permit the rapid low cost production of multielement data for numerous elements difficult to determine by other techniques.

REFERENCES

Abbey, S.

1977: Studies in "Standard Samples" for Use in the General Analysis of Silicate Rocks and Minerals. Part 5: 1977 Edition of "Usable" Values; Geological Survey of Canada, Paper 77-39, 31p.

1980: Studies in "Standard Samples" for Use in the General Analysis of Silicate Rocks and Minerals. Part 6: 1979 Edition of "Usable" Values; Geological Survey of Canada, Paper 80-14, 30p.

Bergeron, M., Buffet, G., Higgins, M.D., and Shaw, D.M.

1983: Variations in Boron Distribution in Altered Basalts; Geological Association of Canada, Program with Abstracts 8, A6.

Gladney, E.S.

1980: Elemental Concentrations in NBS Biological and Environmental Standard Reference Material; Analytica Chemica Acta, Volume 118, p.385-396.

Higgins, M.D., and Shaw, D.M.

1983: Boron Abundance and Distribution in the Mantle, and the Bulk Boron Content of the Earth; Geological Association of Canada, Program with Abstracts 8, A32.

Truscott, M.G., and Shaw, D.M.

1983: Boron in Cherts; Geological Association of Canada, Program with Abstracts 8, A70.

TABLE 5: INTERLABORATORY COMPARISON OF BORON DATA OBTAINED BY DR. D.B. CURTIS, LOS ALAMOS NATIONAL LABORATORY, NEW MEXICO WITH THAT OF HIGGINS *ET AL.* (1983) OF THE MINGS GROUP.

Data for Higgins *et al.* (1983) is presented as values obtained using chemical standards and recalculated to the certified value for NBS-1571, so that a comparison can be made with Curtis.

STANDARD	CURTIS (ppm)	HIGGINS *et al.* 1983 (ppm)	
		Chem. Std.	NBS-1571 Std.
NBS-1571	33 ± 3*	35.0	33*
AVM-197	1.1	2.5	2.35
MH-217	6.6	6.6	6.2
H-12	97.5	107.1	100.7
M30	39.5	43.3	40.7

*Certified value NBS

Grant 014 Development of a Digital Pulse EM Receiver

J. Duncan Crone
Crone Geophysics Limited, Mississauga

ABSTRACT

The development of an advanced, digital Pulse EM receiver is in progress. Software programs for 4 surface and 2 borehole PEM survey methods have been developed. This enables the day's survey data that is stored in a solid state memory to be presented as profiles and data sheets on a field computer each evening. The field profiles have sufficient scale to show fine detail. Noise processing software for use in the receiver has also been written and field tested.

Instrument components have been selected, and specifications have been checked and then tested for temperature, shock, and vibration. Assembly and debugging of the first prototype instrument is now in progress. The instrument is expected to be in production by September 1984.

INTRODUCTION

The purpose of this project is to design, develop, and test an advanced type Pulse EM receiver system. The project was initiated on October 1st 1981, and has now been in operation for a period of 1½ years. This report covers the period of the last research year ending March 31st 1983.

Development of a Pulse EM receiver system is much more complex than conventional EM equipment. The quantity of survey data produced at each reading point is large. It is in the range of 10 to 30 time spaced measurements in 1 to 3 field component directions. The other factor is that Pulse EM is not one method such as H-Loop or Turam, but is a whole variety of methods. At present, 4 different surface methods and 2 borehole methods are used (see Figures in this report). Each method requires separate software programs for field measurement with a microprocessor receiver and also individual software programs for data presentation from a field computer.

A basic aim of the research program is to build a receiver system that will store all this data as it is gathered daily in the field. The data is then transferred to a field computer and automatically plotted, each evening, as the survey progresses. It is essential that the profile presentation contain sufficient amplitude to recognize the presence of fine detail in the recorded anomalies.

In order to achieve these aims, our approach has been to develop a receiver containing a microprocessor and a solid state memory. At the end of each day, the memory was "dumped" into a field computer and the data was presented by a line printer in profile form and numerical print out. Filter operations can also be carried out in the field with this computer. The data was also stored on disc or tape for future fast reference.

This research project can be divided into 3 parts that converge towards the end of the program. These phases consist of:

1. software development
2. component evaluation and testing
3. final instrumentation design, prototype construction, and debugging

SOFTWARE DEVELOPMENT

This is divided into 3 categories:

1. Software programs for the microprocessor in the new PEM receiver to enable surveys to be carried out using the 4 types of surface surveys and 2 types of borehole surveys outlined.
2. Software programs to control and direct the measurement operations of the new receiver; that is the number of samples, sample times, and noise processing capabilities.
3. Software programs used to enable the day's survey data stored in the receiver's solid state memory to be unloaded into the field computer, then to be printed on a line printer as profiles and data sheets. Filter programs for the computer to process this data will improve the accuracy of interpretation.

CATEGORY 1

In this year's research period, software programs were written and field tested for all the 6 field methods mentioned already (Figures 1 and 2). Field testing was carried out using a prototype "Data Logger", a conventional PEM receiver hooked up to an A/D converter and microcomputer. Extensive field testing for all software programs was found to be necessary. This is necessary since flaws in the program are often not detected until abnormal conditions are experienced in the field. It was also found that the early software programs were too complex. This led to field computer error and subsequent program failure. Program simplicity and safety features were built in at the expense of program flexibility.

Although this aspect of the project is almost complete, it is realized that software programs will have to be rewritten and revised on a continuing basis as survey methods are altered and developed.

Moving Coils: Horizontal Survey
(Figure 1 a)

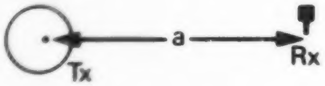

Tx - Small multiturn loop, approximately 15 m diameter
Rx - Vertical component only
"a" - Usually 100 m
Comments - Excellent for shallow exploration in areas of a conductive surface layer
- Maximum penetration of 75 to 150 m
- Battery power supply

Moving Coils: In - Loop Survey
(Figure 1 b)

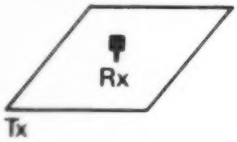

Tx - Single turn, usually 100m x 100m
Rx - Vertical component with optional one or two horizontal components.
- Reading at centre of Tx loop.
Comments - Used in areas of high surface conductivity such as Australia.
- Penetration of 100 to 200m being greater for conductors with a flat upper surface.
- Requires open surface conditions for easy movement of Tx loops.
- Battery power supply.

CATEGORY 2

Software programs to control and direct the measurement operations of the receiver could not be initiated until we had firm ideas as to the final component content of the receiver. This in turn was dependent on testing and evaluation of components; a process that is in its final stages. These software programs, therefore, have just been initiated and will be developed over the next 6 month period. Software programs to reduce powerline noise were produced and were field tested during this research period.

CATEGORY 3

Software programs for the field computer part of the system were designed to produce a data profile of high quality that could be used for detailed interpretation as well as for final report presentation. The software programs were set up to produce various horizontal axis scale options as well as vertical axis plots with linear or linear-logarithmic scale options.

Also, programs were written using filter techniques to improve interpretational accuracy. A Fast Fourier Transform (FFT), high pass filter program was developed as well as a Fraser Filter program. Both filter techniques were evaluated using field data. The programs have proven to be very effective when surveys are carried out in areas of high background effects from geological conductors or cultural conductors such as powerlines and pipelines (Figures 3, 4, and 5). This part of the software development will also be a continuing process because we are just beginning to "scratch" the potential of data processing in the field of mineral exploration.

COMPONENT SELECTION, EVALUATION, AND TESTING

Before instrument design can be finalized, all major component parts and circuit boards containing them must be checked to see if they meet design specifications. These are then subjected to temperature, shock, and vibration testing. A tendency exists among component manufacturers to overstate the capabilities of their products as new components are rapidly developed. This routine testing is therefore absolutely essential to the development of high quality, reliable instrumentation.

During the last year, the following components and circuit boards have been evaluated, tested, debugged, and selected for the prototype instrument:

1. CPU and memory boards for microprocessor
2. multiplier board
3. A/D conversion board - 16 bit
4. D/A converter board - 12 bit
5. crystal clock timing system
6. crystal clock synchronization board
7. crystal clock indicator circuit
8. display LDC module
9. heater system for LCD module
10. print out module system
11. keyboard module

All key components and circuit boards have been tested, except for a final decision on the crystal clock thermal enclosure.

An improved prototype receiver coil was also designed and constructed to reduce its weight and facilitate 3 component measurement. Field testing of this new coil is yet to be carried out.

Borehole Pulse EM Survey Methods
(Figure 2 a)

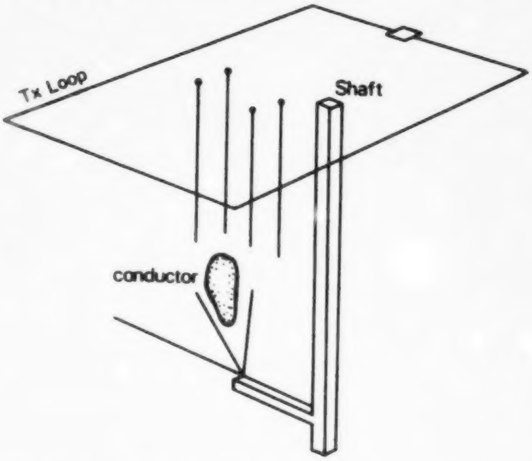

Tx - Single turn, usually 300 m x 300 m to 1000 m x 1000 m.
- Large transmit loop used to survey a number of holes drilled from surface or underground.

Comments - Conductor location determined by changes in the anomaly from hole to hole.
- Push rods available for underground flat holes.

(Figure 2 b)

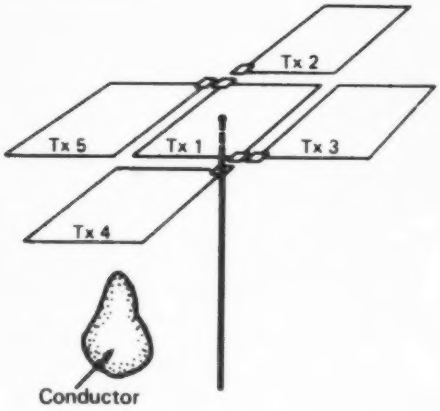

Tx - Single turn, with one side 1/3 to 1/2 depth of hole.
- Multiple transmit loops used to survey an isolated drillhole.

Comments - Conductor location and shape determined by change in anomaly shape from each transmit loop.

Downhole cable systems come in three basic sizes: 500m, 1000m, and 2000m.

'Deepem': Large TX Loop Survey
(Figure 2 c)

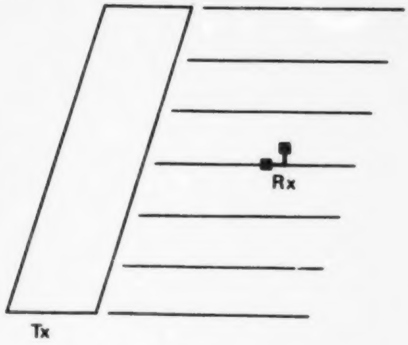

Tx - Single turn varying in size from 100 m x 100 m to 500 m x 1000 m

Rx - Both vertical and horizontal (along line) components are measured. Optional second horizontal component.

Comments - Deep penetration method (500 m and more dependent on Tx loop size) for large conductors with a steep dip.
- Use of the method with smaller Tx loops is ideal for small, isolated conductors with a steep dip.
- Filter techniques must be used in areas of a conductive surface layer to remove ring current response.

Large In - Loop Survey
(Figure 2 d)

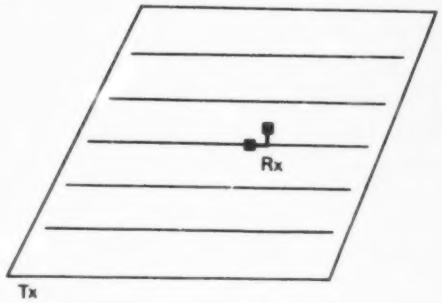

Tx - Large single turn loop in order of 1000 m x 1000 m

Rx - Both vertical and horizontal components are measured, optional second horizontal component.

Comments - Deep penetration method (700 m and more) for conductors with a 45° dip or less, or with a flat upper surface.
- Filter techniques must be used in areas of high surficial conductivity.

Figure 2 Borehole pulse EM survey methods.

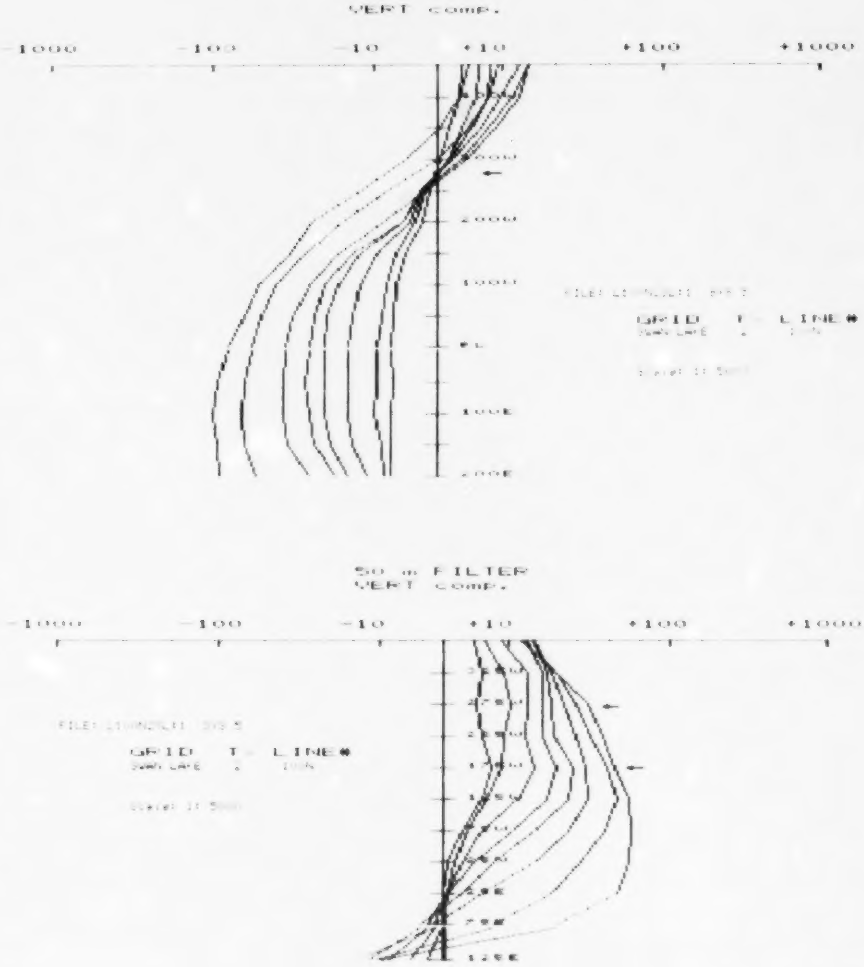

Figure 3. Reduced field computer profiles, vertical deep EM component, Fraser filter.

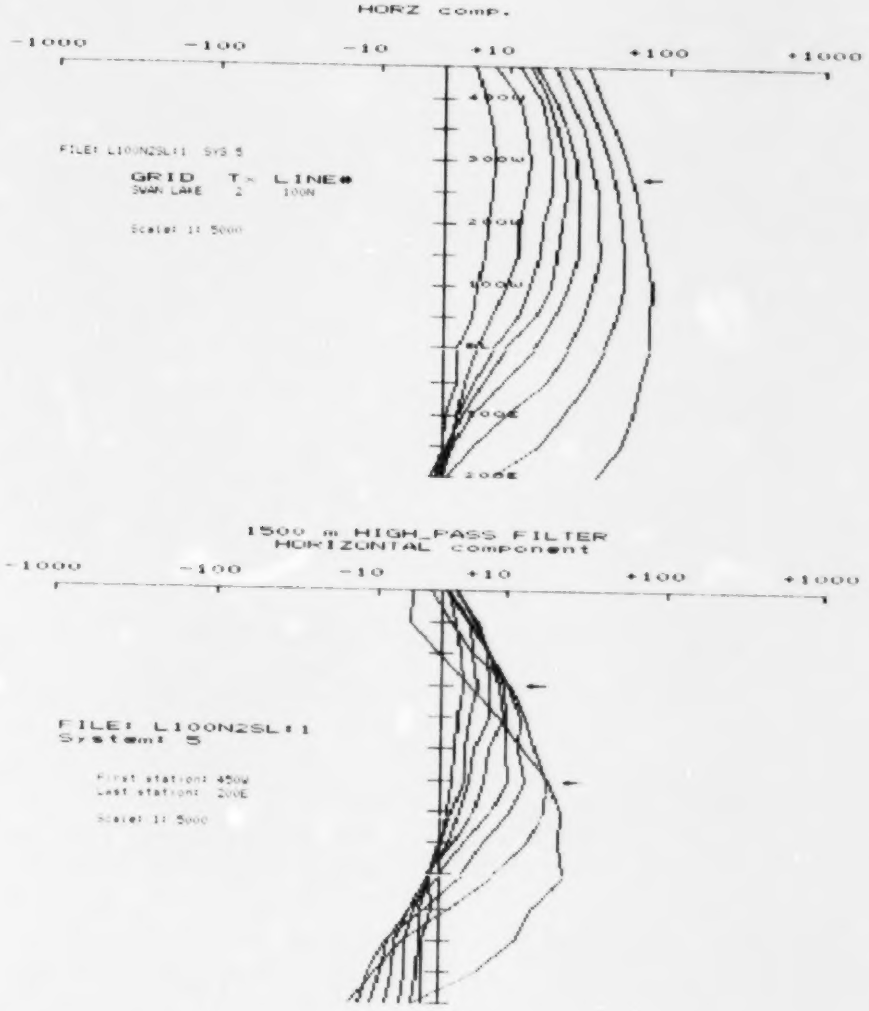

Figure 4. Reduced field computer profiles, horizontal deep EM component, FFT filter.

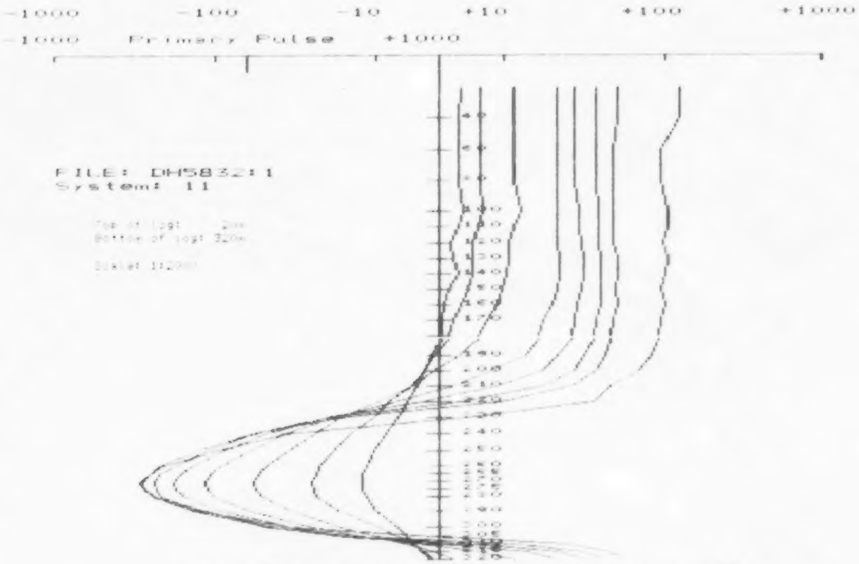

Figure 5. Reduced field computer profiles, borehole pulse EM.

Figure 6. Field test of prototype. Crone pulse EM receiver system.

FINAL INSTRUMENT DESIGN, PROTOTYPE CONSTRUCTION, AND DEBUGGING

This final stage in the development of the new receiver has just started. This stage involves bringing together all the preparatory work on software programs and component hardware into the finalized design concept with the construction of the first prototype receiver system.

Initial work started on this prototype includes:

1. flow charts
2. program modules software
3. microprocessor programs software

The shell of the first prototype instrument case has been designed and the fitting of component boards initiated.

CONCLUSION

Research and development of the new Pulse EM receiver system is proceeding on schedule. No major difficulties have been encountered. The plan to manufacture and market the system by September 1984 should be attainable.

Grant 018 Development of a Four Frequency Helicopter Electromagnetic System

E.B. Morrison
Geotech Limited, Markham

ABSTRACT

Geotech Limited has developed a new Helicopter Electromagnetic Exploration System, the EMEX-1 System. This system provides continuous in-phase and quadrature data from 4 independent frequencies. Two of these frequencies have been assigned to the coplanar configuration and 2 to the coaxial configuration. The range of frequencies offered has been expanded and falls between 380 Hz and 9 KHz for any coil set. An initial set of frequencies may be chosen to suit individual applications. A major feature of the system, however, is ease of frequency changes. The changeover of frequencies can usually be done on site by qualified personnel in a matter of hours.

The light weight and "button on" aspect of earlier systems has been maintained, making the EMEX-1 System suitable for use with most light turbine helicopters such as the Aerospatiale A-Star.

INTRODUCTION

In 1981, Geotech Limited began development of a "state of the art" helicopter, towed bird, electromagnetic exploration system (EMEX-1). This work culminated the following year in the successful field trials of this system.

A major objective of this development has been to produce a superior helicopter prospecting system to extract the maximum data per line-kilometre at a reasonable cost.

The Geotech EMEX-1 is the first airborne electromagnetic system to incorporate 2 pairs of coplanar coils and 2 pairs of coaxial coils. This configuration allows the operation of 4 frequencies simultaneously (Figures 1 and 2).

The basis for this configuration has been an in-depth study of the requirements for an automated computer interpretation software program. Geotech engineers decided that data from the earlier model, Geotech-3, 3 frequency system, was inadequate for this type of advanced analysis. It was also determined that even 4 standard frequencies may not be adequate for proper interpretation under some geological environments. Thus, a completely flexible design was incorporated, one that offered a choice of any 4 frequencies in a range of 380 Hz to 9KHz, operating 2 coplanar coil pairs and 2 coaxial coil pairs. No restriction has been placed on selection of frequencies over this range, except such technical consideration as harmonic relationships between frequencies.

Figure 1. The airborne configuration of the EMEX System showing suspension details and the mounting of a VLF sensor and magnetometer bird.

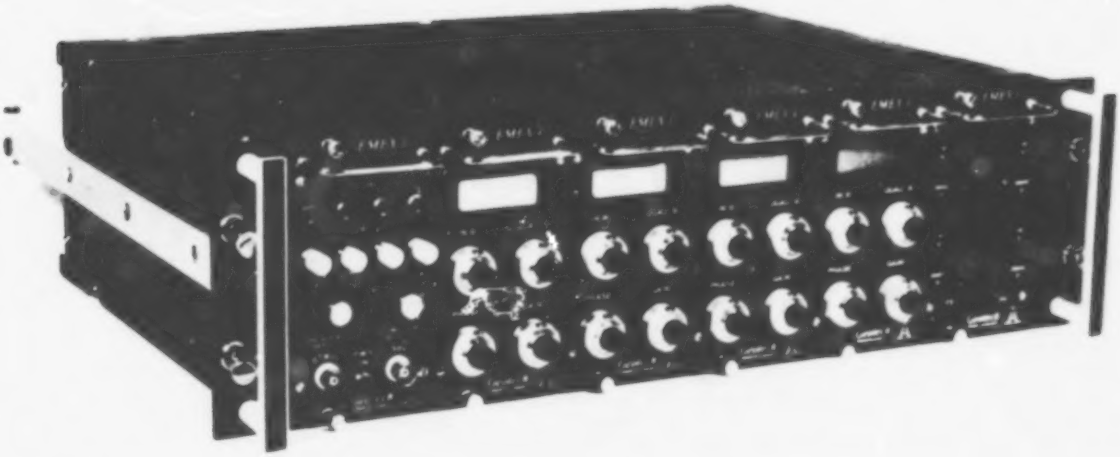

Figure 2. The EMEX electronic console showing the modular construction and compact design

The Geotech EMEX-1 System is the only system available with this feature. This flexibility has been made possible by the design of an electronic system (patent pending) which can remove the interference between receiving coils in any multi-frequency system without predisposing the system to baseline drift. The frequencies may be operated to within 1% of each other with no adverse affects.

DEVELOPMENT AND RESULTS

Although the design and development of the EMEX-1, 4 frequency system was built on the proven technology of the earlier Geotech 3 frequency helicopter electromagnetic system, many major difficulties presented themselves. The aim to make this system more flexible in design, thus allowing a choice in frequencies and orientations, was a major departure from the earlier system. The selection of the range of frequencies was extended to the lower and upper limit based on practical considerations. The bottom end of the scale was set no lower than 380 Hz because of the necessary weight increase of the coil sets required to operate in this region. Increases in weight may cause increased bending moments as well as increase the load on the helicopter. The higher limit for the frequency range was somewhat predetermined by the accompanying decrease in dipole moment necessary to keep the operating voltages and currents at manageable levels.

Under operating conditions, these frequency limits present their characteristic difficulties. The low end of the spectrum is sensitive to microphonics and cultural interference, the high end is the first to be affected by spheric noise and electric field problems. Attention to design may offset many of these problems to a large extent.

The lower frequency of 380 Hz provided by the EMEX-1 System increases penetration of any conductive overburden to allow sufficient energy to excite the conductors beneath, thereby securing improved detection of these difficult targets. Helicopter systems in general have an additional advantage in penetrating conductive overburden as compared to large scale systems, since their configuration energizes only a small part of the ground which reduces the unwanted response from lateral conductive overburden. The higher range of frequencies available assures responses from more resistive targets and fault locations and is invaluable in many engineering applications.

The system was tested over the range of 300 Hz to 9 KHz and orthogonal coil sets were operated to within 1% of each other in frequency with no adverse effects.

One of the important applications of the EMEX System is geological mapping. The feasibility of this for any system is heavily dependent on baseline drift characteristics. Much of the redesign of the system involved incorporating new methods of reducing drift. Major headway has been made in this area and ongoing changes to further stabilize the baseline are taking place as a history of the system develops.

Along with the flexibility in frequency change-over, Geotech Limited has attempted to make the system as modular as possible. Complete transmitter units may be plugged in for replacement in minutes. All signal processing units in the main console, which is located in the helicopter, are of a modular nature. Additionally, the receiver electronics section of the bird is a plug-in type, thus making repairs or trouble shooting in the field greatly simplified. Many of these innovations were necessary for ease of on site frequency change-over.

A major and innovative breakthrough during this development has been the development of the Geotech electronic crosstalk removal system. This allows total removal of unwanted frequencies from any signal channel without predisposing the system to baseline drift such as might occur if traditional filtering were used. Geotech Limited has applied for patents on this method since it may be generally applicable to multi-frequency systems.

Mechanical design for this type of project is perhaps more important than electronic design, since a change of 1 PPM in coil separation will give rise to a change of 3 PPM in signal amplitude.

Internal structures were constructed of low thermal expansion materials, and great attention was given to assure rigid mechanical design.

A Kevlar composite material was chosen for the bird shell material in order to maintain a maximum stiffness/weight ratio.

The increase in weight caused by the addition of the fourth frequency has partially been offset by a general redesign of many areas of the system hardware, with a view towards weight reduction. However, there is a weight penalty, of course, if lower frequencies are extensively selected for use.

The EMEX System has been designed with parallel output integrators for all 8 channels. The rise times for each channel are 0.1 second and 0.5 second. It is advised that 0.1 second rise time data be recorded on magnetic tape for post processing.

Calibration of the EMEX-1 System is accomplished by means of a completely external inductor-resistor combination. This calibration coil is placed in maximally coupled mode a calculated distance from the receiver coil. The value of the resistor is set so that upon completing the L-R circuit, equal in-phase and quadrature components of the calculated magnitude are induced into the system receiver coil. This method assures error free calibrations. Calibration units are measured in PPM of the primary field at the receiver.

DISCUSSION

The EMEX-1 development was undertaken in order to offset the growing need for the more sophisticated hardware required to handle the rapidly expanding areas of application of this technology.

The EMEX System was designed with this aim specifically in mind. The multi-geometry and flexible multi-frequency approach should make the system ideal for many applications. The traditional role of conductor detection has been expanded to include, among others, applications in water resources, bedrock and overburden delineation, and geothermal work. Increasing applications are being found in engineering work such as highway route investigation.

The significant growth of geological mapping as an application of airborne EM systems over the past few years has been a direct result of the development of multi-frequency EM hardware along with the simultaneous development of interpretative software. The EMEX Series

TABLE 1: HELICOPTER ELECTROMAGNETIC SYSTEMS AND SERVICES AVAILABLE IN CANADA.

MANUFACTURER	Model	Maximum Number of Frequencies	Coaxial Frequency Number 1	Coplanar Frequency Number 1	Coaxial Frequency Number 2	Coplanar Frequency Number 2	Coil Seperation	Contract Service Available
Dighem Limited	Dighem II	1	918 Hz	4000 Hz or 870 Hz	–	–	8M	Dighem
	Dighem III	3	918 Hz	4000 Hz or 870 Hz	–	380 Hz or 7200 Hz	8M	Dighem
Geonics Limited	EM33-1	1	736 Hz	–	–	–	6M	Geoterrex
	EM33-2	2	380 Hz	–	3630 Hz	–	5.4M	–
	EM33-3	3	380 Hz	2860 Hz	3630 Hz	–	5.4M	Geoterrex
Geotech Limited	Geotech II (Conversion)	2	933 Hz	4400 Hz	–	–	6M	Geophysical Surveys Ltd
	Geotech III	3	933 Hz	1800 Hz	4400 Hz	–	7M	Apex Ltd Geophysical Surveys Ltd Aerodat Ltd
	EMEX-1	4	380 Hz to 9 KHz	380 Hz to 9 KHz	380 Hz to 9 KHz	380 Hz to 9 KHz	7M 8M	Aerodat Ltd HMS Inc
Sander Geophyics Limited	EM3A	1	500 Hz to 4KHz	–	–	–	7M	Sanders
Scintrex Limited	HEM 802	2	735 Hz	–	3320 Hz	–	8M	Scintrex

Frequencies listed are nominal values and may vary slightly in practice

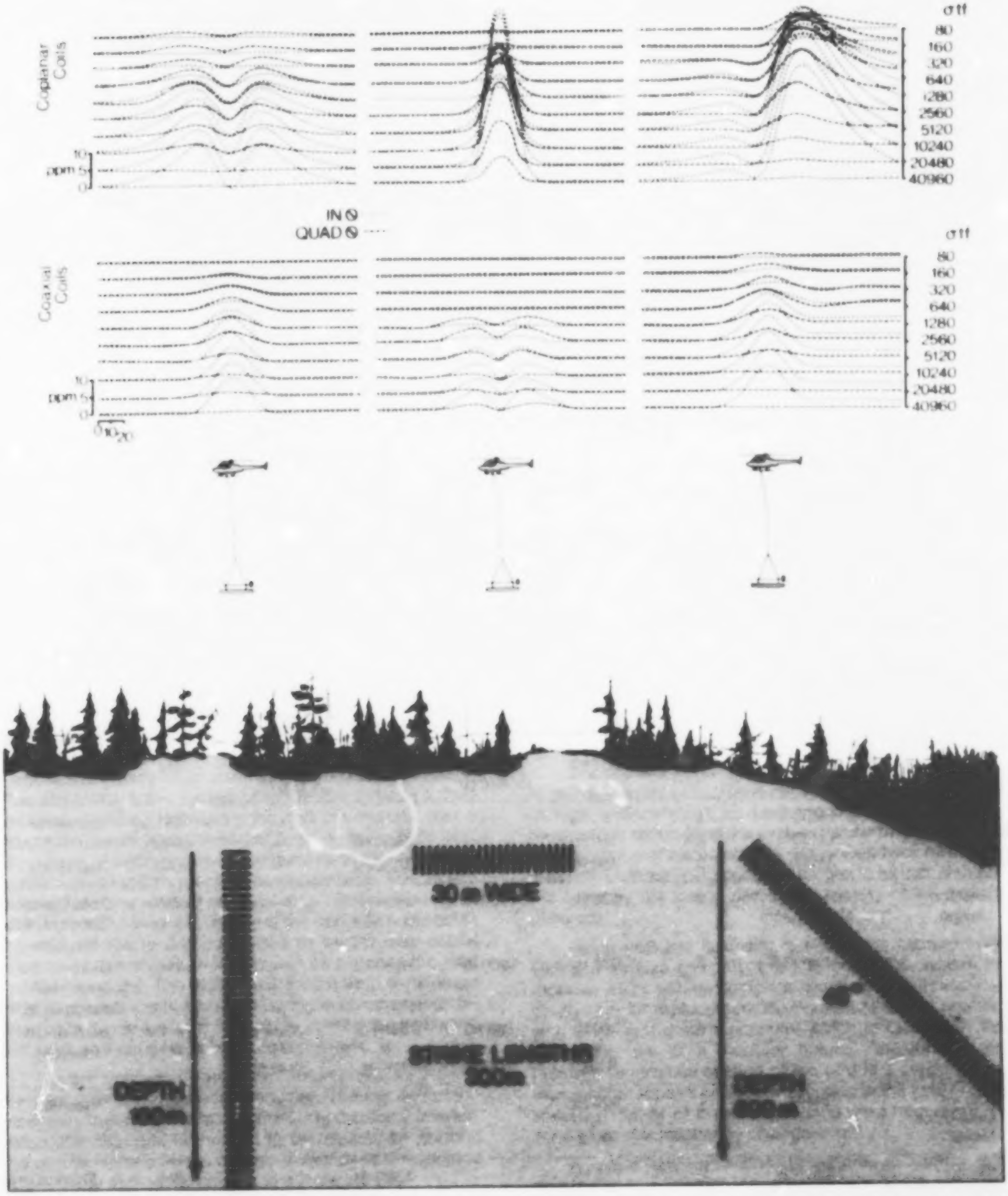

Figure 3. Chart of computer produced responses of coaxial and coplanar coil sets to 3 types of conductor geometries. Note the improved interpretation of conductor geometry possible when data is collected in both coplanar and coaxial modes.

has been developed specifically with geological mapping as one of its major applications (Figure 3).

A serious source of error in geological mapping by EM surveys is caused by baseline drift in the recorded data. This error can be minimized by flying to an altitude out of ground effect at the end of each survey line. This establishes the baseline drift rate and permits correction by post processing. This method is only partly successful due to the non-linear characteristics of the drift. Geotech Limited has incorporated into the design of the EMEX Series, construction techniques and electronic circuits to minimize baseline drift to the greatest extent possible. This eliminates, in many cases, the need to use up valuable survey time flying the system out of ground effect just to establish the baseline drift. Apparent resistivity and the thickness of 1 or more layers of a horizontally stratified conducting media may be determined using data collected by the EMEX System. These data may be presented in the form of contoured maps to delineate the overburden and rock types. Geological mapping may be used to help delineate any geological feature where a resistivity contrast exists.

The compatibility of accurate radar positioning systems with the EMEX Series and its high resolution data combine to provide a tool which eliminates the need for much of the ground follow-up work previously required. Radar navigation provides a valuable addition to the multi-frequency EM data. In many cases, expensive and time-consuming ground surveys can be eliminated by the use of economical, fast, helicopter methods.

FUTURE PLANS AND CONCLUSIONS

The development of the EMEX System has produced a "state of the art" instrument. However, numerous ways to further improve this new system have become evident during field trials. Starting with a working system, we will incorporate these improvements one by one over the upcoming period. The need for system flexibility has been well illustrated by the recent emphasis on gold exploration, where the EMEX System may be converted if necessary to a more suitable range of higher frequencies, and then, if needed, easily reconverted to suit the next application.

Helicopter electromagnetic systems in general have become very popular in recent years, having outlived many of their earlier fixed-wing competitors. This increased recognition and utilization has spurred both hardware and software development related to these systems. Computer interpretation of the data is becoming increasingly mandatory with the advent of 8 channels of EM data from the EMEX System.

Geotech Limited has embarked on a major program in this regard. The aim of this program is to provide automated computer interpretation software for the majority of data, allowing for manual intervention in special cases. As part of the ETDF program, Geotech Limited has completed model studies at the University of Toronto's modelling facility. Work on this software program is continuing and it is expected that first deliveries could occur by the end of the year.

REFERENCES

Fraser, D.C.
1979 The Multicoil II Airborne Electromagnetic System. Geophysics, Volume 44, p.1367-1394.

Frischknect, F.C.
1967 Fields about an Oscillating Magnetic Dipole Over a Two-layer Earth. Colorado School of Mines, Volume 62, Number 1.

Grant, F.S., and West, G.F.
1965 Interpretation Theory in Applied Geophysics. New York, McGraw-Hill Book Company Incorporated, p.456, 501, 502, 526, and 571.

Lodha, G.S., and West, F.G.
1976 Practical Airborne EM Interpretation Using a Sphere Model. Geophysics, Volume 41, p.1157-1169.

Paterson, N.R.
1971 Airborne Electromagnetic Methods as Applied to the Search for Sulphide Deposits. Canadian Institute Mining Bulletin, January, p.29-38.

Pemberton, R.H.
1962 Airborne EM in Review. Geophysics, Volume 27, p.691-713.

Sinha, A.K.
1973 Comparison of Airborne EM Coil Systems Placed Over a Multilayer Conducting Earth. Geophysics, Volume 38, p.894-919.

Sengpiel, K.
1983 Resistivity/depth Mapping with Airborne Electromagnetic Survey Data. Geophysics, Volume 48, p.181-196.

Grant 019 Development of a Portable Helium Detector

G.M. Denham and R. Raz

alphaNUCLEAR Company, Mississauga

ABSTRACT

This paper describes the development of a field-portable exploration tool for the *in situ* measurement of the helium levels in soil, gas, and natural water systems. Two techniques were considered to have potential. The first choice did not work and has been abandoned. The second choice is presently being worked on and is based on a system launched by NASA to probe the upper atmosphere of the planet Venus.

INTRODUCTION

The objective of this project is the development of a field-portable exploration tool for *in situ* measurement of helium levels in soil, gas, and natural water systems.

The product needs to be rugged, reliable, light-weight, and sufficiently sensitive to register helium anomalies which occur over deeply buried uranium mineralization. Helium is a stable, inert gas which is mainly produced by the radioactive decay of uranium and thorium. Measurable levels of helium in surface soil and groundwater have been related to uranium mineralization at a depth of 200 m.

This project, to design a portable helium detector, was started in the last quarter of 1981. A literature search indicated that mass spectrometry or gas chromatography using a plasma emission spectrograph were the 2 techniques that would allow helium gas measurement at the sensitivity required for use in mineral exploration. The latter combination of techniques was favoured initially because mass spectrometer systems using classical sampling techniques are heavy, bulky, and have high power consumption.

EXPERIMENTAL RESEARCH

All work up to June 1982 involved the development of a flow-through plasma emission cell. This was done for us by a sub-contractor, MONITEQ Limited, with considerable experience and expertise in the area of high energy-source lamps, and in trace element determinations by various electro-optical techniques.

The work conducted by MONITEQ Limited was initially to establish detection limits and identify interference lines. The helium emission line at 1.0830 μm was chosen as the detection wavelength. Argon carrier gas gives the least interference at this wavelength. To minimize any argon interference at the detector, a narrow bandpass optical filter centred at 1.0830 μm was chosen to transmit the helium emission. The experiments were conducted with sealed lamps and various mixtures of helium and argon at about 8 torr pressure, and excited by a RF oscillator at 95 MHz.

A clear helium spectrum was reported under these conditions. However, major difficulties arose when experiments were conducted with the flow-through cell. The experimental procedure with the flow-through lamp involved considerable effort and equipment. The specially constructed lamp with a quartz window was coupled to an optimized optics assembly which included the interference filter and a mechanical chopper. This assembly was in turn coupled to a silicon photodiode and amplifier, followed by a phase sensitive detection circuit. The entire assembly was shielded from RF noise and local electrical interference by being encased in an aluminum cylinder. A flowing source of helium at a concentration of 92 ppm in argon was used with a flow-rate of 2.5 ml per minute (approximately the flow expected from a gas chromatograph). The RF frequency was initially set at 122 MHz with a power input of 7 watts, a level at which the plasma filled the lamp cavity. The pressure in the lamp was controlled by a back pressure valve between the lamp and a vacuum system set to provide 4 torr in the lamp.

Emission intensity was optimum with the lamp pressure between 4 and 7 torr. As the pressure was raised toward more realistic levels, the plasma became unstable, containing discharge balls which floated and hence varied in intensity. With a helium concentration through the lamp of 92 ppm, a net negative signal was seen compared to that obtained from pure argon. Higher helium concentrations of up to 35% were then allowed to flow through the cavity. A plot of intensity versus helium concentration suggested that helium was simply acting as a dilutant of the argon plasma.

DISCUSSION OF RESULTS

The most significant problem encountered was the higher than expected signal level from the argon plasma. This indicated that we could not attain the 5 ppB helium sensitivity level unless the argon signal could be reduced to a level equivalent to the expected helium signal to be measured, e.g. a microvolt signal requires an argon background of ~ 10 millivolts assuming the signal/noise ratio to be fixed.

The requirement of argon signal exclusion indicates that a dispersive optical system, using a grating, should be utilized. The interference filter is not suitable.

The second area of concern is the lack of helium emission in any lamp system containing a buffer gas.

The operational theory of the detector method was that, at a reasonable vacuum (~20 torr), the mean free path in a plasma would accelerate the electrons. A proportion of the electrons would give sufficient energy during collision with a helium atom to excite the upper level of the transition phase. In this transition, an emission at 1 083 μm would occur. The probability of this occurrence is now thought, due to the lack of signal from helium, to be exceedingly slight. The range of electron energies is probably foreshortened by the limitation of the ionization potential of argon. This limitation may be overcome by a greater power input into the plasma; this is available, for example, in a direct current excitation such as an arc or spark.

Moving to a gas of higher ionization potential, such as neon, was expected to increase the probability of helium emission. The plasma of neon was weakly coupled, not filling the cavity, although RF power supplied was at the maximum of 15 watts. More intense investigation of neon plasmas would be required to find the correct pressure and optimize the RF coupling. A spectrum of the helium in neon plasma, as expected from the weak plasma, gave a few of the stronger neon lines between 200 nm to 700 nm, but no indication of helium emission.

The lack of signal may be due to the effect of self absorption, or even the extreme case of self-reversal, where the emission in the centre of the plasma is absorbed in the colder gas layers at the walls of the cavity.

The sub-contractor submitted various recommendations and suggestions for further work on this approach. These included:

1. measurement of a different helium emission line
2. re-design of the lamp and excition assembly.

If a further experimental programme with these modifications proved the technique to still have limitations, suggestions for other approaches would be provided.

At this time (July 1, 1982), we decided to abandon the approach suggested by MONITEQ Limited.

THE NEW APPROACH

This left the mass spectrometer technique as the alternative, but some innovative modifications and optimization would be required to use this inherently sensitive, usually bulky and power-consuming technique, and to render it truly field portable.

We have now rationalized our approach to the problem, and it is probable that one of the solutions will be patentable. The basic system: electron guns, focusing, accelerating, and extraction system, the drift tube and magnet array, and to some extent the detector, is based on the one launched by NASA as part of the Venusian upper atmosphere probes. This results in a light-weight, miniaturized system, but unlike NASA's application in space and the outer edges of the Venus atmosphere, 2 major problems remained to be solved. The first of these is a typically heavy and power consuming vacuum pumping system necessitated by classical sampling techniques. The second, but lesser problem, is the very wide dynamic range (10^7) required from the ion detector.

We believe the latter of the 2 problems will be solved by incorporation of a specially constructed channeltron. This will provide the ability to measure ion current at high helium concentrations, yet retain its inherent ability to count individual ions at low helium levels. This is accomplished by a 2-stage electron multiplier incorporating an intermediate "current collector grid", thus providing dual output. Such devices are not commercially available, but have been made in the past for NASA. The manufacturer in this instance has indicated a willingness to custom manufacture for us.

The other major problem associated with mass spectrometers is the method employed for introducing a sample into the system. In a typical laboratory system, a part of the whole sample would be injected directly into the ionization area of the vacuum system. The introduction of a whole air sample into an ultra high vacuum requires that a very high volume (high power and heavy) vacuum pump be used. We propose to overcome this pumping problem by using a novel sample induction method which excludes all of the sample, except its helium and hydrogen components. With only this minute part of a sample being admitted into the system, a very small, light-weight, lower power pump is all that would be necessary to maintain the system's ultra high vacuum.

All detailed manufacturing drawings were completed during the first quarter of 1983.

Grant 020 Application of Vibra-Corer Drills for Rapid Overburden Sampling

C.W. Archibald[1], J.F. Archibald[2],
A.A. Archibald[3], and J.H. Nantel[2]

[1]C.W. Archibald Limited, President
[2]Mining Engineering Department, Queen's University, Kingston
[3]C.W. Archibald Limited, Operations Manager

ABSTRACT

A research and development program to assess the performance criteria of a novel overburden drilling device was initiated under the auspices of the Government of Ontario's Exploration Technology Development Program. Both field and laboratory performance characteristics of the Vibra-Corer, a vibratory overburden coring drill, indicate that it is safe to operate, and can perform satisfactorily in all material, especially in "wet" material.

INTRODUCTION

A program to assess the new Vibra-Corer drill system was carried out by C.W. Archibald Limited of Toronto under the direct supervision of C.W. Archibald, and by the Department of Mining Engineering, Queen's University, Kingston, Ontario under the supervision of Professor J.H. Nantel. The primary objectives of the research were to quantitatively assess the operating parameters of the Vibra-Corer drill units, and to subsequently determine whether modifications of the system could be implemented to improve penetration rate and core recovery.

SYSTEM BACKGROUND

The present commercial drill unit is rented under a lease arrangement in Ontario from Sonic Soil Sampling Incorporated, of Toronto. The drill unit developed by Fred Wink consists of 3 main components: a drive motor, a flexible drive cable, and a vibratory drill head. The head weighs approximately 12 kg, and is driven using the flex-cable take-off which is powered by a 5 or 7 horsepower gasoline engine, weighing approximately 45 kg. The drill unit, which weighs approximately 70 kg, less rods, is quite portable, and can be easily operated on site by a crew of 3 persons. The drill rods are common 5-foot long BQ casing sections that use an open, untoothed steel bit for cutting in overburden. The largest pieces of equipment are the drill rods. These pose no transport problems for small pickups or station wagons. The portability of the Vibra-Corer drill system makes it ideally suited for remote helicopter-assisted programs.

The Vibra-Corer operates on the principle of drill-string oscillation, and requires no water or air injection. The bit element consists of a case-hardened steel drive shoe, thus eliminating the need for expensive diamond or carbide-tipped bits. The rods do not rotate, as in conventional drilling operations; friction wear and excessive replacement costs are thus reduced.

Vibrations produced by the drill head are transmitted directly to the drill rods and the overburden immediately adjacent to the machine. Energy imparted to the overburden material at the cutting head causes a soil column to fluidize. This allows the drill column to settle into the unconsolidated overburden. As the drill is allowed to penetrate the soil layers, an undisturbed sample flows into the hollow rod casing. Externally, the fluidized overburden is packed and acts as a rough hole casing which remains open, allowing the rods to be removed and to be replaced without caving. Exceptions occur only where very wet overburden layers are encountered. After sample drilling, the rods are lifted to extract full, continuous, essentially-undisturbed samples of the unconsolidated overburden. In very few cases, however, will penetration of bedrock, large cobbles, or consolidated organic materials be accomplished. Where penetration is achieved through consolidated ground or dry aggregate materials, such as coarse sands, rates of penetration are appreciably slowed.

PERFORMANCE TRIALS

A series of performance tests was initiated by the authors at a variety of sites throughout the Provinces of Ontario and Quebec during the 1982 and 1983 summer months. A summary of site geology, including overburden characteristics, and performance data, are presented for each of the study locations. In addition, tests were also conducted using prepared materials in the laboratories of the Mining Engineering Department of Queen's University, Kingston, Ontario.

SITE A

Penetration tests were conducted in a water-saturated unit of Abitibi clay and mill tailings, comprising layers of organic material and organic sediments, and varying thicknesses of placed clay, sand, and mixed aggregate material. Tests were conducted during April 1982. The test location is approximately 12 km north of the city of Noranda, Quebec, and lies immediately adjacent to the north pit wall of the Noranda Mines Limited, Gallen Mine. A series of 6 BQ exploratory holes were drilled vertically downward from the top of the mill tailings, into the Abitibi clay unit. At all stages, maximum drill speeds, approximating 12 000 rpm, were maintained.

Observations of the penetration rate indicated the following general trends to exist:

1. Slow penetration rates, in the order of 0.1 m/min, were recorded within the surface layer of tailings. The presence of frozen ice lenses within this layer was found to be responsible. The depth of the tailings material varied from 2 to 4 m across the sites chosen.
2. Slow penetration rates also were noted within the layer of organic material. This is due to the presence of substantial root networks adjacent to the remains of tree stumps. Maximum rates, approximating 0.5 m/min, were attained in layers with no obstructive vegetative matter. The organic layer, averaging 0.6 m thick, was also characterized by the presence of occasional ice lenses.
3. Significant high rates of advance were attained during the drilling of the underlying Abitibi clay unit; rates in the order of 12 m/min were recorded during drilling cycles, to maximum depths of 30 m of the clay. The greatest amount of field time was taken to retrieve the drill rods, recover the entrained samples, and to reinsert the drill sections into the hole.

The average depth drilled to bedrock for all the holes is about 20 m. Of this depth, the upper 5 m of the drillholes was through rubble and organic cover which impeded the drilling rates. During a 3-day interval period, 281 m of drilling was completed to bedrock. Sampling data obtained from logs for typical holes, shown in Figure 1, illustrate the results of field and laboratory studies on material recovered.

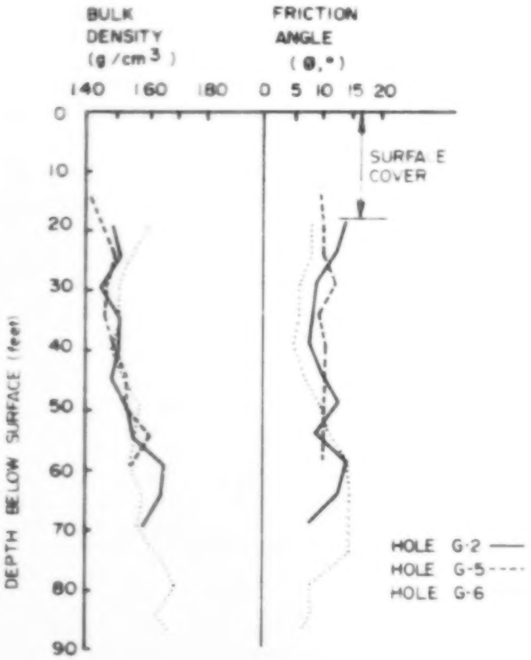

Figure 1. Physical parameters for Gallen Mine Vibra-Cored clay samples, Site A.

SITE B

A series of drilling tests, similar to those described in the preceding section, was carried out in a dry, varved clay at a site located approximately 4 km south of Site A in northern Quebec.

Four holes were drilled. Maximum drive head speeds, as previously mentioned, were maintained during all tests.

In contrast to the results obtained at Site A, however, slow rates and minimum depths of penetration were obtained when the varved clay material was drilled. Rates of penetration of the order of 0.1 m/min were achieved, but not exceeded. In no cases were depths in excess of 1 m obtained.

Because of the lack of success observed at Site B, tests were discontinued. In no cases were the tests in varved clay materials successful using the Vibra-Corer drill.

SITE C

A series of drillholes was completed on top of a tailings disposal site, averaging 7 m in depth, at the Cordova Mine located in the vicinity of Madoc, Ontario. Such tests were conducted to assess the suitability of Vibra-Corer drill application to the sampling of mine tailings.

A total of 6 holes, varying in depth between 2.3 and 9.2 m, was completed during a 2-day interval. The tailings were found to be overlain by crusted tailings and vegetation to a uniform depth of approximately 1.7 m. This upper layer did not permit successful use of the Vibra-Corer drill, and was therefore augered to collar holes before satisfactory implementation of vibratory coring tests. Sampled tailings material below the surface layer exhibited moisture contents averaging approximately 8.5%. A brief summary of penetration rate response is listed in Table 1.

The penetration rate was found to decrease with increasing depth within the tailings material. For all test holes, significantly reduced rates occurred when drilling had progressed into the zone, immediately above the bedrock layer, where dense logement till exists.

SITE D

A series of performance tests was carried out at a sandfill excavation located on the Hinchinbrooke Road, approxi-

TABLE 1. SAMPLE DRILL DATA FOR CORDOVA MINE TAILINGS SITE.

	DRILL DEPTH (m)	PENETRATION TIME (min)	PENETRATION RATE (m/min)
SITE C-8	1.52 – 3.05	0.17	9.1
	3.05 – 4.57	0.22	6.9
	4.57 – 6.10	0.20	7.6
	6.10 – 7.62	0.27	5.6
	7.62 – 9.15	0.35	4.4
SITE B-7	1.83 – 3.05	0.45	2.7
	3.05 – 4.57	0.35	4.4
	4.57 – 6.10	0.47	3.2
	6.10 – 6.25	0.20	0.8

TABLE 2. HINCHINBROOKE SANDFILL SITE TEST DATA SUMMARY

TEST SERIES	PENETRATION RATE (m/min)	TAILINGS MOISTURE CONTENT (% H_2O)	TAILINGS BULK DENSITY (g/cm^3)
A) 7 Sites, 2 days after rainfall, steel rods, single 1.5 m pass	2.29	19.9	---
B) 2 Sites, with organic layer removed, steel rods, single 1.5 m pass	6.32	19.2	---
C) 5 Sites, PVC 1.5 m rods, 1 week after last rainfall, single pass	0.70 – 2.15	14.5	2.04
D) 4 Sites, steel rods, single 3.0 m pass	5.37	14.3	---
E) 2 sites, 0.60 m split-tube sampler, 4 pass to 2.4 m in 0.60 increments at arbitrary penetration rate	2.00	a) 17.4 b) 14.5 c) 15.7 d) 11.3	a) 1.69 b) 1.99 c) 2.05 d) 1.86

mately 60 km north of Kingston, in southeastern Ontario, and adjacent to Highway 38. The excavation site consists of a layer of approximately 5 m of coarse sand and silt on top of bedrock. A 20 cm layer of organic material, primarily grass, exists as cover on top of the sand. Tests were conducted using standard 1.5 m lengths of BQ drill rod. Tests comparing standard lengths with 1.5 m lengths of 5 cm diameter Schedule 40 PVC tubing and 0.60 m long split tube sampler units were also made. The data in Table 1 provide a partial summary of results obtained. Grain size characteristics and physical property data are similarly illustrated in Figure 5.

Single pass penetration tests with standard BQ rods to depths of 1.5 m indicated appreciably higher penetration rates when the covering organic layer was removed at closely adjacent sites. Subsequent tests using single pass attempts, with standard BQ rods to depths of 3.0 m, show quite similar penetration rate behaviour. A decrease in penetration rate behaviour between each group of tests was observed. This decrease should have been anticipated due to the difference in soil moisture conditions. Deep level tests were conducted through drier materials, and would be expected to exhibit slower penetration rates.

Where steel rods were used, recovery of overburden samples, based upon a column length of recovered soil, was determined to be approximately 60%. The reasons for this poor recovery are not clear. Possible explanations are:

1. The retained sample within the drill tube may have become more dense, due to the vibrating action. This creates a column shortening effect.
2. The material within the tube, and the tube itself, may have compacted the overburden ahead of the sampling tube, thereby preventing it from entering the drill string.

Subsequent tests were conducted using a 0.60 m long split tube assembly at slow and arbitrary penetration rates of 2.0 m/min. Several holes were drilled in depth increments of 0.60 m, to final depths of 2.4 m. For the initial 0.60 m pass, sample recovery was found to approximate 55 to 60% (see Table 2 for average results). At successively deeper intervals, 100% recoveries were achieved.

LABORATORY TESTS

A series of limited tests upon "prepared" columns of uniformly-graded sand were performed in the laboratories of the Mining Engineering Department, Queen's University. Construction grade building sand, with the grain size distribution illustrated in Figure 2, was moistened and compacted within PVC cylindrical pipe sections 20 cm in diameter by 1.5 m in length. Material of variable characteristics, forming layers of known density and moisture contents, were prepared, and were subjected to single pass drill penetration tests. For each sample trial, data were recovered to establish relationships between recovery, engine speed, penetration rate, and water content variables.

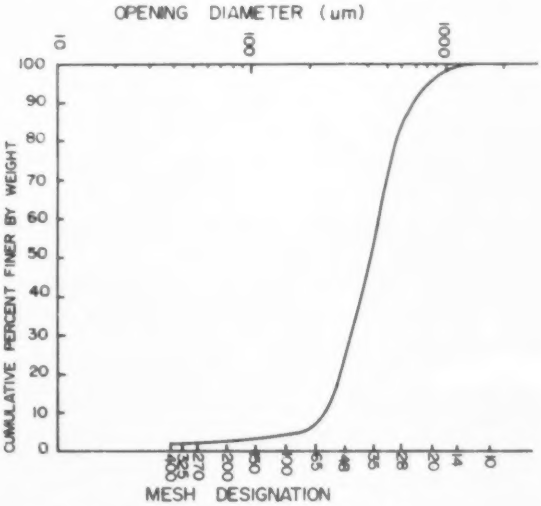

Figure 2. Size distribution of laboratory sand.

Sample densities were restricted to the range between 1.55 and 1.79 g/cm^3. In no cases were sand densities in excess of 1.79 g/cm^3 achieved using hand-tamping techniques. Within this range, the bulk sand samples exhibited porosity characteristics between 37.09% and 42.5%, typical of loosely-compacted, cohesionless sands.

Recovery percentages were determined by measuring differences between the theoretical full casing weights of sand for known casing internal volumes and sand densities, and the actual weights of sand recovered after drilling. The data were analyzed in terms of material recovery versus engine speed and penetration rate versus water content, as illustrated in Figures 3 and 4.

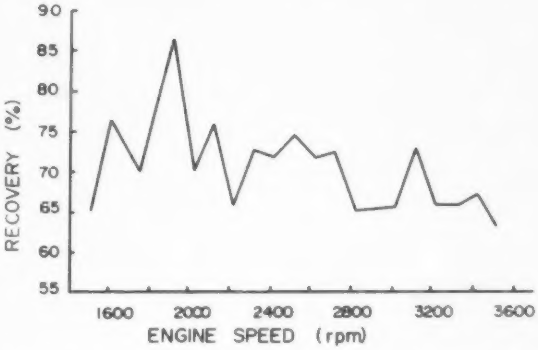

Figure 3. Sand recovery versus engine speed for manufactured material.

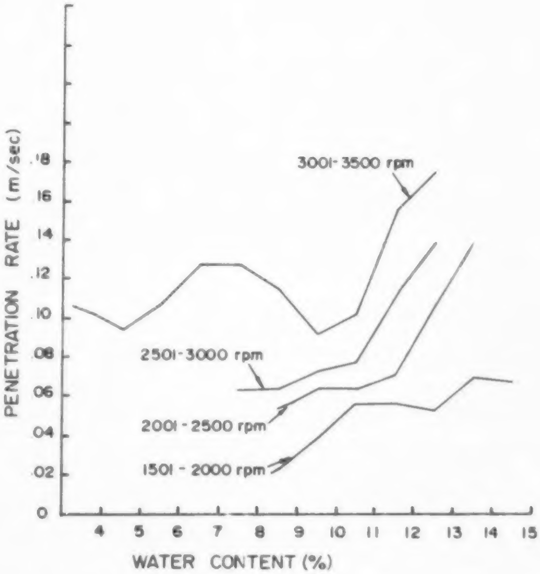

Figure 4. Penetration rate versus water content for laboratory manufactured samples.

The data plotted in Figure 3 indicate that <100% material recovery was obtained for all tests conducted. Peak recovery was 87%, and minimum recovery, 60%. Maximum sample recoveries were observed to occur at drive engine speeds approximating 2000 rpm. At higher and lower engine speeds, reductions in sample recovery percentages were noted.

Figure 4 shows that for all engine speeds selected, the penetration rate increased with increasing water content over the range of water contents (5% to 15%) of the samples tested. Similarly, the penetration rate was also observed to increase with increases in engine drive speed. For an engine drive speed increase from 1500 rpm to 3500 rpm, penetration rates were found to increase from 3.3 m/min to 7.8 m/min. In no cases could fully saturated sample mixtures be prepared under laboratory conditions.

The results of laboratory experiments agree favourably with the recorded field data in that:

1. Penetration rate often is high through overburden which exhibits a high moisture content. In dry, sandy soils, low rates of penetration are encountered unless the medium is "fluidized" by the application of water down the hole.
2. Incomplete recovery will often result where loosely-compacted or highly porous, underconsolidated materials are drilled. The material, which is caused to flow into

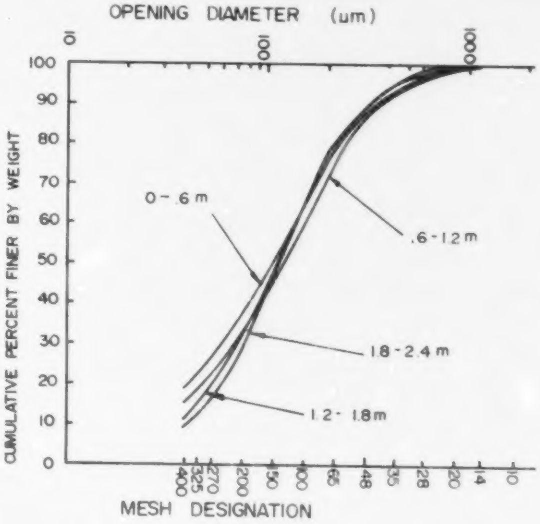

Figure 5. Sizing curves for split tube samples.

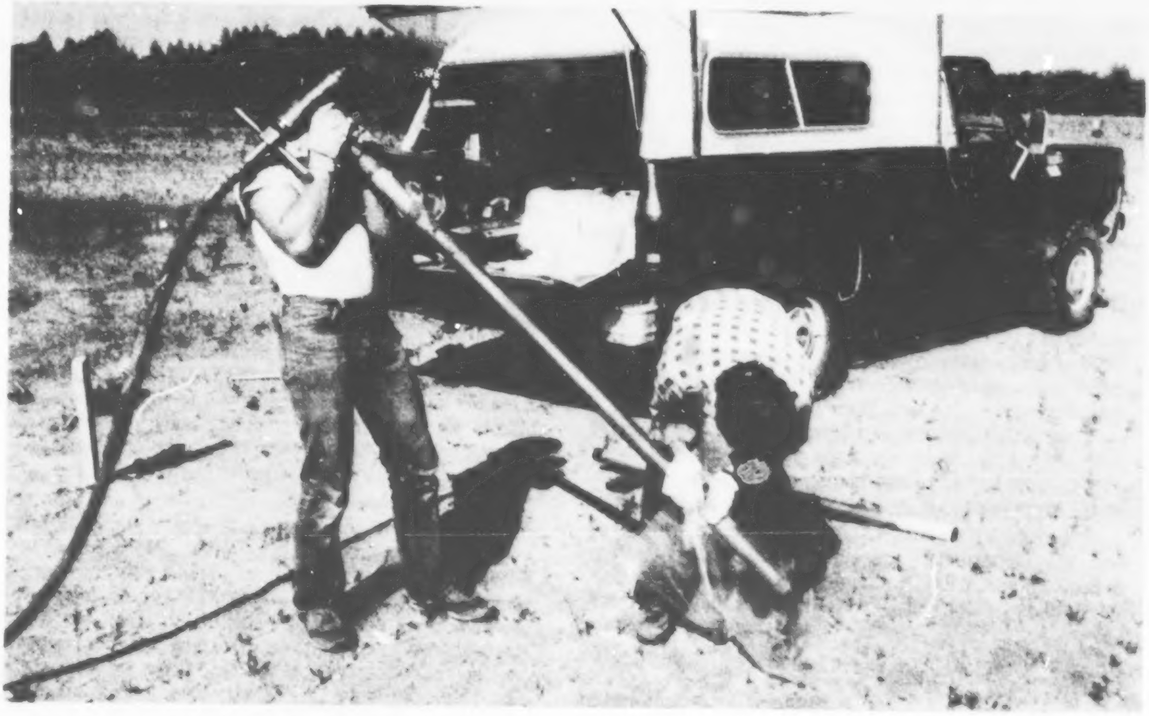

Figure 6. Photograph illustrating equipment used.

the hollow drill casing, will, under the rod vibration action, become slightly compacted and restrict material ahead of the bit from entering it.

In total, 160 sample penetration tests were completed during this study phase.

DISCUSSION

A significant number of field tests have been conducted on a variety of overburden material types to assess the performance of the Vibra Corer drill. The materials include sand, gravel, glacial till, clay (varved and homogeneous saturated), and mixtures of these materials at depths of up to 40 m.

Dry varved clay materials and certain other types of clays found in southern Ontario are drilled with difficulty and penetration rates observed are low when the Vibra Corer unit is used. Nevertheless, in all other types of materials, rapid rates of advance and high recovery rates are common. The speed of penetration in such soils, notably loose, cohesionless materials, varies significantly with changes in soil moisture content and the frequency of drive head vibration achieved. A direct correlation between increasing water content and increasing penetration rate has been established. A similar correlation is observed to occur between an increase in frequency of the drive mechanism and penetration rates for materials exhibiting uniform moisture content conditions.

No established correlation between penetration rate and depth has, as yet, been observed. In timed field trials at a tailings overburden site, a general decrease in penetration rate versus depth was recorded for the majority of test holes observed. In several test holes, however, a steady increase in penetration rate with depth was noted to occur. Such increases in penetration rate would occur with depth due to several factors, these are:

1. The increasing weight of drill rods, at greater hole depths, thereby increasing the vertical driving force.
2. Overburden moisture content increasing with depth toward the local water table horizon.

Penetration rates would be expected to decline with depth in cases where little change in soil moisture content exists. Such conditions would be typical in loosely compacted, granular aggregate materials, such as coarse sands, where excellent drainage conditions and depressed water table elevations may exist. Therefore, it is feasible to assume that frictional resistance between the dry soil/drill rod interface would increase linearly with depth, thereby restricting penetration, as has been observed.

Recovery potential, from both laboratory and field tests, appears to be variable, with the least recovery obtained in laboratory tests using loosely compacted sand material (density ranging between 1.50 and 1.79 g/cm^3) without a core retainer within the drill string. Recovery values varying between 60% to 87% were obtained from laboratory tests. Similar field estimates occur when drilling cobble or large granular aggregate materials.

Sample recovery in laboratory and field testing was found to vary considerably; 100% recovery was noted to be the norm in the field and lower recovery was obtained during laboratory tests. This would probably be due to differences in sample density and porosity characteristics between man-made and naturally-occurring soil mixtures.

Future tests are being devised to improve penetration response in resilient clays by the use of either water lubricants injected through the drive head, or novel cutting bit designs.

Specific tests were also implemented to establish breakdown parameters pertaining to operating safety and equipment durability. The drive head casing was subjected to loading stresses in excess of 40 MPa, without undergoing failure. Under standard operating conditions, peak loading stresses in the order of 20 MPa were recorded, but not exceeded.

A Vibra-Corer unit was allowed to operate in impenetrable ground without lubrication within the drive head to the point at which bearing failure was promoted. It was found that several mechanisms exist to stop violent drive head failure. Should the drive unit seize up, one or all of the following conditions may occur:

1. the engine clutch disengages
2. the drive engine gear box yields
3. the male connecting end of the power flex-drive cable shears through

In all cases, no danger to the operators of the Vibra-Core unit are foreseen. There appears to be sufficient built-in safeguards to make the equipment quite safe.

Additional work, presently underway, includes the adaption of wire-line equipment and split tube core barrels for easier recovery of completely undisturbed samples, suitable for geotechnical analysis. Such work may be complemented by the adoption of thin-walled plastic liner tubes fitted within the present core barrel structures.

Grant 023 Aeromagnetic Gradient Characterization of Altered Volcanic Rocks

W.R. Lechow

Questor Surveys Limited, Mississauga

ABSTRACT

The vertical aeromagnetic gradiometer has been in limited use for at least 18 years. Application has been primarily with hydrocarbon exploration projects requiring large sensor spacing and a dual towed-bird installation. Technological refinements in both optically-pumped magnetometer hardware and compensation instrumentation have permitted decreasing sensor spacings to be used while maintaining a high degree of sensitivity. The Geological Survey of Canada has, in recent years, constructed and tested a rigidly-supported vertical gradiometer on a fixed-wing aircraft. Test results have shown that this type of configuration offers a high degree of immunity from temporal variances in the ambient magnetic field, enhanced depth discrimination, and obvious improvements in both spatial resolution and accuracy over total field instruments. Questor Surveys Limited has recently completed a parametrically similar installation using helium sensors. Initial test flying of this system in Clarendon Township supports the findings of the Geological Survey of Canada, indicating the usefulness of the instrument for detailed mapping in a "greenstone" environment.

Appended to the flying program, magnetic model inversion software utilizing Marquardt's algorithm, and adapted to gradiometer data, was also evaluated. Inversions proved faithful to published ground-truth data where no suggestion of geometrical ambiguity was present in the source geology.

INTRODUCTION

SUMMARY OF GRADIOMETER DEVELOPMENT

The airborne vertical magnetic gradiometer has recently become recognized as a useful tool in mineral exploration programs. The concept is certainly not new, but technological barriers until recently have prevented the development of a useful system. The advent of the high-sensitivity optically-pumped sensor during the late 1950s inspired the construction of early versions of vertical gradiometer during the following half-decade. These early systems employed towed-bird sensor arrangements with relatively wide sensor separation. The wide separation was chosen to provide adequate sensitivity, since the state-of-the-art technology of the day would not provide the low noise levels that are realized in current instruments. For this reason, the gradiometer was primarily attractive to hydrocarbon exploration programs during that period, as the sensor separation represented only a relatively small part of the distance to source rocks of interest, and a useful degree of spatial resolution was still afforded. For similar reasons, the lack of control on the degree of vertical disposition of the sensors, in a towed-bird arrangement, was not considered a significant problem. Noise originating from air turbulence acting on the sensors was a limiting factor on the ultimate performance which could be achieved with these configurations.

A more closely spaced sensor arrangement eventually became viable due to recent technological advancements which have, in general, led to lower noise instrumentation and a subsequent increase in sensitivity.

A rigidly disposed sensor configuration was developed by the Geological Survey of Canada under the direction of Peter Hood (Head of the Regional Geophysics Subdivision, Resource Geophysics and Geochemistry Division; *see* Hood *et al.* 1979). The system was mounted on a Beechcraft B80 Queenair with the sensors incorporated into the tail section. Although the problem of turbulence-induced noise is somewhat lessened, a gradiometer which is physically coupled closely to an aircraft such as this, requires careful and detailed compensation. To this, however, must be added the advantages of virtually constant sensor spacing, greatly improved vertical alignment, and total freedom from swinging or rotation about the vertical axis. With the rigid mounting configuration, much more of the noise is of a common-mode nature, affecting both sensors similarly in both phase and amplitude. Since the system is inherently sensitive only to the difference between sensor signals, common-mode noise is not recognized.

A number of years of test application by the Geological Survey of Canada has led to the conclusion that the vertical gradiometer is certainly a worthwhile device for mineral exploration (Hood *et al.* 1979). Shortly after this conclusion was drawn, Questor Surveys Limited decided to design and construct a rigidly-mounted vertical gradiometer, using a Britten-Norman Trislander aircraft, and optically-pumped helium sensors. This report is based on the initial test flying performed over Clarendon Township with the newly-developed system.

GENERAL FEATURES

The following are the principle advantages of the vertical gradiometer in mineral survey applications, when compared to conventional magnetometers:

1. The vertical aeromagnetic gradiometer allows for the optimum utilization of high sensitivity optically-pumped sensors by operating in the difference mode, thereby rendering the instrument immune to all forms of noise which affect both sensors equally. This includes temporal variations of the ambient magnetic field and allows the acquisition of data which is free of diurnal perturbation. Map compilation procedures then become greatly simplified, requiring little or no levelling effort, and yield a product which is inherently of improved accuracy.
2. The gradiometer is intrinsically more sensitive to residual, or short spatial-wavelength features over the regional aspect of an area. This quality is well appreciated, since a regional-residual separation is the most frequent requirement of post-acquisition processing of conventional total field data.
3. The vertical magnetic gradient above a near-vertical geological contact in an area of high magnetic inclination changes sign. Many parts of the Canadian Shield satisfy these conditions, thereby permitting the use of the gradiometer as an excellent mapping tool. This can be simply accomplished by tracing the zero level of contoured gradient data.
4. The preferential sensitivity to surface, or residual features, and the ability to accurately delineate steeply dipping contacts, give the gradiometer a general superiority in spatial resolution over conventional total field measuring systems.

CLARENDON TOWNSHIP

INTRODUCTION

Clarendon Township is located in northern Frontenac County, southeastern Ontario. The township, dominantly composed of Precambrian rocks in the Grenville Province, is situated east of the Frontenac Axis. Preliminary geological mapping at a scale of 1:15 840 has recently become available for a major part of the township (Map P.2487, Ardoch Area, Pauk and Mannard 1982). The Ardoch map area includes central and eastern Clarendon Township and covers approximately 75% of the area surveyed by the aeromagnetic gradiometer. National Topographic Series coverage of Clarendon Township at 1:50 000 scale is included within map areas 31 C/14, 31 C/15, 31 F/2, and 31 F/3. Relief is moderate in this area, generally being less than 75 m.

EXPLORATION HISTORY

This region saw considerable mining of gold and industrial minerals during the first half of the century and in some instances even earlier. Clarendon Township, itself, experienced very little of this activity. Records indicate that the only early mineral production the township has seen was the Boerth Gold Mine, which went into brief production at the turn of the century, and the James Mine, also an early and very short-lived producer (Hewitt 1964; Smith 1956; Pauk and Mannard 1982). A number of additional mineral occurrences have been recognized and recorded in the township. These occurrences include minerals which have potential economic value, but presumably occur in insufficient grade or volume to warrant development, as well as other minerals which have no intrinsic value, but serve as potential indicators of associative deposits.

A revival of exploration activity was felt in the area in the early 1950s, which led to reinvestigation of the Boerth and James Mine areas, as well as the Webber Property, another early claim which showed a promise of gold potential. The Boerth, James, and Webber localities occur on the the same stratigraphic horizon, a contact between clastic and carbonate metasediments along an anticlinorial crest. Exploration activity during the 1950s and 1960s generally took the form of diamond drilling in the vicinity of the early prospects. Later, during the 1970s, a more widely based reconnaissance geochemical approach was favoured. An increasing emphasis was placed on exploring the uranium potential of the area during the late 1950s. This activity centred on the Cross Lake Pluton and structurally associated rocks. Uranium exploration in the area reached peak activity during the mid 1970s after which it abruptly declined due to the drop in global uranium demand.

GEOLOGY

Clarendon Township lies within the Central Metasedimentary Belt of the Grenville Province. The metamorphic grade increases from west to east along the belt; the map area is underlain by rocks of amphibolite grade.

The township lies on a Late Precambrian metavolcanic-metasedimentary sequence which has been intruded by both felsic and mafic rocks (Figure 1). The oldest rocks in the township are the narrow bands of metavolcanics striking northeastward across the southern end of the area. The composition of the metavolcanics varies with age. The oldest, mafic band lies beyond the southern margin of the survey area. An intermediate band, included within the area of survey coverage, forms the northern contact of the Cross Lake Pluton. The uppermost unit of the early volcanic sequence consists of interlayered mafic tuffs and carbonate metasediments.

A younger metavolcanic-metasedimentary sequence is represented in the northern half of the township by gneisses of varying composition, including both mafic and felsic components. This sequence is folded to form the Plevna Synform and the complimentary Plevna Antiform which are probably the most distinctive structural features in the township. These structures plunge gently northeastward and represent a later episode of deformation in the area. An earlier deformation is marked by isoclinal folding.

A later carbonate-clastic metasedimentary sequence is represented by widespread occurrences, chiefly of carbonates, across the map area. It is these metasediments which host the gold occurrences described previously.

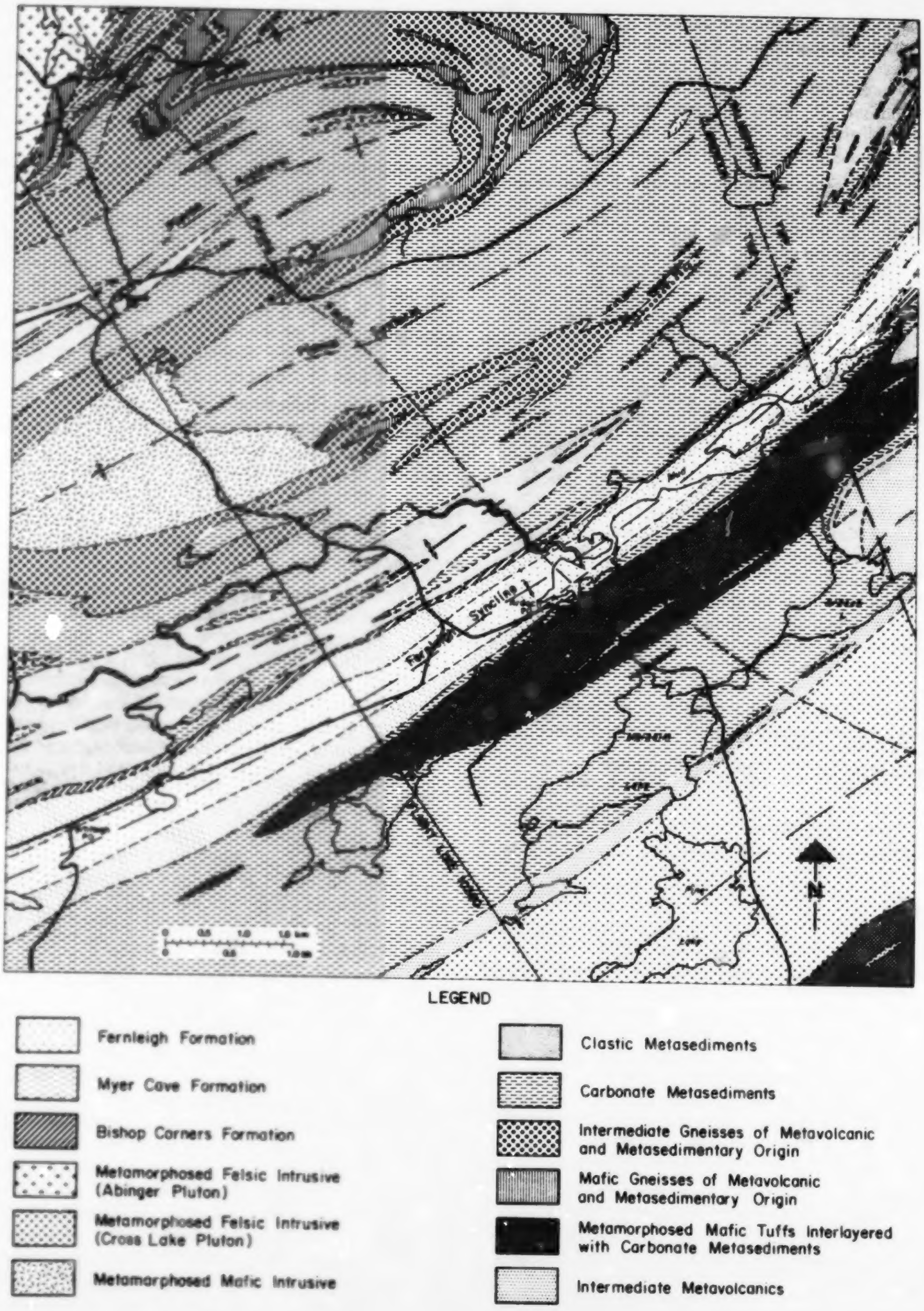
Syncline
N
LEGEND
Fernleigh Formation
Myer Cave Formation
Bishop Corners Formation
Metamorphosed Felsic Intrusive (Abinger Pluton)
Metamorphosed Felsic Intrusive (Cross Lake Pluton)
Metamorphosed Mafic Intrusive
Clastic Metasediments
Carbonate Metasediments
Intermediate Gneisses of Metavolcanic and Metasedimentary Origin
Mafic Gneisses of Metavolcanic and Metasedimentary Origin
Metamorphosed Mafic Tuffs Interlayered with Carbonate Metasediments
Intermediate Metavolcanics

Figure 1. Geology of northern Clarendon Township.

Intrusive events followed the deposition of the sediments. A mafic stock intruded the metasediments and metavolcanics which outline the Plevna Synform. The Cross Lake Pluton formed as a sheet-like intrusion which extensively altered the early volcanic sequence in the southern part of the area. The northwestern part of the township lies on a small part of the Abinger Pluton.

The Flinton Group marks the youngest Precambrian rocks found in the township and is separated from the older units by an unconformity. Three formations are recognized as representative of this group within the survey area. These formations are the Bishop Corners Formation, the Myer Cave Formation, and Fernleigh Formation. The Flinton Group has been the subject of detailed study (Moore and Thompson 1972, 1980). The Group lies within the Fernleigh Syncline, a narrow feature which crosses approximately the middle of Clarendon Township.

Foliation within the study area generally dips steeply northwestward paralleling the axial planes of the earlier folds. The tightest folds occupy the central part of the area, that which lies immediately north of the Fernleigh Syncline.

The predominant fault orientation in the area is northwest-southeast. The Plevna Fault demonstrates this orientation, and is a major fault in the area. This fault shows a lateral displacement only in a few places, and, combined with its orientation, has caused it to be only weakly discernable magnetically. Other faults, which show a northeastward trend, have been inferred from the gradiometer data.

AEROMAGNETIC GRADIOMETER SURVEY

Clarendon Township was flown with the vertical aeromagnetic gradiometer during the 1982 field season. The survey was flown with a 146° nominal flight line orientation at 150 m mean terrain clearance. Flight lines were positioned along a 200 m interval.

Total intensity and vertical gradient data were contoured at 2 nanoteslas and 25 picoteslas/m sensitivities, respectively. In addition to the conventional contour maps, colour contour plots were also generated (Figure 4, Chart A, and Figure 5, Chart B, back pocket). The total intensity data were plotted using a weighted spectrum with a minimum interval of 5 nanoteslas, and a weighting criterion based on a preferred equal-area distribution of the chromatic elements. The vertical gradient data were plotted using a contrast-emphasis spectrum first applied to aeromagnetic gradient data by Peter Hood of the Geological Survey of Canada. This spectrum also demonstrates logarithmic compression toward both ends, with a minimum interval of 25 picoteslas/m at mid-spectrum. Contrast-emphasis is accomplished by adding a yellow constant to alternating intervals.

Comparison between the colour maps of total intensity and vertical gradient information suggests that the gradient data offers a sharper spatial resolution, especially when presented in the contrast-emphasis form. This can be observed in the northeastern corner of the township where an apparently monochromatic high in total intensity information is shown to be sharply delineated when viewed in gradient form. Subtle linear features, which have been inferred as faults, are oriented obliquely to local strike and can be seen as dislocations within, and nearby, the Fernleigh Syncline on the colour gradient map. These are only slightly discernable on the colour total intensity map.

A better appreciation of the gradient data can be realized when the overall amplitude of the data is examined on a relative basis. The colour gradient map was generated using an increment of 25 picoteslas/m about the zero gradient level, and a dynamic range in excess of 17 nanoteslas/m. The displayed gradient data thus spans over 680 times the smallest map unit increment, or approximately 3 orders of magnitude.

In comparison, the colour total intensity map was made using a fundamental increment of 5 nanoteslas (only 2 intervals are represented at this level of sensitivity) with a dynamic range of greater than 1050 nanoteslas. The total intensity data spans more than 210 times the smallest map increment; 105 is a more realistic value since the 5 nanoteslas sensitivity is achieved over only a small part of the total map area.

Both the colour gradient and the total intensity maps divide the represented data into 39 classes, or colours. In order to display the entire range of vertical gradient represented on the map at the highest (25 picoteslas/m) sensitivity, over 17 times the number of classes would be required. For total intensity data, only a 5 times increase would be required to display the entire map range with a 5 nanotesla sensitivity. It can be therefore clearly seen that a contrast of over 3-fold exists between the maps in the degree of compression that has been imposed on the data to accommodate the respective dynamic ranges. In spite of this fact, the gradient data remains obviously abundant in detail. If a smaller, or alternatively, lower contrast survey area were chosen, it would have imposed less constraint due to dynamic range considerations, and the gradient scale could be expanded to better realize the advantages in resolution of gradient over total field data.

EXAMINATION OF PROFILE DATA

A test line (flight line 10380, Figure 1) was arbitrarily selected for a comparison of profile gradient data with geology. In order that the geological information presented on Ontario Geological Survey Map P.2487 could be used to full advantage, a model cross section was constructed along the test flight line (Figure 2). This was accomplished by intercepting contacts, and sketching a structure which conforms to local bedrock attitudes displayed on the map. A generous allowance must be given for error in this section, since no vertical control information was available for its construction. It was felt, however, that this may not be of great consequence, since data from the vertical gradiometer configuration is strongly influenced by surficial geology. Gradient data from the portion of flight line 10380

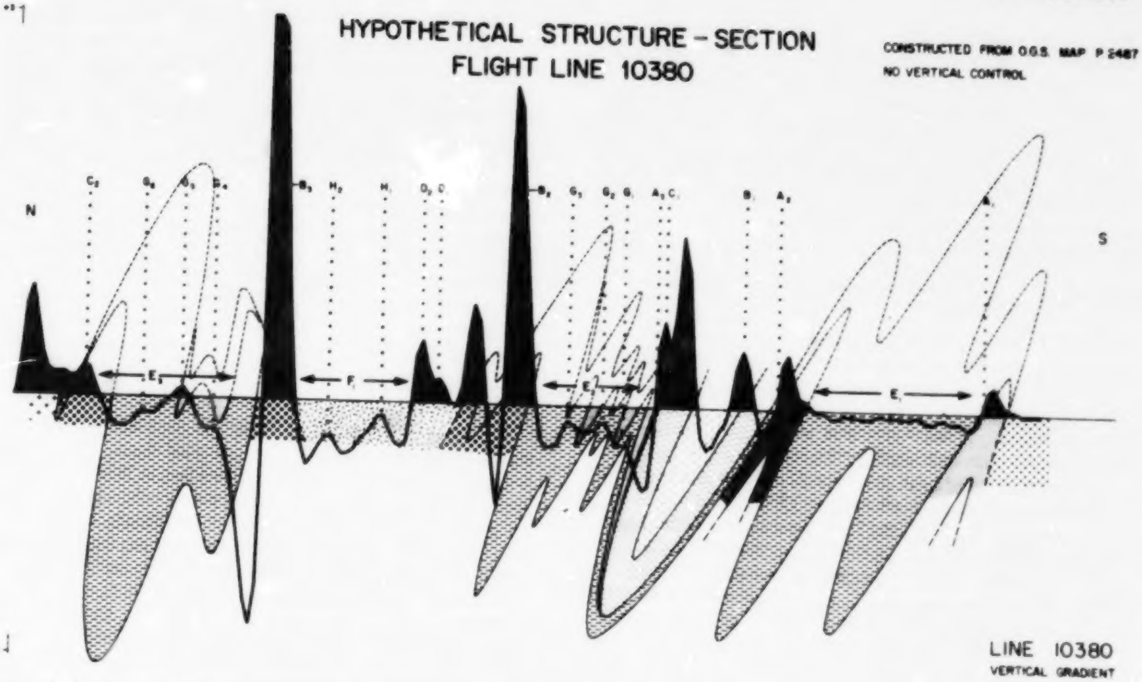

Figure 2. Gradient profile superimposed on model structure section.

which was flown over the representative structure-section, was plotted to scale and superimposed on the structure-section to facilitate direct comparison.

The correlation between the gradient profile and geology was visually assessed using anomaly position, amplitude, and shape criteria. For this purpose, the zero gradient level was used to define anomaly position. Three examples (A_1, A_2, A_3) were identified where the zero gradient level coincided with geological contacts exactly, when visually compared at a scale of 1:30 000. All 3 examples represented the northern flank of a positive anomaly, corresponding to the northern contact of the respective source rocks. It was also recognized that all of these agreements lie on the southerly part of the flight line, perhaps reflecting a more favourable structural situation in the southern part of the survey area for contact mapping using the gradiometer.

Anomalies which misfit the source geology due to lateral offset (B_1, B_2, B_3) are probably the result of mapping errors arising from speculative positioning of a lithic unit between areas of outcrop. In addition, anomalies which are apparently misrepresentative both in width and amplitude (C_1, C_2), probably indicate errors in estimating the subcrop width of bedrock strata during the process of map compilation.

Two adjacent units evidently were missed altogether during mapping (D_1, D_2), probably the result of concealment by swamp. Reference to the colour gradient map verifies the presence of a short stringer parallel with, and immediately north of, the metavolcanics which trace the southern limb of the Plevna Synform.

Areas of laterally sustained negative gradient values accurately mark the presence of marble (E_1, E_2, E_3) and a metamorphosed gabbro (F_1). The latter apparently has undergone sufficient alteration to significantly decrease its magnetic susceptibility, presumably by oxidation.

Interbeds of clastic metasediments (G_1, G_2, G_3, G_4, G_5, G_6) within the marbles, have given rise to weak, positive gradient profiles which are quite uniform in aspect. Two stronger positive anomalies (H_1, H_2) within the metamorphosed gabbro, may represent compositional or textural banding.

In an area of high magnetic inclination and steep geological structure, a vertical gradient profile which agrees in width with that of the source will demonstrate an amplitude which is proportional to the susceptibility of the source. The geology in the Clarendon Township survey area generally fulfills the dip criterion, and on that basis, anomaly amplitude relationships have been examined along the test line. Discrepancies between mapped lithological composition and observed magnetic susceptibility have been noticed in several places along the line. The disagreements are thought to be the result of metamorphic influence on the magnetic constituents within these rocks leading to increased oxidation states. The metavolcanics and metasediments which outline the Plevna Synform, have been classified as felsic and intermediate in composition in the area near the cross section (Pauk and Mannard

Intrusive events followed the deposition of the sediments. A mafic stock intruded the metasediments and metavolcanics which outline the Plevna Synform. The Cross Lake Pluton formed as a sheet-like intrusion which extensively altered the early volcanic sequence in the southern part of the area. The northwestern part of the township lies on a small part of the Abinger Pluton.

The Flinton Group marks the youngest Precambrian rocks found in the township and is separated from the older units by an unconformity. Three formations are recognized as representative of this group within the survey area. These formations are the Bishop Corners Formation, the Myer Cave Formation, and Fernleigh Formation. The Flinton Group has been the subject of detailed study (Moore and Thompson 1972, 1980). The Group lies within the Fernleigh Syncline, a narrow feature which crosses approximately the middle of Clarendon Township.

Foliation within the study area generally dips steeply northwestward paralleling the axial planes of the earlier folds. The tightest folds occupy the central part of the area, that which lies immediately north of the Fernleigh Syncline.

The predominant fault orientation in the area is northwest-southeast. The Plevna Fault demonstrates this orientation, and is a major fault in the area. This fault shows a lateral displacement only in a few places, and, combined with its orientation, has caused it to be only weakly discernable magnetically. Other faults, which show a northeastward trend, have been inferred from the gradiometer data.

AEROMAGNETIC GRADIOMETER SURVEY

Clarendon Township was flown with the vertical aeromagnetic gradiometer during the 1982 field season. The survey was flown with a 146° nominal flight line orientation at 150 m mean terrain clearance. Flight lines were positioned along a 200 m interval.

Total intensity and vertical gradient data were contoured at 2 nanoteslas and 25 picoteslas/m sensitivities, respectively. In addition to the conventional contour maps, colour contour plots were also generated (Figure 4, Chart A, and Figure 5, Chart B, back pocket). The total intensity data were plotted using a weighted spectrum with a minimum interval of 5 nanoteslas, and a weighting criterion based on a preferred equal-area distribution of the chromatic elements. The vertical gradient data were plotted using a contrast-emphasis spectrum first applied to aeromagnetic gradient data by Peter Hood of the Geological Survey of Canada. This spectrum also demonstrates logarithmic compression toward both ends, with a minimum interval of 25 picoteslas/m at mid-spectrum. Contrast-emphasis is accomplished by adding a yellow constant to alternating intervals.

Comparison between the colour maps of total intensity and vertical gradient information suggests that the gradient data offers a sharper spatial resolution, especially when presented in the contrast-emphasis form. This can be observed in the northeastern corner of the township where an apparently monochromatic high in total intensity information is shown to be sharply delineated when viewed in gradient form. Subtle linear features, which have been inferred as faults, are oriented obliquely to local strike and can be seen as dislocations within, and nearby, the Fernleigh Syncline on the colour gradient map. These are only slightly discernable on the colour total intensity map.

A better appreciation of the gradient data can be realized when the overall amplitude of the data is examined on a relative basis. The colour gradient map was generated using an increment of 25 picoteslas/m about the zero gradient level, and a dynamic range in excess of 17 nanoteslas/m. The displayed gradient data thus spans over 680 times the smallest map unit increment, or approximately 3 orders of magnitude.

In comparison, the colour total intensity map was made using a fundamental increment of 5 nanoteslas (only 2 intervals are represented at this level of sensitivity) with a dynamic range of greater than 1050 nanoteslas. The total intensity data spans more than 210 times the smallest map increment; 105 is a more realistic value since the 5 nanoteslas sensitivity is achieved over only a small part of the total map area.

Both the colour gradient and the total intensity maps divide the represented data into 39 classes, or colours. In order to display the entire range of vertical gradient represented on the map at the highest (25 picoteslas/m) sensitivity, over 17 times the number of classes would be required. For total intensity data, only a 5 times increase would be required to display the entire map range with a 5 nanotesla sensitivity. It can be therefore clearly seen that a contrast of over 3-fold exists between the maps in the degree of compression that has been imposed on the data to accommodate the respective dynamic ranges. In spite of this fact, the gradient data remains obviously abundant in detail. If a smaller, or alternatively, lower contrast survey area were chosen, it would have imposed less constraint due to dynamic range considerations, and the gradient scale could be expanded to better realize the advantages in resolution of gradient over total field data.

EXAMINATION OF PROFILE DATA

A test line (flight line 10380, Figure 1) was arbitrarily selected for a comparison of profile gradient data with geology. In order that the geological information presented on Ontario Geological Survey Map P.2487 could be used to full advantage, a model cross section was constructed along the test flight line (Figure 2). This was accomplished by intercepting contacts, and sketching a structure which conforms to local bedrock attitudes displayed on the map. A generous allowance must be given for error in this section, since no vertical control information was available for its construction. It was felt, however, that this may not be of great consequence, since data from the vertical gradiometer configuration is strongly influenced by surficial geology. Gradient data from the portion of flight line 10380

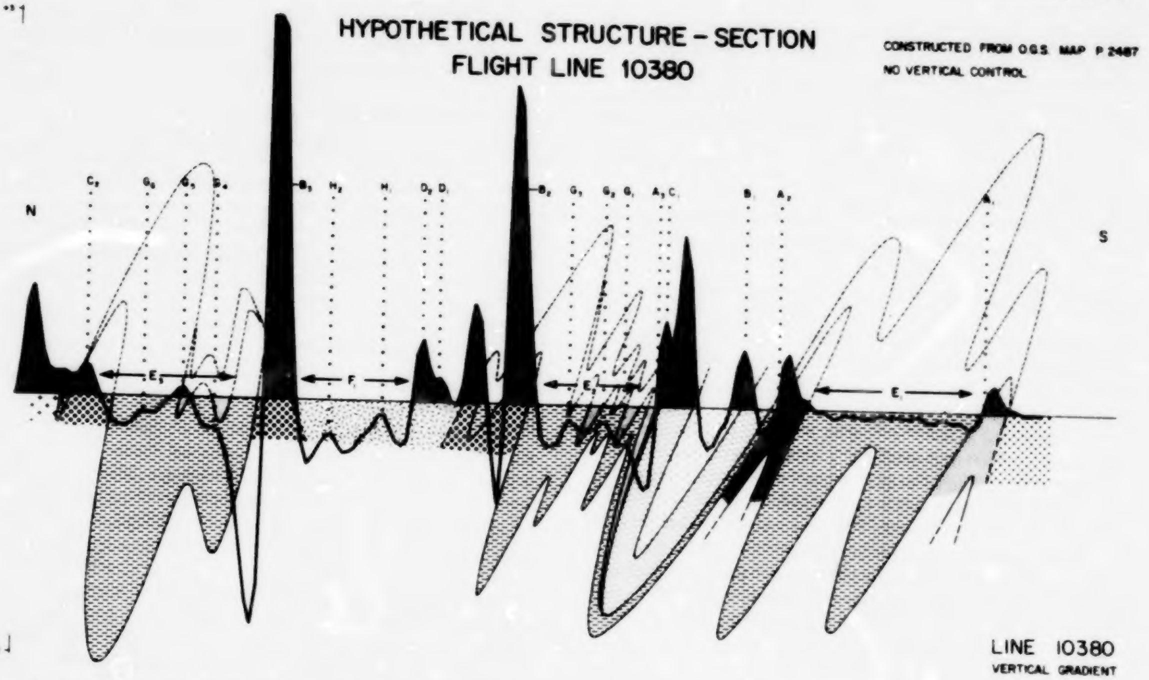

Figure 2. Gradient profile superimposed on model structure section.

which was flown over the representative structure-section, was plotted to scale and superimposed on the structure-section to facilitate direct comparison.

The correlation between the gradient profile and geology was visually assessed using anomaly position, amplitude, and shape criteria. For this purpose, the zero gradient level was used to define anomaly position. Three examples (A_1, A_2, A_3) were identified where the zero gradient level coincided with geological contacts exactly, when visually compared at a scale of 1:30 000. All 3 examples represented the northern flank of a positive anomaly, corresponding to the northern contact of the respective source rocks. It was also recognized that all of these agreements lie on the southerly part of the flight line, perhaps reflecting a more favourable structural situation in the southern part of the survey area for contact mapping using the gradiometer.

Anomalies which misfit the source geology due to lateral offset (B_1, B_2, B_3) are probably the result of mapping errors arising from speculative positioning of a lithic unit between areas of outcrop. In addition, anomalies which are apparently misrepresentative both in width and amplitude (C_1, C_2), probably indicate errors in estimating the subcrop width of bedrock strata during the process of map compilation.

Two adjacent units evidently were missed altogether during mapping (D_1, D_2), probably the result of concealment by swamp. Reference to the colour gradient map verifies the presence of a short stringer parallel with, and immediately north of, the metavolcanics which trace the southern limb of the Plevna Synform.

Areas of laterally sustained negative gradient values accurately mark the presence of marble (E_1, E_2, E_3) and a metamorphosed gabbro (F_1). The latter apparently has undergone sufficient alteration to significantly decrease its magnetic susceptibility, presumably by oxidation.

Interbeds of clastic metasediments (G_1, G_2, G_3, G_4, G_5, G_6) within the marbles, have given rise to weak, positive gradient profiles which are quite uniform in aspect. Two stronger positive anomalies (H_1, H_2) within the metamorphosed gabbro, may represent compositional or textural banding.

In an area of high magnetic inclination and steep geological structure, a vertical gradient profile which agrees in width with that of the source will demonstrate an amplitude which is proportional to the susceptibility of the source. The geology in the Clarendon Township survey area generally fulfills the dip criterion, and on that basis, anomaly amplitude relationships have been examined along the test line. Discrepancies between mapped lithological composition and observed magnetic susceptibility have been noticed in several places along the line. The disagreements are thought to be the result of metamorphic influence on the magnetic constituents within these rocks leading to increased oxidation states. The metavolcanics and metasediments which outline the Plevna Synform, have been classified as felsic and intermediate in composition in the area near the cross section (Pauk and Mannard

1982). The vertical gradient recorded from these rocks, however, is relatively large, exceeding that of all other lithologies represented along the line. This suggests a dominantly mafic composition, a conclusion which has found some additional published support (Sethuraman and Moore 1973). In contrast, the units described as interlayered mafic tuffs and carbonate metasediments (Pauk and Mannard 1982) near the southern end of the section, have only provided a modest gradiometer profile, which is more representative of an intermediate composition.

AUTOMATIC INVERSION TESTS

An adaptation of MAGMOD, version 1.4, was applied to selected gradient profiles along the test line. MAGMOD 1.4 is a magnetic inversion program which computes a theoretical anomaly profile and compares this model to field data using a least-squares technique. Marquardt's algorithm is then followed for model covergence. Initial requirements include the selection of a geometrical model, and parametric data relating to orientation of the model with respect to the ambient field, as well as initial values, and scaling information. Optional switches allow the user to fix, or rigidly define selected parameters, if desired. Other options include weighting of input field data, limits on the flexibility of individual parameters, and a user-imposed convergence time limit.

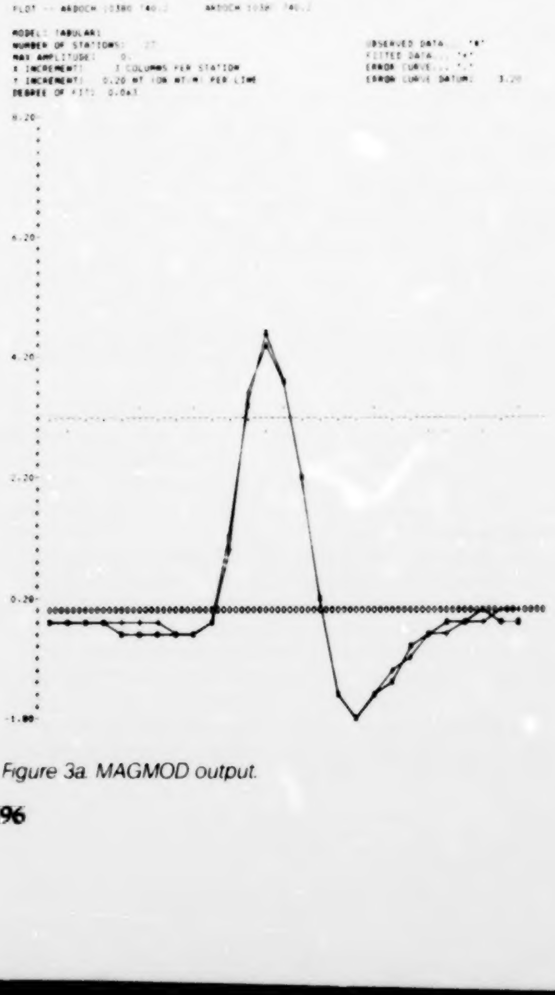

Figure 3a. MAGMOD output.

It would be beyond the scope of this paper to discuss to a great extent the implementation and application aspects of this software tool to gradiometer data. Figures 3a and 3b illustrate a typical example of modeling inversion using MAGMOD. The field data for the example was derived from the highest amplitude gradient anomaly on the test line (Figure 2) discussed previously. This is representative of the volcanic rock which forms part of the northern limb of the Plevna Synform. The tabulated output includes a model dip estimate of 84° SE, in strong agreement with the 82° SE foliation attitude indicated on Ontario Geological Survey Map P.2487, near this location. The depth below ground offered by the model is 1.4 m, which is realistic when considering the indications of nearby outcrop on the geology map. A visual examination of the model profile superposed on the field data (Figure 3a) suggests a reasonably close overall agreement.

In some instances, MAGMOD results have shown some disagreement with the geology map. This is not entirely surprising, since the tight folding in this area would imply that in many places, an apparently singular magnetic anomaly may be reflecting a geometrically composite source, consisting of opposite limbs of a less than isoclinal fold. This would naturally give rise to a dip paradox in the modelling process. Possible examples of this could be the 2 most southerly gradient anomalies on the test line (Figure 2). Map P.2487 indicates the source of these anomalies as being metavolcanics and interlayered tuffs and metasediments, each of which demonstrates a foliation attitude with a northwestward dip direction. In contrast to this, the character of the gradient profiles is suggestive, in both instances, of an opposite or southeasterly dip component within the source geometry. Application of MAGMOD to these profiles has only served to support this observation.

MAGMOD 1.4 was made available under license from Paterson, Grant, and Watson Limited, and was accessed through the VAX 11/780 network operated by Dataplotting Services Incorporated.

REFERENCES

Hewitt, D.F.
1964 Geological Notes for Maps Numbers 2053 and 2054, Madoc-Gananoque Area; Geological Circular 12, Ontario Division of Mines, Ontario Ministry of Natural Resources, p.12.

Hood, P., Sawatzky, P., Kornik, L.J., and McGrath, P.H.
1979 Aeromagnetic Gradiometer Survey, White Lake Ontario; Atomic Energy of Canada Limited, Technical Record TR-11, p.4-8.

Moore, J.M., and Thompson, P.H.
1972 The Flinton Group, Grenville Province, Eastern Ontario, Canada; 24th International Geological Congress, Montreal, Quebec, Proceedings, Section 1, p.221-229.

1980 The Flinton Group: A Late Precambrian Metasedimentary Succession in the Grenville Province of Eastern Ontario; Canadian Journal of Earth Sciences, Volume 17, p.1685-1707.

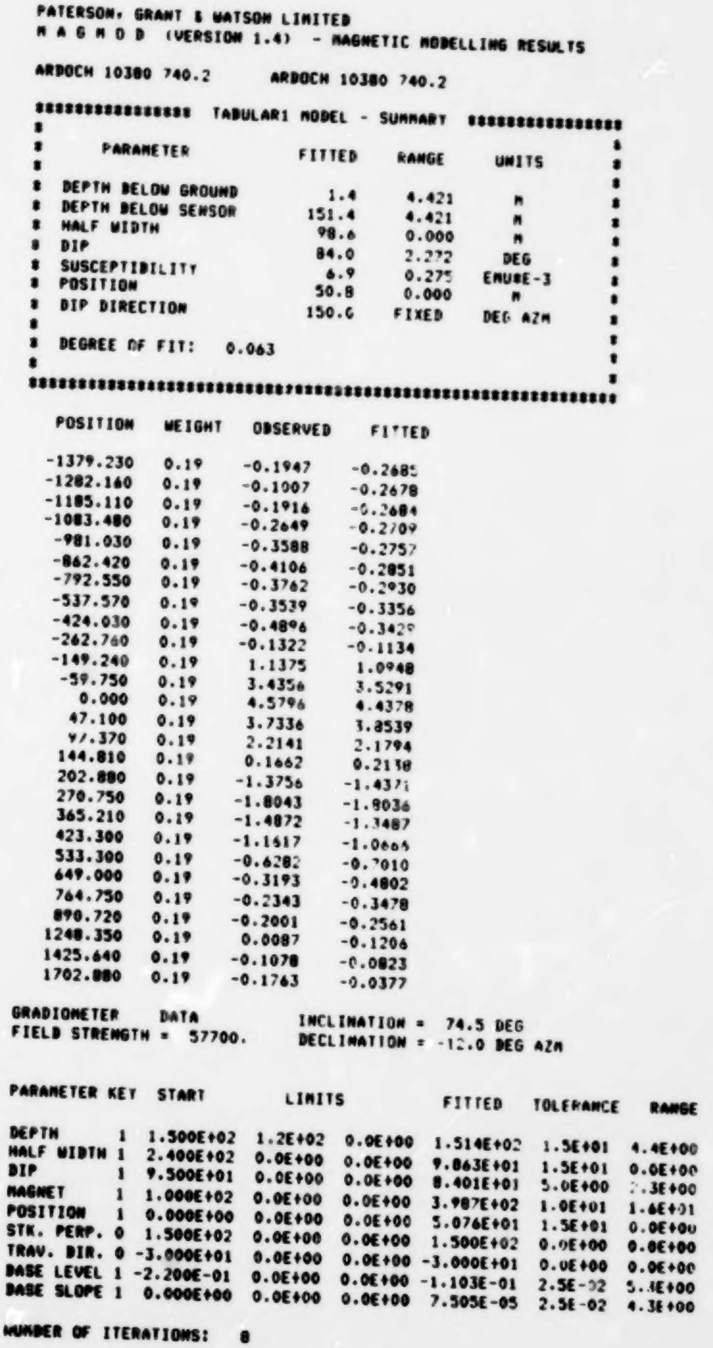

```
PATERSON, GRANT & WATSON LIMITED
M A G M O D  (VERSION 1.4)  - MAGNETIC MODELLING RESULTS

ARDOCH 10380 740.2       ARDOCH 10380 740.2

****************  TABULAR1 MODEL - SUMMARY  ****************
*                                                          *
*      PARAMETER              FITTED    RANGE     UNITS     *
*                                                          *
*  DEPTH BELOW GROUND            1.4    4.421       M       *
*  DEPTH BELOW SENSOR          151.4    4.421       M       *
*  HALF WIDTH                   98.6    0.000       M       *
*  DIP                          84.0    2.272      DEG      *
*  SUSCEPTIBILITY                6.9    0.275    EMU*E-3    *
*  POSITION                     50.8    0.000       M       *
*  DIP DIRECTION               150.0    FIXED    DEG AZM    *
*                                                          *
*  DEGREE OF FIT:    0.063                                 *
*                                                          *
************************************************************

   POSITION   WEIGHT   OBSERVED    FITTED

  -1379.230   0.19     -0.1947    -0.2685
  -1282.160   0.19     -0.1007    -0.2678
  -1185.110   0.19     -0.1916    -0.2684
  -1083.480   0.19     -0.2649    -0.2709
   -981.030   0.19     -0.3588    -0.2757
   -862.420   0.19     -0.4106    -0.2851
   -792.550   0.19     -0.3762    -0.2930
   -537.570   0.19     -0.3539    -0.3356
   -424.030   0.19     -0.4896    -0.3429
   -262.760   0.19     -0.1322    -0.1134
   -149.240   0.19      1.1375     1.0948
    -59.750   0.19      3.4356     3.5291
      0.000   0.19      4.5796     4.4378
     47.100   0.19      3.7336     3.8539
     97.370   0.19      2.2141     2.1794
    144.810   0.19      0.1662     0.2138
    202.880   0.19     -1.3756    -1.4371
    270.750   0.19     -1.8043    -1.8036
    365.210   0.19     -1.4872    -1.3487
    423.300   0.19     -1.1617    -1.0665
    533.300   0.19     -0.6282    -0.7010
    649.000   0.19     -0.3193    -0.4802
    764.750   0.19     -0.2343    -0.3478
    890.720   0.19     -0.2001    -0.2561
   1248.350   0.19      0.0087    -0.1206
   1425.640   0.19     -0.1078    -0.0823
   1702.880   0.19     -0.1763    -0.0377

GRADIOMETER    DATA            INCLINATION =  74.5 DEG
FIELD STRENGTH =  57700.       DECLINATION = -12.0 DEG AZM


PARAMETER KEY  START          LIMITS             FITTED    TOLERANCE   RANGE

DEPTH       1  1.500E+02  1.2E+02  0.0E+00   1.514E+02   1.5E+01   4.4E+00
HALF WIDTH  1  2.400E+02  0.0E+00  0.0E+00   9.863E+01   1.5E+01   0.0E+00
DIP         1  9.500E+01  0.0E+00  0.0E+00   8.401E+01   5.0E+00   2.3E+00
MAGNET      1  1.000E+02  0.0E+00  0.0E+00   3.987E+02   1.0E+01   1.6E+01
POSITION    1  0.000E+00  0.0E+00  0.0E+00   5.076E+01   1.5E+01   0.0E+00
STK. PERP.  0  1.500E+02  0.0E+00  0.0E+00   1.500E+02   0.0E+00   0.0E+00
TRAV. DIR.  0 -3.000E+01  0.0E+00  0.0E+00  -3.000E+01   0.0E+00   0.0E+00
BASE LEVEL  1 -2.200E-01  0.0E+00  0.0E+00  -1.103E-01   2.5E-02   5.4E+00
BASE SLOPE  1  0.000E+00  0.0E+00  0.0E+00   7.505E-05   2.5E-02   4.3E+00

NUMBER OF ITERATIONS:    8
```

Figure 3b. MAGMOD output.

Pauk, L., and Mannard, G.
1982: Precambrian Geology of the Ardoch Area, Southern Ontario; Ontario Geological Survey, Map P.2487, Geological Series-Preliminary Map, scale 1:15 840 or 1 inch to ¼ mile. Geology 1980.

Sethuraman, K., and Moore, J.M.
1973: Petrology of Metavolcanic Rocks in the Bishop Corners-Donaldson Area, Grenville Province, Ontario; Canadian Journal of Earth Sciences, Volume 10, p.591.

Smith, B.L.
1956: Geology of the Clarendon-Dalhousie Area; Ontario Department of Mines, Volume 65, Part 7, p.38-39.

Grant 025 The Development of an Omni-Directional Multi-Frequency Airborne EM System

S.J. Kilty
Dighem Limited, Toronto

ABSTRACT

In June of 1982, Dighem Limited began the development of a multi-coil and multi-frequency helicopter-borne electromagnetic system which would extend the resistivity mapping capability of the DIGHEM^{II} system.

The system was conceived as consisting of 1 coaxial coil-pair and 2 coplanar coil-pairs operating over a frequency range of 380 Hz to 50 000 Hz. This would allow the mapping of earth resistivities from 0.1 ohm-m to 50 000 ohm-m.

The DIGHEM^{III} development required extensive redesign of the electromagnetic sensor ("bird") and electronic hardware. The addition of the higher frequencies also required extensive software development in order to make full use of the additional information.

INTRODUCTION

Dighem Limited is an airborne geophysical company that became federally incorporated in August 1967. Three years later, the original DIGHEM^{I} system was introduced to the mining community. This system consisted of a single vertical transmitter coil plus 3 orthogonal receiver coils. The 3 receiver coils measured the 3 spatial components of the anomalous field vector and, therefore, provided information on strike and dip of planar geologic conductors. Helicopter EM systems were held in low esteem prior to 1970 because of their shallow depth of exploration. With a depth of exploration of 100 m, and the vector EM recording, DIGHEM^{I} represented a significant improvement in helicopter EM technology.

DIGHEM^{I} evolved into DIGHEM^{II} in 1975. This system caused a renewed popularity of helicopter-borne EM exploration. As of January 1981, there were 6 DIGHEM^{II} systems in operation. Four systems were owned and operated by Dighem Limited, and the federal governments of West Germany and Austria owned 1 each.

The DIGHEM^{II} system consists of 2 maximum-coupled transmitter-receiver coil-pairs, one having a vertical coaxial orientation and the other having a horizontal coplanar orientation. This design pioneered 2 important features: the coplanar orientation, and the use of common frequencies on both coil-pairs. The operation of the 2 orthogonal coil-pairs at a common frequency allows a geometric analysis of conductors to be carried out. The DIGHEM^{II} system was the only helicopter EM system to feature this geometric analysis until the advent of DIGHEM^{III}.

DIGHEM^{III}

DIGHEM^{III} (Figure 1) was initially conceived as a rigid, towed boom system that would provide universal coupling to conductors and also have a dual frequency capability. This would result in improved detection and analysis of

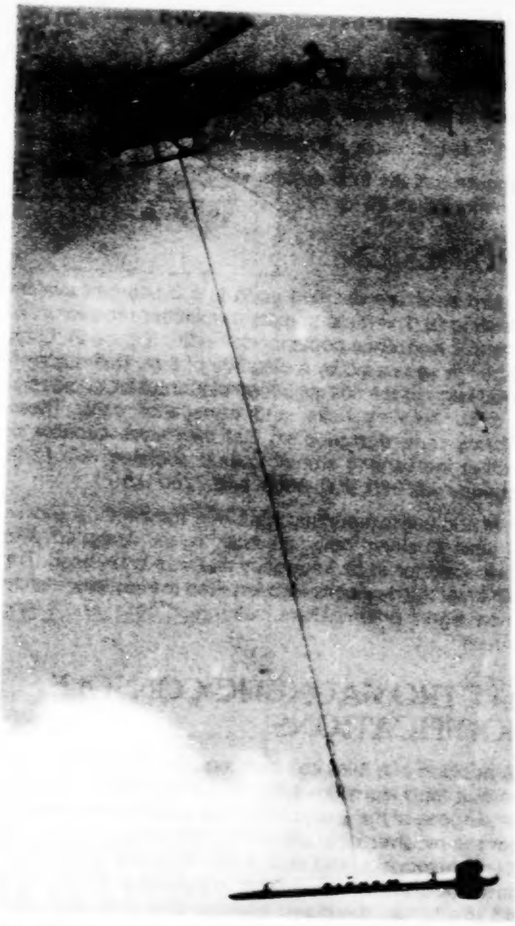

Figure 1. Photograph of the DIGHEM^{III} airborne electromagnetic system.

conductors. As system development began, it evolved into a 3 coil-pair system consisting of 1 vertical coaxial coil-pair and 2 horizontal coplanar coil-pairs operating at any combination of 380, 900, 3600, 7200, and 50 000 Hz. Frequency selection is dependent upon the specific application.

The initial design work commenced during the last week of June 1982; work initially concentrated on the mechanical configuration within the bird structure. The initial design criteria required several basic elements of the DIGHEM^{II} system to remain intact:

1. dipole moment of 225 ampere-turns/m^2
2. coil separation of 8 m
3. noise levels of 1 to 2 ppm
4. instrument drift of 0.5 ppm per minute or less
5. 2 orthogonal coil-pairs operating at approximately the same frequency

In addition to these criteria, the DIGHEM^{III} design had to:

1. provide multi-frequency capability
2. extend the dynamic range of the resistivity calculations
3. provide geometric information on a conductor
4. ensure that the total system weight would increase by no more than 25 kg

BIRD DESIGN

The bird structure decided upon is a 3 coil-pair system consisting of 1 vertical coaxial transmitter-receiver coil-pair and 2 horizontal coplanar coil-pairs (Figure 2). Each coil-pair is separated by a distance of 8 m. This required the redesign of the coil mounting platforms for the receiving coils, bucking coils, and transmitter coils. These platforms were designed so that they were capable of handling the varying size of coils associated with each frequency (i.e. 380, 900, 3600, and 7200 Hz).

In addition to mounting platforms, transmitting, receiving, and bucking coils all had to be designed and constructed for each frequency that was to be used. The addition of the new coils also required the implementation of new signal preamplifiers, calibration coils, and wiring harness.

ELECTROMAGNETIC CONSOLE MODIFICATIONS

The addition of a third coil-pair required the implementation of a third signal analyzer in the instrument console. The purpose of the analyzer is to take the incoming signal from the receiver coil, extract the secondary signal (the ground response), and split it into in-phase and out-of-phase components with respect to the primary transmitted field. In addition, the signal analyzer also outputs a noise monitor channel which indicates the presence of external noise sources (either powerline noise or atmospheric bursts).

The DIGHEM signal analyzers are modular in form. Thus, with the addition of the third module, it was upgraded into a 3 coil-pair configuration. Each console is frequency dependent, and thus is only capable of handling the signal from a specific coil-pair operating at a predetermined frequency. The resulting 3 channels of information (i.e. in-phase, out-of-phase, noise monitor), produced by the signal analyzer, made modifications to both the analog and digital recording instrumentation necessary. This involved both the physical space to record the information and an increase in the dynamic range of the recorder in order to handle increased signal size due to the higher frequency (7200 Hz).

TEST RESULTS

The prototype system was first flown in the Toronto vicinity in late July 1982 with the coaxial coil-pair and 1 coplanar coil-pair operating at 900 Hz, and the third (coplanar) coil-pair at 7200 Hz. Short term (or high frequency) noise normally associated with bird bending was generally within the original specifications of 1 to 2 ppm, but the system did exhibit both phasing and long term (or low frequency) drift problems on the 7200 Hz configuration.

LONG TERM DRIFT

The first problem to be attacked was to locate the source of the low frequency noise and find a solution. Examination of the transmitter for the high frequency coil-pair revealed that the linear type drivers used in the transmitter electronics were failing at this frequency and causing the transmitted frequency to drift by up to 10%. The long term drift of the in-phase and out-of-phase channels from the high frequency module was attributed to this frequency drift. The solution was to redesign the transmitter assembly using Field Effect Transistors (FET) in the driver circuit. This design was completed and, when tested, exhibited drift characteristics which were within the original design specifications.

PHASING

The phasing of the system is necessary to accurately separate the in-phase and out-of-phase components of the secondary signal. At lower frequencies, this is accomplished by generating a pure in-phase response through the use of ferrite cylinders on the ground. Testing revealed that secondary fields resulting from high surficial conductivity can cause a phase shift at the higher frequency such that ferrite phasing of the system may be inaccurate. In order to avoid this problem, a coil was designed with a very high Q-factor such that, when it was shorted, it resulted in a predominantly in-phase response. This allows the system to be phased outside of any ground effects, i.e. during flight.

These modifications to the original design resulted in an electromagnetic system that was equal to the specifications defined at the commencement of the project.

This prototype system was then used to conduct a series of tests over several known deposits of varying geophysical properties. These sites included parts of Caledon Township and the District of Cochrane over known sand and gravel deposits, the Whistle Mine near Sudbury, the Montcalm deposit near Timmins, and the Ontario Geological Survey Nighthawk Lake test site (Barlow 1981; Barlow *et al.* 1982).

SURVEY RESULTS OVER KNOWN GEOLOGY

The most significant contribution that DIGHEM^{III} is making to the exploration community is the increase in the dynamic range of helicopter-borne electromagnetic systems. The use of 7200 Hz allows the mapping of a range of resistivities from 0.1 ohm-m to 8000 ohm-m. This provides 2 important benefits to the mining community:

1. The broader range of resistivities provides a better geological (both structural and formational) mapping tool.
2. The ability to detect conductors with resistivities in excess of 3000 ohm-m means that poorly conductive zones of mineralization (previously unmapped by other airborne electromagnetic systems operating in the range of 385 Hz to 4500 Hz) are now detectable. This is

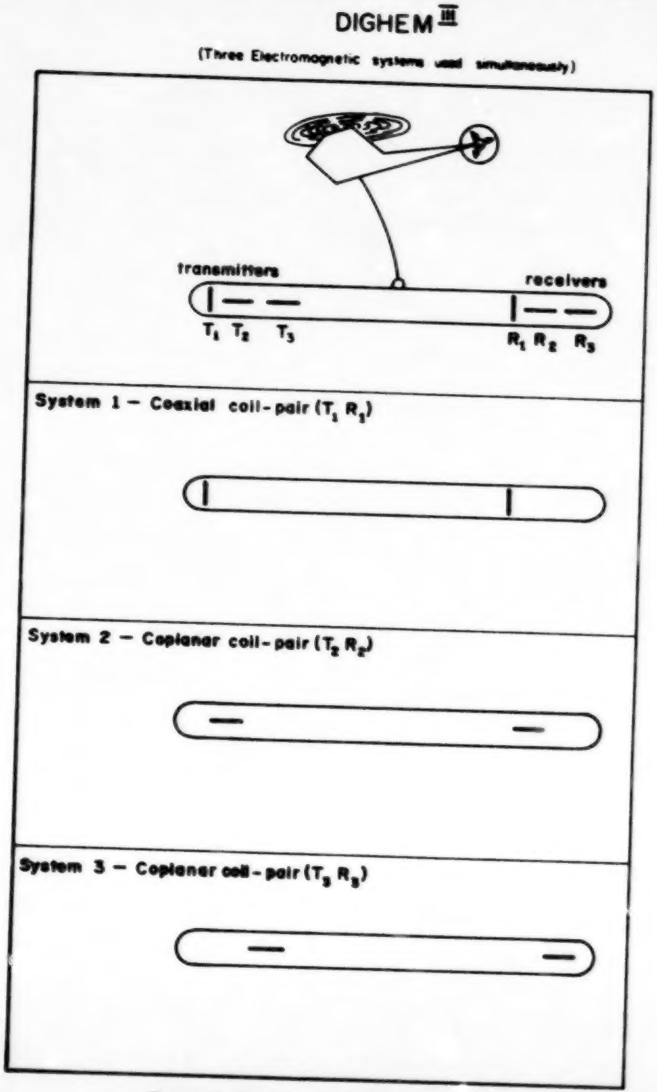
DIGHEM III
(Three Electromagnetic systems used simultaneously)
transmitters
receivers
T1 T2 T3
R1 R2 R3
System 1 — Coaxial coil-pair (T1 R1)
System 2 — Coplanar coil-pair (T2 R2)
System 3 — Coplanar coil-pair (T3 R3)

Figure 2. Coil configuration of DIGHEM^{III}.

very significant in the gold mining camps of Ontario.

This paper presents 2 examples of the ability of the DIGHEM^{III} system to map bedrock conductors located in 2 different geological environments.

NIGHT HAWK LAKE GEOPHYSICAL TEST RANGE

The Night Hawk Lake Geophysical Test Range is located in the northeastern corner of Thomas Township. The conductors consist of several graphite bodies covered by 87 m of sand and gravel. The conductive zones have been drilled and have been interpreted as being due to non-economical graphite shear zones. Ground geophysical surveys utilizing the MaxMin III horizontal loop and the EM-37 transient electromagnetic techniques have been carried out and the results published by R.B. Barlow of the Ontario Geological Survey (Barlow 1981; Barlow *et al.* 1982).

The horizontal loop and the transient system indicate the presence of 2 conductors located immediately adjacent to one another.

Figures 3 and 4 present the DIGHEM^{III} results over the Night Hawk test range.

Flight line profiles over the conductors are shown in Figures 3a and 3b. (The channels are defined in Table 1). These profiles present the processed data from flight line A-A' at 2 different survey altitudes. Profile 3a presents the data at a bird survey altitude of 35 m. Anomalies A and B reflect 2 conductors at a depth of 87 m, i.e. at a distance of

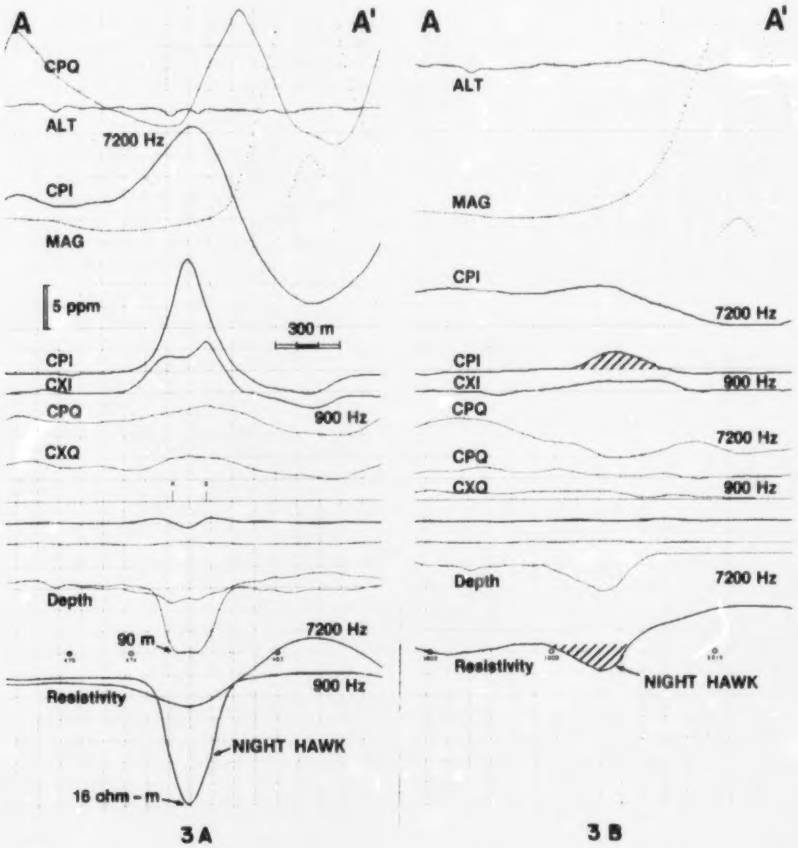

The Night Hawk test range is located near Timmins, Ontario, Canada. The conductor is a graphitic body buried beneath 87 m of glaciofluvial outwash sands. Note how the resistivity and depth channels identify a good conductor at depth. The EM bird was at a height of 122 m (400 ft) over the conductor on the left profile, and 183 m (600 ft) on the right.

Figure 3. Night Hawk Lake profiles.

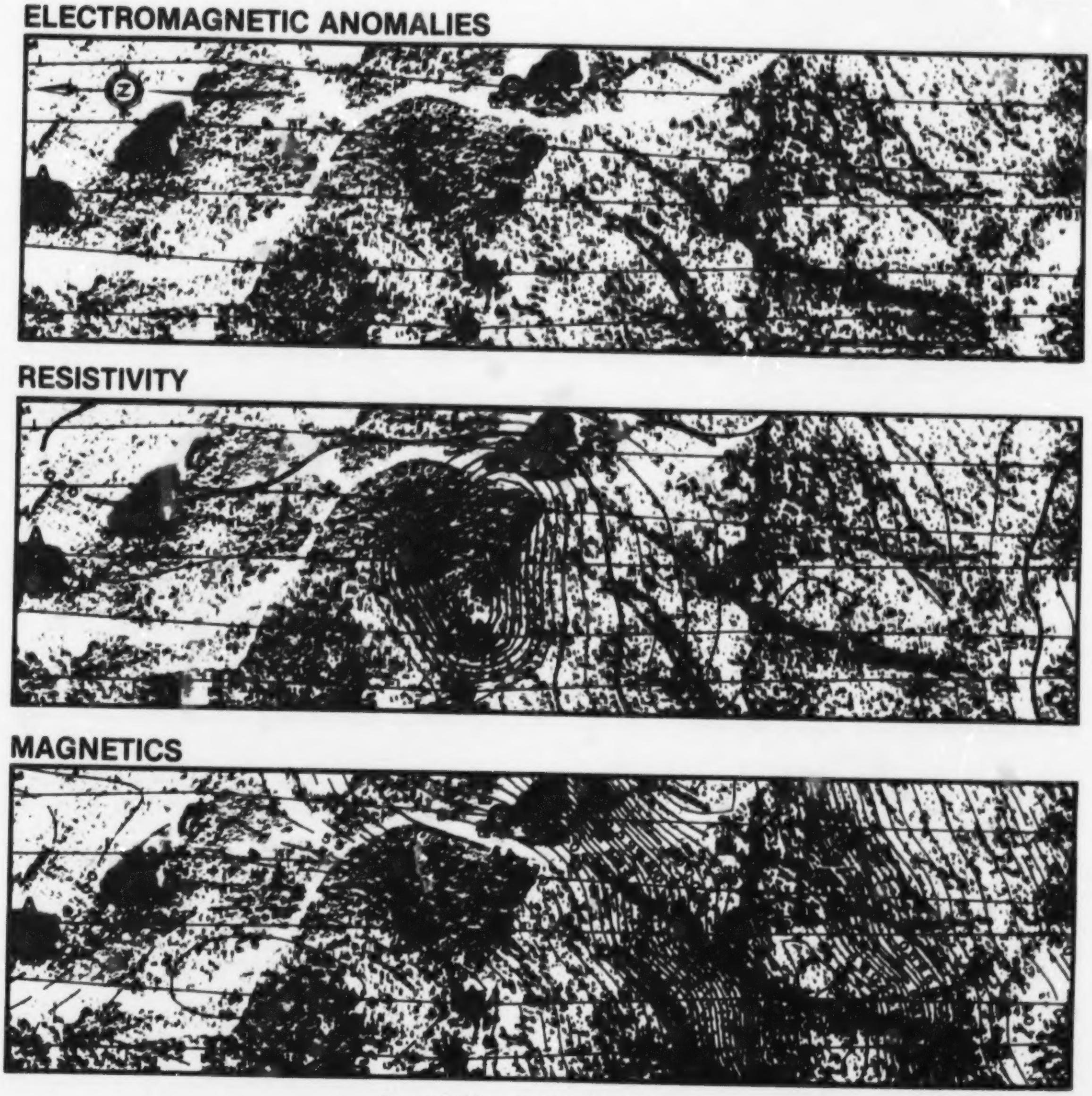

Figure 4. Night Hawk Lake plan views.

122 m below the bird. Figure 3b is a profile along the same flight line, but with the bird at an altitude of 96 m above the ground or 183 m above the conductor. The electromagnetic response at the higher survey altitude is predominantly a coplanar in-phase (CPI) response.

Figure 4 presents a plan view of 3 standard DIGHEM products over the test site. The resistivity contour map readily identifies the test site conductors, as well as giving an indication of the resistivity of the surrounding material. It is, for instance, readily apparent that the surrounding resistivities increase towards the south. This is probably indicative of a decrease in the thickness of the surficial cover.

HEMLO GOLD BELT

Figure 5 illustrates results of DIGHEM^{III} flying in a very resistive environment. This profile represents a typical line of data from the Hemlo area.

TABLE 1: DEFINITION OF CHANNELS FOR FIGURES 3 AND 5.

ALT	Altimeter
MAG	Magnetics
CPI 7200	Coplanar Inphase at 7200 Hz
CPI 900	Coplanar Inphase at 900 Hz
CXI 900	Coaxial Inphase at 900 Hz
CPQ 7200	Coplanar Out-of-phase at 7200 Hz
CPQ 900	Coplanar Out-of-phase at 900 Hz
CXQ 900	Coaxial Out-of-phase at 900 Hz
Depth 900	Depth to conductor calculated from the 900 Hz coplanar coil-pair
Depth 7200	Depth to conductor calculated from the 7200 Hz coplanar coil-pair
Resistivity 7200	Resistivity calculated from the 7200 Hz coplanar coil-pair
Resistivity 900	Resistivity calculated from the 900 Hz coplanar coil-pair

It is obvious from the resistivity profiles that the dynamic range of 0.1 to 1000 ohm-m of the 900 Hz coils is inadequate in defining zones of weak conductivity. Anomalies C and E are very weak responses on the four 900 Hz channels, but are very strong on the two 7200 Hz channels. These high frequency responses are important in this area because they are often associated with fault zones or contacts.

SUMMARY

DIGHEM^{III} was introduced to the mining community for commercial survey applications in December 1982, and, in the time interval between then and June 1983, over 10 000 line-km of survey flying has been completed using DIGHEM^{III}. The system has been operated successfully in 2 configurations: 900/900/7200 Hz in Canada, United States, and Europe, and in the 900/900/380 Hz configuration in Australia. The system has seen extensive use in both resistive and conductive environments.

The research and development of a 50 000 Hz coil-pair was also begun under the funding of this Ontario Exploration Technology Development Grant, but was not completed due to lack of funds. Dighem Limited is presently continuing the research and development of this system with the assistance of a grant from the National Research Council of Canada. This will lead to the DIGHEM^{IV} system which will consist of 4 coil-pairs operating at any combination of 380, 900, 3600, 7200, or 50 000 Hz. This frequency range will give a comparable resistivity range of 0.1 to 50 000 ohm-m. The high frequency will be primarily a structural mapping tool similar to a VLF instrument, but considerably improved because it will be a small scale active system.

SELECTED REFERENCES

Barlow, R.B.
1981: No. 25 Night Hawk Lake Geophysical Test Range Results Using Two Electromagnetic Systems, District of Cochrane; p.152-159 *in* Summary of Field Work, 1981, by the Ontario Geological Survey, edited by John Wood, O.L. White, R.B. Barlow, and A.C. Colvine, Ontario Geological Survey, Miscellaneous Paper 100, 255p.

Barlow, R.B., Pitcher, D.H., and Wadge, D.R.
1982: No. 22 Night Hawk Geophysical Test Range Results, Night Hawk Lake, District of Cochrane; p.152-161 *in* Summary of Field Work, 1982, by the Ontario Geological Survey, edited by John Wood, Owen L. White, R.B. Barlow, and A.C. Colvine, Ontario Geological Survey, Miscellaneous Paper 106, 235p.

Fraser, D.C.
1972: A New Multicoil Aerial Electromagnetic Prospecting System; Geophysics, Volume 27, p.518-537.

1973: Magnetite Ore Tonnage Estimates from an Aerial Electromagnetic Survey; Geoexploration, Volume 11, p.97-105.

1978: Resistivity Mapping with an Airborn Multicoil Electromagnetic System; Geophysics, Volume 43, p.144-172.

1979: The Multicoil II Airborne Electromagnetic System; Geophysics, Volume 44, p.1367-1394.

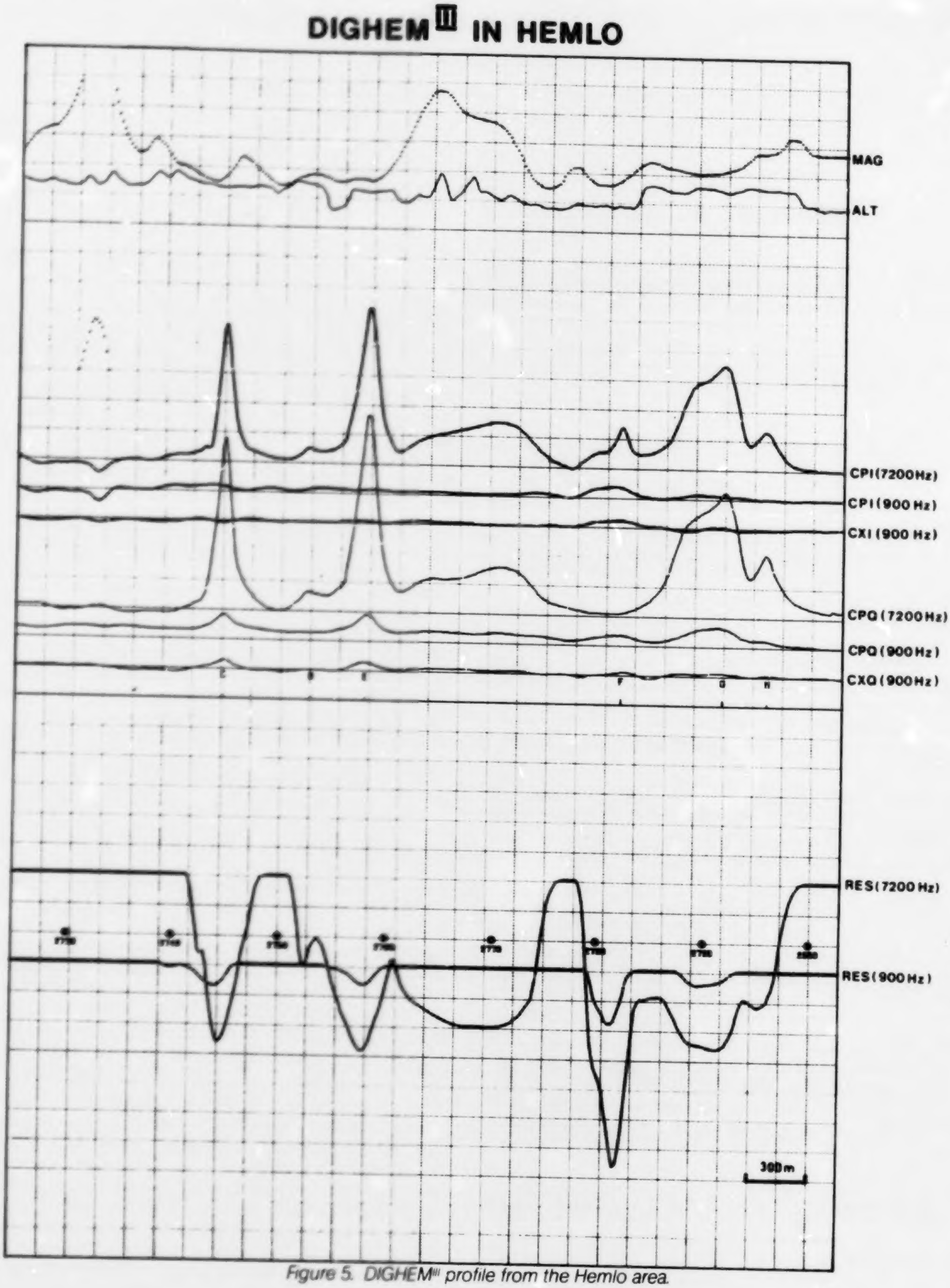

Figure 5. DIGHEM^{III} profile from the Hemlo area.

Grant 028 TOTEM-2G Continuous Recording Ground VLF EM

Alex Herz[1], A.B. Routledge[2], and
K.D. Naujok[3]
[1]Herz Industries Limited
[2]RIGHT BY DESIGN Incorporated
[3]Tri-C-onics Limited

ABSTRACT

Assistance was provided under the Ontario Exploration Technology Development Fund for instrumentation to be designed, built, and made commercially available for continuous reading dual channel and gradient, Very Low Frequency (VLF) ground surveys, with data stored in removable solid state memory modules. This instrumentation will be of particular value in mapping geological structures and for the evaluation, recognition, and assessment of disseminated conductive targets, and of good conductors under overburden. Detailed and cost effective coverage will result from speed and automation of survey, ease, and simplicity of field data acquisition, and the ability to review data in the field using a simple printer.

Data resolution, hence interpretability of survey results, will be considerably enhanced by the continuity of the data, and the ability to insert "comments". Field data may be gathered as rapidly as once a second, for example, at every pace. Depending on the amount of data being recorded, from 1 to 4 memory modules will contain 1 day's data. Solid state storage permits a large amount of data to be rapidly, conveniently, and accurately transferred to processing.

INTRODUCTION

The main objective of the project described in this paper was to produce a commercial exploration instrument capable of gathering geophysical data with greater detail, accuracy, speed, and economy than is currently possible with Very Low Frequency (VLF) electromagnetic (EM) ground instrumentation. VLF has been widely employed for mapping geological structures, for the recognition and assessment of disseminated conductive targets, and for the recognition of good conductors under glacial overburden.

The VLF EM method has demonstrated its viability for many years in both airborne and ground survey applications. Ground surveys of small line mileage are much easier and inexpensive to mount than airborne surveys, but airborne data provides better resolution and continuity required for interpretation purposes. Ground data at 50- to 100-foot intervals is often poorly connected. To make closely spaced measurements, say every 5 feet with conventional VLF EM methods, would be intolerably slow and would result in massive quantities of data. The features incorporated in the TOTEM-2G instrument overcome these limitations, and permit fuller exploitation of the VLF method.

CURRENT SURVEY PRACTICE

Current ground VLF EM instruments require that the operator stop at each station, take measurements, and that he orient the instrument in some way to establish the parameters of the field. This must be repeated for each station frequency. Each reading is recorded in the field notebook. A great proportion of field time is spent walking between stations. In addition, some instruments do not define the quadrature component.

Airborne VLF EM systems, of course, do provide continuous measurements, but need either an electric field phase reference or an expensive time clock, or require a complex gyroscopic reference (and of course an aircraft). For the purpose of providing a phase-free and gravity-reference-free airborne VLF system, Herz Industries Limited previously developed the TOTEM-1A and TOTEM-2A Airborne VLF systems currently in commercial use.

The principles of measurement of total field strength and vertical elipticity used in the TOTEM systems readily lend themselves to use in a continuous-reading ground system without the need for complex mechanical orientation or difficult electric field measurements.

Although a field notebook suffices for recording intermittent measurements taken manually, it is necessary to have an electronic data logging device for continuous automatic readings. This could take the form of a chart recorder, a magnetic tape recorder, or a solid state memory.

The chart recorder and magnetic tape recorder suffer the disadvantages of weight, mechanical unreliability in cold or dirty conditions, and power consumption.A battery powered random access memory (RAM), on the other hand, is reliable, power frugal, lightweight, and reusable.

TECHNICAL DEVELOPMENT

Development of a new VLF EM system ground survey instrument requires 4 steps:

1. Original design of microprocessor driven signal processing and memory module hardware.
2. Modification of the existing TOTEM-2A Airborne VLF EM system for ground use, with some original design to permit interface with the microprocessor-driven hardware. The principles employed for signal acquisition, dual heterodyne conversion, and certain proprietory techniques to maximize signal processing accuracy, were preserved. Value engineering was applied to permit the cost reductions necessary for a high volume ground instrument.
3. Development of algorithms and machine code for vector computation, noise filtering, display and control functions, and data storage and retrieval.
4. Integration of the VLF EM and microcomputer hardware, testing of the operating software, and field trial of the completed instrument package.

MODIFICATIONS OF TOTEM-2A

Modifications were made as required to accomodate changes in packaging, controls, and displays, output interface, and in particular to achieve cost and weight reductions essential for a ground instrument by means of value engineering.

The VLF part of the design is described in general terms only, as it is commercially proven and proprietary, and constituted only a small part of the development effort.

Primary field excitation is provided by distant VLF Radio transmitters at frequencies in the band 15 to 25 KHz. The modulated VLF station signal in the band 15 to 25 KHz is received via 3 orthogonal antennae. It is heterodyne converted to a common internal frequency, band filtered, and rectified to d c signals representing the magnitude and phase of the field components.

Measurement is made at 2 station frequencies simultaneously, optimised for approximate orthogonality of primary field directions, and has facility for the measurement of the GRADIENT of the field. Measurement requires only an additional sensor head that is vertically or horizontally spaced.

The 1-man portable Receiver Console comprises a 3 orthogonal axis antenna head or heads and a control and processing console which resolves the field elipse of polarisation.

The measured parameters are (as in the airborne TOTEM models) the magnitude of the total field and the vertical elipticity. These parameters are essentially independent of antenna orientation, hence may be determined continuously without the need for operator alignment or other intervention.

Modifications were made to permit gain switching under microprocessor control for the purpose of accommodating very large anomalies, and to signal to the CPU various alarm conditions and control settings. In addition, various clock timing and control signals were modified. The vector computation and output filtering boards of the TOTEM-2A Airborne system were removed as their functions are now performed digitally. A preamp buffer also was removed as the antenna is now close to the console.

MICROPROCESSOR HARDWARE

The processor design is based on a CMOS device (low power consumption service). The NSC 800 (microprocessor unit), Random Access Memory (RAM), and Read Only Memory (ROM) and all decoding and selection devices are also CMOS (as is the logic in the VLF section).

The architecture of the hardware was kept general purpose to permit futher expansion and comprises up to 16K of EPROM (changeable form of ROM) and system RAM (12K of EPROM is used currently) and up to 48K of Data RAM (dumping facility).

Data RAM is in a removable Data Memory Module (DMM) and is backed by a lithium battery which is good for 5 to 10 years. Currently, the DMM is equipped with 16K bytes of RAM.

The main hardware design effort was in the Input-Output (I/O) device and Digitizer (A/D) board where the interface between the processor and the VLF section occurs.

A hand held console with display, keyboard, and audio sounder for the VLF signal and alarms was also designed.

PROCESSING ALGORITHMS

Operation of the instrument is completely automatic and continuous. The instrument is continuous reading, that is, a reading may be made on a regular periodic time basis, or it may be triggered by the operator's steps through the survey area. As the operator walks, or under control of an internal clock, the receiver computes the total field magnitude and the vertical ellipticity. The computed and filtered data are continuously recorded in a solid state removable memory module whilst online. Data may therefore be recorded typically every second, or at every pace. A keyboard permits alpha-numeric data to be entered manually at any time into the data stream. This may typically take the form of SURVEY IDENTIFICATION information or COMMENTS such as would otherwise appear in a log book.

A connection on the instrument permits the recorded data to be read out and transferred to disk by the base camp computer, for use by the end user's Application Program, e.g. for interpretation or plotting. Alternatively, memory modules may be accumulated for head office computation, as they are rugged, inexpensive, and lightweight. The battery-less memory modules are of course reusable, and may be returned to the field after transfer and erasure of old data.

The microprocessor software of the receiver divides logically into 2 parts, that for computation and filtering of the data, and that for display, control, and memory storage and retrieval.

The main routines are:

1. digitizer (A/D) conversion
2. statistical and linear filtering (including range changing)
3. vector computation of TOTAL & QUAD (quadrature-inphase, out of phase) values
4. compression and storage of data
5. wake up and HEADER entry
6. keyboard scan and display drive
7. data output, i.e. dump and print (and erase)
8. debug monitor (non-resident)
9. diagnostic tests and alarms

Operator communication is via a numeric and a function keyboard. In the office modes, the operator may PRINT, DUMP, ERASE, VIEW (all 12 recordable channels may be previewed on the display), NULL (used for station direction finding), or go to HEADER.

In HEADER, all the survey description is entered, and a selection of certain special instrument features can be made (e.g. FILTER, which puts in a spike removing algorithm).

From HEADER, the operation may go ONLINE. In this mode, certain other functions are possible, both from the keyboard and 2 special buttons:

1. STEP in manual mode causes data to be recorded
2. FID causes a situation number update
3. FEATURE marks the data record with a token
4. REMARK (number) marks the data record with a numbered token which may be used to signify a particular type of geological or cultural feature
5. OFF LINE returns to the VIEW mode

INTEGRATION AND FIELD TESTING

A prototype instrument with only the basic conversion, processing and storage machine code in place, was field tested during December 1982 over the Cavendish Test Site. The plotted line traversing the Cavendish conductors shows the importance of close spaced readings (Figure 2).

Subsequent to the test, the hardware configuration was finalized, and the software developed to permit a high degree of operational flexibility whilst offering user friendliness.

CONCLUSION

The proposed TOTEM-2G development has produced a commercial instrument to support increased efficiency and effectiveness in mineral exploration.

The instrument is ground portable, and its use combines previously proven techniques in aid of geological mapping, recognition, and assessment of disseminated conductive targets and of good conductors under overburden, with innovative improvements. The significant benefit is from the continuous data acquisition and signal processing hardware and software for real-time collection and interpretation of field data. This permits VLF ground survey with greater speed, more detail, 2 stations (and optional gradient), and direct computer compatibility. Considering survey cost in terms of manpower and equipment, the overall benefit is more information available at less cost than before.

```
TOTEM 2 G CONTINUOUS RECORDING GROUND VLF EM SURVEY RECORD


------------------------SURVEY PARAMETERS----------------------

AREA CODE                           294.6374.01
DISTANCES IN                        METERS
LINE SPACING                        75
STATION SPACING                     25
DATE: YY MM DD                      821203
FREQUENCY LINE  kHz                 21.4
FREQUENCY ORTHO kHz                 17.8
MODES:
MANUAL                              NO
AVERAGING TIME SECS                 2
AUTO RECORD INTERVAL SECS           2
GRADIENT                            YES
HORIZONTAL QUADRATURE               YES
RESOLUTION %                        1
ANOMALY THRESHOLD %                 0

LEVEL LINE  %                       100
LEVEL ORTHO %                       100
LINE NUMBER & DIRECTION             01E
STATION NUMBER & DIRECTION          00N
SURVEY DIRECTION                    N
----------------------------------------------------------------

                        DATA RECORD
             LOWER                             UPPER
     ORTHO            LINE            ORTHO            LINE
TOTL VQAD HQAD TOTL VQAD HQAD TOTL VQAD HQAD TOTL VQAD HQAD
ONLINE
 100    2 -  1  100 -  3    1  100    2    0   98 -  5    4
TIME : 0038
  99 -  2    1   98 -  5    3  100 -  2    0   98 -  5    4
  99    0    0   99 -  5    3  100 -  1    1   99 -  6    3
  99 -  1 -  1   98 -  5    2  100 -  1    0   99 -  6    3
 101 -  1    0   99 -  4    2   99 -  2    0   99 -  5    3
 100 -  1 -  1   97 -  5    1   99 -  2 -  1   99 -  4    3
  99 -  1    0  100 -  4    2  100 -  3    0   98 -  4    2
STATION # 000
 100 -  1 -  1   98 -  3    2  101 -  1 -  1   98 -  3    2
  99 -  1 -  2   99 -  3    2   99 -  1 -  2   97 -  3    2
 101 -  1 -  2   99 -  3    2  101 -  3 -  1   98 -  3    3
  99 -  2 -  1   98 -  3    3  100 -  2 -  1   96 -  4    3
 101 -  2    0   99 -  5    2  100 -  2 -  1   97 -  4    2
STATION # 000
 100 -  3 -  1   99 -  4    3  101 -  4    1   98 -  4    5
 101 -  1    1   99 -  4    1  101 -  3 -  1   98 -  4    3
 101 -  3    0   99 -  3    2  100 -  4    0  100 -  3    6
 100 -  3    1  100 -  4    2  101 -  2    1   99 -  4    3
  99 -  3    1  100 -  5    2   99 -  3 -  1   99 -  4    3
STATION # 000
 101 -  3    0  100 -  4    2  100 -  3    0   99 -  4    3
STATION # 000
 101 -  3    2  100 -  5    3  100 -  3 -  1   99 -  5    3
 100 -  3    1  100 -  4    3  101 -  4    0  100 -  4    1
 101 -  3    1  101 -  6    3   99 -  4    0  100 -  5    3
 100 -  4 -  1  101 -  4    4  100 -  2    0  101 -  5    3
 100 -  2    1  100 -  5    3  101 -  2    0  101 -  5    4
 100 -  3    1  100 -  5    4  101 -  3    0  100 -  5    3
 101 -  4    1  102 -  4    3  101 -  4    1  101 -  4    3
 102 -  2    1  102 -  5    3  100 -  5    1  101 -  5    3
```

Table 1. Data obtained from TOTEM-2G continuous recording ground VLF EM.

```
101 -  3    0  103 -  5    4  101 -  4    0  103 -  6    5
101 -  5    0  105 -  4    3  101 -  4    2  102 -  6    4
103 -  3    1  104 -  5    4  101 -  4    1  103 -  6    3
102 -  3    1  106 -  4    2  103 -  4    1  104 -  4    4
103 -  4    3  106 -  3    2  103 -  3    1  104 -  5    3
103 -  3    2  106 -  5    3  103 -  3    0  105 -  4    3
103 -  4    2  107 -  5    5  103 -  4    0  106 -  4    5
103 -  5    1  107 -  4    4  103 -  2    1  106 -  4    3
103 -  3    1  107 -  5    4  103 -  3    1  106 -  5    3
103 -  3    3  109 -  5    4  103 -  3    2  108 -  5    5
103 -  4    2  108 -  5    4  103 -  4    1  107 -  5    4
STATION # 000
 104 -  3    2  109 -  5    4  105 -  4    1  109 -  5    5
STATION # 000
 104 -  4    1  111 -  5    6  104 -  4    3  109 -  5    5
 106 -  5    2  112 -  6    6  104 -  4    3  110 -  7    5
 106 -  3    3  113 -  5    5  106 -  4    3  112 -  7    6
 106 -  4    3  114 -  5    7  106 -  4    2  112 -  6    6
 106 -  3    4  116 -  7    7  106 -  3    3  114 -  7    5
STATION # 000
 108 -  3    3  116 -  7    7  107 -  3    4  115 -  8    6
 109 -  2    4  118 -  7    8  107 -  3    3  117 -  8    6
 108 -  3    3  119 -  8    9  108 -  3    2  119 -  9    8
 109 -  1    4  120 - 10    5  107 -  3    2  119 -  9    5
 108 -  2    2  121 -  9    6  111 -  2    3  121 - 11    7
 110 -  3    2  125 - 12    6  111 -  1    5  122 -  8    5
 110 -  2    1  127 - 11    4  113 -  1    4  124 - 12    5
 112 -  1    3  128 - 11    4  111 -  1    1  127 - 12    4
 111 -  1    1  130 - 12    5  114 -  2    3  128 - 12    5
 113 -  1    1  132 - 13    3  114 -  1    1  131 - 14    4
 114 -  1    3  134 - 13    3  114    0    2  131 - 13    4
 116     0    3  133 - 15    2  116 -  1    2  133 - 15    3
 118     0    2  138 - 16    4  117    0    1  135 - 14    4
 115 -  1    3  139 - 18    2  118 -  1    1  135 - 16    3
 121 -  1    3  143 - 17    3  118    0    1  139 - 17    2
 STATION # 000
  122    0    2  145 - 18    2  122    0    2  143 - 19    2
  124 -  1    1  149 - 18    1  123    2    0  147 - 20    1
  128    0    0  156 - 20 -  1  125    2 -  2  153 - 21    0
 SCALE 2
  130    0 -  2  162 - 22 -  3  131    2 -  2  161 - 21 -  2
 SCALE 1
  135 -  2 -  4  169 - 15 -  5  136 -  1 -  6  168 - 15 -  4
 STATION # 000
 SCALE 2
  137 -  9 - 10  173 -  7 -  7  136 -  9 -  8  172 -  9 -  6
 STATION # 000
  135 - 12 -  6  171    1 -  1  134 - 15 - 10  170 -  3 -  2
 SCALE 1
  130 - 17 -  7  165    3    3  130 - 17 -  6  163 -  1    2
  127 - 19 -  3  159 -  3    4  127 - 20 -  2  159 -  4    6
  123 - 18    1  158 -  6    4  125 - 19    0  157 - 10    5
 SCALE 2
  121 - 18    1  168 - 10    4  123 - 17    2  165 - 10    3
 STATION # 000
 SCALE 1
  121 - 15    3  162 - 11    3  119 - 15    2  162 - 12    3
  119 - 13    2  165 - 12 -  1  121 - 15    3  165 - 14    0
 SCALE 2
  123 - 13    2  175 - 10 -  3  121 - 13    3  173 - 10 -  2
 SCALE 1
  121 - 13    2  175 -  4 -  7  119 - 14    1  171 -  4 -  3
 SCALE 2
  117 - 15    2  171    2 -  3  119 - 16    3  169    4 -  3
```

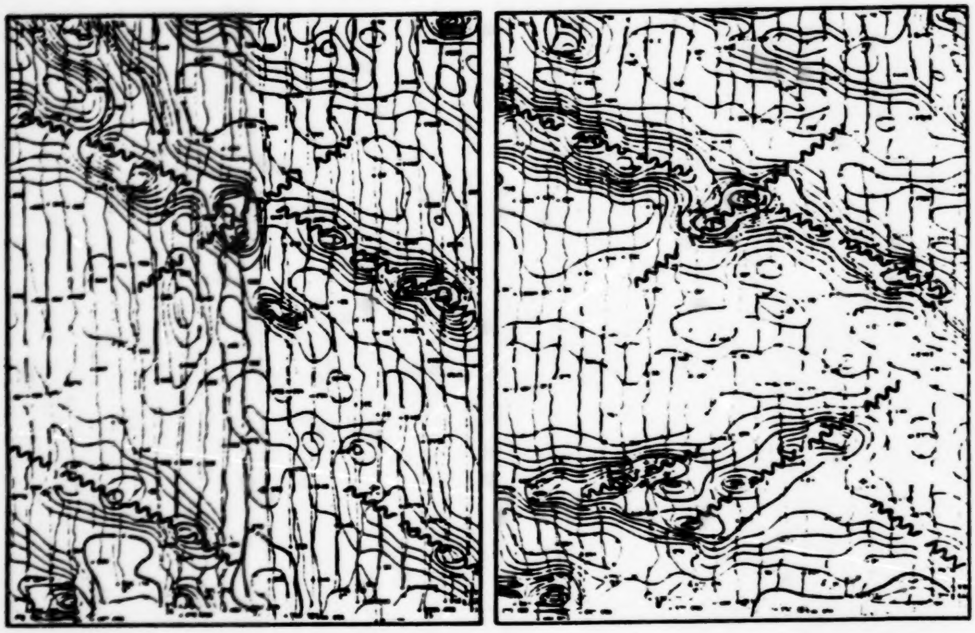

Figure 1. VLF EM (TOTEM-2A) total field contours and quadrature profiles, Precambrian terrain, Northern Ontario, showing relative enhancement of conductors striking near to the azimuth of the transmitting station. Left: Transmitter NSS, Annapolis, Azimuth 148; Right: Transmitter NPM, Hawaii, Azimuth 264.

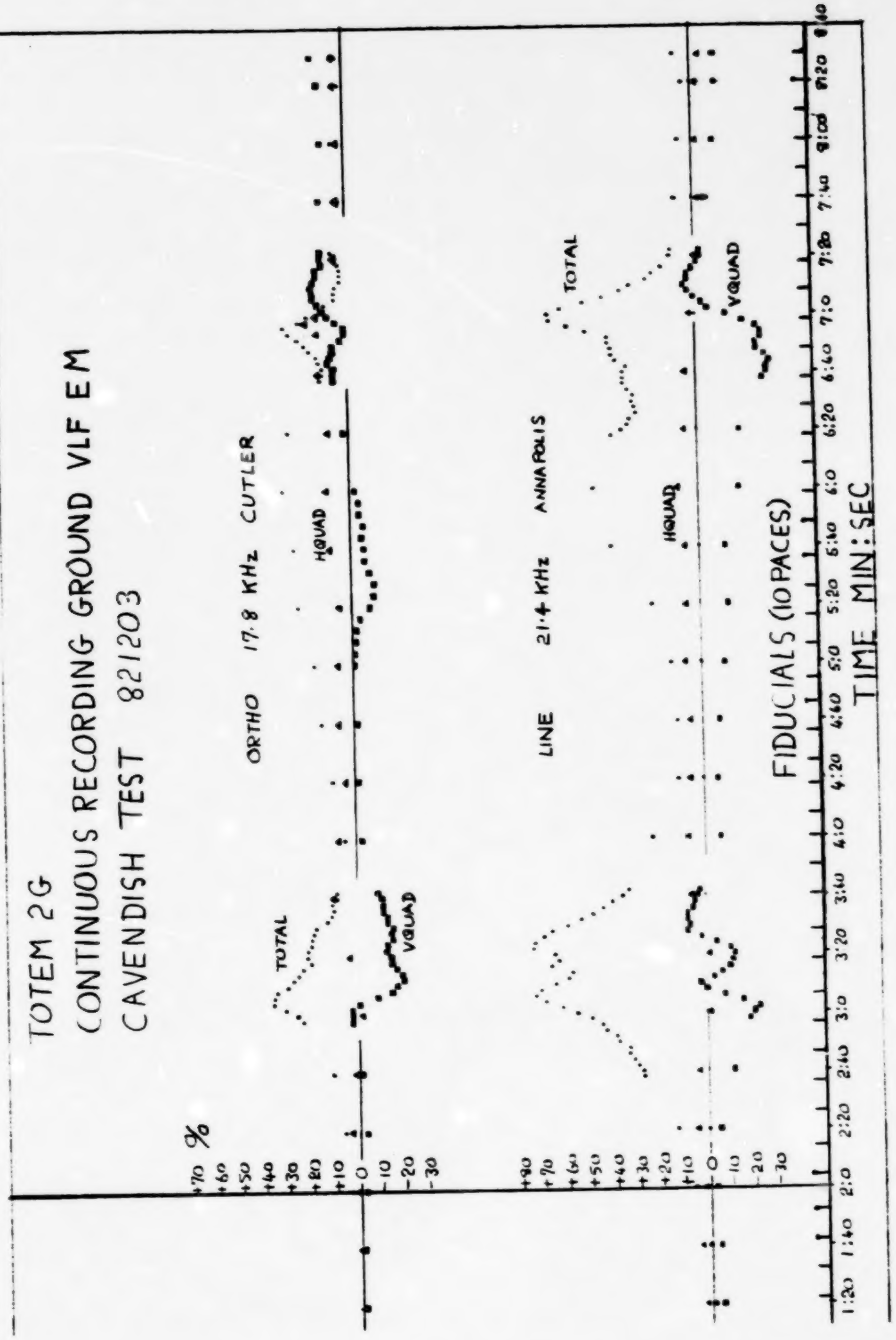

Figure 2. TOTEM-2G, continuous recording ground VLF EM system.

Grant 030 A User-Friendly Electromagnetic Prospecting System

Mitsuru Yamashita
Chief Geophysicist, McPhar Instrument Corporation, Willowdale

ABSTRACT

The system called 'GEM5' is a portable, flexible, microprocessor-operated electromagnetic system. Measurements of the parameters of the ellipse of electrical polarization, in terms of tilt angle and ellipticity, can be made at 5 frequencies, 70, 210, 630, 1890, and 5670 hz. No reference cable or radio link between the transmitter and the receiver is required. The system is extremely flexible in selecting optimum survey mode configurations for various applications. The system can be operated at transmitter-receiver separations of up to 300 m. Precise transmitter-receiver separation is not critical. The system is operated by 2 people, 1 receiver operator, and 1 transmitter operator. Receiver operation is simple with LCD character prompt routines. The data measured are automatically stored into RAM (Random Access Memory) memory; the receiver is equipped with an RS232C port to permit the transfer of stored data to a printer, cassette recorder, modem, or a small computer-operated plotter.

INTRODUCTION

McPhar Instrument Corporation currently manufactures a GEM8 electromagnetic prospecting system. This 8-frequency, high power system measures electrical-polarization ellipse parameters from which the tilt angle and ellipticity of an electromagnetic field are derived. This approach does not require a reference link between the transmitter and receiver, thus permitting considerable flexibility in survey design. As Dey and Ward (1970) concluded, the tilt angle and ellipticity are amongst the most diagnostic parameters that can be used for inductive sounding. In addition to their use in sounding, these parameters are very effective in the search for, and detailing of, conductive bodies that may contain economic mineralization.

The high power McPhar GEM8 system has proven that measurement of ellipse parameters is an extremely effective method of geophysical exploration. Because of the physical size of the system, crew size requirements, and

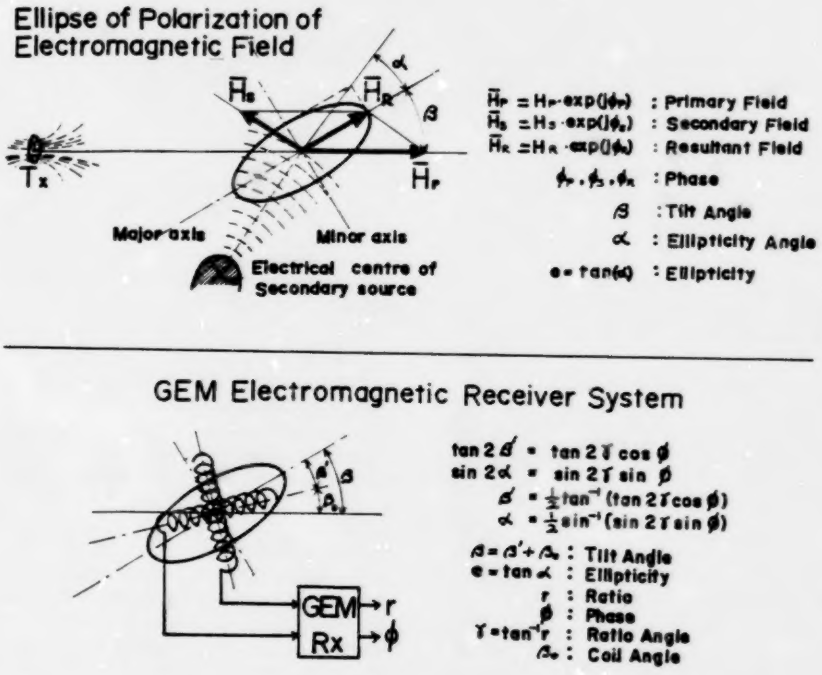
Ellipse of Polarization of Electromagnetic Field
$\bar{H}_s$
$\bar{H}_R$
α
β
Tx
$\bar{H}_P$
Major axis
Minor axis
Electrical centre of Secondary source
$\bar{H}_P = H_P \cdot \exp(j\phi_P)$: Primary Field
$\bar{H}_S = H_S \cdot \exp(j\phi_S)$: Secondary Field
$\bar{H}_R = H_R \cdot \exp(j\phi_R)$: Resultant Field
ϕ_P, ϕ_S, ϕ_R : Phase
β : Tilt Angle
α : Ellipticity Angle
$e = \tan(\alpha)$: Ellipticity
GEM Electromagnetic Receiver System
β'
β
β_0
GEM Rx
r
ϕ
$\tan 2\beta' = \tan 2\gamma \cos \phi$
$\sin 2\alpha = \sin 2\gamma \sin \phi$
$\beta' = \frac{1}{2}\tan^{-1}(\tan 2\gamma \cos \phi)$
$\alpha = \frac{1}{2}\sin^{-1}(\sin 2\gamma \sin \phi)$
$\beta = \beta' + \beta_0$: Tilt Angle
$e = \tan \alpha$: Ellipticity
r : Ratio
ϕ : Phase
$\gamma = \tan^{-1} r$: Ratio Angle
β_0 : Coil Angle

Figure 1. Ellipse of polarization of the electromagnetic field and ellipse parameter.

high cost, its application may not be optimal for locating conductors in a near-surface environment.

To take advantage of the ellipse parameter measurements and experience with the GEM-8 system, the development of a simplified, low cost, light-weight, user friendly system has been undertaken with emphasis on employing advanced CMOS microprocessor technology for digital signal enhancement, signal processing, and automatic data storage.

SYSTEM CONCEPTS

The transmitter (Tx) radiates an electromagnetic primary field at a given frequency. The primary field induces a current in a conductor which produces a secondary field. The secondary field is electromagnetically polarized because it differs in phase from the primary field, also, the magnitude and direction of the secondary field are different from those of the primary field. Figure 1 illustrates this relationship. The magnitude of the phase shift and the amplitude and direction of the secondary field depend on the conductivity, geometry, location, depth of the conductor, conductivity of the host rock, aplied frequency, and direction of the primary field moment.

The polarized secondary field induces signals in the orthogonal receiver coils. The signals from each coil are first processed to provide the amplitude ratio and the phase angle between the 2 coils. A microprocessor and associated software are employed to automatically derive the ellipse parameters in terms of tilt angles and ellipticities, using the relationships indicated in Figure 1. The tilt angles and ellipticities at various frequencies are then analyzed to provide information about a conductor in the ground. The information may also be used to study rock structures and to assist in geological mapping.

THE GEM5 SYSTEM

As the foregoing discussion demonstrates, the GEM5 system is conceptually very simple. Because no primary field reference link is required, the transmitter (Tx) dipole can be oriented in any direction. The only transmitter requirement is that the signal be coherent, i.e. that the phase be constant for a given frequency. All measurements at the receiver (Rx) are inherently normalized as amplitude ratios and phase differences between the orthogonal receiving coils.

TRANSMITTER (Tx)

The transmitter system is physically composed of 3 major components: the power source, the transmitter console, and the transmitter loop. It is designed for 1 man to carry and operate. Figure 2 shows the prototype GEM5 transmitter system. In a field survey, the console and the power pack are back-packed.

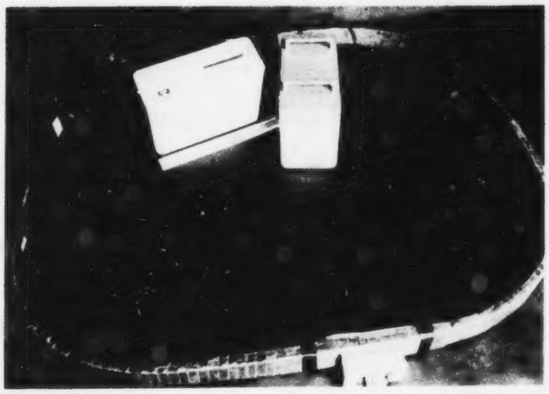

Figure 2. The GEM5 prototype transmitter system showing console, power pack, and transmitter coil.

POWER SOURCE

The power source is normally a rechargeable, sealed, lead-acid battery with voltage selection capability depending on the maximum Tx-Rx (transmitter-receiver) separation requirement, as follows:

Supply voltage	Tx moment at 70hz	Weight	Maximum Tx-Rx separation Co-planar	Co-axial
12V	175NAI	4.5kg	200 m	250 m
24V	350NAI	9.0 kg	250m	300 m
48V	700NAI	18.0kg	300 m	350 m

With a 24 volt battery pack, continuous operation for 8 hours is possible under normal conditions. The 48 volt, 18 kg battery pack, however, lasts for only 4 hours. Thus, 2 batteries are required during a full day, 1 in the morning, the 2nd in the afternoon. Other types of DC power source, between 12 volts and 48 volts, such as snowmobile batteries or portable generators are equally usable.

TRANSMITTING LOOP

The loop is a framed air-core coil, 90 cm by 105 cm in size, with a weight of approximately 10 kg, on a rotatable stand. The frame and stand are designed for easy use in the field. A survey can be performed in the horizontal-loop, vertical-loop, or tilted loop mode as desired.

TRANSMITTER CONSOLE

A crystal oscillator permits selection of any one of 5 different driver frequencies: 70, 210, 630, 1890, and 5670 hz. The operation is extremely simple. Figure 3 shows that front panel operation is performed entirely by push button: Power On, F1, F2, F3, F4, F5, and Power Off. Buttons F1 to F5 select the transmitting frequency. The console weighs approximately 2 kg.

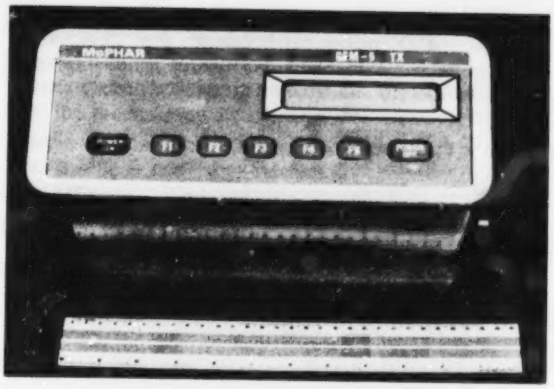

Figure 3. Front panel of the GEM5 transmitter console.

RECEIVER (Rx)

The receiver consists of a receiving coil and a console with a built-in rechargeable battery, and is shown in Figure 4.

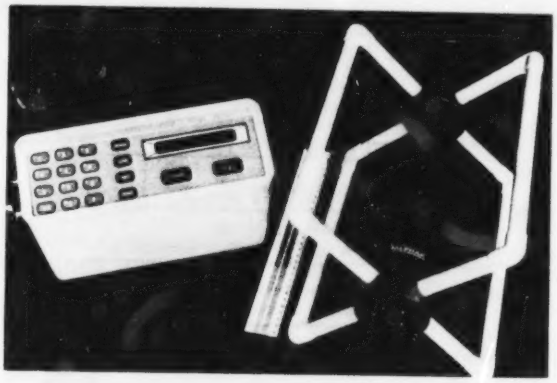

Figure 4. The GEM5 prototype receiver system showing console and receiver orthogonal coil.

RECEIVING COIL

The receiving coil system has 2 orthogonal coils and is self-standing. Because the coils are air-cored, the system is more stable and independent of wind noise, temperature change, and coupling effects due to nearby metallic objects. Coil levelling in uneven terrain is not required. An electrical clinometer measures coil angle with respect to the horizontal. This data is fed into the receiver console for automatic tilt angle correction. The coil system dimension is 30 cm by 30 cm and weighs 1.5 kg. The 2 signals from the 2 orthogonal coils are amplified by a 2-channel built-in amplifier, then fed into the console.

RECEIVER CONSOLE

The receiver console is composed basically of a power source, CPU microprocessor, analog processing selection, RAM data memory, interfacing section, and key-display front panel. The console is 10 cm by 27 cm by 20 cm in size, and weighs approximately 5 kg. The operating temperature range is -40°C to 80°C. Figure 5 shows a schematic block diagram of the console.

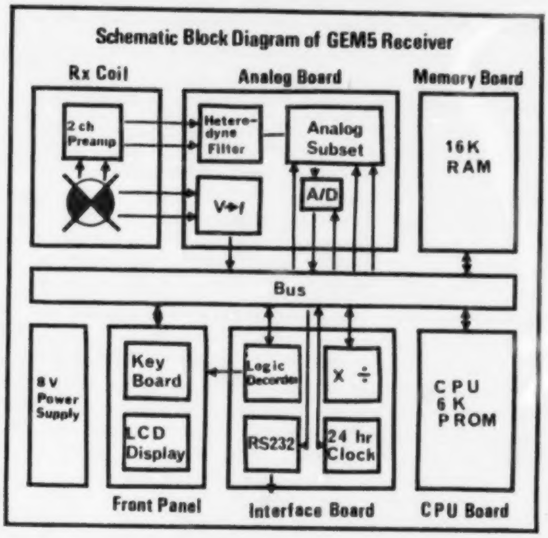
Schematic Block Diagram of GEM5 Receiver
Rx Coil
Analog Board
Memory Board
2 ch Preamp
Hetero-dyne Filter
Analog Subset
A/D
V→f
16K RAM
Bus
8V Power Supply
Key Board
LCD Display
Logic Decorder
X ÷
RS232
24 hr Clock
CPU 6K PROM
Front Panel
Interface Board
CPU Board

Figure 5. Schematic block diagram of GEM5 receiver.

The power source is a built-in rechargeable battery. The 5 AH battery supports at least 10 hours of continuous operation and 30 hours of RAM and system backup.

The analog processing section performs automatic gain-control, frequency selection, filtering, and signal conversion to digital data. It is designed to receive transmitted signals at any of the 5 frequencies, 70, 210, 630, 1890, and 5670 hz.

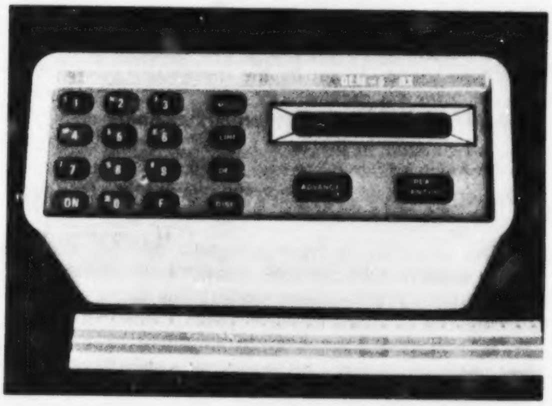

Figure 6. Front panel of the GEM5 receiver console.

The front panel has an 18-key board and a 16-character LCD display as indicated in Figure 6. The LCD display is automatically heated if the temperature drops below -20°C.

The CMOS Z80 based microprocessor with 6K of ROM memory performs the signal processing, calculation, storing of data, and interfacing with external devices.

It also controls the receiver operation. An automatic operator-keyboard prompt routine with the 16 character LCD display makes the operation very easy, and is independent of the quality of data input by the operator. The microprocessor is programmed to require minimum keyboard data entry. For example, following completion of measurements at 1 station, a station number is automatically advanced to the next station and displayed. The receiver displays all requests, warnings, and the required statistical needed data to verify signal quality. The operation can be interrupted at any time to change mode, line, station specifications, display data, and to delete current record.

The interfacing section of the receiver console contains an RS232 port to allow transfer of stored data from the RAM memory into an external permanent recording device. The information and data listed below are stored in ASCII in the 16K RAM non-volatile memory. Each record size is 32 bytes and designated by a header gate character:

Mode header—a header character, unit number, job number, survey mode, operator number, data and time.

Line header—a header character, Tx line, Rx line, station increment.

Station header—a header character, Tx station, Rx station, time, battery voltage.

Measurement data—frequency, coil angle; ratio, standard deviation; phase, standard deviation; tilt angle, standard deviation; ellipticity, standard deviation; number of stacking samples.

MEASUREMENT AND SIGNAL PROCESSING

SIGNAL PROCESSING

Figure 7 illustrates the signal processing. First, a transmitting frequency is set by the transmitter operator on request from the receiver operator. A resultant electromagnetic field is received by the orthogonal coils. The induced voltages in the coils are fed into the 2-channel amplifier with a 50 to 60 hz rejection filter. The coil system is also equipped with an electrical clinometer to measure the coil angle, thus eliminating coil levelling.

The amplified 2-channel signals are fed into the analog section of the console. A super-heterodyne circuit converts both channel signals to 8 hz. The microprocessor switches the sampling signal from the X-coil to the Y-coil and from the Y-coil to the X-coil, and sets a proper gain after checking the initial A/D converted signal. The switching sequence for 1 measurement is X-coil to Y-coil to Y-coil to X-coil over 2 seconds, eliminating relative drift problems between amplifiers.

After the A/D conversion, the digital signals are sampled at 1000 points per frequency cycle, stacking 4 times for each X-signal and Y-signal for 1 measurement. The 2-channel signals are then processed and converted into 2 complex numbers.

From the 2 complex numbers, the ratio and phase shift between X and Y coil are derived. Then 2 final ellipse parameters, tilt angle, and ellipticity, are calculated. The results are updated approximately every 2 seconds and the final results can also be stacked if further signal-to-noise improvement is required.

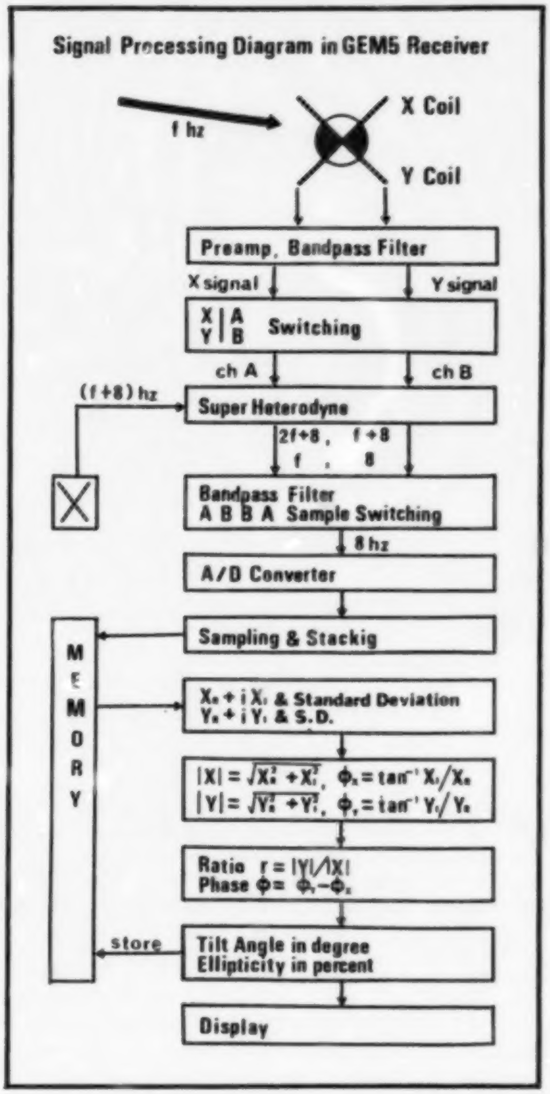
Signal Processing Diagram in GEM5 Receiver
f hz
X Coil
Y Coil
Preamp, Bandpass Filter
X signal
Y signal
X | A
Y | B
Switching
ch A
ch B
(f+8) hz
Super Heterodyne
2f+8, f+8
f, 8
Bandpass Filter
A B B A Sample Switching
8 hz
A/D Converter
M E M O R Y
Sampling & Stackig
$X_0 + iX_1$ & Standard Deviation
$Y_0 + iY_1$ & S.D.
$|X| = \sqrt{X_0^2 + X_1^2}$, $\phi_x = \tan^{-1} X_1/X_0$
$|Y| = \sqrt{Y_0^2 + Y_1^2}$, $\phi_y = \tan^{-1} Y_1/Y_0$
Ratio $r = |Y|/|X|$
Phase $\phi = \phi_y - \phi_x$
store
Tilt Angle in degree
Ellipticity in percent
Display

Figure 7. Diagram showing signal processing in the GEM5 receiver.

MEASUREMENTS

The final results, with statistical data are displayed on the 16 character LCD display. If a receiver operator is satisfied with the results, they are stored in the RAM memory. The results can first be stacked, then stored, if desired.

The measurement sensitivities of tilt angle and ellipticity are 0.1° and 0.1%. A tilt angle is automatically corrected by the coil clinometer data.

DATA STORING

The total data from approximately 80 stations, with all 5 frequency measurements, from approximately 120 stations with 3 frequencies, or from approximately 160 stations with 2 frequencies, can be recorded.

OPERATION AND SURVEY MODE

Because the ellipse parameters are inherently normalized at the receiver, the system does not require any reference link, cable or radio, between Tx and Rx, and precise Tx-Rx separation is not critical. This fact, in addition to measuring the resultant field, instead of a particular projected component, makes the system very flexible for various survey modes.

TRANSMITTER OPERATION

After moving to a specified station, the transmitter loop with the stand is placed on the ground and rotated to a horizontal or vertical position according to the survey mode.

There are 2 common methods of surveying: a) with the transmitter coil vertical but either with the plane of the vertical loop at right angles to the line between the transmitter and receiver (in-line mode) or with the plane of the vertical loop in the direction of the receiver (broadside mode); and b) with the transmitter coil horizontal for both the in-line mode and the broadside mode.

The transmitter is activated and ready to transmit by pressing the "Power On" key. At the receiver operator's request, the transmitter operator presses the specified "Frequency No." key. After all measurements at the station are performed, the operator moves to the next station.

RECEIVER OPERATION

At a station, the receiver operator places the orthogonal receiver coil frame on the ground. Levelling of the frame is not required. The angle off the horizontal is automatically fed to the console. In the broadside mode, the common intersecting line of the orthogonal coils is pointed approximately at the transmitter. For the in-line mode, the intersecting line is set approximately perpendicular to the transmitter direction.

With the microprocessor-controlled operator-keyboard prompt routine, the receiver console operation is very easy and nearly automatic.

SURVEY MODE

A GEM5 survey can be performed without cutting clear survey lines. This, in addition to not requiring a cable link between the transmitter (Tx) and receiver (Rx), is especially important in ecologically sensitive areas. The following survey modes, also illustrated in Figure 8, can be selected to obtain the best results.

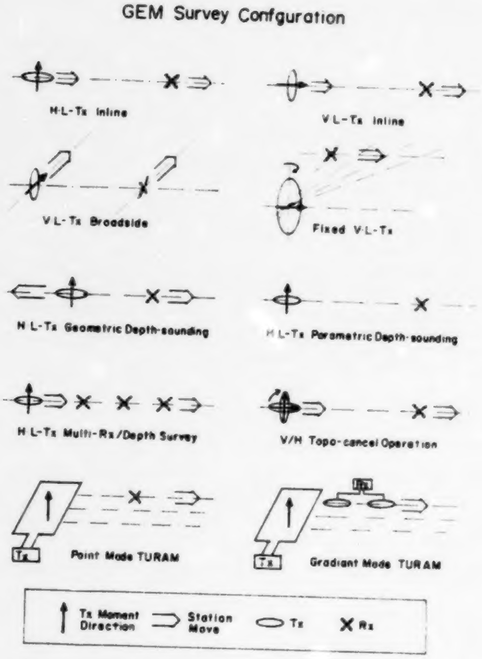

Figure 8. Summarized illustration of GEM5 survey modes.

HORIZONTAL TRANSMITTER LOOP, INLINE MODE

This mode is suitable in searching for steeply dipping tabular-shaped conductors and simultaneously studying structural formations such as overburden and basement. For reconnaissance surveys, measurements may be made at 2 frequencies only. Measurements at all 5 frequencies are justified only when detailed data, such as depth, conductivity-thickness and dip, are required on previously located conductors.

VERTICAL TRANSMITTER LOOP, INLINE MODE

This mode has advantages in searching for vertical conductors under an area of conductive overburden since it is less sensitive to horizontal conductors. More signal strength is available at the receiver position than for other modes, providing the largest Tx-Rx separation capability.

HORIZONTAL TRANSMITTER LOOP, BROADSIDE MODE

If the geological strike is known approximately, this mode has advantages in locating conductors by typical "cross-over type" response. Also, conductive overburden gives a relatively reduced response. This mode is free from terrain effects due to elevation differences between Tx and Rx on tilt angle measurements. The broadside mode can readily be employed because there is no cable link between the Tx and Rx.

VERTICAL TRANSMITTER LOOP, BROADSIDE MODE

This mode is similar to the horizontal Tx loop, broadside mode, except it offers better response to steeply dipping tabular conductors.

MULTI-RECEIVER OPERATION

Because there is no link between Tx and Rx, more than 1 receiver can be operated simultaneously with 1 transmitter. For example, 1 receiver 100 m from the Tx and a second receiver 300 m from the Tx on the same traverse line can be used to explore different depths.

SIMULTANEOUS MULTI-MODE OPERATION WITH MULTIPLE RECEIVERS

More than 1 receiver in different modes can be operated simultaneously with 1 transmitter. For example, 1 receiver may be in the inline mode while the second receiver is in the broadside mode. In this way, anomalies can be better resolved, and 2 survey lines may be run with 1 traverse.

SHOOT-BACK-TYPE OPERATION FOR ROUGH TERRAIN

Although the ellipticity response is insensitive to terrain elevation effects, the tilt angle is not. To eliminate the elevation effects, a shoot-back-type operation can be performed by rotating the transmitter loop from horizontal to vertical and making measurements for each position.

PARAMETRIC-GEOMETRIC COMBINED DEPTH SOUNDING OPERATION

A depth sounding survey can be performed to study layered structures to a depth at 150 m with the horizontal loop transmitter. The sounding response covers approximately 3 decades of ground resistivity with the present frequency range. The coverage can be increased to 4 decades by combining geometric sounding, for example, employing 100 m and 300 m Tx-Rx separations.

GEM5 RESPONSE

CONDUCTIVITY SPECTRUM

The frequency range of 70 hz to 5870 hz is designed to obtain sufficient data to evaluate conductors having conductivity-thickness values of 0.1 mhos to 2000 mhos. The range for massive sulphides is generally 1 mho to 500 mhos. Figure 9 shows the GEM5 conductivity spectrum over steeply dipping conductors for various modes. Some examples of conductivity-thickness values of mineral deposits are indicated.

Figure 10 indicates the GEM5 conductivity spectrum for a homogeneous earth having conductivity values of various ground and rock types.

RESPONSE CURVES

Anomalous responses over steeply dipping dikes are summarized in Figure 11 for various modes, depths, and dips. The 2 ellipse parameters, ellipticity, and tilt angle, are approximately equivalent to "Out-of-phase" and "In-Phase" response, respectively.

A magnitude of the ellipticity response is small at low values of σt (conductivity-thickness). As σt increases, the magnitude increases to a maximum value. Beyond the maximum value of σt, the ellipticity decreases with increasing σt. The tilt angle response, however, increases with increasing σt over the entire range toward saturation. This behaviour is similar to the "Quadrature" and "In-Phase" response of conventional EM systems, and is diagnostic of anomalous sources.

The lowest frequency provides excellent depth penetration in a highly conductive overburden environment with Tx-Rx separations of up to 300 m.

TERRAIN EFFECTS AND THE REMOVAL OF TERRAIN EFFECTS

As previously mentioned, the ellipticity is insensitive to terrain effects due to elevation difference between the Tx and Rx. The tilt angle parameter is sensitive, and the removal of the terrain effects on data obtained in a topographically rough area is important to achieve proper interpretation.

The most convenient way is to normalize to the lowest frequency by subtracting the tilt angle value at the lowest frequency from those at higher frequencies. This method is done on the assumption that a tilt angle response at the lowest frequency is small and can be ignored. In the case of strong response from a highly conductive zone, over-correction will result.

If there is detailed information on terrain, often after a gravity survey, the correction can be performed simply by subtracting the calculated tilt angle response due to the elevation difference between Tx and Rx.

The third method is a shoot-back-type operation by taking measurements with a horizontal Tx loop then a

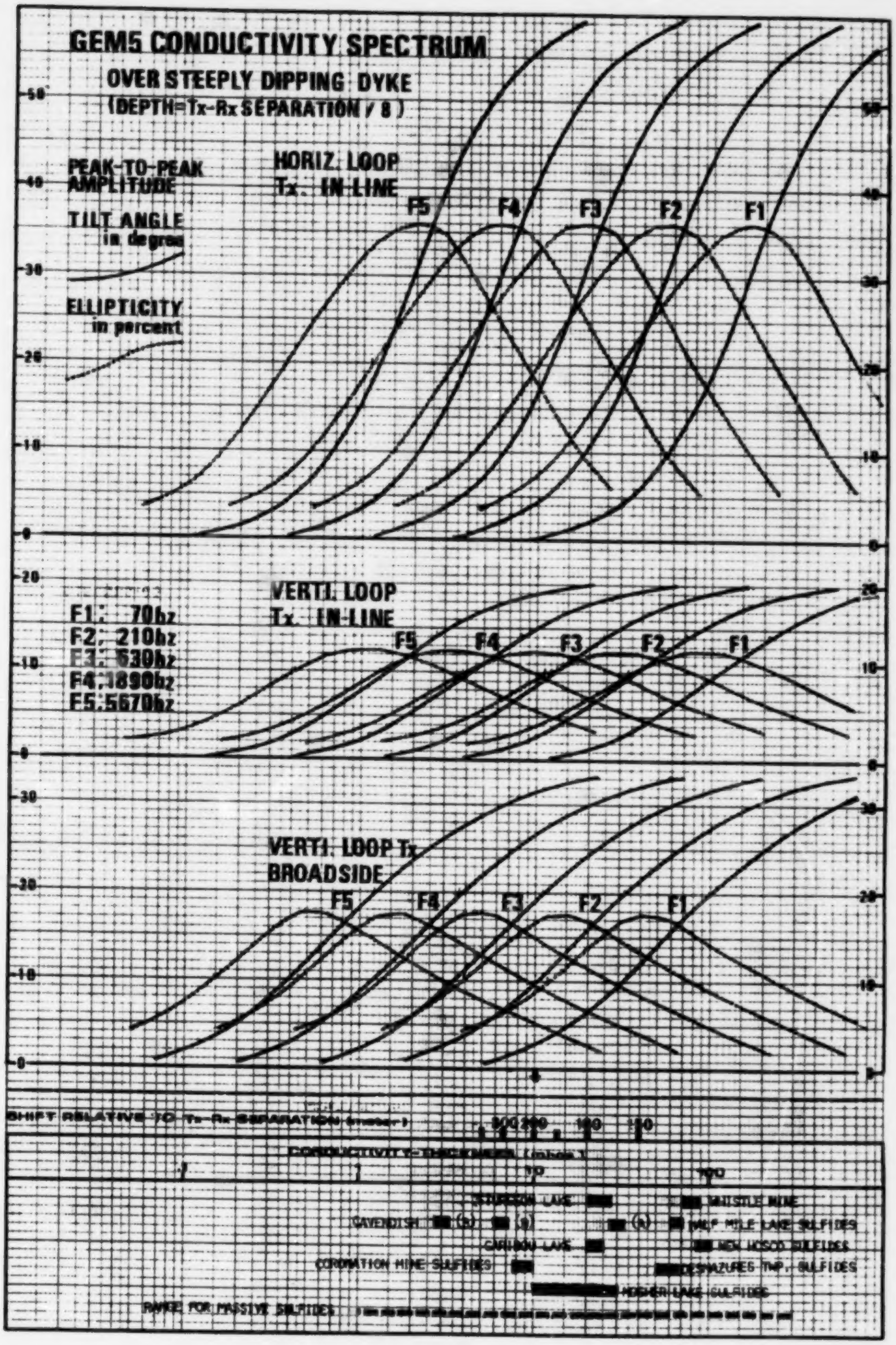

Figure 9. GEM5 conductivity spectrum of various survey modes over steeply dipping dikes with conductivity-thickness reference to ore deposits of some mines.

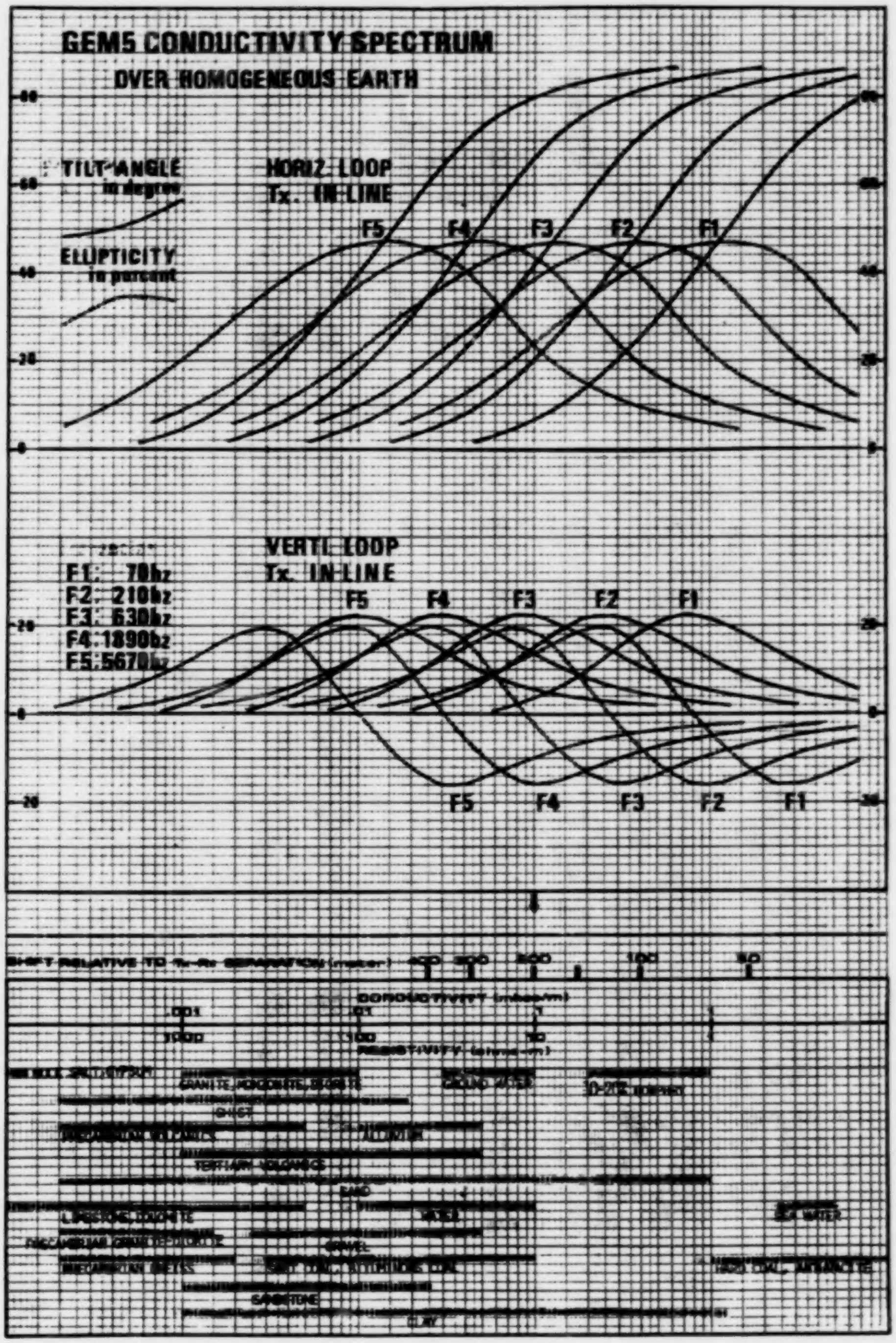

Figure 10. GEM5 conductivity spectrum of 2 survey modes over homogeneous earth with conductivity reference to various geology.

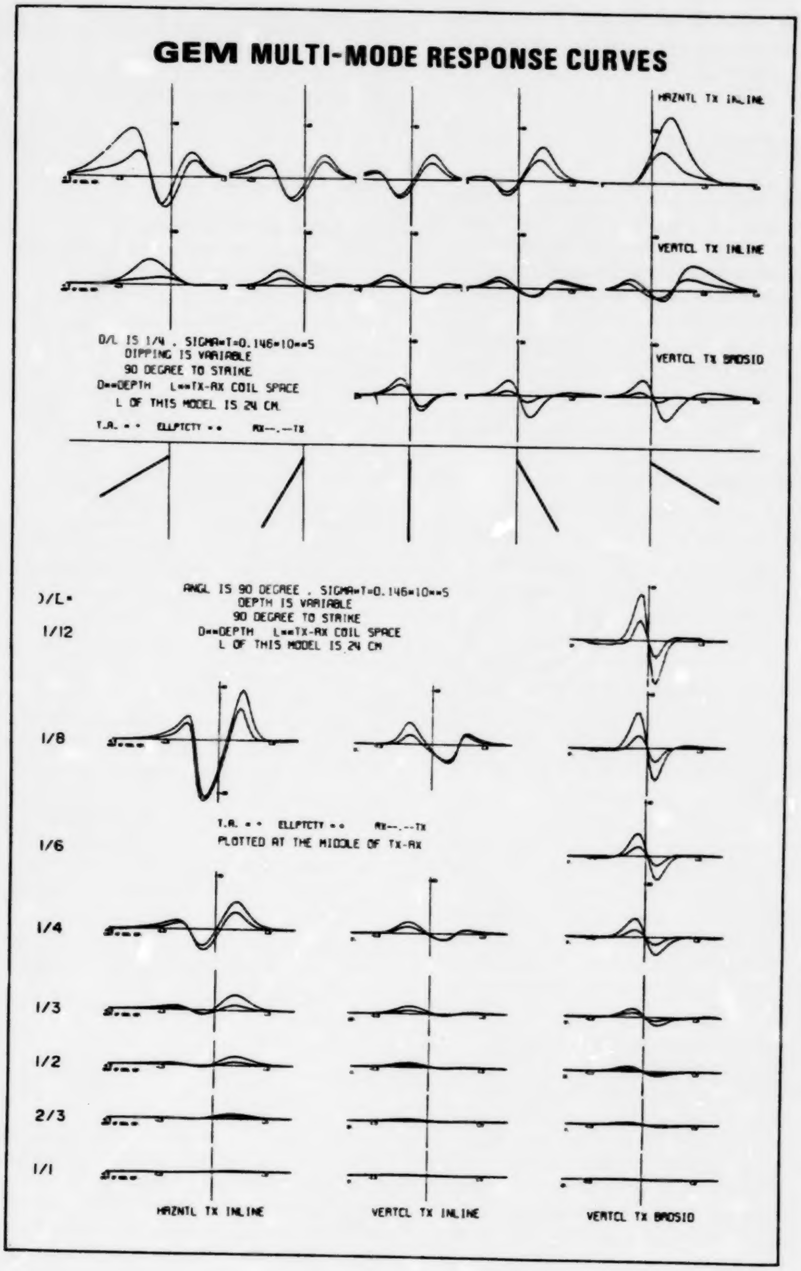

Figure 11. Summarized GEM5 responses over steeply dipping dikes for various survey modes, depths, and dips.

vertical Tx loop. This method works well if the Tx-Rx orientation is within ±20 degrees or the Tx coil can be tilted aiming at the Rx to within ± 20°.

INTERPRETATION

Even though the GEM5 performs signal processing digitally, and the GEM8 is mostly analog, the results from both devices are absolutely equivalent. Therefore, all interpretation methods and tools for GEM8 can be used for GEM5 data interpretations. Interpretations can be made to estimate conductor location, depth of conductor, dip and conductivity-thickness value, and to obtain "stratigraphic" information such as overburden conductivity and thickness or depth to basement.

FUTURE PLANS

The system should be available for sale, lease, or contract survey to the public in 1983.

REFERENCE

Dey, Abhyit, and Ward, Stanley H.
1970: Inductive Sounding of a Layered Earth with a Horizontal Magnetic Dipole; Geophysics, Volume 35, Number 4, p.660-703.

Grant 031 The Geoport Project

D.J. Dodds

Huntec (70) Limited, Scarborough

ABSTRACT

The most expensive part of geophysical exploration is the cost of mobilizing field crews into remote areas. Therefore, it is essential to make most effective use of field operations. Reduction and interpretation of field data on site can ensure data quality and allow field crews to do immediate follow-up of anomalies of interest.

Computers are now available at a size, cost, and computation power that makes them highly attractive for use in geophysical, geochemical, and geological field surveys. However, appropriate editing, plotting, and interpretation software is not commercially available, particularly for use by non-experts. In addition, not all computer hardware is rugged enough for use under typical field conditions.

The objective of this project is to develop a line of practical hardware/software computer systems for geoscience exploration. The major emphasis will be on designing menu-driven software for a range of geophysical applications, built around a common database core software package. Care will be taken to ensure, as far as possible, machine-independence of the software so that it will not become obsolete with expected advances in hardware. In addition, a novel transit case-work station will be incorporated into hardware design. Both hardware and software will be extensively tested under field conditions.

This 3-year program will develop a wide range of application software. It is expected that a commercial product will be marketed world-wide before the end of the program.

INTRODUCTION

It has been estimated that data collection typically represents about 80% of the total cost of a geophysical survey. Exploration costs are rising rapidly, largely due to increased costs of mobilizing field crews into remote areas. At the same time, computers are becoming smaller, more rugged, and less expensive. Therefore, field computers will be used increasingly to improve the effectiveness of field personnel, and to reduce the costs and risks of field operations.

This project addresses specification of a computer system appropriate to use in geophysical field conditions, and preparation of commercial-quality software for a range of geophysical applications. Both hardware and software will be marketed worldwide.

Huntec Limited has identified several important improvements which can be made in geophysical field instruments using state-of-the-art technology. Some of these are:

1. better interaction between the operator and equipment through menu-selectable commands thus simplifying operating procedures
2. faster data acquisition and improved data quality made possible by more powerful microprocessors capable of more extensive real-time signal processing
3. fast on-site data reduction to permit anomalies to be followed up while the crew is still in the area

This development program will be aimed at incorporating these concepts into a hardware/software system that could be used not only with Huntec instruments, but with most types of geophysical instrumentation through standard digital interfaces. Software for a variety of geophysical data interpretation applications will be developed.

THE GEOPORT SYSTEM

Over the last 2 years, with the support of the Ontario Board of Industrial Leadership and Development (B.I.L.D.) Exploration Technology Development Program, Huntec Limited has devoted considerable effort to the development of a portable computer system for the analysis of geophysical data. Although a rugged and transportable hardware configuration is an important part of the system, the bulk of the work has been in the design of a cost effective software system.

The cost of software development and maintenance is a significant factor in all areas of computer applications. A related problem is the design of the interface between the applications software and the user; a consistent and friendly user interface may be essential to user acceptance of a software system, but may substantially increase the software development cost. These problems are of particular importance in the geophysical industry because of the relatively limited market for any particular geophysical application.

The database concept has been used successfully in commercial applications to reduce software development costs and to provide a consistent user interface. A database is a collection of information combined with facilities for efficiently adding information to the database and retrieving information from it. Usually a database system includes programs which permit a non-programmer to search, view, and edit information in the database. But applications programs may also be written which access the database directly. These may compute results from the information in the database, then store those results back in the database.

The word "database" is used by software professionals to cover a wide range of programs and techniques. Certain ideas are fundamental to the concept, however. A database consists of a collection of data which is permanently stored in a computer, together with the means to efficiently and effectively access that data.

A database, in the full sense of the word, must also have the following characteristics. It must permit the user to view the data it contains in multiple ways. It must be flexible enough to permit new categories of information to be added to existing data. The database must contain some description of its own structure. It must allow the non-programmer to find and display desired information within the database in an efficient manner. Finally, the database must provide a means for the programmer to write applications software which can efficiently find, use, and modify the data which it contains.

Let me enlarge upon each of the following characteristics by giving an example of its significance in the context of a database which contains geophysical survey data. First, consider the need to view the data in multiple ways. It has become common practice to process ground magnetometer data by correcting for fluctuations observed at a base station magnetometer. To insert these corrections (manually or by means of software), it is desirable to step through the data in order of date and time. However, to plot the data, we must ideally access it by line and station number. These 2 ways of looking at the data are illustrated by the 2 profiles in Figure 1; the first is presented in order of time, the second in order of location.

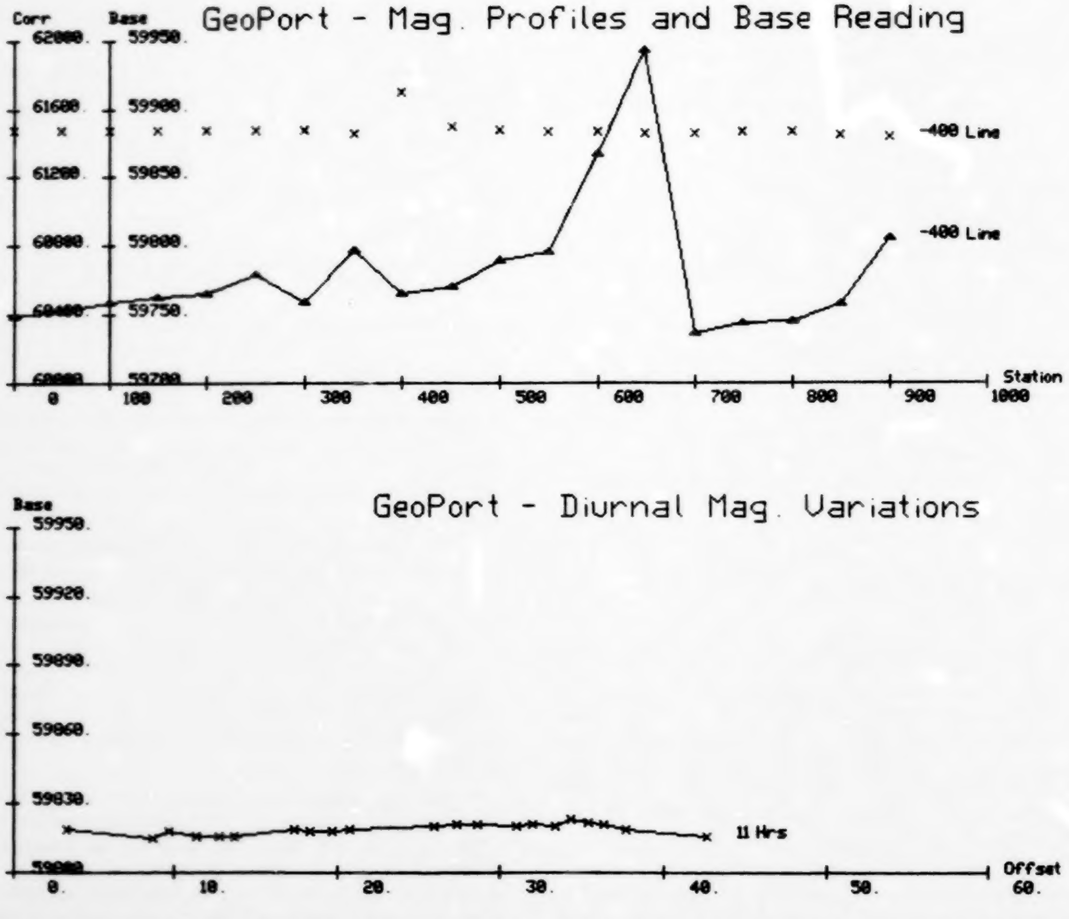

Figure 1. The database facilities allow the user to look at data in many ways; in this case the data are viewed in order of time and in order of station number.

```
Month  Day  Year  Hrs  Min  Sec  Line  Station  Base    Offset  Rdg     Corr
                                                Gamma   Gamma   Gamma   Gamma

    8   25  1981   14   37   40  -400        0  59885.    -45.  60437.  60392.
    8   25  1981   14   39   40  -400       50  59884.    -44.  60461.  60417.
    8   25  1981   14   40   20  -400      100  59884.    -44.  60516.  60472.
    8   25  1981   14   41    0  -400      150  59884.    -44.  60549.  60505.
    8   25  1981   14   41   40  -400      200  59884.    -44.  60569.  60525.
    8   25  1981   14   42   40  -400      250  59884.    -44.  60672.  60628.
    8   25  1981   14   43   20  -400      300  59885.    -45.  60523.  60473.
    8   25  1981   14   44   20  -400      350  59882.    -42.  60814.  607
    8   25  1981   14   45    0  -400      400  59912.   -102.
    8   25  1981   14   45   40  -400      450  598
    8   25  1981   14   46   20  -400
    8   25  1981   14   4
    8   2
```

```
Month  Day  Year  Hrs  Min  Line  Station  Gobs      Gb
                                           m Gal   m Gal

    8   25  1981   16   20  -400        0    3.3    22.4
    8   25  1981   16   26  -400       50    3.2    22.4
    8   25  1981   16   31  -400      100    3.3    22.5
    8   25  1981   16   38  -400      150    2.3    22.3
    8   25  1981   16   43  -400      200    4.5    22.7
    8   25  1981   16   49  -400      250    1.1    22.2
    8   25  1981   16   55  -400      300    3.9    23.8
    8   25  1981   17    1  -400      350    3.6    23.0
    8   25  1981   17    7  -400      400    2.4    24.3
    8   25  1981   17   14  -400      450    2.0
    8   25  1981   17   20  -400
    8   25  1981   17
    8   2
```

```
Line  Station  Base    Offset  Rdg     Corr      Gobs     Gb
               Gamma   Gamma   Gamma   Gamma   m Gal   m Gal

-400        0  59885.    -45.  60437.  60392.    3.3    22.4
-400       50  59884.    -44.  60461.  60417.    3.2    22.4
-400      100  59884.    -44.  60516.  60472.    3.3    22.5
-400      150  59884.    -44.  60549.  60505.    2.3    22.3
-400      200  59884.    -44.  60569.  60525.    4.5    22.7
-400      250  59884.    -44.  60672.  60628.    1.1    22.2
-400      300  59885.    -50.  60525.  60473.    3.9    23.8
-400      350  59882.    -42.  60814.  60772.    3.6    23.0
-400      400  59912.   -102.  60624.  60522.    2.4    24.
-400      450  59887.    -37.  60593.  60556.
-400      500  59884.    -44.  60761.
-400      550  59883.
-400
```

Figure 2. The database concept allows different categories of data to be combined easily; in this case, gravity and magnetic data.

In Figure 2, 2 sets of data collected on the same survey line are shown. One is magnetometer data, the second is gravity data. They can be combined as shown, by adding a new field to one of the sets of data. This is not a particularly straight-forward task using more conventional techniques. Separate applications programs designed to operate on magnetometer data and gravity data would not typically work on data in a new file format combining both kinds of data. However, the approach in a database system is to have the applications software query the database for the category of data which is required by name, rather than expecting data to be in a fixed format. Therefore, if 2

```
GeoPort Data Base Listing - B:MAG+GRAV.DB

 Line  Station  Base    Offset   Rdg      Corr     Gobs      Gb
                Gamma   Gamma    Gamma    Gamma   m  Gal   m  Gal

  -400     550  59883.    -43.   60808.   60765.     7.1     25.1
  -400     600  59883.    -43.   61379.   61336.     5.5     27.3
  -400     650  59882.    -42.   61985.   61943.    17.5     35.5
     0     300  59819.     21.   60665.   60686.     5.9     25.6
     0     400  59818.     22.   60669.   60691.     9.1     27.2
     0     450  59819.     21.   60948.   60969.     7.9     28.3
     0     500  59821.     19.   61925.   61944.    11.8     32.9
     0     550  59821.     19.   61555.   61574.    19.9     39.0
     0     600  59820.     20.   60753.   60722.    20.7     41.8
```

```
FIELD NAME     INDEX    RELATION    VALUE
Corr               1       GT       60600.000
Gb                 1       GT           0.025
```

Figure 3. The user can select and access data according to his own criteria.

databases are combined, the applications programs which could be used on each will be usable on the combined result because data categories are identified by name.

The identification of data by name is one aspect of the database's capacity to describe itself. In geophysical applications, the database might also contain permissible ranges of values of certain types of data. It would then prevent the user from storing data outside of the permitted range. It could contain specifications of the physical units in which measurements are expressed, scales to be used in plotting data, and the like. With this kind of information already in the database, the inputs needed from the user to an applications program are greatly reduced, making results more accessible and less error-prone.

Figure 3 illustrates the facility which can help make data accessible to the non-programmer. At the bottom of the figure is a specification for selecting records from the database. It has been entered by the user, who wants to see all records in which Bouger gravity is greater than 25 mgal and total magnetic field is greater than 60 600 nT. The resulting listing is shown at the top of the figure.

Of course, geophysicists do not often find listings a satisfactory way to display data. In Figure 4, gravity and magnetic data have been displayed using a generalized graphing program. To access the data, the user has specified the names of the fields which are to be used as abscissa ("station") and as ordinates ("Corr" and "Gb"). Default scaling information has been obtained from the database, although the user has the option of modifying the scales. The user has also specified that a separate graph is to be drawn for each survey line. Because the graphing program is quite general, the user can easily request plots which combine different kinds of data (in this case, gravity and magnetic data). Graphic packages designed for specific types of data would not have this capability.

By making the context of the database accessible to the programmer, specific applications software can be written more quickly. Figure 5 illustrates the concept. Input, output, editing, and graphing of all data can be handled by generalized programs. These common functions are therefore eliminated from programs for calculation and interpretive modelling, which can get data directly from the database and store results in it.

Over the past year, the database concepts described here have been incorporated in a software system which is presently installed on an 8-bit microcomputer system (Figure 6). The software system contains the following major components:

Data Base Edit—permits the user to display the database on the CRT screen, scroll through it, search it, select data for editing by pointing with the cursor and edit the selected data

Data Base List—select and tabulate fields and records on printer

Data Base Graph—select user-specified records and graph a user-specified field, producing profiles, decay curves, spectra and other plots on the CRT screen, graphics printer, or optional plotter

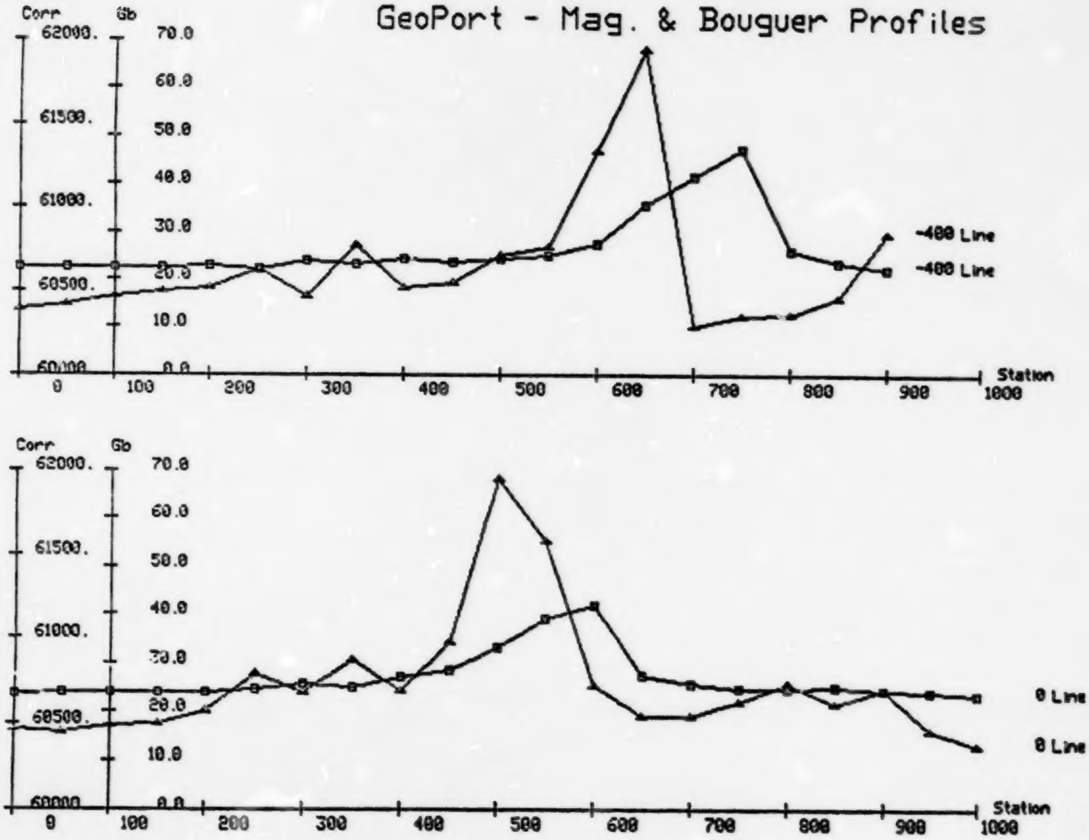

Figure 4. A generalized graphing program can easily produce specialized plots, like this one which combines gravity and magnetic data.

Data Base Map—select user-specified records and post the values from a user specified field on a plot, producing maps, sections and pseudo-sections

Data Base Initialize—create a database and specify its size, record format, and field names

Data Base Copy—copy the contents of one database to another while selecting, adding or deleting records and fields, to permit editing, and merging of the database

Data Base Formula—allows the user to specify calculations to be performed on the contents of a database

Data Base Input—copies a data file in an arbitrary format into a database

This software is now fully operational, and was in fact used to produce the listings and graphs in Figures 1 to 4.

In summary, the database concept allows a wide variety of functions to be handled by a few general programs with carefully designed user interfaces. Where specialized software is needed, the necessary input, output, and display functions can be handled by these programs. The database concept therefore reduces the cost of software development, and eliminates the need for the development of many specialized programs.

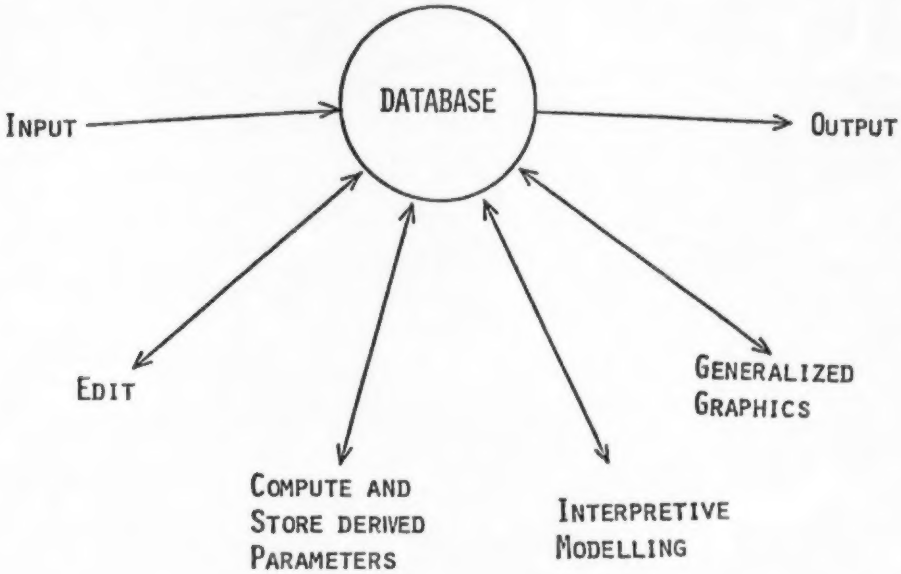
DATABASE
INPUT
OUTPUT
EDIT
GENERALIZED GRAPHICS
COMPUTE AND STORE DERIVED PARAMETERS
INTERPRETIVE MODELLING

Figure 5. The requirement to input, output, edit and display data is common to all geophysical techniques. Calculations and interpretive modelling are application specific.

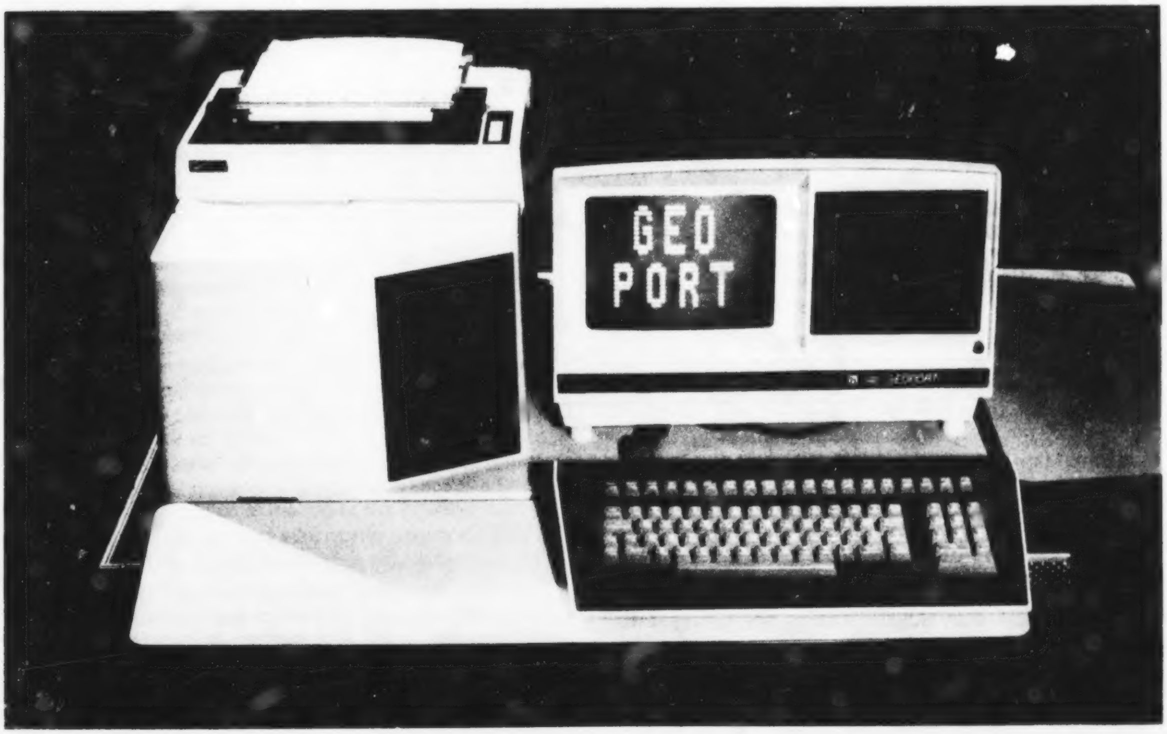

Figure 6. GEOPORT hardware.

Grant 039 Single Receiver, Frequency Scanning Fixed Source Electromagnetic System

Andrew Rogozinski
Androtex Limited, Mississauga

ABSTRACT

The system Androtex Limited is developing will be a new version of the Turam fixed source electromagnetic method. It will combine the high sensitivity and the frequency scanning capability of the present "ELFAST" system, with single coil measurements instead of using the conventional 2 receiving coils connected to a compensator bridge (receiver).

This new configuration will enable surface measurements to be carried out by 1 operator, rather than the present 2-man crew, and will at the same time considerably increase survey productivity. Moreover, the capability of measuring 3 orthogonal field components is retained and simplified.

In drillhole surveys, measurements are made in the same manner as in surface surveys. It will no longer be necessary to use the "compensator" configuration with a fixed reference coil and an increasing distance between reference and measuring coils with the new system.

The multifrequency, high power transmitter will provide output power of 2000 W and an adjustable output voltage from 100 to 800 V. This is necessary to energize deep conductors and overcome the effects of surface conduction, particularly at lower frequencies.

Large areas of potentially mineralized formations in Ontario are covered by a thick layer of conductive unconsolidated Quaternary deposits. It is particularly in this type of geological environment that wide-spectrum fixed-source methods are indispensable tools in the search for base-metal bodies. Many examples of successful surveys with these methods exist in Ontario, and even more striking results have been obtained in recent years in the Athabasca Basin.

The present Elfast system permits a daily production of 4 to 5 km, using 3 frequencies and including loop laying, to be easily achieved. A single coil system will make a 50% improvement in productivity possible. Cost effectiveness will be significantly increased without any attendant loss in data quality.

The transmitter for the new system, with a stabilized output current and a power capability of 2000 watts, has been designed and is described. The next stage of research and development is the development of a single coil receiver with solid state memory and a computing/plotting support system.

INTRODUCTION

Deep exploration ground electromagnetic equipment has gained a strong interest during the past decade as the search for mineral deposits is directed to greater depths as well as in more difficult geological environments. Wide band systems using a large fixed transmitting source have become more popular when exploration depth is the main concern. Other important factors are quality of results, efficiency of operation (cost effectiveness), and reliability in the field.

The well known frequency domain Turam method has been used successfully for many years without significant improvements to the instrumentation. The Elfast Extra-Low-Frequency Auto-Scanning Turam System, introduced in 1979, was a step forward, and has been used successfully reaching exploration depths up to 500 m.

The proposed new system, based on recent advances in electronics, will consist of a single coil receiver instead of the conventional 2-coil system (gradient measurements). Moreover, it will eliminate the unsatisfactory configuration with the stationary reference coil at the surface in drillhole survey measurements. Assymmetry effects of 2 coils and separate channels at the receiver will also be removed. Field productivity, particularly in rugged terrain, will be considerably improved.

A built-in solid state memory module in the receiver, for recording the great volumes of data collected daily, will further increase field productivity. The data accumulated in memory will be transferrable to a computing system for processing and plotting, permitting the operator to evaluate the survey results on a daily basis.

The new, microprocessor-controlled receiver will be made automatic by means of full synchronization with the transmitted timing and programmable frequency pattern.

An increase of the transmitter power to 2000 W with stabilized output current will further improve the signal-to-noise ratio, particularly at the lowest frequencies, and in areas where a high level of man-made (power lines) noise is present. Long continuous profiles could be measured for reconnaissance work or surveys for deeply buried targets can be made by using a single transmitting loop set-up. The transmitted frequency will be programmable and set, as required, for a particular survey environment. Each frequency can be set for a pre-selected length of time depending on field conditions. All parameters will be pre-synchronized with the receiver at the beginning of the survey. Identical high stability frequency clocks in both the transmitter and receiver will ensure accurate measurements throughout a full day's survey without radio or other tenuous links for a reference signal.

PROGRESS OF PROJECT

The research supported by the Ontario Board of Industrial Leadership and Development Exploration Technology Program commenced at the end of December 1982 and covers 3 main phases in the development of the Single-Receiver Frequency-Scanning Fixed-Source Electromagnetic System:

1. design of transmitter with a stabilized output current and power capabilities of 2000 W
2. single coil receiver with solid state memory and computing/plotting support system
3. borehole attachment to the receiver

TRANSMITTER

A single coil receiver must have a constant energized electromagnetic field throughout the survey. In other words, the transmitting loop must be energized with a stable current at each frequency. This will also ensure accurate secondary field calculation when surveying for deep targets. Variation, due to loop resistance (temperature effect) or ground resistance if transmitter is used in galvanic mode, as well as changes of voltage from the power source (generator), has to be compensated by a high stability current regulator at the transmitter. This is necessary to ensure proper overall operation of the single coil receiver with borehole capabilities. A block schematic of the high output power transmitter with current regulator is presented in Figure 1.

The power section consists of a 3-phase transformer in "Δ" to "Y" at the output connection with several taps providing a full range of output voltage from 100V to 800V in 100V increments. Three solid state relays (SSR) act as the main ON/OFF power switch at the input, which is controlled by internal electronics, including protection circuits and controls at the front panel. Each SSR is protected against inductive effects from the power transformer and excessive voltage spikes which might occur during switching.

The output voltage from the transformer is connected to a 3-phase module consisting of 6 silicon-controlled rectifiers acting as high efficiency current regulators. The output current adjustment is externally controlled and regulated in a closed fast-acting loop-feedback system. Measuring and sampling is done throughout by an isolated sensor located at the output terminal of the transmitter.

A smoothing filter in π configuration supplies the main output converter, which consists of 4 inverter type silicon-controlled rectifiers connected in bridge configuration. When 1 pair of SCR's are switched on simultaneously, the full supply of DC voltage is applied across the load in 1 polarity. In that time, the second pair of SCR's are off or open. The supply voltage across the load will change polarity when both pairs of SCR's are in the appropriate state. Thus, voltage is applied alternatively across the load, dependent only upon the switching action of the driver controlled by digital logic circuits.

Current in the input and output lines is monitored by fast-acting sensors providing signals to the protection circuits so that in case of excessive current in either line, the main power line is automatically disconnected. If the output current drops below 0.5A, the output is also shut down as this is considered a no load condition (open loop).

The power supply connected to 1 phase of the input voltage provides stable +12V, +6V, -12V, and -6V outputs to the internal-supporting electronics and monitoring signals on the front panel.

The digital programmer driven from a high stability temperature-compensated crystal-contolled oscillator gives 5 fundamental output frequencies: 25, 75, 225, 675, and 2025 Hz. The programmer is connected with the auto-switching circuitry and programmable frequency selector. Any 1 of 5 output frequencies can be selected with a set of toggle switches for any frequency pattern required for a particular survey.

It is possible to set precisely at 10, 20, 30, and 40 second periods, with the timing subsystem driven from the crystal oscillator, for each transmitting frequency in the multi-mode operation, depending on the signal-to-noise

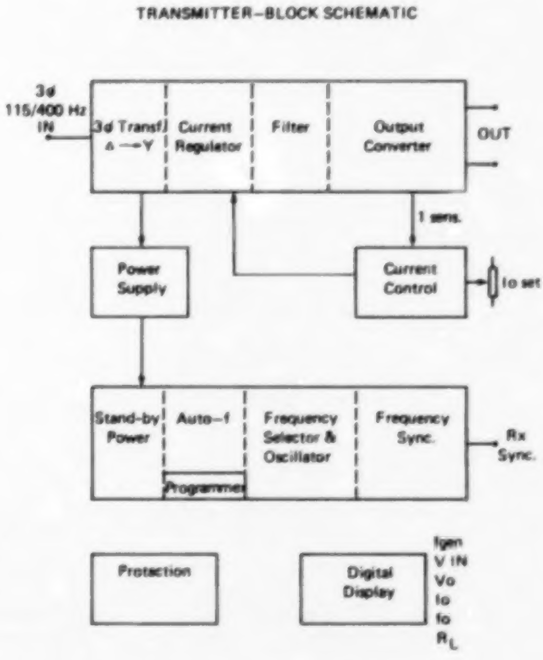

Figure 1. Block schematic diagram of transmitter.

ratio (longer stacking time at the receiver) or terrain conditions. The timing circuits are disabled when a single frequency operation is chosen.

The digital circuits are designed in a Complementary Metal-Oxide Semiconductors (CMOS) technique. This kind of logic was selected for the control section of the transmitter mainly because of its high noise immunity characteristics and low power consumption.

A separate connector is provided to synchronize transmitter timing and frequency pattern with the receiver at the beginning of the survey.

To ensure continuity of full synchronization with the receiver, when, for any reason, the motor generator stops operating, an internal standby rechargeable battery automatically takes over supply of all digital circuits, i.e. crystal oscillator, programmer, and timing system. In this case, the initial synchronization with the receiver is still valid and does not require corrections. Moreover, when the output power is disabled by protection circuitry (overload, open loop) synchronization is not required. After a period of 3 hours, the timer disconnects the standby system. This internal standby feature further improves the efficiency of field operation.

The protection system is connected to fast acting current and voltage sensors at the input and output of the power section of the transmitter and will automatically turn off voltage supply from the generator when:

1. input voltage from the generator is beyond limits
2. output current exceeds maximum or drops below desirable limit (open loop)
3. internal overheating of transmitting occurs
4. current regulator reaches limits
5. high voltage switch is used or frequency or timing pattern is changed
6. emergency stop is used

Lamps located on the front panel indicate separately the reason for power-off stage.

An operator at the transmitter can monitor the following switch selected parameters on the digital display:

1. generator frequency which indicates motor generator's RPM
2. input voltage from alternator
3. transmitter output voltage
4. transmitter ouput frequency
5. load resistance

The display printed circuit board consists of an A/D converter with multiplex output driving a 3½ digit display.

Load (loop) resistance, which is measured using separate terminals, allows the operator to use maximum power at a certain load which varies depending on the loop size.

A floating output and the front panel of the transmitter (Figure 2) are isolated from high voltage for safety of the operator. Also, a ground terminal is provided.

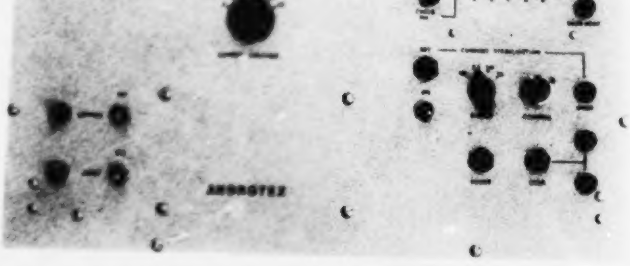

Figure 2. Transmitter

TRANSMITTER PARAMETERS

Output:
Power–2000 VA
Voltage–100 to 800 V
Current–10A maximum stabilized to within ±.05% for variation of load ±25% and input voltage ±10%
Waveform–Square wave
Frequencies–25, 75, 225, 675, 2025 Hz

Operating Temperature Range: -40°C to +70°C with +75°C limit

Load Limits: 11.0A maximum, .5A minimum

Input Voltage Limits: 125 V maximum, 100 V minimum

Input:
Power–2200 VA
Voltage–115V Nominal
Phase–Three

MOTOR GENERATOR SET

As a highly dependable electrical power source in the field, an alternator with a permanent magnet was chosen. This type of alternator does not require external excitation and has several major advantages over a conventional alternator such as:

1. Minimum maintenance because: a) ball bearings are sealed and lubricated for life; b) no brush/commutator
2. Excellent dependability
3. High overload capacity
4. Compact design
5. High efficiency

Another consideration for choosing this type of alternator was its availability versus aircraft alternators which are disappearing from the market.

The alternator is driven by a single cylinder 4 stroke Briggs & Stratton gasoline engine. The principal considerations for deciding to use the highly reliable Industrial-Commercial version were:

1. cast iron cylinder sleeve for long operating life
2. positive valve rotation ensuring maximum power over a long period of time
3. ball bearings on crankshaft

Figure 3 illustrates the motor generator which is mounted on a reinforced steel plate, with shock mounts and mechanical limiters. A large gasoline tank provides for continuous operation over an 8 to 10 hour period under full load.

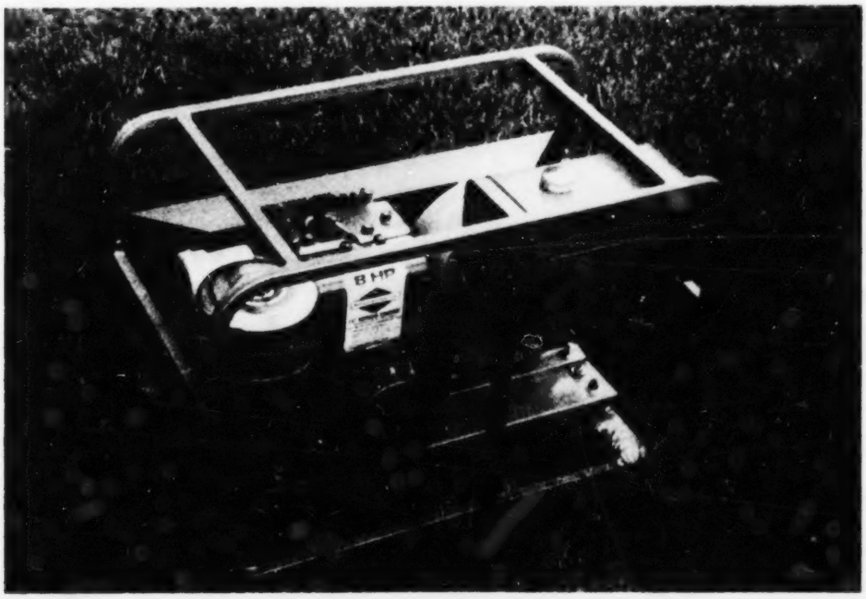

Figure 3. Motor generator.

MOTOR GENERATOR PARAMETERS

Engine: Briggs & Stratton 4 stroke 8 HP SAE, I/C type
Alternator: 3 phase 115V/400 Hz at 1700 RPM
Output Power: 2200 VA
Dimensions: 42 cm by 74 cm by 48 cm
Weight: 60 kg

Design and testing of the motor generator is completed but some minor adjustments to the mechanical design will be done during final documentation.

Testing of the assembled transmitter is also in the final stage.

This project is proceeding on schedule and we are now in the initial stages of developing the single coil receiver.

POOR

QUALITY

ORIGINAL